THE BIOPHYSICAL AND PHARMACOLOGICAL PROPERTIES OF PRESUMPTIVE SEROTONERGIC NEURONES RECORDED INTRACELLULARLY FROM THE DORSAL RAPHE NUCLEUS IN THE IN VITRO SLICE PREPARATION

by

Donald Gordon Rainnie

Thesis presented for the degree of

Doctor of Philosophy

University of Edinburgh

1988

In accordance with the requirements of regulation 3.4.7 this thesis has been composed by myself and the work presented herein is my own.

Donald G Rainnie

ACKNOWLEDGEMENTS

Firstly, I would like to thank all the people in the department of Pharmacology at Edinburgh for their friendship and encouragement during the last three years.

Secondly, and most importantly, I would like to thank my family for their constant support and belief in me.

ABSTRACT

Presumptive serotonergic neurones recorded intracellularly from the dorsal raphe nucleus in the *in vitro* slice preparation had a high input resistance Rm (203 ± 7MΩ), a linear current-voltage relationship in the hyperpolarising direction and a long membrane time constant τ (29 ± 1.4ms). Spontaneous rhythmically firing action potentials (0.5-2Hz) were seen at the resting membrane potential (-59 ± 0.8mV). The rhythmicity resulted from a four stage pacemaker potential cycle; 1) a slow depolarising prepotential leading to 2) a broad (2ms) overshooting action potential followed by 3) a rapid afterhyperpolarisation (AHP, 10-20mV) and 4) a gradual (≈200ms) return to the resting membrane potential. Several time and voltage dependent ionic conductances were found to underlie the pacemaker potentials. A Co^{2+} sensitive low threshold (-60 to -55mV) depolarising prepotential was seen to be mediated by a transient inactivating inward calcium current. The subsequent action potential consists of a) a TTX sensitive, fast sodium spike and b) a TTX insensitive, high threshold (-40mV) component. The latter potential was blocked by Co^{2+} as was the following AHP. The AHP was found to reverse direction between -80 to -90mV consistent with a potassium mediated event. In voltage clamp depolarisation evoked a transient inward current followed by a TEA-sensitive outward current. The AHP was therefore assumed to be mediated via a calcium dependent potassium conductance, $I_{k(Ca)}$. Apamin, a known inhibitor of $I_{k(Ca)}$, blocked the AHP irreversibly. 5-HT appeared to have no direct effect on AHP size or duration. A second more transient outward current was observed that required hyperpolarisation from the resting membrane potential to remove channel inactivation. This outward current was insensitive to TEA but 4-aminopyridine (4-AP) caused a 60% reduction in amplitude. The inactivation and activation properties of the current (Vhalf -74 and -49mV respectively) were characteristic of I_A. 5-HT had no apparent effect on I_A. A third non-inactivating outward current was observed with depolarising voltage commands to -40mV, or more positive. Transient hyperpolarising voltage step commands produced an inward current relaxation and on termination of the pulse an outward relaxation was observed. This current, reminiscent of I_M, could act as a rectifier and oppose prolonged membrane depolarisations.

5-HT (50-100μM) caused a membrane hyperpolarisation (4-18mV) and a concomitant decrease in Rm (15-20%) and τ (24-32%). The reversal potential for the 5HT effect was -91mV. This was close to the K^+ equilibrium potential. Chloride loaded cells showed a depolarising response to 10mM GABA application whereas 5HT under the same experimental conditions still evoked a hyperpolarisation. Baclofen, believed to activate a G protein mediated potassium conductance also caused a longlasting hyperpolarisation together with a decrease in Rm and τm which reversed at -90mV. The selective 5-HT_{1A} agonists 8-hydroxy-2-(di-n-propylamino)teralin (8-OHDPAT), dipropylcarboxamidotryptamine (DP-5-CT) and the novel anxiolytic buspirone caused a marked longlasting hyperpolarisation with an associated decrease in Rm and τ at concentrations lower than required for an equivalent response to 5-HT. All three compounds had reversal levels similar to that of 5-HT. Methysergide (100μM) and S_2 (100nM-5μM), a purported $5HT_1$ antagonist, were ineffective in antagonising the 5HT induced response. Spiperone (30μM) caused a 60% reduction in the 5HT induced response. Furthermore spiperone caused a gradual increase in Rm and τ possibly by blocking a local tonic release of 5HT or dopamine.

In conclusion this study has demonstrated that DR neurones posses the necessary voltage gated conductances needed to maintain an intrinsic pacemaker activity. Exogenous application of 5HT does not affect any presently characterised conductance but appears to produce inhibition via an increase in potassium conductance. It is postulated that this response is mediated primarily by the activation of a $5HT_{1A}$ receptor-G protein complex. Hence the anxiolytic action of buspirone may be attributable at least in part to the activation of this same receptor - G protein complex.

CONTENTS

CHAPTER 1

GENERAL INTRODUCTION

One way to achieve a greater understanding of the functioning of the central nervous system (CNS), with respect to both normal and aberrant conditions, is to elucidate cellular responses within specific brain regions. Essential to this understanding is the identification of neurotransmitters and the determination of their mechanisms of action. In order to determine whether or not a specific compound may be regarded as a neurotransmitter a number of experimental criteria have been developed (Werman 1966, Orrego 1976). Strictly speaking, a substance cannot be regarded as a transmitter at a particular synapse of a neurone unless the following criteria are met :

1. It is synthesised within the neurone.

2. It is present in the presynaptic terminal and is released in sufficient amounts to exert its proposed action on the affected neurone or effector organ.

3. When applied exogenously in reasonable concentrations it should mimic exactly the actions of the endogenously released transmitter.

4. If possible, exogenous application should be competitively antagonised by blocking agents shown to inhibit endogenously released transmitter action.

5. A specific mechanism exists for inactivation either by enzymic metabolism or by a high affinity reuptake system at its site of action.

In the CNS it is often impossible to satisfy all the criteria at a given synapse. The criteria assume that specific neurones can be selectively stimulated and that the transmitter released can be detected in the amounts released by single nerve endings after a single action potential. Perhaps most importantly a detection system must be employed that does not disrupt the functional integrity of the brain region under study. Early neurological studies employed both surgical and chemical lesions to show changes in post synaptic receptor number and localisation, as measured by ligand binding studies, to aid the identification of putative neurotransmitter substances. However the disruption of functional integrity was still quite gross and involved the non-selective destruction of neuronal pathways. The discovery of specific neurotoxins, such as 5,7 dihydroxytryptamine a specific serotonergic neurotoxin, has greatly helped the understanding of the morphological distribution of specific

neuronal pathways. Unfortunately the problem of identification of released substances still remains. Biochemical investigations of the brain had been centered mainly on brain tissue content of various chemicals. This however did not allow the separation of intracellular and extracellular content. Any attempt to look at synaptically released transmitter required a technique that would allow measurement of only the extracellular fluid. The development of the push-pull cannula by Gaddum (1961) allowed the first measurement of perfused extracellular environment. With the introduction of *in vivo* microdialysis in conjunction with high performance liquid chromatography (HPLC) some of these problems have been partially overcome (Ungerstedt et al 1982).

Any attempt to study post synaptic transmitter action at the cellular level will by its very nature be problematical. However the electrophysiological approach has given scientists a greater understanding of cellular biophysics. This thesis is primarily addressed to the analysis of events mediated by serotonin in the rat CNS *in vitro* with particular reference to both the passive and active membrane responses of dorsal raphe (DR) neurones when recorded using intracellular microelectrodes.

Mechanisms of transmitter action.

In central neurones the ultimate consequence of a chemical transmitter interacting with a specific receptor is either an excitatory or inhibitory effect on action potential generation in the postsynaptic neurone. However the simple classification of a receptor as being excitatory or inhibitory does not reveal any direct information about the membrane mechanisms involved. The question still remains as to how the receptor is coupled to specific ion channels, and indeed what type of ion channel is the receptor involved with.

Over a hundred years ago (Sydney) Ringer showed that the solution perfusing a frog heart must contain salts of sodium, potassium, and calcium mixed in definite proportions if the heart is to continue beating over a long period. At about the same time (1888) Walter Nernst derived an equation to express the electrical potential arising from the diffusion of electrolytes across a membrane in solution :

$$Es = \frac{R\,T}{Z\,F} \ln \frac{[S]2}{[S]1} \qquad \text{Equ. 1.1}$$

Where Es = the equilibrium potential for ion S

R = the gas constant

T =the temperature in degrees Kelvin

F = the Faraday constant

Z = the valency of ion S

and [S]2, [S]1 are the concentrations of ion S on opposite sides of the membrane.

In 1902, Julius Bernstein proposed the theory that excitable cells are surrounded by a membrane that is selectively permeable to K+ ions at rest and that the concentration ratio determines the resting potential of the cell. Consequently the Nernst equation could be appied, to give

$$E_k = \frac{R\,T}{F} \ln \frac{[K]_o}{[K]_i} \qquad \text{Equ. 1.2}$$

Where $[K]_o$ and $[K]_i$ are the potassium concentrations outside and inside the cell respectively. In the 1940's intracellular recording from the squid giant axon showed this theory to be an over-simplification.

In order to determine the nature of the ion channel involved in receptor function it is first necessary to know the transmembrane distribution of the major ionic species. The electrical potential across a neuronal membrane is dependent both on the distribution of sodium, potassium and chloride ions across the membrane and on their relative permeabilities. It was Hodgkin and Huxley (1952) who first considered the membrane to consist of separate channels for each ion, each channel being selective for one species of ion. In consequence the membrane potential can be derived from a simple equivalent electrical circuit in which each channel type is represented by a battery in series with a resistor (Fig. 1.1). By application of Ohm's Law to this circuit,

$$Em = \frac{gK.EK + gNa.ENa + gCl.ECl}{G} \qquad \text{Equ. 1.3}$$

Fig. 1.1

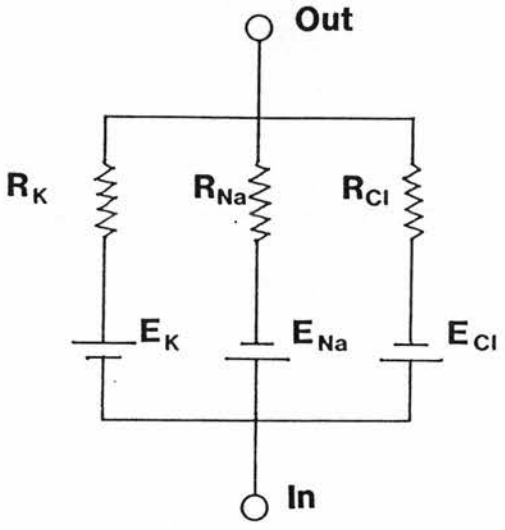

where Em = the membrane potential.

EK, ENa, ECl = the equilibrium potential of the individual ion species, that is the membrane potential at which an electrochemical gradient no longer exists.

gK, gNa, gCl = the conductance of the individual ions across the membrane.

and G = gK + gNa + gCl

In order to understand the effects of a neurotransmitter on neuronal membrane potential we can further simplify the model and assume that at rest the total conductance and the membrane potential can be described by a single resistor and battery in series; the action of a transmitter that opens additional ion channels can then be represented as an additional parallel conductance pathway. In Fig. 1.2 then, suppose that ϵ and r represent new channels opened during transmitter action this would be equivalent to closing switch S1. If ϵ does not equal E current will flow. Its value will be given by ;

$$I = (\epsilon - E)/(R + r) \qquad \text{Equ. 1.4}$$

and the change in the potential (e) caused by the transmitter action will be ;

$$e = R (\epsilon - E)/(R + r) \qquad \text{Equ. 1.5}$$

As this model indicates the magnitude and polarity of the response is dependent on the membrane potential of the neurone. The membrane potential at which the transmitter no longer causes a change in membrane potential is called the reversal potential (E rev), or equilibrium potential, ie where $E = \epsilon$. This value is measurable and of particular importance as it can give an indication of the specificity of the conductance change if only a single ion species is involved (Ginsborg 1973). In order to fulfill the criteria required for transmitter action nerve stimulation and application of the putative transmitter must share not only a similar excitatory or inhibitory action on postsynaptic membranes but the ionic mechanisms underlying these responses must also be similar.

The most widely used method for determining the reversal

potential of transmitters was first described by Fatt and Katz in 1951. Called the constant current method, it employed two intracellular microelectrodes, one to record the membrane potential and the other to pass constant current to shift the membrane potential to new steady state levels. This technique can also be achieved with a single microelectrode which when used in conjunction with a bridge balanced amplifier can both record and pass current. The membrane can then be hyperpolarised or depolarised and the voltage response to putative transmitter action measured. This technique allows either the direct measurement of the reversal potential or its value to be extrapolated, if the membrane resistance and the conductance change caused by the transmitter are independent of membrane potential over a sufficient range. Thus if R and r are constants in the equation

$$e = [\ R/(r+R)\ ](\ Erev - Vm\ ) \qquad \text{Equ. 1.6}$$

the response (e) to the transmitter will vary linearly with the displacement of the membrane potential from the transmitter equilibrium potential (Erev) (and as already described, will be nullified if the membrane potential is equal to the reversal potential).

However for many cell types within the CNS membrane resistance does vary with membrane potential.

Membrane Time Constant

In addition to containing many channels the lipid bilayer of neuronal membranes separates the intra and extracellular fluid by an extremely thin insulating layer. The gap between the two conducting solutions forms a significant electrical capacitator. Hence the equivalent circuit of Fig. 1.2 should be redrawn to incorporate the capacitance of the membrane, Fig 1.3(a). If a current I is passed across the membrane with S open, then the membrane potential change will follow the equation

$$Vm = IR_m(1-e^{-t/\tau m}) \qquad \text{Equ. 1.7}$$

Fig. 1.2

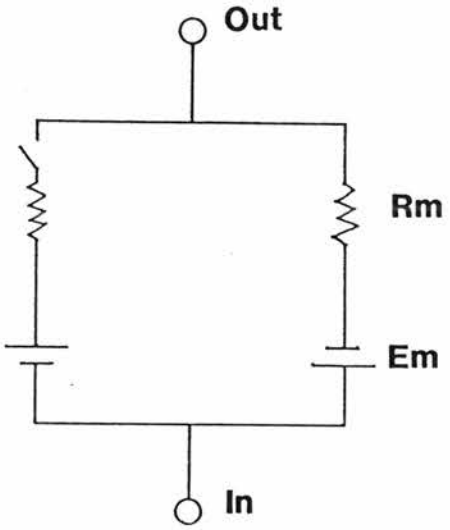

Fig. 1.3

a)

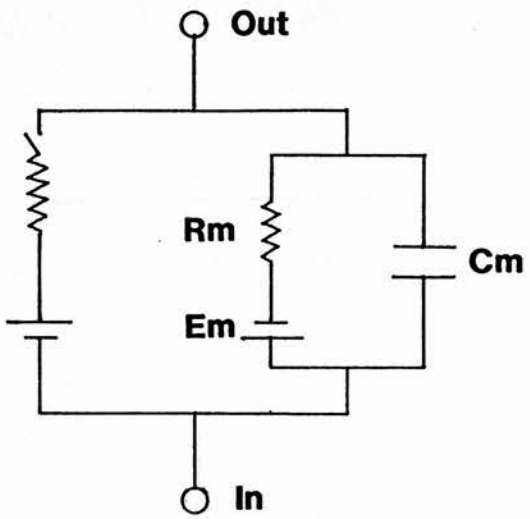

b)

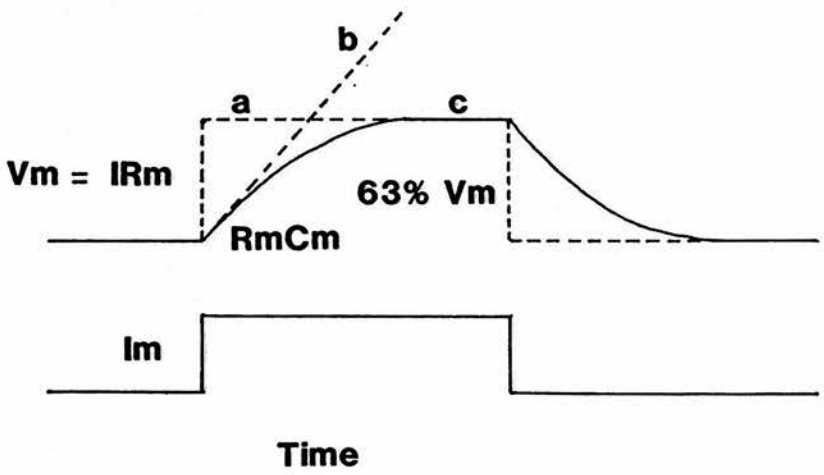

where the parameter τm = RmCm is the membrane time constant and is the time taken for the change in membrane potential to reach 63% of its maximum value.

The value of τm is of particular importance in the integration of synaptic inputs. Both excitatory and inhibitory postsynaptic potentials result from brief synaptic currents, as mentioned above, in response to neurotransmitter action. The rising phase of a post synaptic potential is dependent on both the active and passive properties of the membrane. The falling phase is however only on the discharge of the capacitor through the membrane resistance and consequently is a function of τm. Hence the greater the τm value of a neurone the greater the possibility of temporal summation and to a lesser degree spacial summation of synaptic inputs.

5-Hydroxytryptamine as a Neurotransmitter

Since the original paper by Dahlström and Fuxe (1968) reporting the presence of 5 hydroxytryptamine (5-HT) containing neurones in the central nervous system several studies have attempted to elucidate their possible function. Histochemical studies have revealed that 5-HT containing neurones can be divided into several distinct raphe nuclei, designated B1 - B9. Each of these nuclei have areas of specific efferent innervation. The medullary nuclei send projections mainly in the caudal direction (Bowker et al 1983, 1987). In some of these nuclei 5-HT has been shown to co-localise with the neuropeptides, substance P (Hökfelt et al 1978), enkephalin (Leger et al 1986) and/or somatostatin (Taber-Pierce et al 1985) and are believed to be involved in the regulation of nociceptive pathways within the spinal cord (Ogren et al 1985). Of the midbrain raphe nuclei the dorsal raphe nucleus (DRN), B7, has been shown to contain the largest cluster of 5-HT containing neurones. The efferent projections of the DRN have been mapped using 5,7 dihydroxytryptamine a selective 5-HT neurotoxin (Bjorklund 1973), combined with autoradiography (Tabier-Pierce et al 1976; Bobillier et al 1976) and immunohistochemistry (Steinbush 1981; Steindler et al 1983). It was found that the DRN innervates a multiplicity of areas within the mid and forebrain, particularly the thalamus, amygdala, cerebral cortex, hippocampus, septum and lateral habenula. Given these facts it is interesting to note that DR neurones appear to innervate frontal brain regions mainly in an ipsilateral

manner, although some contralateral innervation has been observed (van der Kooy & Hattori 1980a). This group also noted that the majority of raphe neurones projecting to the substantia nigra also projected to the caudate and putamen and were situated primarilly in the dorsal aspect of the nucleus. Additionally a large population of neurones projected solely to the caudate putamen and were situated in the ventral aspect of the nucleus (van der Kooy & Hattori 1979b). The DRN has also been shown to innervate more caudal structures including the locus coeruleus, and pontine and medullary reticular nuclei (Taber-Pierce et al 1976) and it has been suggested that these connections may regulate the reciprocal firing of raphe and reticular neurones during the sleep cycle. Raphe activity is seen to decrease dramatically during REM sleep (Adrian & Lanfumey 1986; Trulson 1985).

Early in vivo electrophysiological experiments on the dorsal raphe nucleus using extracellular unit recording showed single neurones to have a slow continuous firing rate of 0.5 - 3 Hz and a biphasic extracellular potential (a positive then negative wave form). This activity could be inhibited by systemic administration of the potent hallucinogen lysergic acid diethylamide (LSD) (Aghajanian et al 1968). The effects of LSD were assumed to be mediated via 5-HT due to the similarity of action of 5-HT and LSD in smooth muscle preparations (Gaddum 1953). To determine the role of tonic 5-HT release on DRN excitability, animals were pretreated with p - chlorophenylalanine (p-CPA). When given alone, the specific 5-HT synthesis inhibitor p-CPA (Koe & Weissman 1965) did not appreciably affect DRN firing rate (Aghajanian et al 1970). However monoamine oxidase inhibitors (MAOI's) such as pargyline caused a marked decrease in baseline firing rates suggesting the negative feedback was due to the extracellular accumulation of 5-HT or dopamine etc. . Pretreatment with p-CPA almost totally prevents the inhibitory effect of MAOI's in keeping with the suggestion that it is 5-HT release which plays an important role in DRN firing regulation. Pretreatment with p-CPA however had no effect on the reduction in baseline firing rate seen with systemic administration of LSD. Consequently it was suggested that LSD must act at a point secondary to 5-HT release. Pretreatment with the 5-HT precursor L-tryptophan also caused a reduction in baseline firing rates which could not be prevented by p-CPA pretreatment. In a parallel study it was shown that preloading with L-tryptophan, the 5-HT precursor, caused a marked increase in histochemical fluoresence of

presumed serotonergic neurones in the DRN. The increase in fluoresence however was resistant to pretreatment with p-CPA (Aghajanian & Asher 1971). These confusing effects were eventually reconciled by the hypothesis that p-CPA acts differentially causing a marked reduction in histofluorescence in forebrain terminals but not in the perykarya, possibly due to continued synthesis of new tryptophan hydroxylase in cell bodies (Aghajanian et al 1973). The role of LSD as a specific 5-HT uptake inhibitor was excluded when Sheard et al 1972 showed depletion of 5-HT stores with p-CPA to inhibit the reduction of baseline firing rate normally seen following treatment with tertiary amine 5-HT uptake blockers such as chlorimipramine, (see also Scuvée-Moreau & Dresse 1979), LSD however still produced a marked decrease in baseline firing rates.

Using direct microiontophoresis Bramwell & Goyne (1973) confirmed that 5-HT itself caused a reduction in baseline firing rate in DR neurones. However, the possibility of a negative feedback loop could not be excluded.

Any possible negative feedback loop may employ one or more of the afferent inputs to he DRN. Early histochemical fluoresence studies had shown the presence of a direct noradrenergic input to the DRN (Loizou 1969; Riozen & Jacobowitz 1976). A subsequent study using electron miroscopic autoradiography proved that this noradrenergic input terminated on serotonergic neurones and formed synaptic specialisations (Baraban & Aghajanian 1981). Using a retrograde tracing technique Aghajanian and Wang (1977) demonstrated that the dorsal raphe also recieves a dense innervation from the substantia nigra, medial preoptic nucleus and the lateral habenula. Electrical stimulation of the substantia nigra was shown to cause a frequency dependent suppression of raphe activity (Stern et al 1979a). In a parallel study Stern et al (1979b) demonstrated that single unit activity of DRN neurones was substantially depressed following stimulation of the lateral habenula. This supported the hypothesis that lateral habenula stimulation produced a greater inhibition in firing of proposed serotonergic neurones compared to non-serotonergic neurones in the DRN (Wang & Aghajanian 1977a). Electrical stimulation of the lateral habenula has also been shown to cause a reduction in [^{3}H] serotonin release within the substantia nigra and cuadate

nucleus. Inhibition of release within the substantia nigra was shown to be antagonised by local application of picrotoxin, a GABA antagonist, in the DRN (Reisine et al 1982).

Haigler & Aghajanian (1974) attempted to explore the feedback loop hypothesis by showing transection of the brain between the diencephalon and mesencephalon not to prevent the inhibition of firing caused by direct iontophoresis of 5-HT (see also Mosko & Jacobs 1977). Intravenous administration of LSD still caused a decrease in baseline firing rates. This technique however does not exclude the possibility that a feedback mechanism exists within the midbrain or brainstem.

Following pretreatment with RO4-4602, an aromatic amino acid decarboxylase inhibitor, shown to cause an increase in 5-hydroxytryptophan (5-HTP) within the perykarya and projection systems of serotonergic neurones (Carlsson & Lindqvist 1971) Gallagher & Aghajanian (1976) showed there to be a reduction in the inhibition of DRN firing caused by L-tryptophan treatment. Further RO4-4602 significantly reduced the amount of dorsal raphe 5-HT in the presence of L-tryptophan even though p-CPA is ineffective. Thus it was proposed that a local increase in 5-HT in the vicinity of the perykarya after tryptophan loading is sufficient to produce inhibition of raphe firing. Consistent with this hypothesis is the fact that microiontophoretic application of both LSD and 5-HT continued to cause a decrease in raphe firing rate after pretreatment with RO4-4602. Further support came from push-pull cannulae experiments showing that a steady state release of [^{3}H] 5-HT occured following local superfusion of [^{3}H] tryptophan in the DRN <u>in vivo</u>. A marked increase in the release was also observed following local DRN depolarisation with potassium chloride (Hery et al 1982).

Among the negative feedback loops available, the most direct route would be via 5-HT axon collaterals. In a report on the effects of DRN stimulation on amygdaliod activity it was noted that antidromic stimulation of DR neurones causes a period of post stimulus inhibition (Wang & Aghajanian 1977a). In a follow up study it was demonstrated that antidromic activation of dorsal raphe neurones produces a period of post stimulus inhibition even when the the major frontal afferent pathways are lesioned, including the habenula and preoptic hypothalamus (Wang & Aghajanian 1977b). The antidromic inhibition however is lost after the destruction of 5-HT pathways by 5,7 DHT but not by destruction of other pathways eg the noradrenergic pathways by

6 hydroxydopamine. Although γ-aminobutyric acid (GABA) can also inhibit DR neurones this effect is preferentially blocked by picrotoxin (Gallager & Aghajanian 1976) leaving the action of iontophoretic 5-HT application and antidromic stimulation unaltered (Wang & Aghajanian 1977b). Recently with improved immunocytochemical and ultrastructural techniques serotonergic dendro-dendritic contacts as well as 5-HT containing axon terminals have been observed in the cat DRN (Chazal & Ralstron 1987; Harandi et al 1987). These findings raise several possibilities a) direct local actions occur between serotonergic neurones (Wang & Aghajanian 1982), b) the existence of recurrent collaterals (Mosko et al 1977), and c) the possibility of regulation by serotonergic contacts from other raphe nuclei. However, the recent introduction of brain slice preparations (Mosko & Jacobs 1976) raised a fourth possibility, d) that the post-spike inhibitory period is part of the inherent oscillatory activity of DR neurones (Mosko & Jacobs 1977, Trulson et al 1982).

The in vitro Slice Preperation

Despite the fact that the original paper demonstrating that brain slices could be maintained in vitro was first published in 1957 (Li & McIllwain) it was a number of years before the technique was routinely applied to electrophysiological studies. Even then early studies concentrated on extracellular recordings of synaptically driven population spikes (Anderson et al 1971) and the regulation of spike size and frequency with drug treatment. The popularity of the technique increased dramatically with the demonstration that high quality, long lasting, intracellular recordings could be obtained (Yamamoto 1972, Swartzkroin 1975) from neurones within the slice. This technique allowed the full experimental advantages of the slice preparation to be exploited.

Not only does the slice preparation have features in common with the whole brain in situ, it also has features in common with cell culture preparations. As with tissue culture preparations the blood brain barrier is absent and hence neurones within the slice can be treated with any compound that freely diffuses through the extracellular space. This feature made it possible to study the effects of changes of extracellular ionic composition on neuronal function and allowed defined drug concentration to be applied to the

cell. Positioning of recording and stimulating electrodes under direct microscopical control into defined areas of the preparation is also possible, overcoming the problems inherent in stereotaxic techniques. Electrode possitioning is also aided by the fact that the slice maintains the original morphological integrity of the whole brain in situ. Hence particular fiber tracts, ventricles and in some instances individual neuclei can be used to orientate the positioning of the microelectrode. Consequently in the DRN slice preparation the electrode could be positioned with resonable confidence in the largest cluster of serotonergic neurones within the DRN (see methods) by placing the electrode in the isthmus of the periaqueductal grey formed by the median longitudinal fasiculus. The retention of morphological integrity also ensures that the neurones are buffered from drug action by the surrounding tissue in a manner similar to that of any drug that may cross the blood brain barrier in vivo. In laminated structures such as the hippocampus preservation of anatomical integrity allows transmitter or drug sensitivity to be mapped over the surface of the neurone by local iontophoresis. In such a way the high dendritic sensitivity to both glutamate (Dudar 1974) and baclofen (Inoue 1985) has been demonstrated in hippocampal pyramidal cells.

The ability to record intracellularly for long durations has enabled the characterisation of postsynaptic responses to a number of neurotransmitters. In the DRN for example a noradrenergic excitatory input and an inhibitory serotonergic input have been demonstrated (Yoshimura & Higashi 1985a,b). The technique has also allowed characterisation of particular neuronal types on the basis of biophysical properties within a given nuclei. More recently experiments have been performed where the microelectrode has been used not only to inject current but also to inject channel blockers or putative second messengers into neurones (Freedman & Aghajanian 1987).

This thesis is concerned with the biophysical and pharmacological responses of proposed serotonergic neurones recorded intracellularly in the DR slice preparation. Chapter 2 will describe the methods employed for the visualization, recording, data aquisition and handling of DR neurones. In Chapter 3 the inherent passive and active membrane properties of DR nerones will be shown and discussed with respect to the known firing pattern of these neurones. The pharmacological profile of DR neurones will be shown in Chapter 4. In particular the neuronal responses to exogenously applied 5-HT agonists

/ antagonists are shown and the underlying ionic conductance mechanisms mediating autoreceptor activation are discussed with respect to 5-HT receptor subtypes shown by ligand binding studies. Finally in Chapter 5 the biophysical and pharmacological characteristics of DR neurones will be discussed with reference to the known characteristics of hippocampal CA_1 and facial motoneurones, two areas which show distinct but differing responses to 5-HT application.

CHAPTER 2

METHODS

The dorsal raphe nucleus lying in the middle of the lower midbrain, is of great interest to those working with systems mediated by 5-HT. In 1965, Dahlstrom & Fuxe demonstrated in one of the earliest fluorescence histochemical studies that this nucleus constitutes the largest serotonergic nuclei in the brain and that neurones in this nucleus project to many areas in the central nervous system. This observation has been repeatedly confirmed using a variety of newer and more sophisticated techniques (Aghajanian 1976; Jahnsen 1980; Steinbush 1981).

Subsequent biophysical and pharmacological characterisation of this neuronal cluster has lead to a greater understanding of its role in CNS. Experimental investigation into the biophysical properties of neurones necessitate the use of intracellular recording electrodes. Problems with impalment stability in in vivo preparations (Aghajanian & Vandermaelen 1982) initially limited experimenters to looking at pharmacological alterations of extracellular unit activity (Aghajanian et al 1970; Bramwell & Goyne 1973; Mosko & Jacobs 1977).

With the introduction of the in vitro slice preparation (Li & McIlwain 1957) came the prospect of recording from specific brain regions using extracellular and intracellular electrodes. Although certain brain regions, such as the hippocampus, were found to be readily amenable to electrophysiological studies in the in vitro slice (Johnston & Hablitz 1979) it was not until 1983 that stable intracellular recordings were first obtained from dorsal raphe neurones in the in vitro slice preparation (Crunelli et al 1983). The in vitro dorsal raphe slice preparation subsequently became a powerful tool for studying the biophysical and pharmacological properties of the individual neurones of this major serotonergic nucleus.

Preparation of the Dorsal Raphe Slice

Male Sprague-Dawley Cobb rats (200-250g) were decapitated and the brain quickly removed. The cortex was reflected and two coronal cuts were made : one at the rostral end of the thalamus, the other at the rostral end of the cerebellum. Two parasagital cuts, each 3-4mm from the midline, were then made. The resulting block of tissue was then transferred to the chuck of a vibratome slicer (Campden Instruments) using a strip of Whatman filter paper. The tissue block was fixed to the chuck with cyanoacrylate glue with the distal cut

surface uppermost. Movement of the tissue block during cutting was limited by positioning a 4% agar block against the ventral surface of the tissue block. The chuck was then transferred to the bath of the vibratome containing oxygenated (95% O_2, 5% CO_2) artificial cerebrospinal fluid (ACSF) at 4°C, consisting of (in nM) : NaCl 134, KCl 6.25, HEPES 1.25, $MgSO_4$ 2, CaCl2 2, $NaHCO_3$ 16 and glucose 10. Under microscopical control 400μm transverse sections were obtained, cutting dorso-ventrally. Only sections in which the cerebral aqueduct (Aq) retained its integrity and the medial longitudinal fasiculus (mlf) could be observed (Fig. 2.1) were selected.

Slices were transferred to the recording chamber using a fine spatula. The slices were supported on a fine Nylon mesh and superfused from beneath with ACSF at 37°C flowing at approximately 1ml per minute. The entire procedure from decapitation to placement of the slice in the recording chamber, took from 5 to 12 minutes. Following an equilibration period of 1hr recording began.

The recording chamber was an adaptation of the Haas bath (Haas et al 1974), (Fig. 2.2). Briefly it consists of a thermostatically controlled heated water bath above which is situated the incubation chamber. Artificial CSF is gravity fed through the water bath and into the well of the incubation chamber. The overflow of the well is channelled through the Nylon netting, on which the slice rests, to a tissue paper wick which syphons the ACSF into a collecting funnel. The slices rest at the interface between the ACSF and warmed humidified gas (95% O_2, 5% CO_2) which is gently bubbled through the heated water bath and enters the incubation well containing the brain slice via a port situated above the well. Flow rate is regulated by an adjustable membrane flow regulator positioned between the ACSF reservoir and the input port of the recording chamber.

Drug administration

Routinely drugs from frozen stock solutions were dissolved in oxygenated ACSF to the required concentration immediately before the start of the administration. The diluted drug was then superfused over the slice by switching a stopcock from control ACSF to buffer containing the drug. All the drugs superfused at μM concentrations were administered as above, stock solutions at the appropriate mM concentrations were usually prepared with double distilled deionised

water. The exceptions were noradrenaline prepared in a pH 4 stock solution containing 100μM ascorbic acid, to avoid oxidation, and spiperone (free base) prepared as a mM stock solution in 0.5% acetic acid. During administration of 4-aminopyridine (4AP) and tetraethylammonium (TEA) the mM concentration of NaCl was reduced by an equal molar quantity. In low Ca^{2+}/ high Mg^{2+} containing medium, the Ca^{2+} concentration was lowered to 0.2mM and the Mg^{2+} concentration raised to 4mM. Addition of Co^{2+} required no change of the ACSF constituents because HEPES rather than phosphate was used as the pH buffer in control ACSF.

Identification of Serotonergic Neurones within the Dorsal Raphe Nucleus.

In order to maximise the possibility of recording from serotonergic neurones it was important to determine the area of the dorsal raphe with the highest concentration of serotonergic neurones. The localisation was achieved using an immunohistochemical technique.

Whole brains were fixed by in vivo perfusion with a 4% paraformaldehyde, 0.5% gluteraldehyde solution in 150 - 200gm rats anaesthetised with 25mg / kg pentobarbitol. The brain was then removed and placed in a 20% sucrose solution in 0.2M phosphate buffered saline (PBS) for at least 10 hours. A block of tissue containing the DRN was prepared as outlined above. The block of tissue was mounted onto the chuck of an open top cryostat (Bright's) with OTC compound (Tissue Tech.) and frozen to -25°C. Transverse 50μm sections were cut in the region believed to contain the dorsal raphe. Sections were washed in cold PBS and then incubated in a humid atmosphere with rabbit anti-5HT antibody (1:500 dilution) (R.I.A U.K) for 24 hours at 4°C. Following incubation with the primary antibody the sections were washed again in cold PBS and then incubated for 1 hour with sheep anti-rabbit IgG (R.I.A U.K) at room temperature (1:100 dilution). After washing, sections were incubated with a rabbit peroxidase anti peroxidase complex (1:100 dilution) (Capel Laboratories) for 1 hour at room temperature. To visualise the labelled cells the slices were preincubated with diaminobenzidine to reduce any background staining from endogenous peroxidase activity, followed by an incubation with a

diaminobenzidine - H_2O_2 chromogen until the required intensity of stain was achieved. The reaction product causes the serotonergic neurones to stain dark brown with the chromogen.

The neurones showing 5-HT-like immunoreactivity appear to be located in four distinct areas within the DRN. The largest cluster of neurones is situated ventromedially within the isthmus of the DRN formed by the myelinated regions of the medial longitudinal fasiculus. Two smaller lateral clusters can be distinctly seen one either side of the midline; the smallest cluster being located on the midline in the most dorsal aspect of the nucleus. Because of the constantsy of its location most recordings were taken from the ventromedial cluster.

Intracellular Recording Techniques

Intracellular electrodes were made from glass capillary tubing (Kwick fil , GC 120F-10, Clark Electromedical Instruments) on a horizontal puller (Narishige PN-3). In initial current clamp experiments the electrodes were filled with 1M potassium acetate and had resistances between 80-120MΩ. Subsequent experiments were performed with electrodes filled with 3M potassium chloride and resistances between 50-80MΩ. Experiments employing voltage clamp techniques required 3M potassium chloride filled electrodes with resistances between 30-50MΩ. The tip of the electrode was positioned on the surface of the slice in the area of the medial dorsal raphe nucleus under microscopic control (Wilde M5 stereomicroscope). The electrode was then driven through the slice in 2μm steps, using a "Dick Vet" microdrive for 300μm or until a cell was penetrated. Potentials were recorded with respect to a silver/silver chloride pellet placed against the tissue paper wick of the outflow of the recording chamber. Recordings were obtained using a high input impedance DC preamplifier (Axoclamp 2A, Axon Instruments Inc.) with an active bridge facility to enable current injection through the recording microelectrode. Pulses of hyperpolarising current, 100 msec long, were injected into the neurone via the recording electrode at 1 Hz. This allowed changes in membrane resistance to be measured throughout the course of the experiments. The hyperpolarising pulses also give a useful indication of electrode resistance before a cell is penetrated, thus the resistance of the microelectrode at this stage was calculated as :-

$$Re = Ve/Io \qquad \text{Equ. 2.1}$$

Where, Re = electrode resistance

Ve = voltage drop recorded across the electrode

Io = amplitude of the test current pulse

Proximity to a cell was indicated by an apparent increase in the input resistance of the microelectrode. By over compensating the capacitance neutralisation of the the headstage of the preamplifier causing it to oscillate, the electrode was "buzzed" into the cell. Recordings were selectively obtained from cells that showed a resting membrane potential more hyperpolarised than -55mV on the Axoclamp 2A voltage monitor. The absolute resting membrane potential of the cell was measured as the change in potential seen at the end of each experiment on the withdrawl of the microelectrode from the cell. If a residual resistance was observed on withdrawl the cell this resistance was subtracted from the calculated cell resistance for each current step employed.

Intracellular current clamp recording

All current clamp experiments were performed in the bridge balance mode of the axoclamp. In bridge balance mode the microelectrode voltages are monitored continuously and continuous currents can be injected down the microelectrode from a constant current source. Associated with the current flow (Io) down the microelectrode is a voltage drop (Ve) across the microelectrode which is dependent on the microelectrode resistance (Re). In order to record the true membrane potential during times of current injection this voltage drop has to be minimised by bridge balancing. Once inside the cell, and throughout the duration of the experiment, the bridge was balanced by minimising the time independent component of the voltage response evoked by hyperpolarising current pulses. Capacitative currents from both the microelectrode and the cell membrane were reduced to a minimum by negative capacity compensation. In order to set the negative capacitance the Axoclamp was set to discontinuous current clamp and the microelectrode used cyclically to pass current and record voltage, with a 30% duty cycle. The voltage source (Vc) Fig. 2.5 in series with the resistors Ro (100MΩ for the 0.1x headstage used in all experiments) and Re acted as a current source when switch

S1 was closed. Under steady state conditions the voltage (Vo) seen at the amplifier A1 output was the sum of Ve and the membrane potential Vm. In order to sample the true membrane voltage Ve must be eliminated from the voltage records. When switch S1 opened (T open) after 30% of the cycle period current flow stopped and Ve decayed to Vm. Closure of the switch S2 allowed the new membrane potential to be sampled at A2, this was held until another sample of Vm was obtained. Hence the membrane potential could be recorded independently of the voltage drop across the microelectrode. Because the rise time of the voltage drop across the microelectrode was dependent on the capacitance of both the amplifier and the elecrode this could be offset by negative capacitance compensation. During this process current was injected into the headstage to compensate for the current required to charge the capacitors. Over compensation would be seen as an overshoot in the voltage response across the electrode, under compensation as a failure to return to 0 volts before the sample cycle repeated. Once the optimum compensation has been achieved the axoclamp is returned to bridge balance mode. The input resistance of the cell Rm was regarded as the size of the steady state voltage deflection recorded in response to a given hyperpolarising current pulse, provided the bridge is adequately balanced.

$$\text{Thus } Rm = Vm / Io \qquad \text{Equ. 2.2}$$

If during putative transmitter application a change in resting membrane potential was observed, constant DC current of the required polarity was injected into the cell in order to manually voltage clamp the cell to the pre drug membrane potential. This reduced complications in interpretation that may have resulted from voltage dependent changes of the DRN membrane and allowing the absolute effect of the drug on the membrane condutance to be determined.

The time constant for membrane charging (τm) was determined by the time taken for voltage deflections to reach 63% of the final steady state value. Small hyperpolarising rectangular current pulses were used to determine τm to avoid substantial alterations of the charging curve by voltage activated channel activity. A computer generated semilogarithmic plot of log(1-V/Vmax) against time was used to determine τ and test the exponential nature of the charging curve.

The capacitance of the membrane can be calculated from ;

$$Cm = \tau m / Rm \qquad \text{Equ. 2.3}$$

If it is assumed that the neuronal membrane has a capacitance of $1\mu F / cm^2$ and that the neurone is roughly spherical then the approximate radius of the neurone can be calculated from the following equation ;

$$r^2 = \frac{Cm \times 10^5}{4\pi} \qquad \text{Equ. 2.4}$$

where r is in μm and Cm in nF.

Intracellular voltage clamp recording

Most single electrode voltage clamp recording systems are based on an original system outlined by Wilson & Goldner (1975). A variation is implemented in the Axoclamp 2A, Fig. (2.6) (Finkel & Redman 1984) A1 is a high input impedance high speed amplifier to which the impaling microelectrode ME1 was connected via an Ag/AgCl half cell (Clark Electromedical Insts.). A1 measures the voltage potential (Ve + Vm) with reference to the bath ground (B). Vm is the voltage deviation from the resting potental and Ve is the voltage developed on the miroelectrode resistance and capacitance (Re and Ce respectively) by the current Io. Just prior to the timing cycle, T, the membrane potental was sampled (sample 1) by the sample and hold device SH1. At this point Ve had nearly returned to zero, SH1 holds the sampled value (Vms) for the remainder of the cycle. Vms was compared to the voltage step command (Vc) at the differential amplifier A2.The output of A2 was the error voltage (e) at the end of the previous cycle ie Vc - Vms. During the current passing phase, TI, the output of A2, e, was connected via switch S1 to the input of a controlled current source (CCS). Consequently the current generated by the CCS, Io, was injected into the microelectrode due to the high input impedance of A1 ($10^{12}M\Omega$). The current passed was directly proportional to the input voltage e of the CCS. The gain of the system was controlled by adjusting the sensitivity (GT) of the CCS. The square current pulse produced during TI caused Ve to rise at a rate determined mainly by the capacitance of the microlectrode to the surrounding tissue, and the capacitance of the buffer amplifier A1. At a mean sampling

frequency (fs) of 6.1 KHz the current pulse had a mean duration of 0.05 ms (n = 36) which was at least two orders of magnitude shorter than the membrane time constant, τm = 30.87 ms (n = 38), see chapter 3. Hence the current pulse caused only a small linear change in Vm.

At the end of TI, switch S1 changed to the voltage recording (TV) position. In this position the input voltage into the CCS was 0 volts (Vo) hence the output was zero and the microelectrode passively recorded the voltage Ve + Vm. Before the new voltage sample was taken (sample 2) sufficient time was allowed for Ve to decay within a fraction of a millivolt of Vm. The decay of Ve was monitored on a slave scope (HSO) and fs adjusted to allow full decay of Ve, 3.5 - 9 KHz. Sample 2 was then taken and the cycle repeated. Consequently SH1 updated the measurement of Vms at a rate equal to fs and hence Vms changed in small increments. The increments were averaged Vms(ave) before being recorded and viewed on an oscilloscope.

Any change that occured during TV was not noted until the following sample period and could only be corrected for when S1 switched to the current passing position. This caused a delay in the response to membrane potential changes that was dependent on fs. Thus the sample frequency of the system should be faster than the changes of membrane potential to be controlled. Action potentials could not be clamped by this system, an atttempt however was made to clamp the fast transient hyperpolarising potentials seen in DR neurones (see chapter 3). Although the sample frequency was sufficiently high ($\approx$ 6 KHz) to allow adequate sampling of the hyperpolarising potential the voltage clamp did not achieve steady state voltage command (Vc) during the peak of the potential (chapter 3 Fig. 3.19). This was probably due to an inability to reach critical damping, where;

$$\frac{GT\ D\ T}{Cm} = 1 \qquad \text{Equ. 2.5}$$

and GT = controlled current source gain
D = 30% duty cycle
T = cycle duration
Cm = membrane capacitance
derived by Watson & Goldman (1975 Equ. 28).

Equation 2.5 can be rewritten as;

$$GTDT = Cm \qquad \text{Equ. 2.6}$$

The capacitance of the cell Cm could be calculated from the equation ;

$$\tau m = Rm \times Cm \qquad \text{Equ. 2.7}$$

Both τm, the membrane time constant, and Rm the membrane resistance could be calculated from current clamp data and an estimate for Cm found ($\approx$ 0.142 pF). When D = 0.3 and T, calculated from fs, was 160 μs then a value for GT could be calculated for critical damping in nA/mV. Hence ;

$$DGT = \frac{\text{voltage (mV) x capacitance (pF)}}{\text{time } (\mu s)} \qquad \text{Equ. 2.8}$$

Critical damping would therefore have occured at 0.8 nA/mV gain at the controlled current source where fs was 6.1 KHz. During voltage clamp experiments the maximum gain achieved was 0.1 nA/mV. This caused overdamping of the clamp hence further delaying the time at which Vm reaches the step command Vc. Increasing the gain above 0.1 nA/mV caused instability wihtin the clamp and subsequent oscillation. From Equ. 2.6 it can be seen that decreasing T by increasing fs allows G^T to be increased. It was found that decreasing T caused an excessive increase in the noise on the output records.Phase lag or lead could have been used to reduce the noise and increase the gain of A2 however this was avoided for fear of introducing a 'false clamp'. Hence even though a seemingly fast step response can be recorded on Vms, the step response in the cell Vm is much slower.

The current passed by the CCS in response to the voltage step command was continuously monitored and gave a direct indication of the ionic flow across the membrane in response to the step command. Consequently it was thought better to allow the clamp to deviate slightly from Vc, in response to fast transient potentials, to ensure that voltage - current relationhips could be reliably constructed.

Passive voltage - currrent relationships were constructed from current responses obtained with graded hyperpolarising step commands from the resting potential. To determine the voltage dependent nature of membrane conductance, membrane potentials were clamped at pre

determined potentials by direct injection of contant DC current. Graded hyperpolarising voltage step commands were then evoked and the current response measured. As mentioned above action potentials could not be clamped by this voltage clamp system However, most experiments were conducted in the presence of 1μM tetrodotoxin (TTX) to block synaptic transmission and in addition blocked the fast sodium component of the action potential.

Two voltage clamp protocols were employed in studying active current. Firstly graded depolarising voltage step commands were evoked from the resting membrane potential and the currents evoked recorded. Secondly, in order to study the voltage dependency of active currents evoked, a dual pulse protocol was adopted. This protocol allowed two parameters to be studied a) the effects of increasing graded hyperpolarising prepulse step commands on active currents evoked in response to a fixed depolarising step potential and b) the effects of a fixed hyperpolarising prepulse step command on currents evoked in response to increasing graded depolarising step potentials.

In all voltage clamp experiments a downward deflection from the resting level of the current trace was indicative of an inward flow of current. Conversly an upward current deflection was indicative of an outward flow of current from the cell.

Ideally membrane current should be recorded from an area of uniform potential, so that the current comes from a population of channels that were all experiencing the same voltage. Single electrode voltage clamp however is utilised for experimental procedures where direct visualisation of individual neurones is impossible ie the slice preparation or in preparations where the size of the cell soma makes it impracticable to utilise a two electrode voltage clamp system. It does however have intrinsic limitations, primarily that the speed with which a current can be clamped is determined by the switching frequency chosen for the experiment. Hence fast currents may not be accurately clamped.

Monitoring and storage of data

All parameters measured during both current and voltage clamp protocols, membrane potential, injected current, cellular voltage responses, voltage step commands and evoked step currents were continuously monitored on a Gould 1425 digital oscilloscope and stored

on a four channel FM tape recorder (Racal Store 4D). Electrode charging and discharging during discontinuous current clamp (DCC) and single electrode voltage clamp (SEVC) was monitored on a slave scope (Telequipment D63). The data was then transferred from the FM tape recorder onto a Winchester disk (Data Systems DSD 880 x 30) of a PDP 11/73 (Digital) computer via a general purpose , analogue - digital, laboratory interface (Cambridge Electronic Design model 502). Data could be stored at sampling rates as high as 20KHz. Stored data could then be reviewed using a real time FORTRAN package (DA6.FOR) operating within the RT11 version (4) operating system (Digital) and displayed as on a digital oscilloscope either as individual sweeps or as averaged data from a number of sweeps. Several "in house" tailored subroutines have been written to allow rapid data analysis, editing, printing and plotting. Averaged data, current - voltage relationships and exponential plots were routinely printed on a Colorwriter 6320 (Gould) and could be down loaded onto 9" floppy discs for storage.

Inactivation / activation curve construction

For both inactivation and activation curve construction calculations the original data analysis was performed on the PDP11/73. Current and voltage pairs were then entered into a function fitting program via a DCS 286 desk top IBM clone interfacing with the Edinburgh University mainframe computer and the EMAS-A operating system. The interface was achieved via KERMIT23.

Function fitting was performed utilising the SIMPLEX METHOD of Nelder and Mead as imlemented by NAG (Numerical Algorhythms Group) in subroutine E04CCF. Estimates for Vhalf, k and Imax for inactivation were made by fitting:

$$I = \frac{Imax}{1 + \exp((Vstep - Vhalf)/k)} \qquad \text{Equ. 2.9}$$

When Vstep = Vhalf

I = Imax / 2, ie half maximum estimated current

For activation values of Vhalf,k and gmax were estimated by fitting the following function :-

$$g = \frac{gmax}{1 + \exp((Vhalf - Vstep) / k)} \qquad \text{Equ. 2.10}$$

Values for gobs, the potassium conductance, were estimated from observed currents Iobs by

$$g\ obs = \frac{Iobs}{Vstep - E_k} \qquad \text{Equ. 2.11}$$

where E_k was calculated as -83mV from the Nernst equation.

SUBSTANCE	SOURCE	CONCENTRATION
γ-Aminobutyric acid (GABA)	SIGMA	10mM
4-Aminopyridine (4-AP)	SIGMA	5mM
Apamin	SIGMA	50, 100nM
Baclofen	CIBA	15, 50, 60μM
Buspirone	BRISTOL MYERS	10μM
Cobalt	SIGMA	500μM
Cadmium	SIGMA	1mM
Dipropyl-5-carboxy-amidotryptamine (DP-5-CT)	SANDOZ	10μM
Hepes	SIGMA	1.25mM
5-hydroxytryptamine (5-HT)	SIGMA	50, 100μM
8-hydroxy-2-(di-n-propylamino)-tetralin (8OH-DPAT)	Research Biochemicals Inc.	10, 100μM
Methysergide	SANDOZ	100μM
Noradrenaline (NA)	SIGMA	50μM
Spiperone	JANSEN	10μM
Syntex S2	SYNTEX	100nM, 1μM
Tetraethylammonium (TEA)	SIGMA	10mM
Tetrodotoxin (TTX)	SIGMA	1μM

Fig. 2.1 Diagram of the DR Slice

A schematic diagram of the mesencephalic area routinely taken for the DR slice preparation.

Aq = Cerebral aqueduct.

CG = Central grey.

CGD = Central grey dorsalis.

CGM = Central grey medialis.

DpWh = Deep white layer superior coliculus.

DR = Dorsal raphe.

InG = Intermediate grey layer superior coliculus.

Me5 = Mesencephalic trigeminal nerve nucleus.

mlf = Median longitudinal fasiculus.

MnR = Median raphe nucleus.

rs = Rubrospinal tract.

xscp = Decussation superior cerebellar peduncle.

Intraural 1.2 mm ; Bregma -7.8 mm.

Modified from Paxinos and Watson 1982

Fig. 2.1

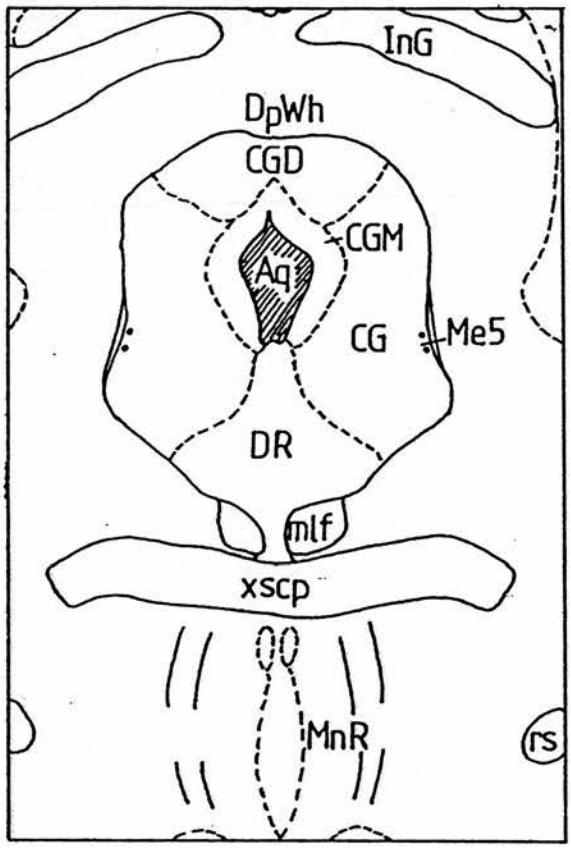

Fig. 2.2 The Recording Chamber (modified from Haas et al 1974)

The tissue preparation (TS) was placed on the nylon netting (J) and perfused by oxygenated ACSF. The ACSF was introduced at port (A), warmed as it passed through the water bath, and entered the incubation well at (B). The water bath was heated with a thermopad (G) (Minco, Cavel Components Ltd U.S.A) the temperature of which was thermostatically regulated with reference to a probe (H). The ACSF flowed through the netting and was syphoned into a collecting funnel (F) by a tissue paper wick.

An O2/CO2 (95:5%) mixture was bubbled from a sintered glass tube (C) through warmed, distilled water and entered the incubation chamber via port (D). On entering the chamber the warmed, humidified gas was deflected across the preparation by a baffle (K). A hole in the baffle allowed access to the slice with microelectrodes. Dotted lines represent fluid levels.

Fig. 2.2

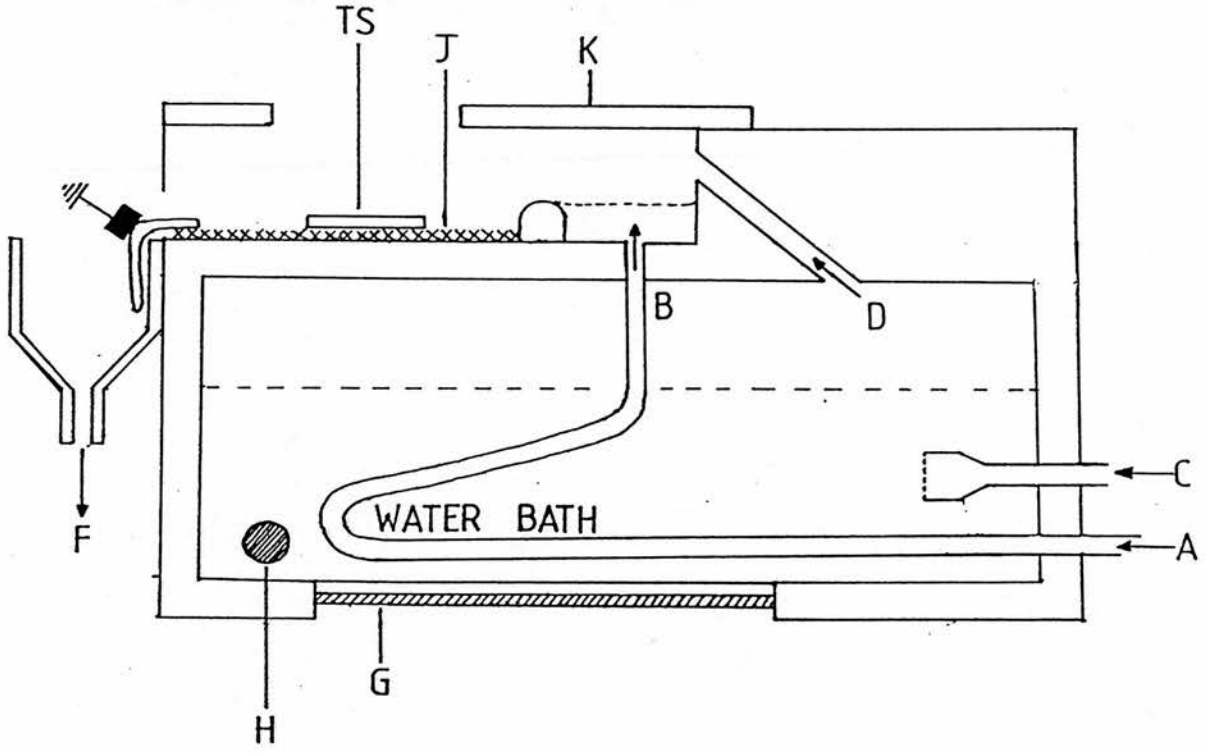

Fig. 2.3 The distribution of serotonergic neurones in the in vitro slice of the midbrain.

Serotonergic neurones within the dorsal raphe nucleus are grouped into four distinct clusters. Two lateral clusters (LC), a small dorso - medial cluster (DMC) situated close to the midline of the central aqueduct (Aqu), and the largest group the ventro - medial cluster (VMC) forming the isthmus of the nucleus. The nucleus lies in the median ventral section of the periaqueductal grey (PAG).

Fig. 2.3

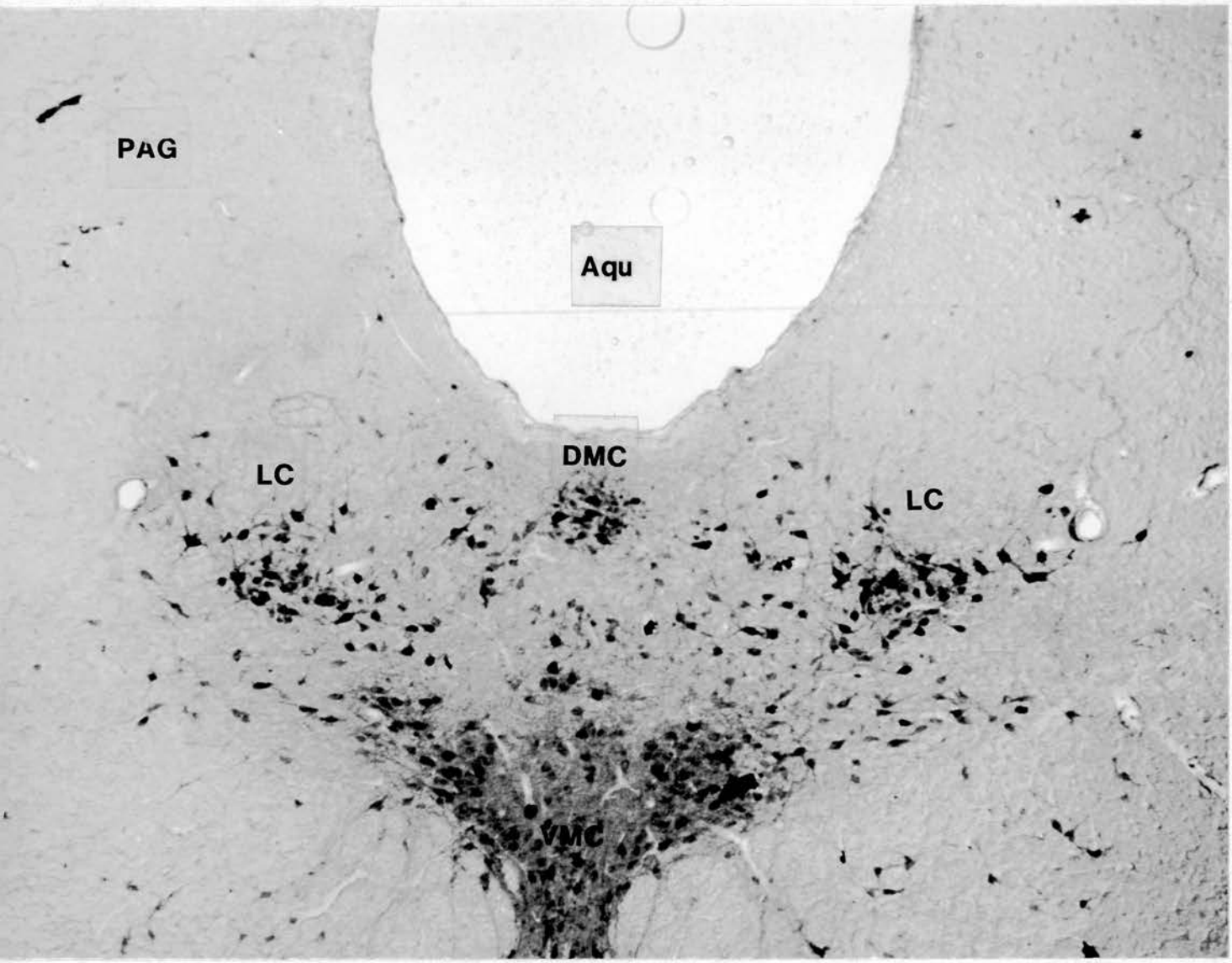

Fig. 2.4 Electrical recording apparatus

Electrotonic potentials were recorded through glass microelectrodes with respect to a silver/silver chloride reference ground attached to the outflow of the recording chamber. Signals were amplified using an Axoclamp 2A preamplifier via a 0.1 current gain headstage. Hyperpolarising and depolarising current pulses applied to the cell were generated via a step command generator activated within the preamplifier by a TTL pulse from a Digitimer D4030. In voltage clamp (v/c) mode the step generator determined the size of the voltage clamp step potential. During dual pulse voltage clamp protocol the hyperpolarising prepulse step command was generated by the v/c stimulator (Omnical 2000, W-P Instruments Inc.) connected to the external v/c command input of the preamplifier. The Digitimer regulated the timing and duration of all current and voltage steps. A calibration pulse (1nA, 10mV) applied at the start of each experiment was generated by an isolated stimulater (Digitimer model DS2). The decay of the electrode discharging was continuously monitored on a slave scope (Telequipment D63) in both discontinuous current clamp (DCC) and single electrode voltage clamp (SEVC). Current and voltage responses were amplified by a 1 - 20 variable gain second stage amplifier before being recorded on an FM tape recorder (Racal Store 4D). Wave forms were monitored from tape on an oscilloscope (Gould) recorder to ensure that no attenuation of the responses occurred during recording. A Schmitt trigger was interposed between the Digitimer and the tape recorder to ensure that the trigger pulse was of sufficient magnitude to drive the PDP11/73 in later data analysis.

Fig.2.4

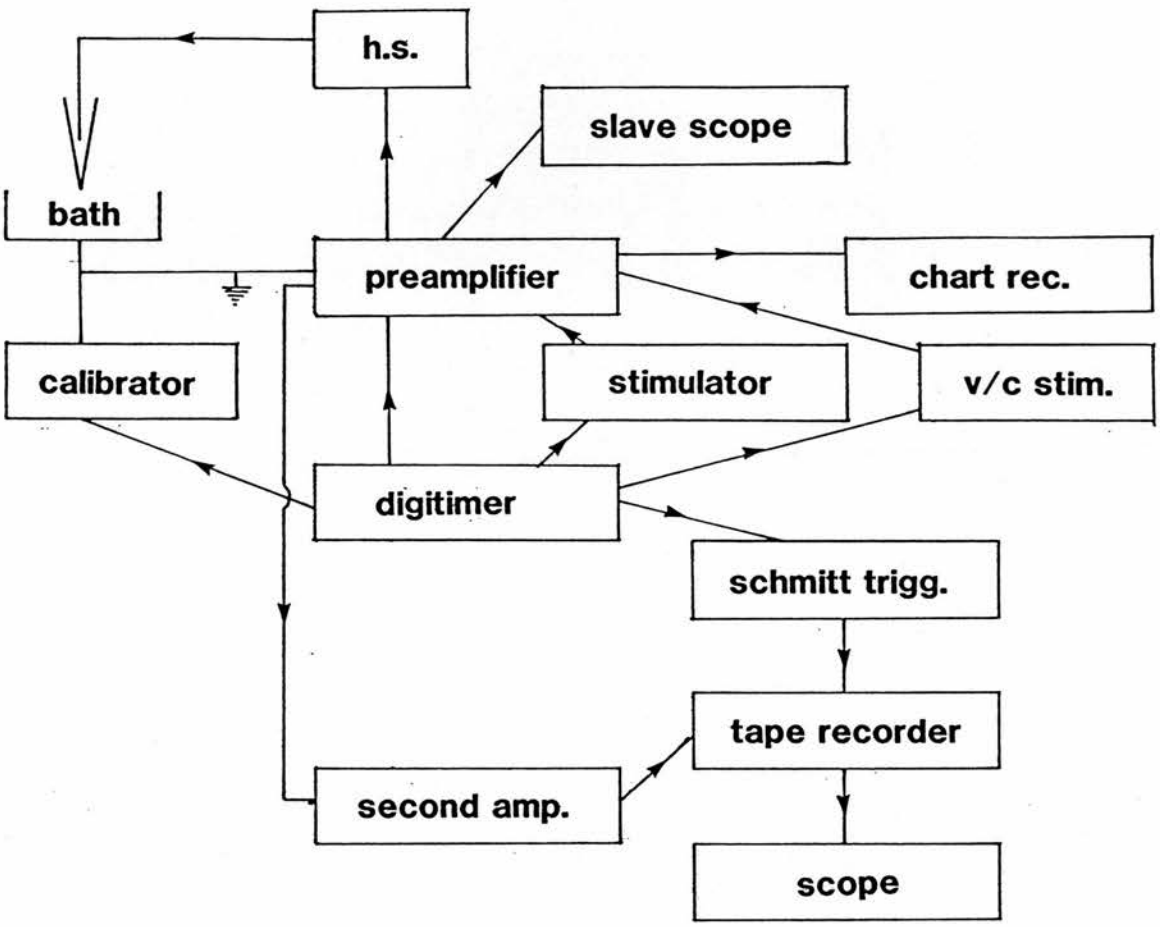
h.s.
slave scope
bath
preamplifier
chart rec.
calibrator
stimulator
v/c stim.
digitimer
schmitt trigg.
tape recorder
second amp.
scope

Fig. 2.5 Circuit diagram for the Axoclamp in discontinuous current clamp mode.

Current Io was injected for 30% of the cycle time. Because of the high input impedance of the preamplifier A1 the current was injected into the cell. During the voltage sampling phase switch S1 changes to the zero volts position, this allowed the voltage drop across the electrode to decay to zero as measured by the differential amplifier A3. Hence when the sample and hold device, switch S2, capacitator and amplifier A2, measured the membrane potential this value was independent of the voltage drop across the microelectrode.

Fig. 2.5

AXOCLAMP CURRENT CLAMP CIRCUIT

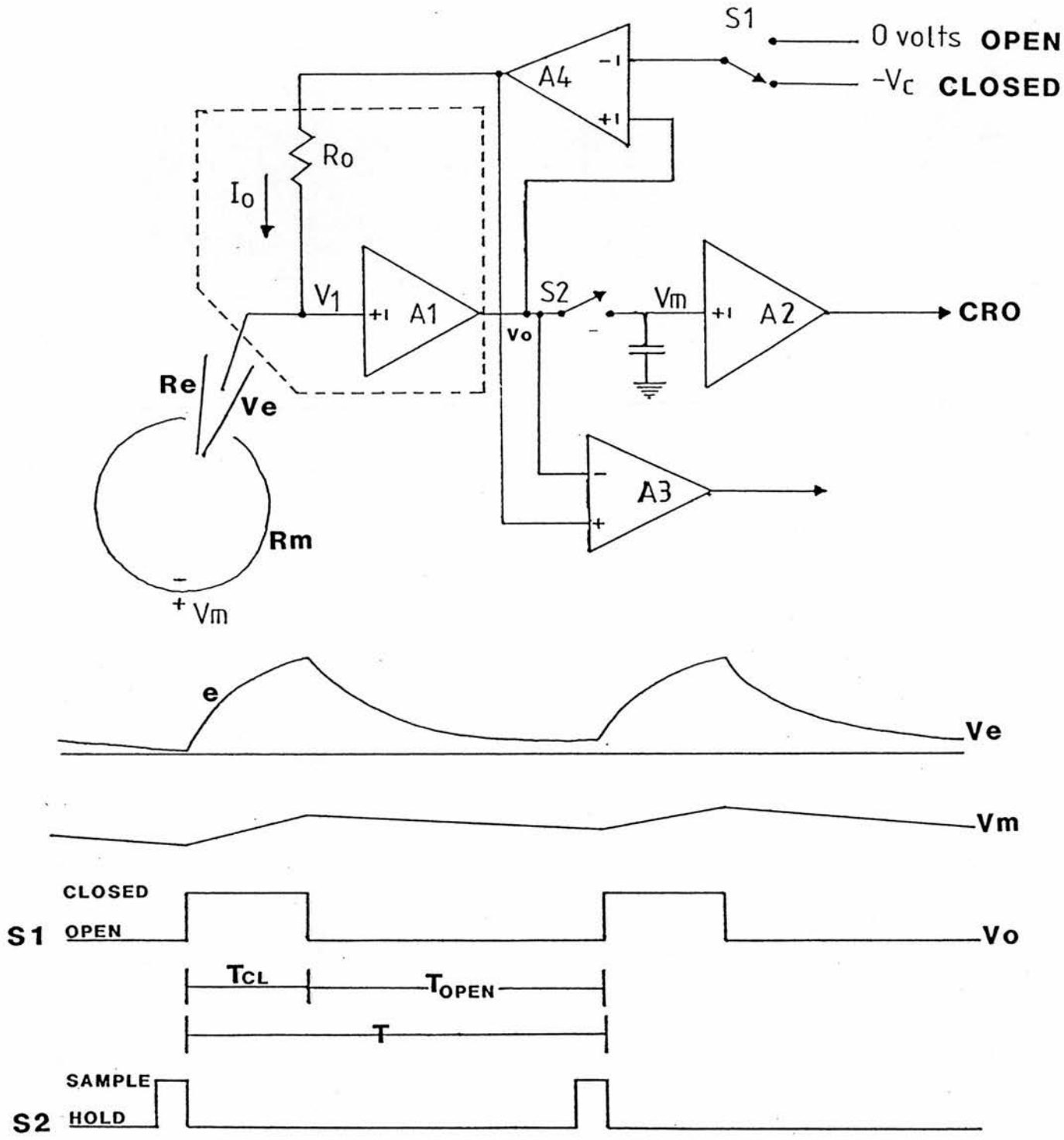

Fig. 2.6 Circuit diagram for the Axoclamp 2A in voltage clamp mode.

The circuit works on a 30% duty cycle ie the current Io was injected for 30% (Ti) of the cycle duration and voltage was recorded for the remainder of the cycle. Because of the high input impedance of the preamplifier A1 the current flows through the microelectrode and into the cell. The voltage response (Vm) evoked was measured by the unity gain A1 and sampled by the sample and hold device SH1 the output of which forms the input into the differential amplifier A2. The second input of which was the voltage step command Vc. The voltage difference between the two inputs forms the output which then drives the constant current source CCS in proportion to the voltage input. The amplitude of the CCS output was determined by the gain Gt set on the CCS. To ensure that the voltage measured was a true representation of Vm switch S1 changes to input 0 volts into the CCS hence no current flowed and the voltage drop across the microelectrode Ve, monitored at HSO, decayed to Vm. The Vm must be sampled when Ve has fully decayed. The cycle starts again when switch S1 returns to the output of A2.

Fig. 2.6

AXOCLAMP VOLTAGE CLAMP CIRCUIT

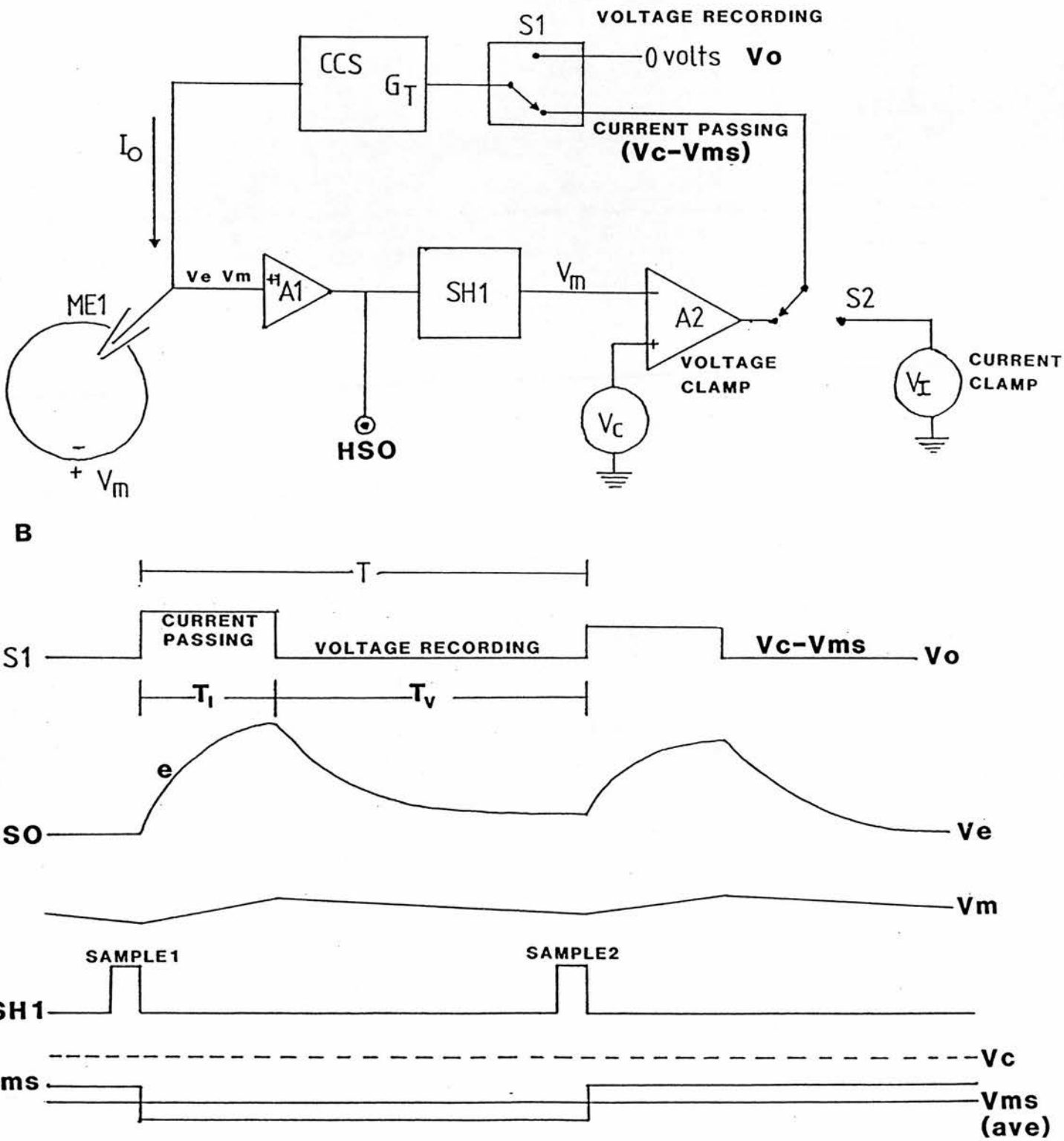

CHAPTER 3

THE BIOPHYSICAL PROPERTIES OF DORSAL RAPHE NEURONES

INTRODUCTION

The initial electrophysiological experiments which provided evidence that the "characteristic" neurones recorded extracellularly in vivo within the DRN were serotonergic were inconclusive. Apart from the known preponderance of serotonergic neurones within the nucleus most studies on the firing properties of purported serotonergic neurones were based on the finding that iontophoretic injection of L-tryptophan from recording microelectrodes caused a marked increase in the histofluorescence of cells at the tip of the recording electrodes in the DRN. These cells had shown 'typical' firing rates of approximately 0.5 - 2 Hz with a regular rhythm, a positive - negative wave form and firing which was inhibited by i.v. administration of LSD (Aghajanian & Haigler 1974). However it was not until 1982 that a definitive recording of known serotonergic neurones was obtained. Using a dual labelling procedure Aghajanian & VanderMaelen (1982a) demonstrated in vivo that intracellular recordings of neurones showing the 'typical' rhythmical firing pattern not only showed fluoresence from intracellularly injected ethidium bromide but also the formaldehyde induced yellow fluorescence of serotonin containing neurones. In a follow up study the same group attempted to further characterise the membrane properties of serotonergic DR neurones (Aghajanian & VanderMaelen 1982b). Because of the instability of the in vivo preparation long term intracellular recording from only a small number of neurones was possible. Nevertheless the cells showed long duration (≈ 2ms) action potentials with amplitudes ranging from 62 - 80 mV and input resistances ranging from 30 - 70 MΩ. The large post spike hyperpolarisation (≈ 6 mV) followed by a gradual interspike depolarisation were a regulatory factor in determining raphe cell rhythmicity and hence termed 'pacemaker potential's.

In a preliminary report on the passive membrane properties of DR neurones Crunelli et al (1983) showed that long duration high fidelity intracellular recordings could be obtained from typical serotonergic neurones in vitro. As with the in vivo preparation spontaneous rhythmical firing was observed consisting of single action potentials occurring at 0.25 - 5 Hz. Similarly action potentials were followed by marked long lasting afterhyperpolarisations (AHP's). However the input resistance was approximately three times greater than that recorded in vivo,(100 - 320 MΩ). The time constant of membrane charging was

characteristically long compared to neurones recorded from the periaqueductal grey matter (PAG) lateral to the cerebral aqueduct. In a parallel study VanderMaelen & Aghajanian (1983) also noted the close similarity between serotonergic DR neurones recorded intracellularly in vivo and those recorded in the in vitro slice preparation. Unlike Crunelli et al however this group reported input resistances closer to those noted in the in vivo preparation.

Earlier Trulson et al (1982) observed that DR neurones recorded extracellularly in vivo maintained an oscillatory firing pattern in the presence of ACSF containing 30mM magnesium to block synaptic activity which did not differ significantly from the firing patterns observed in vivo and in vitro slices bathed in control ACSF. This indicated that the rhythmical firing pattern was not dependent on an excitatory synaptic input and that there may indeed be an intrinsic pacemaker activity in individual DR neurones that dictates the firing frequency of these neurones.

As observed by both Crunelli et al (1983) and VanderMaelen & Aghajanian (1983) the neuronal population of the DRN is not a homogeneous population. Occasionally a second type of neurone was impaled. These cells displayed a fast firing frequency ($\geq$ 10 Hz) and short duration action potentials ($\approx$ 1ms), followed by a small short duration AHP. The input resistance and time constant of these cells were markedly smaller than those of proposed serotonergic neurones. These cells therefore were assumed to be non-serotonergic. Results from such cells will not be included in this study.

In the results section of this chapter the major ionic mechanisms that underlie the passive and active membrane properties will be described in some detail using both current and voltage clamp experiments. At the onset of this study no detailed analysis of these mechanisms had been performed, during the course of the study however other groups have addressed the same topic. Consequently the results of these groups will be referred to as and where applicable.

RESULTS

Passive membrane properties

Stable intracellular recordings were obtained from 103 dorsal raphe neurones. These cells showed resting membrane potentials ranging from -50 to -89 mV with a mean value -59 ± 0.8 mV (n = 103) (this and other values are mean ± S.E.M for the number of observations in parenthesis). Of the 103 cells impaled 77% appeared to be spontaneously active; however few if any remained spontaneously active during prolonged periods of recording.

Input resistance. Membrane voltage responses to hyperpolarising current commands showed a linear current-voltage relationship Fig. 3.1(a). No inward rectification was observed with voltage deflections as negative as -100 mV. Occasionally with voltage steps beyond this level inward rectification could be observed. Current voltage relationships in the linear portion of the curve Fig. 3.1 (b) gave an apparent mean input resistance of 203 ± 7 MΩ (n = 96), range 68 to 405 MΩ.

The apparent input resistance was also determined by measuring the voltage response to constant current pulses at a range of holding potentials Fig. 3.2. Of the 21 cells tested in this way 33% showed a gradual increase in apparent input resistance with increasing steady state hyperpolarisation Fig. 3.2 (a). A further 33% showed no change at all levels of hyperpolarisation Fig. 3.2 (b) and the remaining 33% showed an apparent decrease Fig. 3.2 (c). Subsequently current - voltage relationship calculations were performed at a constant membrane potential using manual voltage clamp.

Time constant. The time course of the potential change (τm) resulting from rectangular current pulses was measured at the resting membrane potential using small hyperpolarising current pulses (≈ 0.05nA).The exponential change in membrane potential had a time constant of 29 ± 1.4 ms (n = 73) Fig. 3.4. By using small hyperpolarising current pulses to determine τm substantial alterations in the charging curve by voltage activated channel activity were minimised. In all the cells studied the charging curve could be fitted by a single exponential (see methods).

The effect of tetrodotoxin (TTX) on passive membrane properties.

TTX is known to block sodium conductances in mammalian neurones (Blankenship 1976). In order to study active conductances underlying spike generation and to avoid problems during voltage clamp procedures (see methods) it was necessary to block the sodium component of the fast action potential. Consequently it was important to determine the effects of bath applied TTX on the passive membrane properties of DR neurones. In control ACSF small depolarising current pulses (0.05nA) were seen to evoke overshooting all or none action potentials. Bath application of TTX (1μM) caused a total abolition of the action potential generated in response to depolarising pulses Fig. 3.3 (a,b). Measurement of plateau voltage deflections in the hyperpolarising direction Fig. 3.3 (a) and the derived current - voltage relationship Fig. 3.3(c) showed input resistances to range from 170 to 335MΩ with a mean 215 $\pm$ 17MΩ and a marked increase in the input resistance following the addition of TTX to the ACSF ranging from 174 to 400MΩ with a mean 255 $\pm$ 22MΩ (n = 10). This increase in input resistance was significantly different from control values at p = 0.001 (paired Students t test). The change in membrane resistance was accompanied by a significant increase in the time constant τ from 28 $\pm$ 3ms (n = 10) to 35 $\pm$ 3ms (n = 10) (p = 0.001). As for the control time constant Fig. 3.4 (a) the τm in the presence of TTX Fig. 3.4 (b) could be fitted by a single exponential.

As shown in Fig. 3.3 (c) TTX administration also caused a small but measurable hyperpolarisation mean 3.5 $\pm$ 0.7mV (n = 10). This could be due to 1) the blockade of a steady state inward sodium current, 2) inhibition of a tonic synaptic input, 3) a direct effect on ion channel activity or 4) a combination of any of the above. Although the reversal potential would normally give a good indication of the ionic mechanisms involved in drug action in TTX the block of presynaptic action potentials and thus postsynaptic channel activity the block of one specific conductance would be masked by the loss of synaptic activity. Consequently as seen in Fig. 3.3 (c) the reversal potential, ie the extrapolated point of intersection of the two regression lines, shows a value of -49mV which is far removed from the expected reversal potentials for any of the known selective ion channels in particular Na^+.

Active Membrane Properties

Synaptic potentials. In a few of the impaled cells spontaneous postsynaptic depolarising potentials (PSDP's) could be observed Fig. 3.5 (a - d) with 3M KCl filled electrodes. The PSDP's were typically fast in onset and then showed a gradual decay back to the resting membrane potential (-59mV). Occasionally the PSDP's are seen to summate (star). During transient hyperpolarising steps to measure cellular input resistance the PSDP's were seen to increase in amplitude (observation not shown). Bath application of TTX caused a total inhibition of PSDP's Fig. 3.5 (e). Although no attempt was made to characterise the transmitter involved in the activation of PSDP's it may be noted that similar results were obtained both *in vivo* and *in vitro* in the hippocampus when recording with KCl filled electrodes (Nicoll et al 1980 ; Alger & Nicoll 1980). Both studies proposed a reversed GABA mediated miniature inhibitory postsynaptic potential (mIPSP) as the cause of the PSDP's.

Action potentials. As mentioned above 77% of all neurones recorded showed spontaneous 0.5 - 2Hz rhythmic action potential generation Fig. 3.6 (a). The generation of spontaneous action potential activity is thought to be due to the inherent membrane properties of the DR neurones. Manual hyperpolarisation of the cell to inhibit action potential generation revealed no excitatory synaptic events to account for the spontaneous activity. Cell viability was determined by the ability of the neurone to produce an overshooting action potential. Cells which could not evoke an overshooting action potential were assumed to be damaged or dying.

The DR neurones display a repeating cycle of membrane potential changes similar to 'pace-maker potentials' seen in certain invertebrate neurones and vertebrate cardiac muscle cells (Noble, 1985). The pacemaker potential in serotonergic DR neurones is seen to consist of a repeating four stage cycle Fig. 3.6 (b). 1) A slow depolarising potential leading to an all or none action potential 2) this in turn leads to a long lasting afterhyperpolarisation (AHP) of 10 - 20mV with a rapid onset 3) and a gradual ($\approx$ 200ms) return to the resting level 4). Individual action potentials Fig. 3.6(c) show a marked increase in membrane charging at the onset of the action potential, time to peak is about 1ms. The falling phase of the action potential can be seen to be biphasic. A shoulder on the falling phase

(arrow) is seen to delay the repolarisation of the neurone. In a number of neuronal types such as dorsal root ganglia (Dunlap & Fischbach 1978) and the locus coeruleus neurones (Williams et al 1984), the shoulder has been shown to be due to a calcium mediated component of the action potential (see also Fig. 3.3(b) and below).

Ionic mechanisms underlying action potential generation. As mentioned above TTX causes the total inhibition of the sodium component of the action potential. Current - voltage relationships constructed from steady state voltage deflections Fig. 3.7 (arrow) show a distinctly asymmetrical response to hyperpolarising and depolarising current steps of similar amplitude Fig. 3.7(b). Depolarising current injections of 0.05nA evoke voltage responses with similar duration τm and amplitude to those observed in response to hyperpolarising current steps of the same amplitude. With depolarising steps above this level in the presence of TTX however membrane charging becomes extremely rapid and with steps above 0.15nA a graded depolarising prepotential is observed. AHP's can be observed following the termination of current steps of sufficient amplitude to evoke depolarising prepotentials. In a number of neurones the low threshold depolarising prepotential can be seen to act as a precursor for a high threshold all or none depolarising potential (Figs. 3.8 & 3.10) followed by a long duration AHP. The ability to generate this high threshold TTX insensitive spike was restricted to a few neurones, addition of 10mm TEA was usually required before spike activity was observed. In a large number of neurones in the absence of TTX an action potential could be observed following the termination of hyperpolarising electrotonic potentials. In these cells the abolition of the spike with TTX unmasked the presence of a rebound slow depolarising potential which could be inhibited by bath application of the calcium channel blocker cadmium Fig. 3.9. These depolarising prepotentials were reminiscent of the calcium potentials observed in cerebellar purkinje cells (Llinas & Sigimori 1980) and inferior olivary neurones (Llinas & Yarom 1981). In experiments to determine the ionic nature of these low and high threshold depolarising potentials in DR neurones the calcium channel blocker cobalt (Co^{2+}) was added to the perfusate (500μM). The high threshold depolarising potential observed in control ACSF, Fig. 3.10, was totally abolished on addition of Co^{2+} as was the AHP following the high threshold spike. Hence it was concluded that the normal action potential involves a

calcium mediated component and that the AHP seen following action potential generation in DR neurones was dependent at least in part on Ca^{2+} entry during spike generation.

Afterhyperpolarisations. The above result indicated that the AHP seen in DR neurones following action potential generation was probably similar to the AHP's seen in a number of different neuronal types and shown to be the result of calcium activated potassium conductances (Barret & Barret 1976; Alger & Nicoll 1980; Hotson & Prince 1980; Krnjevic et al 1980; Wong & Prince 1981). In all of these cell types the AHP is sensitive to Ca channel blockers and to extracellular potassium ion concentration.

As mentioned above GABA mediated IPSP's have been shown to act via an increase in chloride conductance. If the AHP was a chloride dependent potential evoking an AHP in a chloride loaded neurone would be impossible. The AHP however could still be produced in cells recorded with 3M KCl filled electrodes.

If a K^+ conductance was involved in the evoked AHP then it should reverse at or near the K^+ equilibrium potential. Indeed this was found to be the case (Fig. 3.11). AHP's were found repeatedly to reverse between -80 and -95mV (n = 4) which is close to the equilibrium potential for K+ in DR neurones superfused with 6.25mM external K+ concentration. To ensure that the reversal of the AHP was not due to a potassium conductance dependent on a sodium influx the above experiment was repeated in the presence of TTX, Fig. 3.12. The calcium spike generated caused a large AHP ($\approx$ 21mV) which decreased in amplitude with increasingly more hyperpolarised membrane potentials eventually reversing direction at approximately -80mV. This was again consistent with an event mediated by a potassium conductance.

In an attempt to measure the potassium current mediating the AHP directly, voltage clamp experiments were employed where short (10ms) depolarising step commands mimicked the high threshold calcium potentials, Fig. 3.13. An outward tail current was observed following the termination of the depolarising step commands to - 20mV or more depolarised levels. The time constant (τ) of current decay was 84.8ms which is similar to the duration of the AHP decay. The slope conductance of this cell was 12.9nS hence the 0.37nA outward current seen with steps to 0mV would cause a 28mV hyperpolarisation from the resting membrane potential (- 60mV), consistent with the AHP's seen in current clamp.

From the above data it would appear that a calcium dependent potassium conductance was indeed the mechanism responsible for the DR neuronal AHP. To explore this hypothesis further the effect of superfusion of nM concentrations of apamin on AHP production was tested. Apamin is a polypeptide isolated from bee venom. Originally shown to inhibit neurotransmitter - induced increase in potassium permeability in guinea pig taenia coli and hepatocytes (Banks et al 1979) it has subsequently been shown to block calcium dependent potassium conductances in bullfrog sympathetic ganglion cells (Tanaka et al 1986), cat spinal motoneurones (Zhang & Krnjevic 1987), vertebrate sympathetic neurones (Kawai & Wantanabe 1986), and supraoptic neurosecretory neurones (Bourque & Brown 1987). A recent report has demonstrated the distribution of apamin binding sites to be heterogeneous throughout the brain. The raphe nuclei although showing low levels does appear to posses apamin binding sites (Mourre et al 1986).

Superfusion with 100nM apamin Fig. 3.14 in 5 cells showed a marked and irreversible blockade of the AHP following spike generation. Apamin also caused a small depolarisation of the membrane potential 3.8 ± 0.5mV (n = 5) which is possibly indicative of a tonic calcium influx contributing to the resting membrane potential via a potassium conductance. Apamin however had no effect on spike size or duration.

Transmitter actions on AHP's. Previous reports, primarily from the hippocampal slice preparation showed that the calcium dependent potassium conductance ($I_{K(Ca)}$) was sensitive to modulation by certain neurotransmitters. Dopamine has been shown to increase AHP potentials (Bernado & Prince 1982) however a later study showed dopamine to decrease AHP potentials via an action at β adrenergic receptors (Malenka & Nicoll 1986), a decrease in AHP potentials was also observed with noradrenaline (Madison & Nicoll 1982) and histamine (Haas & Konnerth 1983).

Because of the possible role of 5-HT in the regulation of dorsal raphe firing, experiments were performed to determine the effect of bath application of 5-HT on $I_{K(Ca)}$. Superfusion with 100μM 5-HT (both in control ACSF and ACSF containing TTX) caused an apparent reduction in the amplitude of the AHP following spike generation Fig. 3.15. In this cell the AHP was reduced from 17 to 10mV returning to control values on washout. This apparent effect on $I_{K(Ca)}$ however can be fully

explained in terms of input resistance alterations. During 5-HT superfusion the input resistance of the neurone fell from 405 to 195MΩ (see next chapter) hence the membrane response to an $I_{K(Ca)}$ of control amplitude would be reduced irrespective of any direct transmitter action on $I_{K(Ca)}$.

Biphasic responses to the termination of hyperpolarising current step commands. In a small proportion of the neurones impaled, cells that showed a single exponential τm for membrane charging would show on termination of the rectangular current pulse a membrane time constant for discharging that could best be described as the sum of two exponentials Fig. 3.16(a). The biphasic membrane response acts to delay the return to resting membrane potential by many milliseconds (≈ 200ms). The activation of the biphasic response was dependent on the membrane potential from which the hyperpolarising voltage steps were evoked Fig. 3.16 (b-c). The activation range for the second slower component was between -50 and -75mV. As shown in Fig. 3.16(b) at a membrane potential of -75mV the voltage decay almost fits a single exponential. The delay in the membrane potential returning to resting membrane levels was assumed to be due to an activation of a transient outward current with hyperpolarising voltage responses from a set range of membrane potentials. This transient outward current (TOC) was similar to that observed by Segal (1985) who demonstrated that TOC was capable of delaying the onset of action potential generation in DR neurones. Hence it would seem that this TOC could also play a regulatory role in the activity of DR pacemaker potentials. The conductance changes associated with the TOC determined in voltage clamp are discribed on page 35.

Voltage clamp recording.

In order to study the ionic currents across the membrane that are responsible for the membrane potential changes described above voltage clamp experiments were performed.

Step currents evoked during hyperpolarising voltage step commands. The steady state conductance of DR neurones was determined using transient hyperpolarising voltage step commands from a predetermined holding potential and measuring the steady state current responses Fig. 3.17 (a-c). Holding at the resting potential of -60mV (Fig.3.17(a)) transient (100ms) voltage step commands evoke

rectangular current responses with a linear voltage - current relationship and a slope conductance of 4.3nS Fig. 3.18 (stars), and a mean steady state conductance of 6.2 ± 1nS (n = 10). The linear voltage current relationship reflected the lack of inward rectification seen in current clamp data. Moving the holding potential to -50mV showed no alteration of the steady state current response to hyperpolarising step commands Fig. 3.17 (b), the voltage current relationship having a slope conductance of 4.3nS (Fig. 3.18, squares). However a transient outward tail current was observed on termination of voltage step commands beyond -60mV. The peak amplitude of the tail current increased as the voltage step commands increased (Fig. 3.17(b)). Further depolarisation to a holding potential of -40mV Fig. 3.17(c) no longer showed a rectangular current response to hyperpolarising voltage step commands. An additional time dependent component was visible particularly with the current responses to the smaller hyperpolarising step commands. A time dependent inward relaxation (arrow) could be observed which decreased with increasing hyperpolarising step commands. On termination of the step command an outward relaxation could be observed (double arrow). Increasing the magnitude of the step command decreases the inward relaxation observed during the current response. The steady state voltage current relationship showed a slope conductance of almost twice the previously measured conductances 8.1nS Fig. 3.18 (open squares). These results were consistent with similar responses seen in bullfrog sympathetic neurones (Brown & Adams 1980; Adams et al 1982) and in hippocampal neurones (Halliwell & Adams 1982). Termed the M current by Brown and Adams this current has been demonstrated to be a potassium mediated conductance that showed no time dependent inactivation within its activation range and that could be blocked by μM concentrations of muscarine. As with the bullfrog sympathetic ganglia experiments outward relaxations seen in DR neurones on repolarisation from more negative potentials (≥ -60mV) were complicated by the appearance of another more transient outward current.

Step currents evoked in response to depolarising voltage step commands. Depolarising voltage step commands from a holding potential of -60mV evoked both voltage and time dependent outward currents Fig. 3.19. In control ACSF the current response could be seen to consist of at least three distinct phases Fig. 3.19(a), 1) a fast TOC generated with step commands above -50mV, 2) a slowly activating outward current

seen with depolarising step commands above -40mV and 3) an outward tail current following the termination of step commands to -40mV and above.

Tetraethylammonium (TEA) at 10mM concentrations had no effect on the fast TOC, the slowly activating outward current however was drastically reduced and the outward tail current abolished. The TEA sensitivity of the slow outward and tail currents and the voltage activation range were similar to those reported for a calcium activated outward current in guinea pig hippocampal pyramidal neurones (Brown & Griffith 1983a). The inward calcium current was presumably masked by the high amplitude TOC. The slow activating outward current remaining after TEA application Fig. 3.19(b) (arrow) may represent a TEA resistant component of $I_{K(Ca)}$ or more probably may represent the activation of I_M, shown to activate above -50mV (Fig. 3.17(c)) and be resistant to TEA (Brown & Adams 1980). TEA did not appear to affect the decay of the fast transient outward current which showed a time constant of 6ms and 7ms on application of TEA Fig. 3.20. It should be noted however that activation of the TOC with step commands above -40mV causes a breakdown of the voltage clamp hence the decay of the outward current during the early stages of the clamp cannot be regarded as absolute.

The fast TOC and the outward tail current seen on termination of hyperpolarising pulses were similar in nature to a transient outward current seen in invertebrate neurones (Connor & Stevens 1971; Neher 1971; Thompson 1977) and vertebrate neurones (Gustafsson 1982) designated I_A. The current is the result of a transient increase in potassium conductance.

In order study the fast transient outward current in isolation from other voltage activated currents a dual pulse protocol described by Thompson (1977) for isolating I_A in molluscan neurones was adopted. When holding a DR neurone at -67mV and increasing the magnitude of the depolarising voltage step command following a fixed hyperpolarising prepulse Fig. 3.21(a) the TOC increased from 0.31nA with a step to -62mV, to 1.39nA when stepping to -52mV. Conversely inactivation properties could be measured with increasing hyperpolarising prepulse voltage step commands followed by a depolarisation to a fixed potential Fig 3.21(b). The amplitude of the fast TOC increased from 0.47nA with a prepulse hyperpolarisation to -77mV, to 1.66nA stepping to -97mV. The time constant of TOC decay was seen to be dependent on

the current amplitude. In the same cell as Fig. 3.21 the maximal activation current (1.39nA) had a time constant of 25ms and the maximal inactivation current (1.66nA) showed a time constant of 34ms Fig. 3.22. Construction of a steady state inactivation/activation curves Figs. 3.23 & 3.24 gave values for half maximal inactivation (V half inact.) (open circles) of -89mV (mean -74 ± 1.75mV (n = 10)) a slope of 3.8mV (mean 5.1 ± 0.54mV (n = 10)) and a maximum estimated current (Imax) of 1.9nA (mean 1.63 ± 0.26nA (n = 10)). Half maximal activation (V half act.) was -51mV (mean 46.2 ± 5.84mV (n = 3)) with a slope of 4.7mV (mean 5.3 ± 1.0mV (n = 3)) and a maximum estimated conductance (gMAX) of 41.3nS (mean 54.5 ± 6.7nS (n = 3)).

In another cell Fig. 3.25 it can be seen that a 10mV shift in holding potential (-50 to -60mV) causes a parallel shift in the inactivation curve. The V half inact. changed from -63 to -70mV and the Imax decreased from 1.24 to 0.58nA. The slope however remained unaltered at 3.48mV.

I_A is characterised by both its insensitivity to TEA and its selective sensitivity to 4-aminopyridine (4-AP) (Thompson 1977). Bath application of 4-AP (5mM) caused a reduction in the size of the fast transient outward current Fig. 3.26. In control ACSF Fig. 3.26(a) increasing the magnitude of the prepulse step command caused an increase in the TOC amplitude, increasing from 0.47nA with steps to -77mV, to 1.86nA with prepulse steps to -97mV. Application of 5mM 4-AP caused a reduction in the TOC amplitude over all the prepulse step commands tested Fig. 3.26(b). The outward current was abolished with steps to -77mV and reduced to 1.1nA with steps to -97mV. In the presence of 4-AP an inward current (arrows) was observed followed by a delayed outward current which persisted after the termination of the depolarising step command.

Time dependent I_A inactivation. In the same cell the effects of increasing the interval between the prepulse and the step command was observed. In control ACSF increasing the gap duration caused a concomitant decrease in I_A amplitude Fig. 3.30(a), I_A was almost totally abolished following a gap duration of 90ms Fig. 3.31 (squares). Bath application of 4-AP not only reduced the peak I_A amplitude Fig. 3.30(b), 1.8 to 1.1nA with no gap present, but also reduced to 30ms Fig. 3.31 (crosses) the gap duration after which I_A can still be evoked. This effect was seen to recover on prolonged washout Fig. 3.30(c). The baseline current ≈ 0.5nA seen in Fig. 3.31

represented leakage conductance which had not been subtracted from the I_A amplitude

Time dependent opposition of inward and outward currents. During the course of I_A inactivation experiments, it was noted that when holding the membrane potential at -50mV, in order to achieve full inactivation of I_A, a depolarising step command to -40mV evoked an inward current followed by a delayed outward current which persisted after the termination of the step command Fig. 3.32(a). The introduction of increasing hyperpolarising prepulse commands caused an increase in the apparent time to peak (arrow) of the inward current. The apparent time to peak increasing from 10.4ms with no prepulse to 22.4ms with a hyperpolarising prepulse command to -66mV, Fig. 3.32(c). The delay appeared to have no effect on either the amplitude or the time course of the delayed outward current. A prepulse step command to -80mV caused the inward current to be totally masked by a large transient outward A current Fig. 3.32(e). A remnant of the delayed outward current could still be observed (large arrow) indicating that the voltage protocol had not inactivated the presumed calcium activated potassium conductance and that the inward calcium current and the outward I_A must oppose each other at their time of onset. In an attempt to clarify the effect of calcium influx on I_A amplitude experiments in which the extracellular calcium concentration was reduced from 2mM to 0.2mM and replaced by 4mM magnesium were performed. In the presence of TEA (10mM), to prevent contamination by delayed outward potassium currents, peak I_A was seen to be reduced from 0.81 to 0.51nA following a hyperpolarising prepulse to -97mV Fig. 3.33 (a + b). On switching to a TEA, low Ca^{2+} high Mg^{2+} containing ACSF the peak I_A amplitude increased to 1.7nA following a similar prepulse command Fig. 3.33(c). The steady state conductance had however increased from control conductance.

Construction of a steady state inactivation curve showed that the reduction of extracellular Ca caused an increase in the half maximum inactivation voltage (Vhalf) from -68 to -71mV and the estimated maximum current (Imax) from 1.0 to 1.7nA. The slope however decreased from 7.01 to 6.25mV.

Transmitter action on I_A. As mentioned above 5-HT has been shown to have a direct inhibitory effect on raphe cell firing. It was of interest therefore to test the effects of 5-HT application on I_A activity. Results obtained were ambiguous, 5-HT appearing to increase

(n = 1), decrease (n = 2) and have no effect (n = 2) on I_A amplitude. In Fig. 3.35(a) application of 100μM 5-HT reduced the maximum observed I_A current from 2.53 to 2.05nA no recovery was observed on washout with the maximum amplitude declining further to 1.78nA. Steady state voltage - current relationships Fig. 3.35(b) showed that the decrease in I_A amplitude was not due directly to the altered conductance state during 5-HT application. The neuronal conductance decreased from 20nS to 7.1nS on washout having shown an original control conductance of 5.6nS. The reversal potential for the 5-HT action was -80mV. This will be dealt with in greater detail in the next chapter. Steady state inactivation curves plotted for the same cell Fig. 3.36 shows a gradual decrease in both the Imax values 2.56 to 1.75nA and the Vhalf values -73 to -70mV throughout the duration of the experiment. The slope however increased from 4.09 to 5.78mV during 5-HT application, returning to 3.65mV on washout.

Noradrenergic inputs into the DR nucleus have been shown to be an important excitatory regulator of firing frequency. Hence the effects of bath application of 50μM noradrenaline (NA) was examined. NA routinely caused a reduction in the amplitude of I_A (n = 4) Fig. 3.37(a) the maximum current evoked following a prepulse step command to -94mV falling from 0.63 to 0.34nA. Steady state voltage - current relationships Fig. 3.37(b) showed NA to cause a decrease in neuronal conductance from 3.7nS in control ACSF to 2.7nS. The reversal potential, like that of 5-HT , was found to be -80mV. Inactivation curves Fig. 3.38 generated from the above data showed NA to cause a parallel shift to the right. The slope for each plot showed no change 5.81mV compared to 5.98mV during NA application. The Vhalf was reduced from -82 to -77mV and the Imax fell from 0.69 to 0.36nA.

Repeated administration caused a gradual desensitisation of the neuronal response to NA. Fig. 3.39(a) on first application NA caused a marked reduction in I_A amplitude, falling from 3.18nA in control ACSF to 2.34nA. Initially during NA perfusion a marked hyperpolarising DC current was required to maintain the membrane potential at -60mV indicating a depolarising action of NA. This action became desensitised rapidly, on the third time of application no DC current was required to hold the membrane at the control potential. The amplitude of I_A however was reduced from 1.96 to 1.55nA. Hence the depolarising action of NA would appear to be more sensitive to desensitisation than the NA action on I_A where activity decreased from

30% inhibition of I_A to 10% inhibition following repeated NA administration. Once again a parallel shift to the right in the inactivation curve was observed following NA application with Vhalf reducing from -73 to -68mV and Imax decreasing from 2.86 to 1.65nA Fig. 3.40. Unlike the previous cell (Fig. 3.37) the slope was also reduced from 3.79 to 2.86mV. Repeated administration of NA abolished the reduction of both the Vhalf and slope seen with initial NA application. The control (circles) and NA (crosses) inactivation curves being inseparable after repeated NA administration Fig. 3.41. The Imax value however was still reduced from 2.14 to 1.9nA. In contrast subsequent bath application of 4-AP (5mM) produced a further decrease in Imax (1.0nA) together with a reduction in both Vhalf -74 to -72mV and the slope 3.9 to 2.9mV.

DISCUSSION

This chapter has shown that not only do DR neurones posses passive membrane properties that would permit both the temporal and spatial integration of synaptic inputs but in addition active currents that could well account for the proposed pacemaker activity seen in vivo.

The passive membrane properties of DR neurones reported in this study were in close agreement with those reported by Crunelli et al (1983), with cells showing a resting membrane potential of -59 ± 0.8mV, an input resistance of 203 ± 7MΩ and a membrane time constant τm of 29 ± 1.4ms. The neuronal input resistance observed in this study is twice that demonstrated in vivo (Aghajanian & VanderMaelen 1982b). It is possible that this discrepancy occurs due to 1) the removal of a tonic synaptic input or 2) the removal of dendritic or axonal arborisations during slice preparation. A higher input resistance in in vitro preparations however appears to be a common occurrence, Kita et al (1982) concluded that the increased Rm seen in substantia nigra neurones was due to the lack of tonic synaptic inputs. The input resistance of DR neurones was relatively high in comparison to other in vitro CNS preparations where resistances have been seen to range from 40MΩ in thalamic neurones (Jahnsen & Llinas 1984) and 48 ± 155MΩ in hippocampal neurones (personal observation) to as low as 8 ± 3MΩ in facial motoneurones (Larkman et al 1989). Consequently DR neurones are capable of showing marked voltage responses to even the smallest synaptic inputs. This effect would be further enhanced by the long time constant, τm = 29 ± 1.4ms, which would allow temporal summation over a much greater time interval than would be possible in hippocampal neurones (τm = 18.3 ± 1.0ms) or facial motoneurones (τm = 2.9 ± 0.6ms).

The fact that spontaneous depolarising postsynaptic potentials (DPSP's) were observed in a number of preparations would indicate that in the DR slice preparation not all tonic synaptic inputs have been severed. That these DPSP's were not observed when recording with electrodes filled with potassium acetate would imply that the DPSP's, recorded with KCl filled electrodes, were reversed IPSP's due to a change in the Cl^- driving force and that under ordinary conditions the individual spontaneous conductance increases are relatively small and the driving force modest. The DPSP inhibition by TTX would argue that

these spontaneous potentials result from activity dependent transmitter release as spontaneous quantal transmitter release is resistant to TTX treatment (Kuno & Weakly 1972). As mentioned above GABAergic neurones have been shown to be present in the DR nucleus (Belin 1987) and that GABA application inhibits raphe cell firing, an action which can be blocked by local application of picrotoxin (Gallager & Aghajanian 1976). Hence it was assumed that the DPSP's resulted from the spontaneous activity of presynaptic GABAergic interneurones. Inhibition of this tonic GABA mediated input could account at least in part for the hyperpolarisations and increased τm and Rm seen with bath application of TTX.

The spontaneous activity seen on initial impalement of DR neurones was not directly related to a tonic excitatory input as manual hyperpolarisation to inhibit action potential generation did not uncover a sequence of rhythmic depolarising postsynaptic potentials. It was therefore concluded that DR neurones were capable of generating spontaneous rhythmic activity intrinsically. That no bursting activity was ever observed in DR neurones supported the theory that firing was controlled by a regular pacemaker activity.

Several conductances, additional to the expected fast sodium and delayed rectifying K^+ conductance, have been observed which would account for the four stage cycle seen during steady rhythmic activity in DR neurones.

Calcium conductances. Two separate calcium conductances were observed that showed distinct and independent activation properties. A graded low threshold depolarising prepotential could be observed that was resistant to TTX application and abolished by bath application of the calcium channel blocker cobalt (Co^{2+} 500μM). The depolarising prepotential was observed not only following depolarising step current commands from the resting membrane potential but also following the termination of hyperpolarising current step commands from rest. The depolarising prepotentials were reminiscent of the low threshold calcium spikes reported in inferior olivary (IO) neurones (Llinas & Yarom 1981), spinal dorsal horn neurones (Murase & Randic 1983) and thalamic neurones (Jahnsen & Llinas 1984). Unlike dorsal horn, IO neurones or thalamic neurones the low threshold prepotential in DR neurones could be activated from resting membrane potentials without membrane hyperpolarisation. A voltage dependent de-inactivation was seen with the rebound prepotentials following hyperpolarising current

commands. The rebound prepotentials increasing in magnitude and decreasing in the time to onset with increasing hyperpolarising current step commands. This rebound prepotential was also seen to be blocked by Cd^{2+} application.

Under voltage clamp a protocol mimicking the depolarising current clamp step commands from rest showed an apparent transient inward current followed by a slowly developing outward current. Either the inward current inactivated and decayed before the onset of the outward current or the outward current masked a persistent inward current. In hippocampal neurones Johnston et al 1980 reported that in response to depolarising voltage step commands 1) internally applied CsCl decreased the outward current with no effect on the inward transient current 2) barium, a substitute charge carrier in Ca^{2+} channels, caused an increase in the amplitude of the transient inward current and 3) Co^{2+} caused a total inhibition of both the inward and delayed outward currents. Hence it was assumed that the inward current was a voltage dependent inward inactivating calcium current. Although this problem was not addressed in this study Burlhis and Aghajanian (1987) demonstrated that in DR neurones recorded with CsCl filled electrodes a transient inward current could still be evoked in the absence of the delayed outward current. This inward current and the rebound potential observed in current clamp could be abolished by the application of Ni^{2+} a known calcium channel blocker. Hence the current mediating the low threshold prepotentials would appear to be an inward inactivating calcium current. It is interesting however that Burlhis & Aghajanian (1987) were unable to evoke the transient inward current unless inactivation of the channel was removed by membrane hyperpolarisation from the resting membrane potential. In the present study an apparent transient inward current could be evoked with depolarising step commands from -50mV. This may reflect the presence within DR neurones of two separate low threshold Ca^{2+} conductances with different activation properties.

With the introduction of patch clamp single channel recording several types of calcium channel have been observed in vertebrate neurones. Carbone & Lux (1985) reported two voltage - activated, fully inactivating Ca^{2+} channels in chick dorsal root ganglia (DRG). In the same year Fedulova et al (1985) reported the presence of both voltage activated inactivating and non inactivating currents in rat DRG's. Subsequently three distinct channels have been reported in the same

DRG preparation and have been given the following nomenclature; the L channel, a large conductance channel that contributes to long lasting current at strong depolarisations; the T channel, a small conductance channel that underlies a transient current activated at weak depolarisations; and the N channel which requires strongly negative potentials for complete removal of inactivation (unlike L) and strong depolarisations for activation (unlike T) (Nowycky et al 1985). The channel types can be distinguished further by their sensitivity to both antagonists and agonists. Nickel ions antagonise the T current with little or no effect on N and L channel activity. The dihydropyridine nifedipine inhibits the L current but does not reduce T or N currents whereas the N and L channels can be blocked by the polypeptide neurotoxin ω conotoxin (Fox et al 1987).

The sensitivity of the low threshold calcium current to 100μM Ni^{2+} observed by Burlhis and Aghajanian lead them to the conclusion that this current was similar to the T current observed by Fox et al (1987). The prerequisite for a hyperpolarisation from the resting membrane potential before the current was observed however is more reminiscent of N type channel activity. It would be of interest to determine the nature of the inward calcium current activated on depolarisation from resting membrane potentials seen in this study.

A high threshold TTX resistant, Co^{2+} sensitive, current could also be observed that was similar to the high threshold Ca^{2+} currents observed in dorsal horn and IO neurones. As for the Ca^{2+} spikes seen in inferior olivary neurones the threshold for spike activation ($\approx$ -40mV) in DR neurones was above that which would normally activate the fast Na^{+} spike ($\approx$-50 to -55mV). In the absence of TTX a shoulder on the falling phase of the action potential was always observed, it is thus probable that the Na^{+} spike triggers the high threshold Ca^{2+} spike. The high threshold Ca^{2+} spike in Purkinje cells and IO neurones were demonstrated to be non inactivating (Llinas & Sigimori 1980a; Llinas & Yarom 1981). If this were true of the high threshold Ca^{2+} spike seen in DR neurones then repolarisation would occur due to the action of the delayed rectifier and hence produce a shoulder on the falling phase of the action potential. These authors also noted that the high threshold Ca^{2+} spike had a probable dendritic location of origin; this may in part explain the high threshold nature of this current.

In papillary heart muscle preparations the dihydropyridine calcium agonist Bay-K-8644 was shown to cause an increase in the maximum rate of rise, amplitude and duration of slow action potentials (Sada et al 1986). In striatal neurones Bay-K-8644 was demonstrated to cause an enhancement of calcium potentials and inward slowly inactivating currents evoked by depolarising step commands from -50mV or above (Cherubini & Lanfumey 1987). Hence it would appear that the high threshold calcium spikes observed in these preparations are similar in both their activation range and pharmacology to the L channel current previously described by Nowycky et al (1985). It is possible that the high threshold calcium conductance observed in DR neurones is of a similar nature. Cherubini & Williams (1988) have however reported that the L type calcium current is not responsible for the calcium current involved in spontaneous firing in locus coeruleus neurones.

Potassium Conductances.

Calcium activated potassium conductance $I_{K(Ca)}$. The AHP seen in DR neurones following action potential generation appears similar to the AHP's seen in a number of different neuronal types that have been shown to be the result of a calcium activated potassium conductance (Barret & Barret 1976; Alger & Nicoll 1980; Hotson & Prince 1980; Krnjevic et al 1980; Wong & Prince 1981). The demonstration that both low and high threshold calcium currents are associated with AHP production in DR neurones and that the AHP's could be inhibited during superfusion with the calcium channel blocker Co^{2+} supported the hypothesis of a calcium dependent activation. That the AHP could be observed after neuronal chloride loading and that the reversal potential remained within the range expected from a potassium mediated conductance further supported the hypothesis of a calcium activated potassium conductance. Similar results were obtained by VanderMaelen and Aghajanian (1983b). They demonstrated that the AHP reversal potential was dependent on the extracellular K^+ concentration and that magnesium could block AHP production.

More recent experiments have indicated that AHP production may involve at least two independent potassium conductances (Pennefather et al 1985; Fowler et al 1985; Lancaster & Adams 1986; Constantini & Sim 1987). Namely an early, fast, large outward current which was

sensitive to low micromolar concentrations of TEA, given the nomenclature I_c by Brown and Griffith (1983). This early current appears to be responsible for the rapid AHP following spike generation. A second small slow outward current, similar to those seen in the present study following large transient depolarising voltage step commands, has been termed I_{AHP} by Pennefather et al (1985) and shown to be inhibited by nanomolar concentrations of apamin. The inhibition of the AHP seen in the presence of nanomolar concentrations of apamin in this study would point to the presence of I_{AHP} currents in the conductance profile of DR neurones. I_{AHP} may not however be the result of activation of a single K^+ channel type. Constanti and Sim have demonstrated the presence of an I_{AHP} in olfactory cortex neurones that show a similar inhibitory response to NA and TEA but is not inhibited by apamin in high micromolar concentrations.

The action of apamin in blocking the AHP in several neuronal types has been demonstrated to be due to a direct effect on the outward K^+ conductance and not due to an effect on Ca^{2+} influx (Kawai & Watanabe 1986). Care must be taken however in placing too much emphasis on apamin blockade of AHP as direct proof of the presence of $I_{K(Ca)}$ in this study. It would be of interest to study the effect of apamin on the slow low threshold inward calcium current observed in DR neurones, particularly in view of the fact that apamin has been shown to be a specific blocker of slow Ca^{2+} channels in cultured cell reaggregates from chick heart (Bkaily et al 1985).

In a recent report Freedman and Aghajanian (1987) have demonstrated a similar apamin sensitivity of $I_{K(Ca)}$ in DR neurones. They further demonstrated that AHP duration was increased during bath application of the α_1 agonist phenylephrine or NA in the presence of propranolol. The effects were antagonised by prazosin and hence the action was proposed to be mediated via an α_1 adrenoreceptor. Intracellular injection of the putative second messenger myo-inositol-1,4,5-trisphosphate (IP_3) transiently mimicked the actions of α_1 agonists whereas phorbol esters, stimulaters of protein kinase C, caused a suppression of the $I_{K(Ca)}$. Hence it was concluded that endogenous NA acting at α_1 adrenoreceptors may cause an increase in AHP duration by increasing intracellular IP_3 levels.

Increasing the duration of AHP's could be seen as an inhibitory neurotransmitter action on raphe cell firing activity. Consequently it might be assumed that this effect could mediate the inhibitory

response to 5-HT application. 5-HT however appeared to have no direct effect on AHP size or duration and the decrease in amplitude seen in Fig. 3.15 could easily be explained by a shunting effect on voltage responses due to the decrease in Rm seen with 5-HT application. This hypothesis is supported by the observation that 5-HT application had no effect on the inward low threshold Ca^{2+} current and subsequent outward K^+ current seen in voltage clamp (Fig. 6 Burlhis & Aghajanian 1987). This is in contrast to the effects of 5-HT application on AHP activation in hippocampal CA_1 neurones. Here 5-HT has been shown to cause a reduction in I_{AHP} without affecting inward Ca^{2+} currents (Colino & Halliwell 1987).

Voltage gated transient outward K^+ current, I_A. The voltage sensitive biphasic discharging curve observed in response to transient hyperpolarising current steps during current clamp gave the first indication of the presence of an A like current in DR neurones (Fig. 3.16). Dekin & Getting (1984) had reported that in one class of nucleus tractus solitarius neurones a hyperpolarising current prepulse caused a delay in the onset of action potential generation in response to a depolarising current pulse. They also noted that the delay increased with increasing hyperpolarising prepulse commands and was insensitive to Cd^{2+} and acetylcholine and hence not caused by $I_{K(Ca)}$ or I_M. Thus they concluded that this voltage and time dependent outward current was similar to the fast transient outward A current seen in molluscan neurones.

This hyperpolarisation dependent delay in action potential generation was demonstrated in DR neurones. Segal (1985) showed that spike generation in response to depolarising current pulses was markedly delayed when the cell was conditioned with a hyperpolarising prepulse. The delay was overcome by bath application of 4-AP but not cadmium. These responses are characteristic of the A like current seen in molluscan neurones. A direct comparison however required the use of voltage clamp techniques.

This study has demonstrated the presence of a transient outward current during voltage clamp protocols which, although showing slight variations from previously reported I_A characteristics, can best be described as a I_A-type current.

The current showed complete inactivation at membrane potentials about -55mV and required a membrane hyperpolarisation to de-inactivate the channels. Steady state inactivation curves showed a half maximal

inactivation potential (Vhalf)of -71 ± 1.75mV and a voltage dependent slope (k) of 5.1 ± 0.54mV. These values fall neatly between those of previously reported I_A currents. In snail neurones Vhalf for inactivation = -65mV and k = 4mV (Neher 1971) and in dissociated hippocampal neurones Vhalf = -83mV and k = 7.5mV (Numann 1987). The activation curve showed a Vhalf of -46mV and a similar degree of voltage dependency than the inactivation curve with k = 5.33mV. The degree of overlap of the inactivation and activation curves (-67 to -55mV) ensures that at rest (-59mV) there is a steady state activation of the A channels in DR neurones. Consequently any intrinsic or synaptically evoked depolarisation must first overcome the steady state outward rectifying A current before spike threshold can be attained. Spike threshold will be further increased due to the increased conductance state at this membrane potential. Hence at rest I_A will act to stabilise the membrane potential against excitatory inputs and amplify the effect of inhibitory inputs.

The dual pulse protocol allowed the transient outward current to be studied in isolation from other contaminating currents. Because of the extremely rapid rate of rise of the TOC the time course for activation could not be accurately measured using the single electrode voltage clamp technique. The decaying phase however could be seen to follow a single exponential with time constants ranging from 17-46ms. The single exponential decay of I_A has been reported by a number of workers studying a variety of different preparations. The time course for the exponential decay however varies markedly from preparation to preparation. Invertebrate preparations show time constants for inactivation as long as 300-600ms (Neher 1971; Connor & Stevens 1971). The time course of inactivation seen in vertebrate neurones appears to be faster, with values between 20-40ms (this study; Numann et al 1987). The apparent difference in the decay rates could be explained by a slowing of I_A kinetics due to the low temperature recording conditions (5-20°C) in invertebrate preparations, Zbicz & Weight (1985) however showed, in hippocampal CA_3 neurones, I_A to inactivate with a single exponential decay and a time constant of 380ms. It would appear at first glance that two independent I_A channels with different inactivation kinetics exist. Gustafsson et al (1982) have reported that I_A decay in hippocampal CA_3 neurones could not be described by first order kinetics. A rapid initial decay was followed by a slow second phase which could last for several seconds. A subsequent report

by Storm (1986) showed that in CA_1 neurones depolarising voltage step commands from membrane potentials more hyperpolarised than rest elicit a fast-activating TOC that had three components. A fast component that was Ca^{2+} dependent, an intermediate one that was sensitive to 4-AP and a slow one that was both insensitive to 4-AP and Ca^{2+} independent. Hence it is possible that the slowly decaying component may not represent A channel activity due to its insensitivity to 4-AP. Support for a biphasic decay came however from Kasai et al (1986) who demonstrated that single channel activity with a unitary conductance of 20pS observed in guinea pig DRG's could be responsible for an averaged current that decayed with two time constants τ_f (fast) = 100ms and τ_s (slow) = 4,000ms. They concluded that the channels had two different states of inactivation. Although the fast decay reported in DRG's was longer than the decay observed in this study it would be interesting to speculate that the difference between snail and mammalian time constants for decay may be due to the expression of a different inactivation states for the same 20pS conductance channel.

The I_A current observed in DR neurones not only shows voltage dependent activation properties but also time dependent activation. The effect of time dependent activation being observed with increasing the duration of the conditioning hyperpolarising prepulse, reaching a maximum with conditioning prepulses of $\geq$ 80ms. This time dependency would be of particular importance during post spike AHP's. During an action potential spike the I_A would be effectively inactivated, on repolarisation and subsequent fast AHP I_A activation would be fractionally restored. As the AHP gradually decays, as a result of the slow $I_{K(Ca)}$, the membrane voltage would move into the range where activation is appreciable and inactivation is removed. The time dependent nature of I_A activation would counterbalance the progressive voltage dependent inactivation hence prolonging the interspike interval. Since the conductance, g_A ,has been described to be the product of $(activation)^4$ x (inactivation) by Connor (1978), the time course when voltage is changing is not determined by a simple decay process, but by two processes one that increases and one that decays. This causes a surprisingly slow decay for I_A. Connor further demonstrated that in a computer simulation of action potential firing patterns the addition of I_A could reduce the firing frequency from

77Hz to 2Hz. This latter frequency is close to the firing rate of DR neurones observed in this study and suggests that I_A is of importance in DR firing patterns.

The time dependency was seen not only for the removal of inactivation but also for the return to the inactivated state. The observation that a gap of 90ms, between the hyperpolarising conditioning pulse and the depolarising step command, was required for activation to be abolished has profound implications for synaptic integration in DR neurones. Hence any synaptic event that acts to de-inactivate I_A will be "remembered" by the cell for a duration that is presumably also dependent on the duration of de-inactivation. Consequently any EPSP occuring during this period would activate I_A and therefore be reduced in amplitude.

A further similarity to I_A was seen in the pharmacological sensitivity to K^+ channel blockers. The TOC was seen to be resistant to TEA (10mM), known to block the delayed rectifier and a calcium activated potassium conductance, with neither amplitude nor initial time constant of decay being affected. Any TEA blockade of the TOC channel would theoretically be expected to cause a decrease in the outward current amplitude and a reduction in the time course of decay.

Bath application of 4-AP was seen to cause both a reduction of the TOC amplitude and a reduction in the rate of TOC decay in both dual pulse paradigms tested. It was apparent from the results of the time dependency experiments that 4-AP was not acting as a simple blocker of A channels. The blockade of A channel activity was seen to increase with increasing duration of the conditioning prepulse. Since prolonged hyperpolarisation increased the proportion of de-inactivated A channels it would appear that 4-AP was able to interact with the de-inactivated A channel thereby inhibiting channel opening. A similar observation was reported by Thompson (1982) who also noted that the steady 4-AP block was removed by depolarisation. Together with the finding that 4-AP caused the initial I_A decay to increase whilst causing a later slow decline in current lead Thompson to the conclusion that a voltage dependent unblocking of the activated I_A channel could occur at depolarised voltages allowing channel opening and subsequent inactivation. Hence current would flow at times when, in the absence of 4-AP, inactivation would normally be complete.

A similar finding was made in DR neurones Fig. 3.23(a & b , right hand records). In control ACSF the A current could be seen to decay

with a single exponential time constant of 34ms. Following 4-AP application however the decay appeared biphasic with the initial time course of decay reducing to 16ms and the appearance of a second slower decay with a time course of decay of approximately 198ms. It is possible therefore that a process similar to that proposed by Thompson for I_A blockade in snail neurones also occurs in DR neurones. A further possibility could be postulated whereby 4-AP causes a conformational change in the channel protein such that the majority A channels become "locked" in the slow inactivation phase reported by Kasai et al (1986). This would imply that under normal conditions the majority, if not all, of the A channels show a conformational change to the fast inactivation process. Because of problems with interference from other voltage dependent conductances this process was not explored further. It would however be of interest to determine if dendrotoxin (DTX), shown to cause epileptiform action potential burst firing (Docherty et al 1983) and selective blockade of I_A (Halliwell et al 1986), acts to block I_A by a process similar to that of 4-AP.

During 4-AP application it was noted that a low threshold transient inward calcium current (as previously reported) was observed during step commands to depolarised voltage levels where in control ACSF no inward current had been previously observed. The possibility arose that the inward calcium current and the TOC may act to oppose each other over a defined voltage range under normal circumstances. On holding the membrane at -50mV, to inactivate A channels, step depolarisations to -40mV evoked a low threshold inward calcium current and a subsequent $I_{K(Ca)}$ Fig. 3.29(a). Support for the view that this current was opposed by I_A was obtained by showing that increasing the hyperpolarising prepulse evoked an I_A current of sufficient magnitude to mask the inward calcium current. Further support came from the observation that following TEA administration to suppress $I_{K(Ca)}$ and I_K substitution of Ca^{2+} (2mM) with low Ca^{2+} (0.2mM) and high magnesium (4mM) caused a doubling in the amplitude of I_A from 0.8nA to 1.7nA. It had been observed in several earlier studies that changing extracellular calcium concentrations could cause a parallel shift in the activation and inactivation properties of I_A. In contrast to the results reported in this study a decrease in I_A was observed following calcium channel blockade with Co^{2+} (Thompson 1977; Numann et al 1987) and Mn^{2+} (Gustafsson 1982; Zbicz & Weight 1985). It must be noted that

in each of these studies a parallel shift towards more depolarised levels was observed in the activation/inactivation properties of I_A. Frankenhaeuser & Hodgkin (1957) demonstrated that a 5 fold reduction in extracellular calcium caused an equivalent effect to a membrane depolarisation of 15mV. It was proposed that calcium ions were adsorbed at the outer edge of the membrane thereby creating an electric field within the membrane which adds to that provided by the resting membrane potential. The local electric fields set up by charges near the membrane - solution interface could bias voltage sensors within the membrane. In the absence of Ca^{2+} the outer surface bears a net negative charge setting up local negative potentials (surface potentials) and hence altering the electrical field within the membrane. Thus an intramembrane sensor would see a change in field potential equivalent to a depolarisation. Frankenhaeuser & Hodgkin also showed that Mg^{2+} had a membrane stabilising effect that was similar but less effective than Ca^{2+}. This could explain why in this study no parallel shift in the depolarising direction of the inactivation curve was observed with Mg^{2+} substitution, indeed a small shift in the hyperpolarising direction was observed but this was thought to be of insufficient magnitude to cause the two fold increase in I_A following the reduction of extracellular Ca^{2+}. Mayer & Sugiyama (1988) have demonstrated in cultured rat DRG's an order of potency for divalent cations to cause a depolarising shift in the activation curve. The sequence was $Cd^{2+} \geq Mn^{2+} = Co^{2+} \geq Ca^{2+} \geq Mg^{2+}$, hence further supporting the view that, in this study, the increase in I_A observed in low Ca^{2+} ACSF was due to the removal of an opposing inward Ca^{2+} current. A similar conclusion was reached by Burlhis & Aghajanian (1987) who noted that in DR neurones an inward calcium current was observed to peak earlier, when recorded with CsCl filled electrodes, than would normally be observed in the presence of I_A.

In view of the known role of extracellular calcium in neurotransmitter release it may be postulated that the increase in I_A, seen on lowering extracellular Ca^{2+} concentrations, could be due to the inhibition of a TTX resistant local neurotransmitter release that acts to inhibit I_A. The dis-inhibition would be seen therefore as an increase in the I_A amplitude. Although excitation - release coupling can be controlled by Ca^{2+} influx through all three of the known Ca^{2+} channels it is proposed that N channels play a dominant role in neuronal neurotransmitter release (Tsien et al 1988). Hence it would

be of interest to examine the effects of bath application of Ni^{2+}, a specific T channel blocker previously shown to block low threshold inward calcium currents in DR neurones, on I_A amplitude. Theoretically this treatment would still allow TTX resistant release whilst inhibiting the voltage gated low threshold Ca^{2+} current. If an increase in I_A was still observed then an effect of low Ca^{2+} on neurotransmitter release would seem improbable.

Neurotransmitter mediated changes in I_A. Because of the inhibitory effect of 5-HT on extracellular firing activity in DR neurones it was important to determine if this purported neurotransmitter had any direct effect on I_A activity.

In a series of experiments to determine the effect of 5-HT on I_A no conclusive evidence was obtained; 5-HT caused an increase, a decrease or had no effect on I_A. In one experiment Fig. 3.35 5-HT could be seen to cause a small reducion in I_A together with a large increase in conductance. On washout the conductance state returned to control levels, and I_A further reduced. It is possible that the increased neuronal conductance seen during 5-HT application decreased the efficiency of the space clamp and hence caused an apparent decrease in I_A to be observed. This theory however would not account for the further decrease in I_A amplitude seen on washout when the conductance returned to control values. An action of 5-HT on a second messenger system can not be overlooked. The progressive decay in I_A may be due to the slow activation of a second messenger which was independent of the receptor mediated increase in conductance. The variability in the results however would tend to indicate that the changes in I_A amplitude observed during 5-HT application were probably coincidental with changes in impalement damage during the course of the experiments. That 5-HT probably had no effect on I_A was supported by the observation of Burlhis & Aghajanian (1987) that showed 5-HT had no effect on I_A amplitude at concentrations shown to suppress prepotential generation. Consequently it is unlikely that the inhibitory effect of 5-HT was mediated by an increase in I_A amplitude, as might be expected if 5-HT was to decrease DR firing activity by an action on I_A.

These results would suggest that 5-HT receptor activation had no direct effect on I_A channel activity. An alternative hypothesis may be proposed however whereby a tonic TTX resistant 5-HT release within the DR nucleus maximally activates I_A in control ACSF. Consequently any

further application of 5-HT would be ineffective in increasing I_A amplitude. It would be of interest therefore to determine the effects of known 5-HT antagonists on I_A amplitude before a definite conclusion is arrived at for the action of 5-HT on I_A.

Unlike the inhibitory effect of 5-HT extracellular application of noradrenaline (NA) showed an excitatory effect on raphe cell firing activity (Baraban et al 1978). These workers later demonstrated that the excitation could be inhibited by pretreatment with alpha - adrenoceptor antagonists. The order of potency of adrenergic agonists in evoking DR neurone firing gave the first indication that the receptor mediating the excitation was of the α_1 adrenoceptor category (Baraban & Aghajanian 1980). Further support came from the observation that prazosin a specific α_1 antagonist could antagonise the excitatory response to NA application in DR neurones (Marwaha & Aghajanian 1982). A subsequent preliminary intracellular study of proposed serotonergic neurones in the in vitro slice showed NA to evoke an increase in the spontaneous firing rate (VanderMaelen & Aghajanian 1983).

If NA was to increase the excitibility of DR neurones by an action on I_A it would be expected that a reduction in I_A amplitude would be observed. This was found to be true. Bath application of NA caused not only a marked decrease in I_A amplitude (Figs. 3.37 + 3.39) but also caused a decrease in membrane conductance and a hyperpolarising DC current was required to maintain the cell at the holding potential. The reversal potential for NA action was calculated to be -80mV which is close to the estimated reversal potential for a K^+ conductance as derived by the Nernst equation. Consequently NA would appear to act by closing membrane K^+ channels and thus causing a depolarisation. It is posssible that a non specific closure of K^+ channels was responsible for the decrease in I_A amplitude on NA application. On repeated administration however the depolarising effect of NA was seen to desensitise whereas NA could still evoke a decrease in I_A amplitude. This would suggest that NA acts as an agonist at two different subpopulations of receptors that are linked to different populations of K^+ channels. NA was seen to evoke a positive shift in the I_A voltage inactivation curve on initial application, on subsequent application the positive shift in the voltage inactivaton curve was abolished. This theory is however hard to reconcile with the observatiion of Aghajanian (1985) that NA acts

to alter the TOC by an action at an α_1 receptor. It would be of interest therefore to see if any residual effects of NA application on I_A occured following pretreatment with prazocin.

Voltage gated non-inactivating outward current, I_M. Although not thoroughly investigated, the non-inactivating outward current has all the characteristics of the I_M current first reported in vertebrate neurones by Brown & Adams (1980). The proposed outward potassium current was activated at membrane levels more depolarised than -40mV, and was characterised by an inward relaxation seen during hyperpolarising pulses. Support for a K^+ mediated conductance came from the observation that, with increasing hyperpolarising pulses, the inward relaxation decreased as the steps moved towards the K^+ reversal potential. This was also true of the outward relaxation seen on termination of the transient hyperpolarising pulses. The inward relaxation during the transient hyperpolarising pulse indicated that the potassium channels carrying the M current gradually close during the time course of the test pulse. Channel closure was indicated by the fact that membrane conductance falls during this relaxation, the fast ohmic step being larger at the start of the step than at the end. An opening of the M channels at -40mV is further supported with the observation that the steady state conductance doubles from 4.3 to 8.1nS with holding potentials changes from -50 to -40mV.

This non-inactivating outward current, although not directly involved in the regenerative pacemaker potential cycle, plays a direct role in the overall regulation of DR firing activity. The outward K^+ current and the concomitant increase in conductance activated at membrane potentials more depolarised than -40mV may in part be responsible for the apparent rectification seen with depolarising steps in current clamp experiments in the presence of TTX. This would therefore act as an important regulator of DR activity during periods of sustained excitatory synaptic inputs.

The M channels have been shown to be primarily regulated by cholinergic activation of muscarinic receptors (Brown & Adams 1980; Halliwell & Adams 1982) with acetylcholine acting on muscarinic receptors to cause an inhibition of I_M. In frog sympathetic neurones where I_M is activated at the resting membrane potential cholinergic inputs have been demonstrated to cause a slow depolarising post synaptic potential (Adams & Brown 1982). Similarly in hippocampal CA_1 neurones carbachol administration has been demonstrated to inhibit I_M

and cause a membrane depolarisation of sufficient magnitude to evoke burst firing (Malenka et al 1986). Several workers using different preparations have now shown that a variety of putative neurotransmitters act to inhibit I_M including leutinising hormone releasing hormone (LHRH), bradykinin and substance P (for a review see Brown 1988). In temporal hippocampal CA_1 neurones Colino & Halliwell (1987) have reported that bath application of 5-HT evoked a biphasic membrane response, hyperpolarisation followed by a depolarisation. The later depolarisation was associated with an inhibition of I_M. Although no depolarisation is observed following 5-HT application on DR neurones (see next chapter) it would be of interest to determine if 5-HT acts to modulate I_M in DR neurones.

In conclusion, this chapter has demonstrated that DR neurones posses a collage of passive and active membrane properties that would be required to maintain the constant intrinsic pacemaker activity reported in vivo. Further more detailed work is required to dissect the mechanisms by which neurotransmitters act on the individual conductances to alter this activity.

FIGURE LEGENDS

Fig. 3.1

Electrotonic potentials recorded intracellularly from DR neurones in reponse to graded hyperpolarising current steps. A. At the resting membrane potential, -63mV, hyperpolarising current steps of -.02nA evoke electrotonic potentials that showed no rectification with voltage deflections in the hyperpolarising range to -100mV. B, the current - voltage relationship in the hyperpolarising direction was linear and in this cell showed a membrane input resistance (Rm) of 174MΩ.

Fig. 3.1

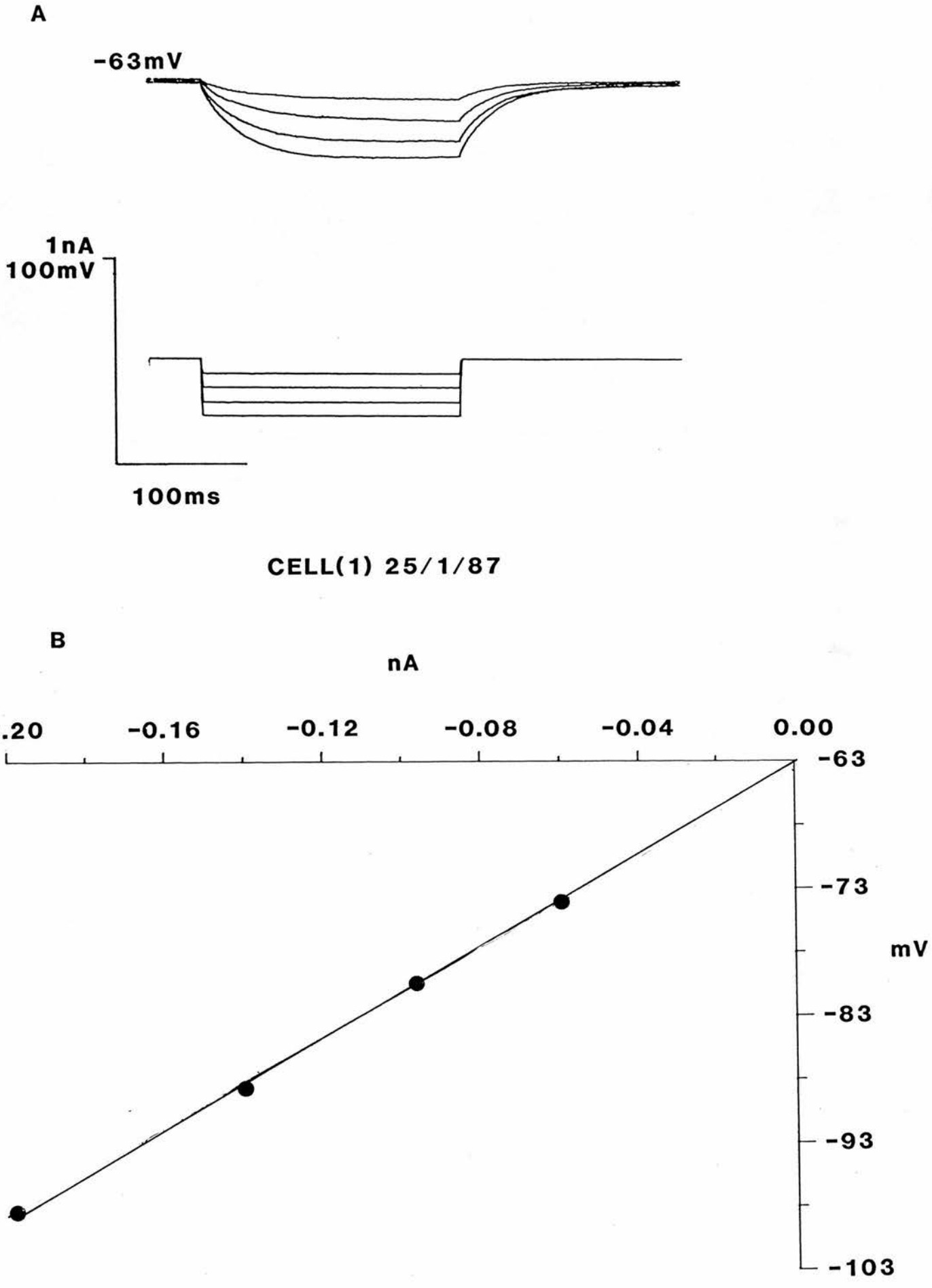
A
-63mV
1nA
100mV
100ms
CELL(1) 25/1/87
B
nA
-0.20
-0.16
-0.12
-0.08
-0.04
0.00
-63
-73
-83
-93
-103
mV

Fig. 3.2

The effect of changing membrane holding potential on the apparent input resistance. The reponse of DR neurones to manual voltage clamping at varying levels of hyperpolarisation fell into three distinct categories. Trace A, those that showed an increased membrane resistance at more hyperpolarised voltage levels. In this cell the resistance increased from 99MΩ at -60mV to 215MΩ at - 90mV. Trace B, those that showed no change in input resistance irrespective of the mebrane holding potential. In this cell the input resistance was 298MΩ at - 60mV and 290MΩ at -100mV. Finally trace C, those that showed a decrease in input resistance at more hyperpolarised holding potentials. In this cell the input resistance fell from 220MΩ at -60mV to 160MΩ at -100mV.

Fig. 3.2

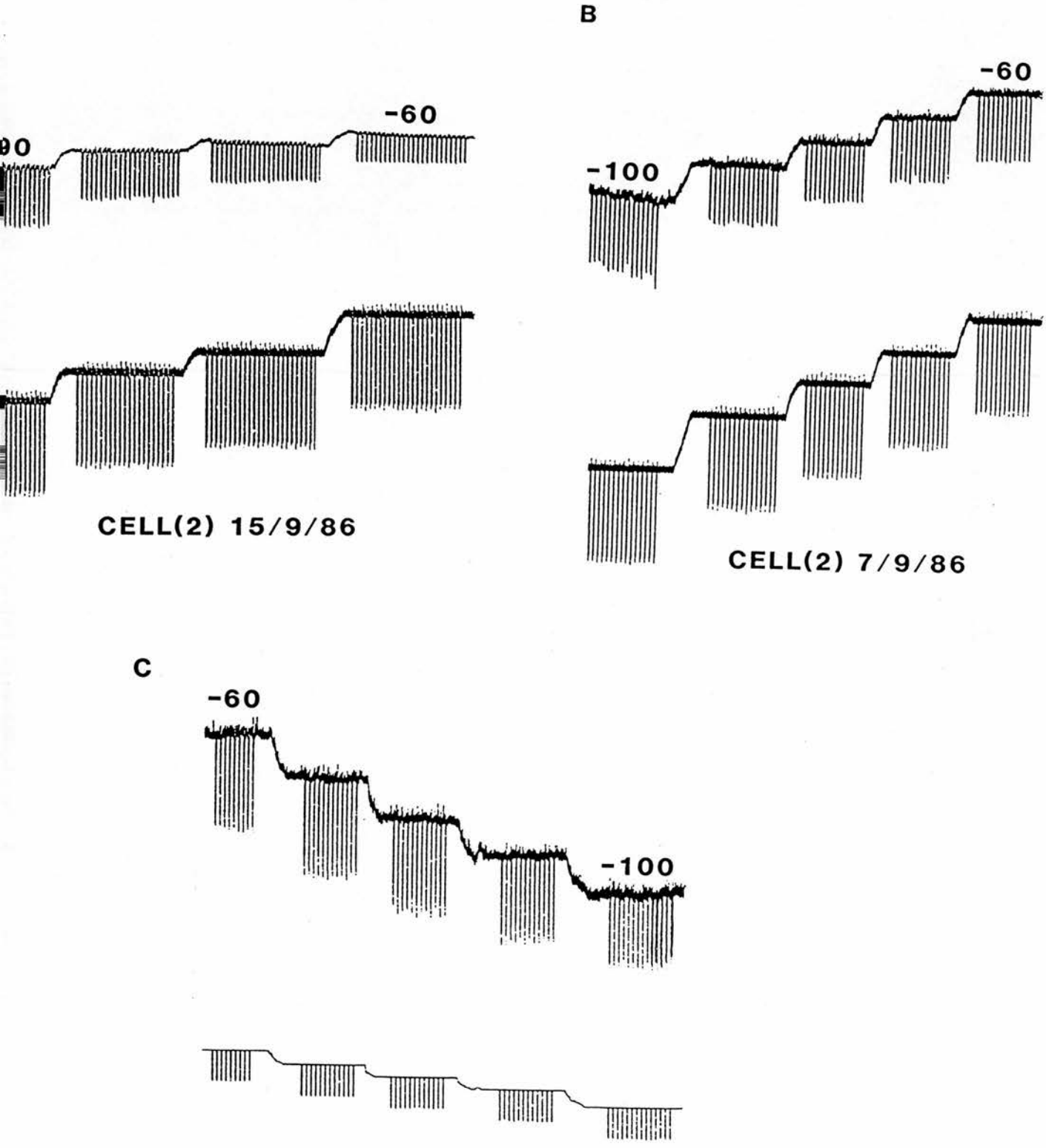

Fig.3.3

The effect of tetrodotoxin (TTX) on active and resting membrane properties of dorsal raphe neurones in vitro. In control artificial cerebrospinal fluid (ACSF), upper trace (A) the voltage response evoked by the application of graded (200 msec) hyperpolarising and depolarising current pulses, lower trace. Small (0.05 nA) depolarising pulses evoke an all or none action potential (-71 mV) followed by a characteristic AHP. In (B) bath application of TTX (1μM) graded (200 ms) hyperpolarising current pulses evoke greater voltage deflections than seen in (A). Depolarising current pulses up to 0.3nA failed to evoke an all or none action potential however a small slow depolarising potential was observed. In (c) current-voltage plots obtained from (A) and (B) plateau values (arrows). The membrane input resistance, as determined by the slope of the individual regression lines, increased from 184MΩ in control ACSF to 252MΩ in 1μM TTX. Membrane hyperpolarisation (7mV) in the presence of TTX was offset by the injection of positive DC current. Extrapolation of regression lines for control and TTX treatment showed a reversal potential of -49mV.

Fig. 3.3

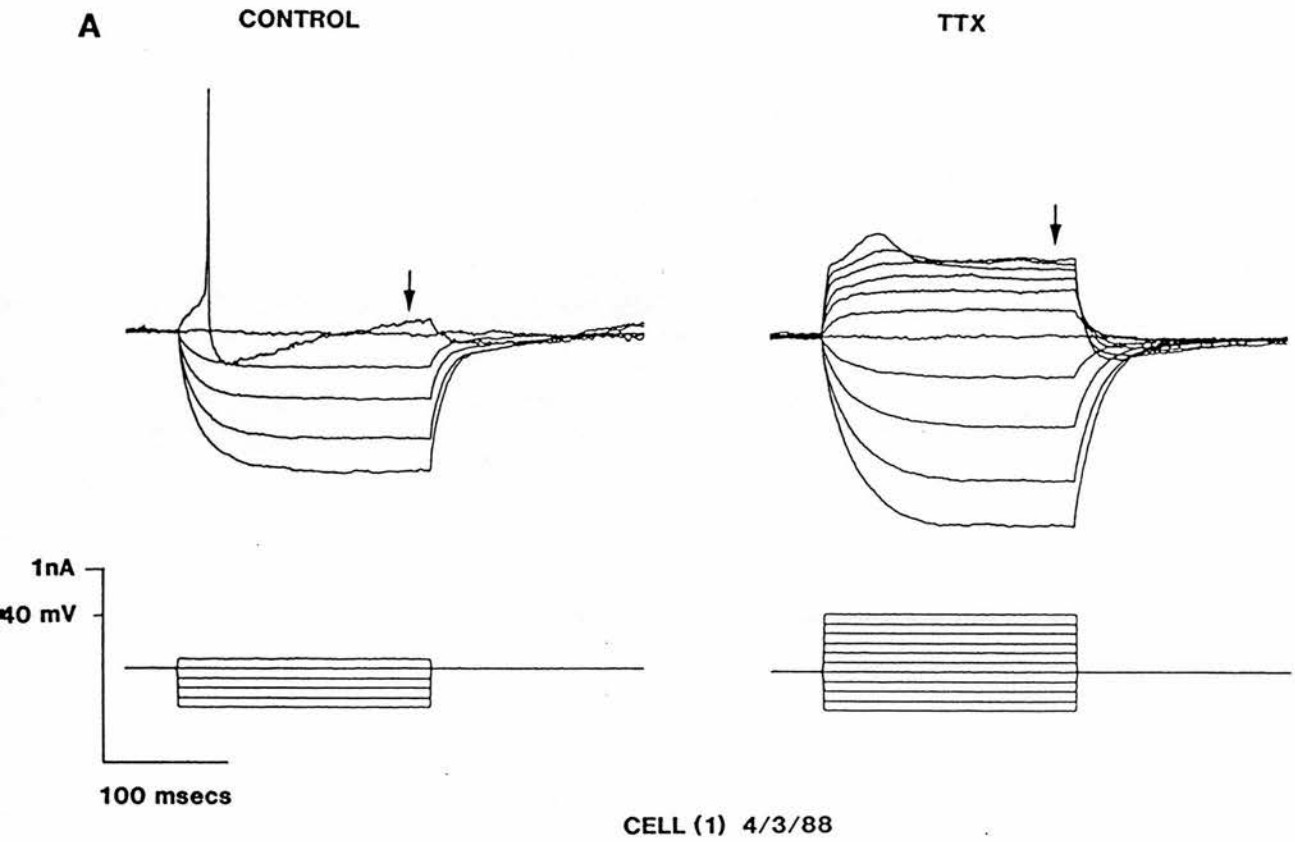
A
CONTROL
TTX
1nA
40 mV
100 msecs
CELL (1) 4/3/88

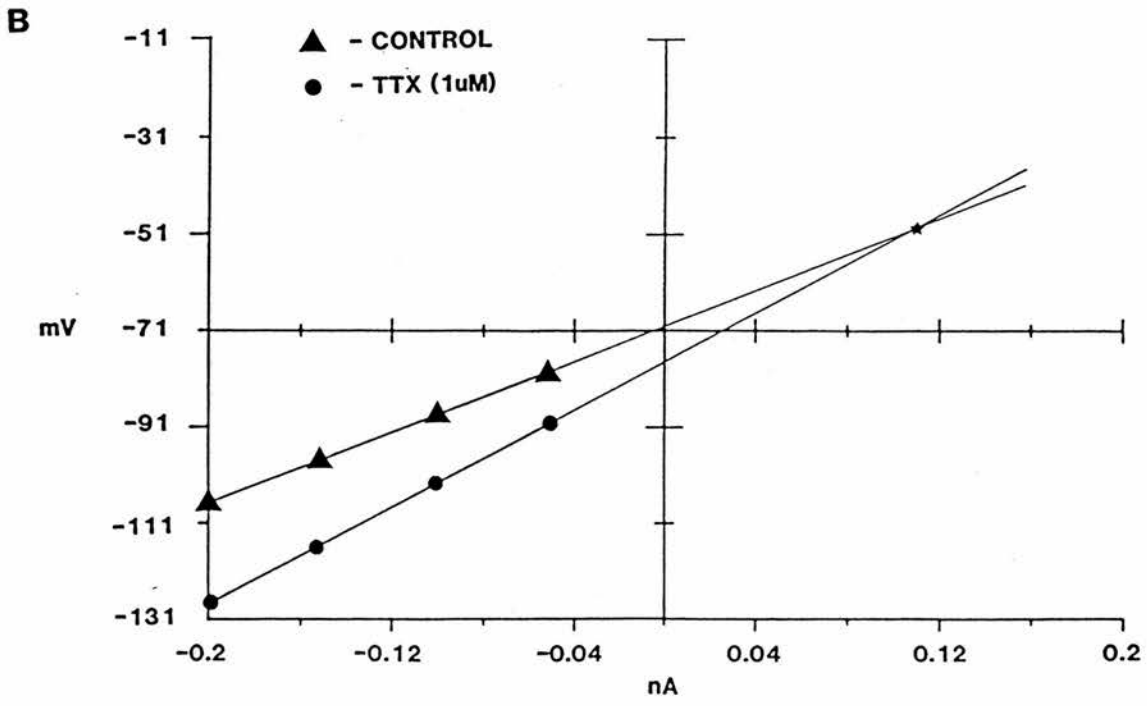
B
▲ - CONTROL
● - TTX (1uM)
-11
-31
-51
mV
-71
-91
-111
-131
-0.2
-0.12
-0.04
0.04
0.12
0.2
nA

Fig.3.4

Semilogarithmic plots of log(1-V/Vmax) against time to determine the time constant (g) of the exponential membrane charging curve. In the same neurone as Fig.3.3 the voltage response to the smallest hyperpolarising current step (0.05nA) was used to calculate g and hence avoid any voltage activated membrane properties that may be activated with larger current commands. In control ACSF (A) membrane charging produced a straight line single exponential fit with a time constant (g) of 15 ms. (B) in the presence of TTX (1μM) the g increased to 24 ms.

Fig. 3.4

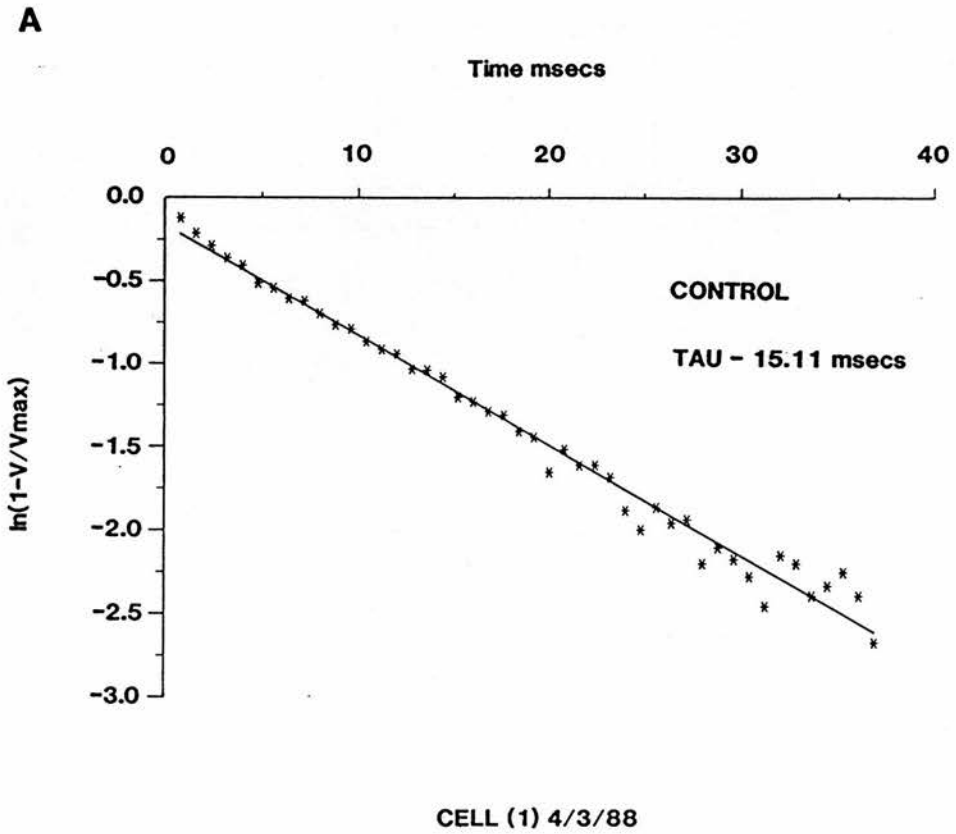

CELL (1) 4/3/88

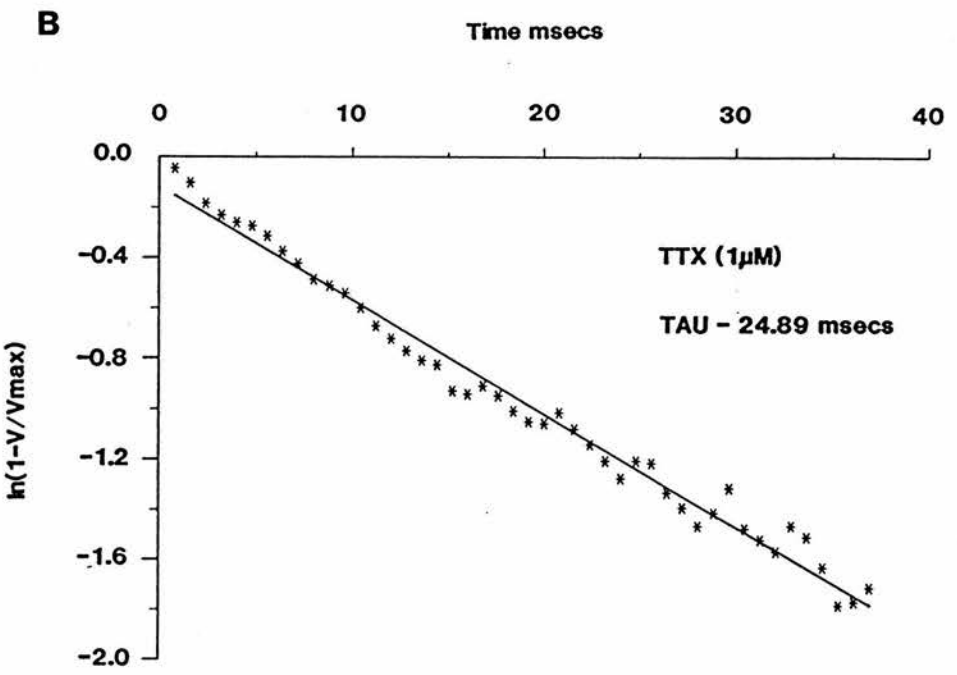

Fig.3.5

The effect of TTX on spontaneous postsynaptic potentials recorded with 3M KCl filled glass microelectrodes. At rest (-59mV) many small fast rising potentials can be seen on continuous oscilloscope sweeps, traces A-D. The initial downward deflection in trace A is a 10mV calibration pulse. Occasionally the depolarising potentials can be seen to summate (star, sweep D) Within 10 minutes of TTX application, trace E, the spontaneous depolarisations are abolished.

Fig. 3.5

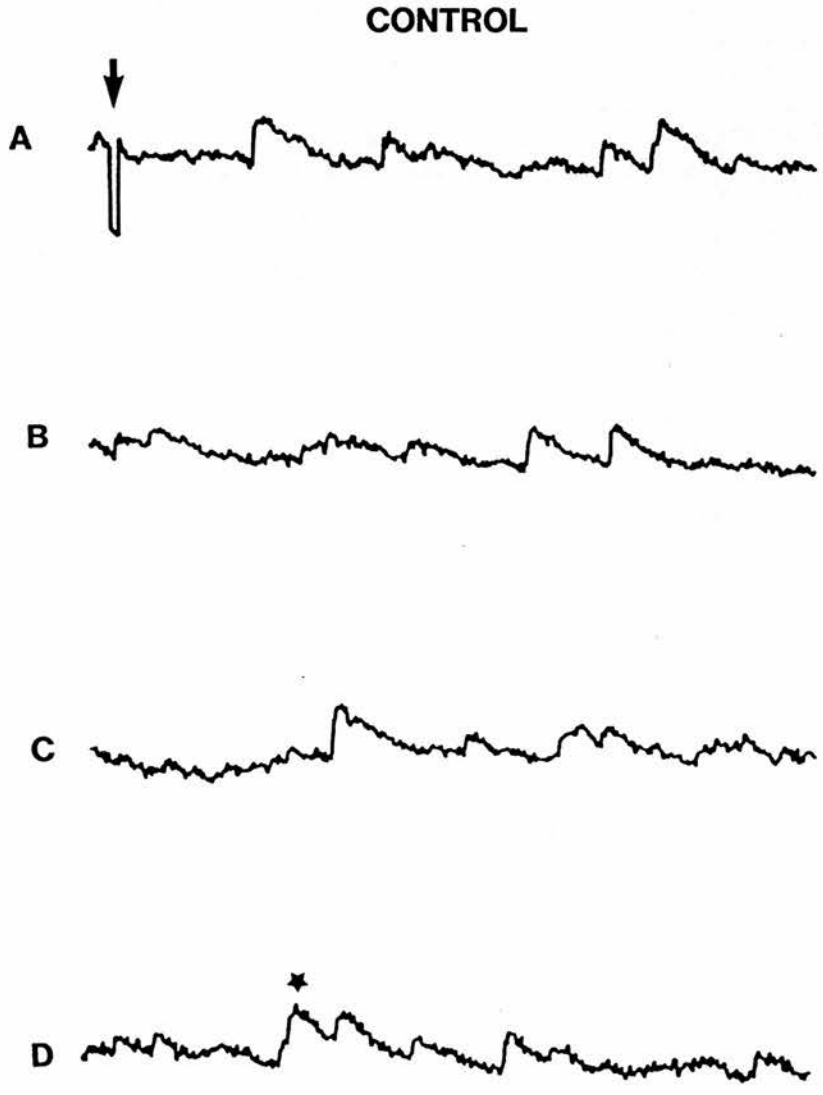

Fig. 3.6

Intracellular recordings from dorsal raphe neurones in vitro. Cells were impaled using glass microelectrodes (20 -90 MΩ) filled with 3M KCl. (A) Upper trace, spontaneous action potentials recorded intracellularly from a dorsal raphe neurone. Firing frequency ranged between 0.3-2 Hz. Resting membrane potential was -60 mV with fast overshooting 88 mV spikes. (B) Middle trace, on a faster time base a sequence of events can be observed to make up the spike related events 1) a slow depolarising prepotential which precedes an all or none fast action potential 2), leading to a long lasting afterhyperpolarisation (AHP) with a rapid onset 3), and a gradual (200 ms) return 4) to the resting membrane level before another sequence is initiated. (C) Lower trace, in the same neurone at a still faster time base the action potential can be seen to consist of a rapid rising phase, time to peak from resting potential was 1 ms. The falling phase showed a marked shoulder probably in part due to a calcium mediated component of the action potential. The repolarisation overshoots the resting membrane potential to produce a transient AHP of 13 mV.

Fig. 3.6

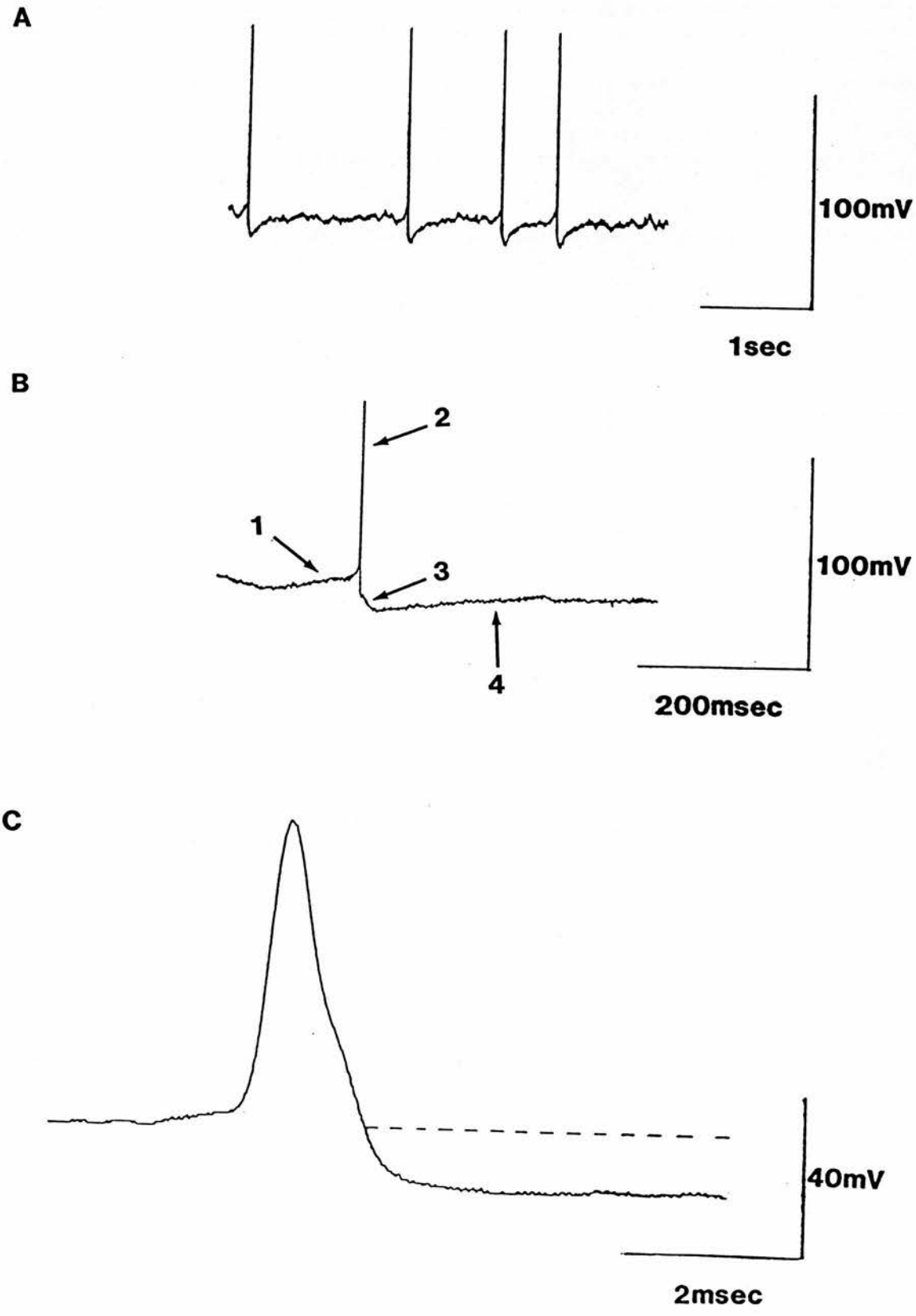

CELL (1) 14/2/87

Fig.3.7

Asymmetrical electrotonic potentials recorded in response to graded (200ms) hyperpolarising and depolarising curent steps. A , in the presence of TTX, voltage deflections, upper trace, evoked by hyperpolarising current steps were always seen to be larger than those produced in response to depolarising current steps of a similar amplitude. Note that AHP's follow the larger depolarisations. B, a current-voltage plot of the plateau responses recorded in A (arrow). The current-voltage relationship was linear for hyperpolarisations. In the depolarising direction however the responses showed a marked rectification.

Fig. 3.7

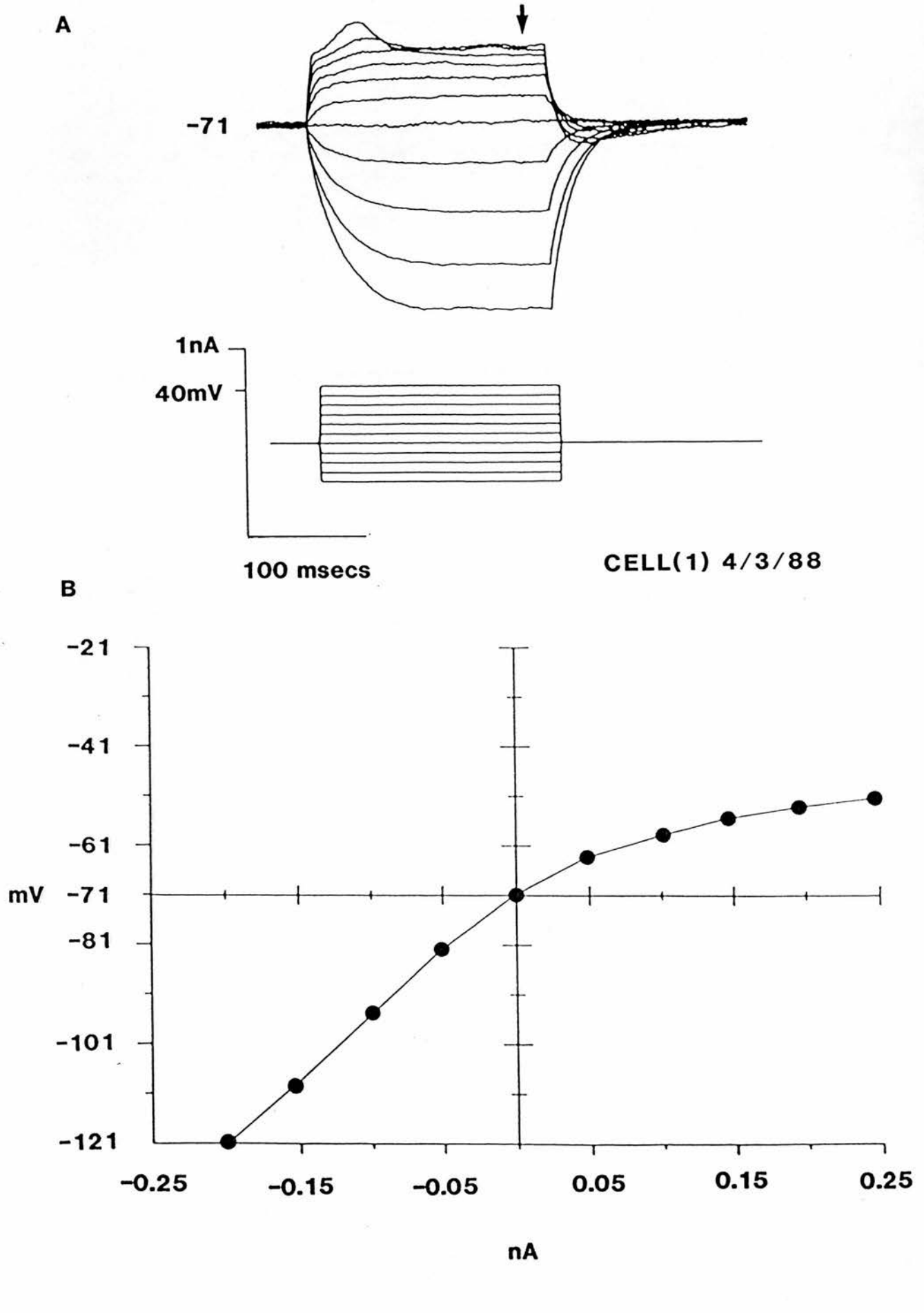
A
-71
1nA
40mV
100 msecs
CELL(1) 4/3/88
B
-21
-41
-61
mV
-71
-81
-101
-121
-0.25
-0.15
-0.05
0.05
0.15
0.25
nA

Fig.3.8

Voltage dependent depolarising potentials in the presence of TTX. When the resting membrane potential was manually voltage clamped at -69mV, with depolarising DC current, a 200 ms 0.1nA depolarising current step (lower traces) evoked a passive membrane perturbation. At rest, -59mV, a similar current step evoked a low threshold depolarising prepotential. Manually clamping at -49mV with hyperpolarising DC current injection the same current step evoked a low threshold depolarising prepotential on which rides a TTX resistant high threshold all or nothing depolarising potential (80mV) followed by an AHP.

Fig. 3.8

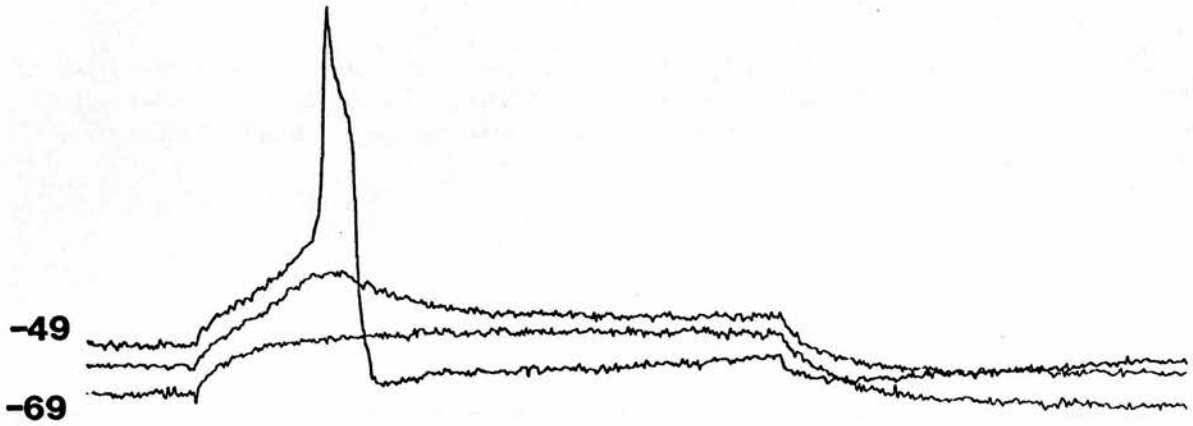

CELL (2) 12/9/86

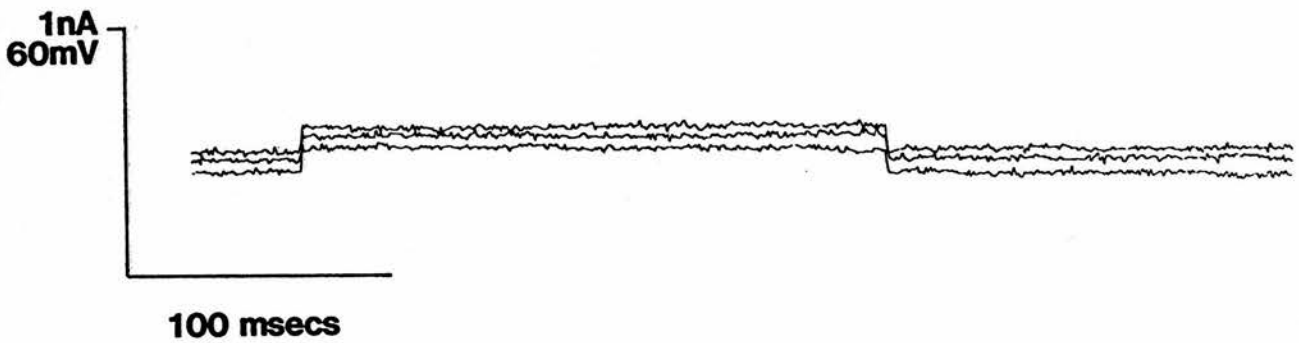

Fig. 3.9

The effect of TTX and Cd2+ (1mM) on rebound potentials observed following hyperpolarising electrotonic potentials. In control ACSF, A, an action potential followed by an AHP could be observed following a hyperpolarising electrotonic potential evoked in response to a 0.1nA hyperpolarising current step (lower trace). No spike activity was observed in the absence of a hyperpolarising current command. Following bath application of TTX (1ΩM) the action potential was abolished however a small slow depolarising potential and subsequent AHP were recorded on termination of the hyperpolarising current pulse. Addition of Cd2+ (1mM), a calcium channel blocker, abolished the rebound prepotential and following AHP. Note Cd2+ caused a 10mV depolarisation hence the cell was manually voltage clamped at the pre cadmium membrane potential, -58mV.

Fig. 3.9

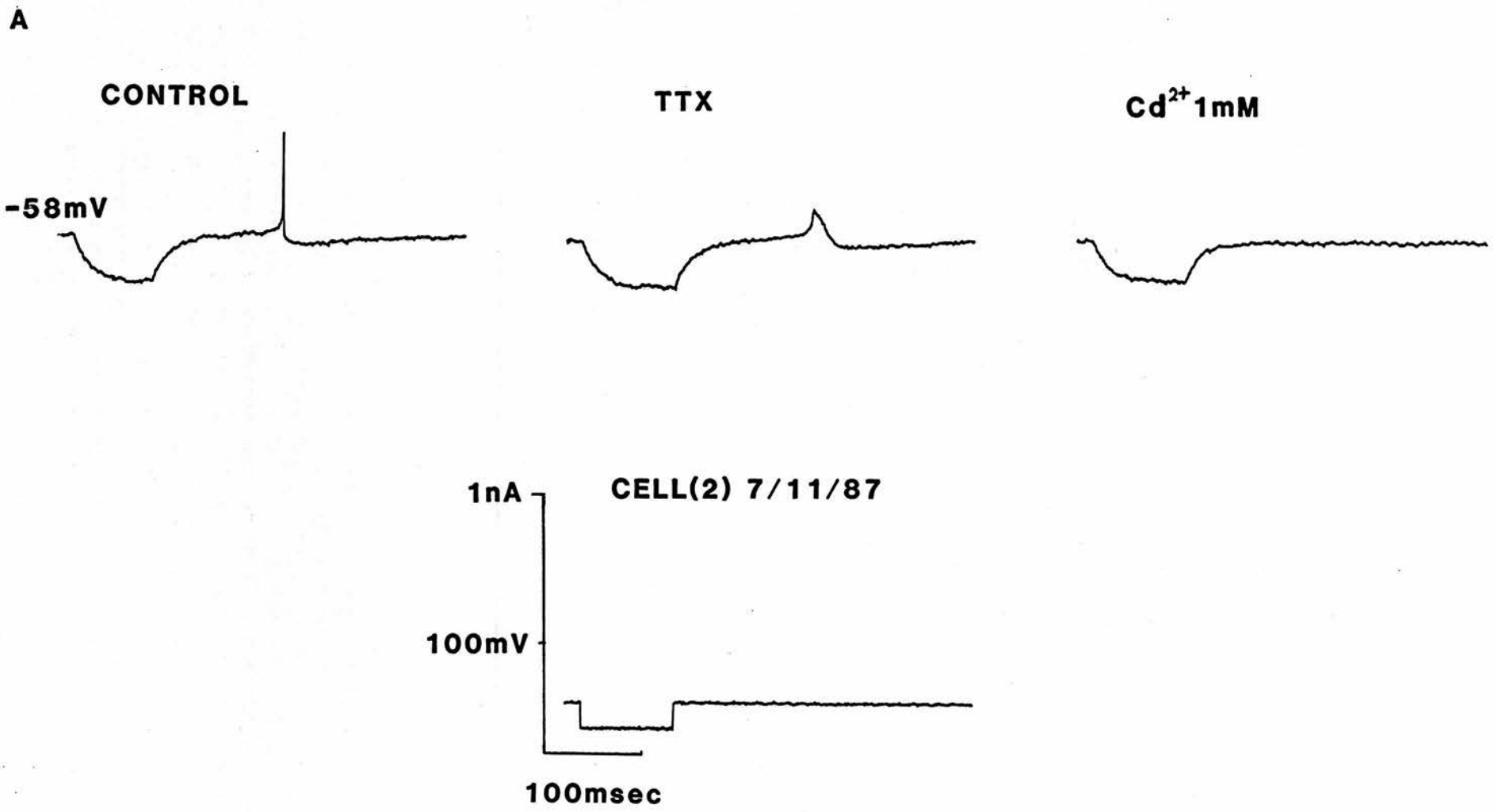

Fig. 3.10

The effects of the Co2+ on high threshold depolarising potentials in dorsal raphe neurones. A, graded (150ms) depolarising current steps to 0.1nA (lower trace), evoke a high threshold all or none depolarising potential (63mV) (upper trace). B, in the same cell pretreatment with 500μM Co2+ abolishes the high threshold depolarising potential to 100ms depolarising current steps as high as 0.3nA. Pretreatment with Co2+ also abolished the afterhyperpolarisation associated with the high threshold depolarising potential.

Fig. 3.10

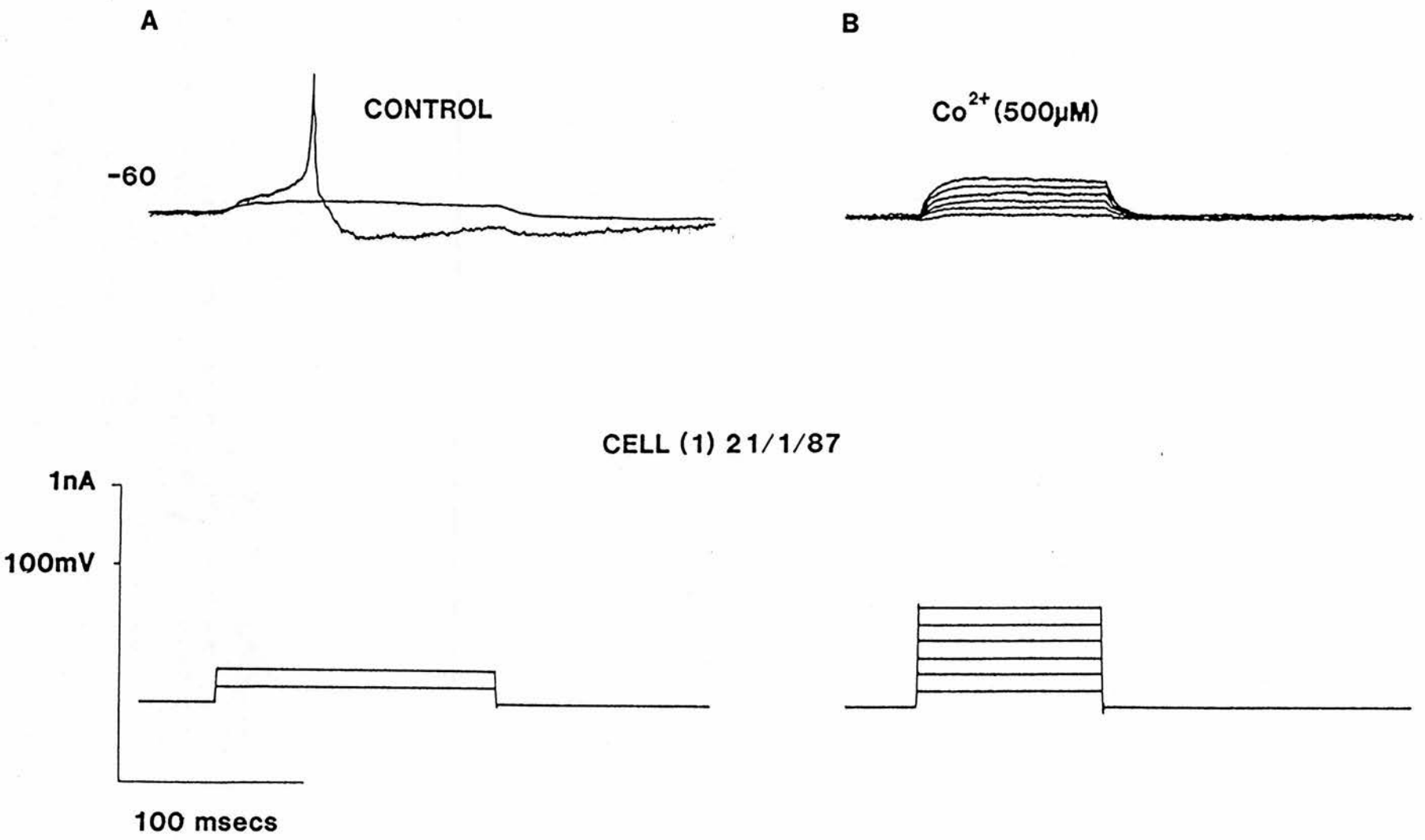

Fig.3.11

The effect of membrane potential on the afterhyperpolarisation (AHP). A, at -77mV a 3ms, 0.3nA depolarising current step generates a fast 2ms action potential followed by an AHP reaching a peak of 9mV after approximately 15ms. B, manual voltage clamping at -87mV by injection of hyperpolarising DC current causes a reduction in the AHP to 4mV. A further hyperpolarisation to -97mV caused the reponse to reverse, producing an afterdepolarisation. Note the peak action potential amplitude in each figure is 74mV. The peak of the action potential is truncated during the digital conversion of the analogue response. The reversal potential of the AHP must lie between -87 and -97mV.

Fig. 3.11

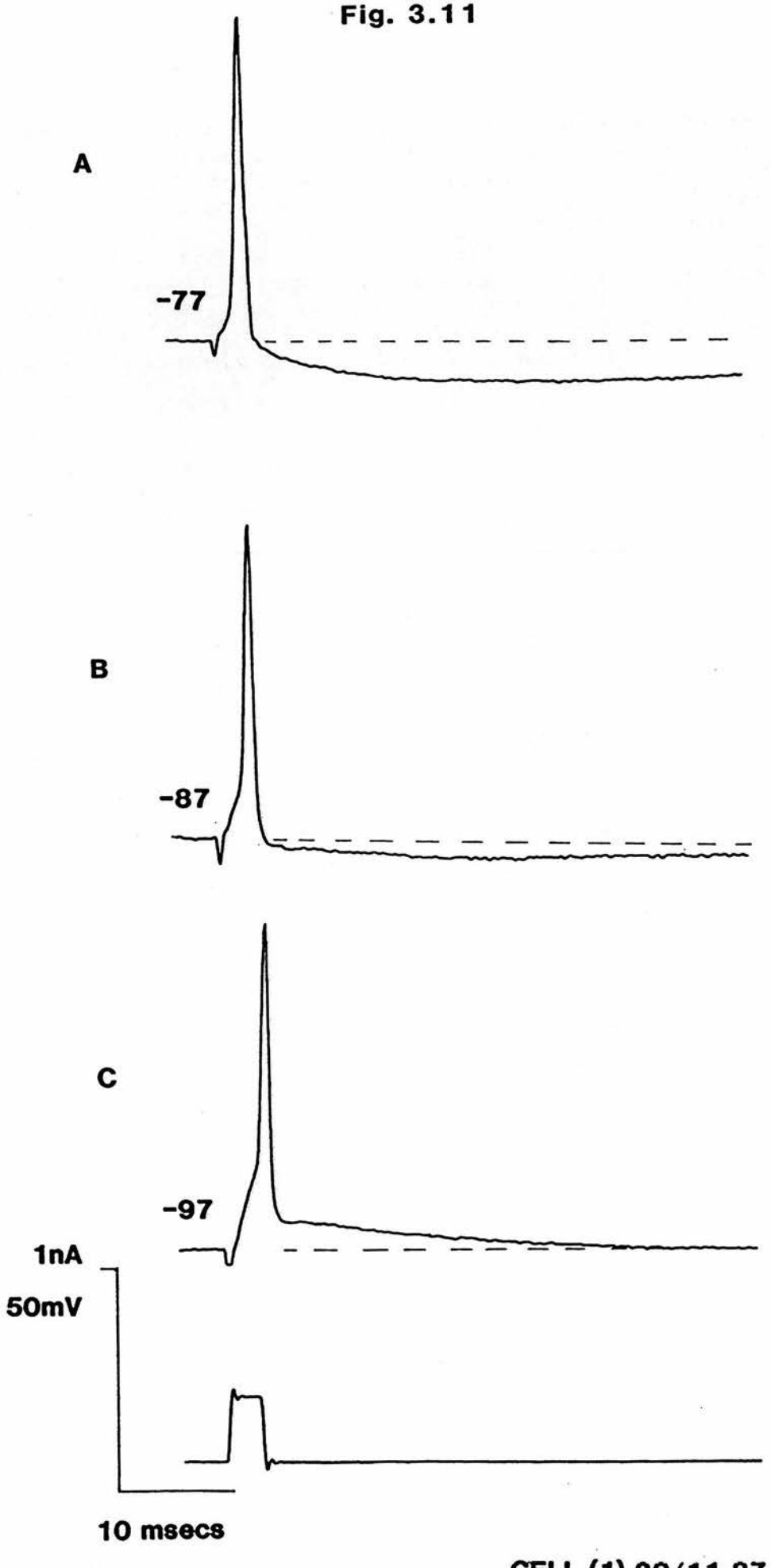

Fig. 3.12

Voltage dependent reversal of the AHP observed following high threshold spike generation in TTX. In the presence of 1μM TTX activation of a high threshold calcium spike by a short (3ms) suprathereshold (1.8nA) depolarising current pulse evoked a 17mV AHP which slowly returned to the resting membrane potential (-68mV) after periods of greater than 150ms. Manual voltage clamping at -78mV reduced both the amplitude (8.5ms) and the duration (150ms) of the AHP. At -88mV the voltage deflection reverses and the high threshold calcium spike evokes an afterdepolarisation. Clamping at -98mV caused both the amplitude and the duration of the afterdepolarisation to increase. Hence the reversal potential of the AHP following calcium spike generation lies between - 78 to -88mV.

Fig. 3.12

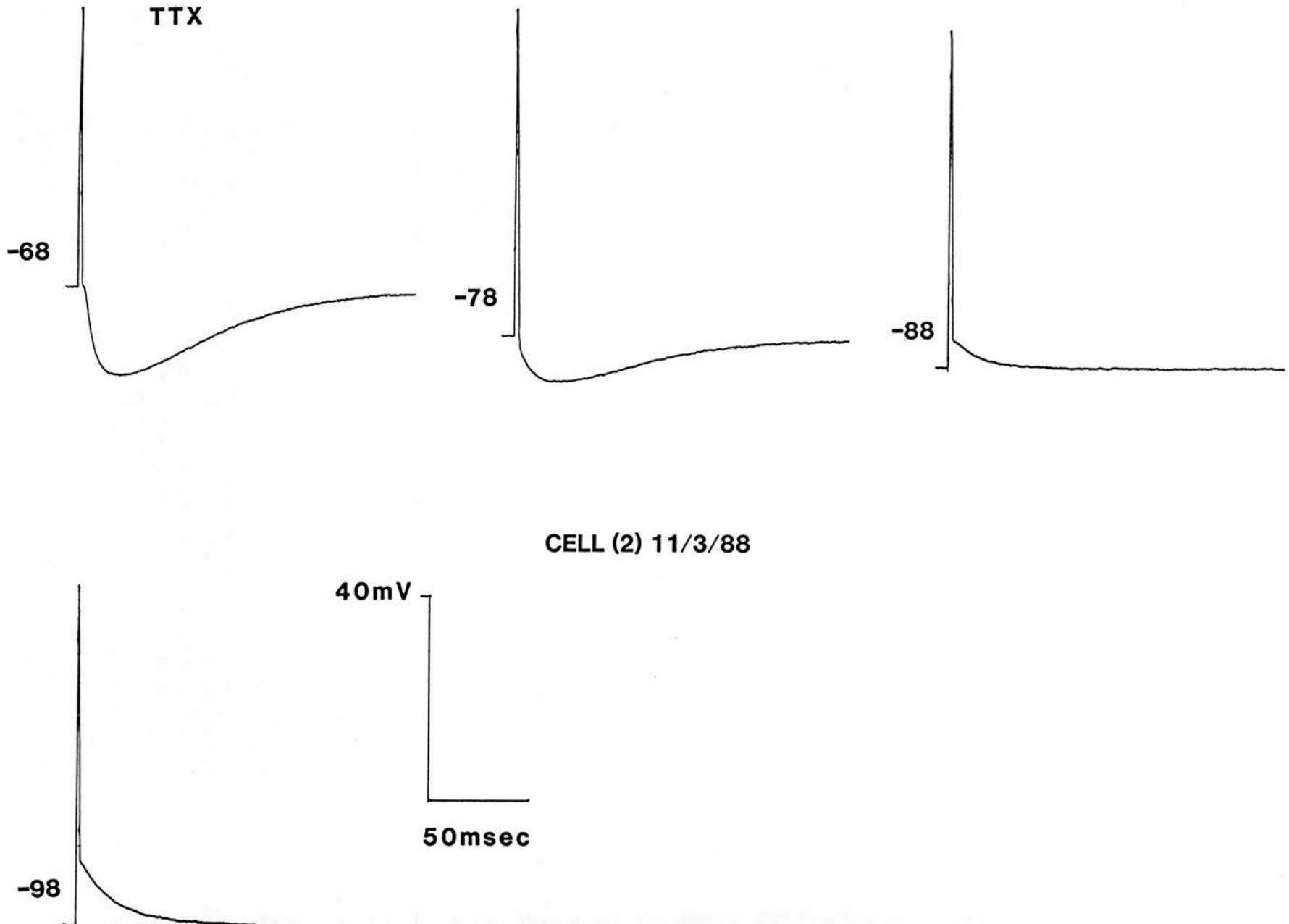

Fig. 3.13

Voltage dependent outward tail current following short duration depolarising step commands in voltage clamp in the presence of TTX. The cell was voltage clamped at -60mV with a holding current of +0.09nA. Increasing (10ms) step commands from -30 to 0mV in 10mV increments caused the onset of a voltage dependent outward tail current. Holding the cell at -60mV and steping to -30mV evoked no tail current (A). Steping more positive than -30mV evoked a graded outward tail current. Peak current amplitude ranged from 0.14nA at -20mV to 0.37nA at 0mV steping potential, with time constants (τ) of 29ms and 84.8ms respectively. Note voltage step commands to potentials greater than -20mV were not fully acheived due to problems with the voltage clamp. Tail current values should therefore be regarded as qualitative not quantitative.

Fig. 3.13

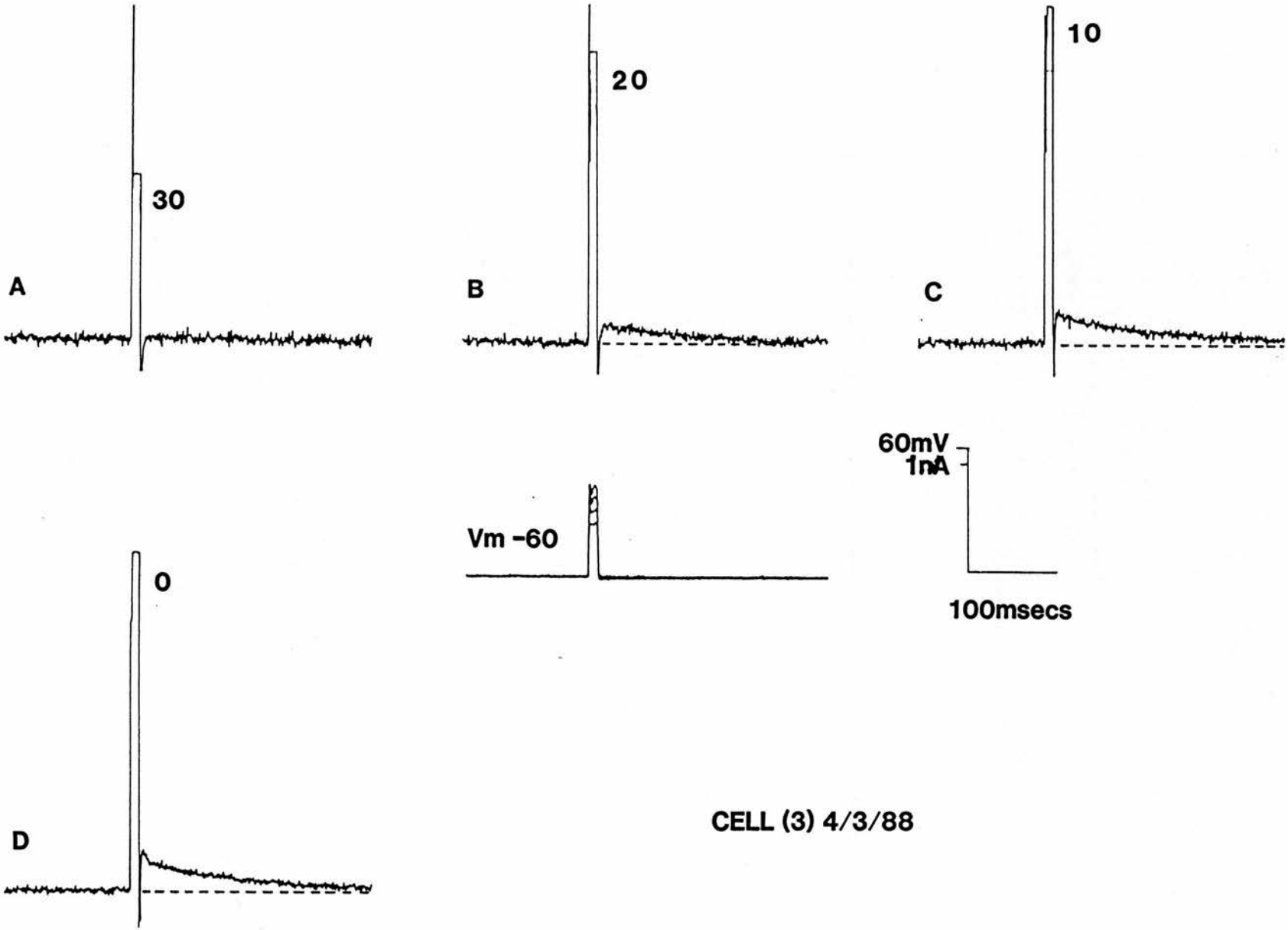

Fig. 3.14

The effect of apamin on AHP's. A, at rest -77mV short (3ms) depolarising current pulses (0.3nA) evoke an all or none action potential followed by an AHP which reaches a peak (9mV) after approximately 15ms. B, bath application of apamin (100nM) caused a long lasting inhibition of the AHP. Full recovery was never observed after prolonged washout of 100nM apamin. Note the action potential peak amplitudes in A and B had been truncated during either analogue to digital or digital to analogue conversion, as in Fig. 3.10.

Fig. 3.14

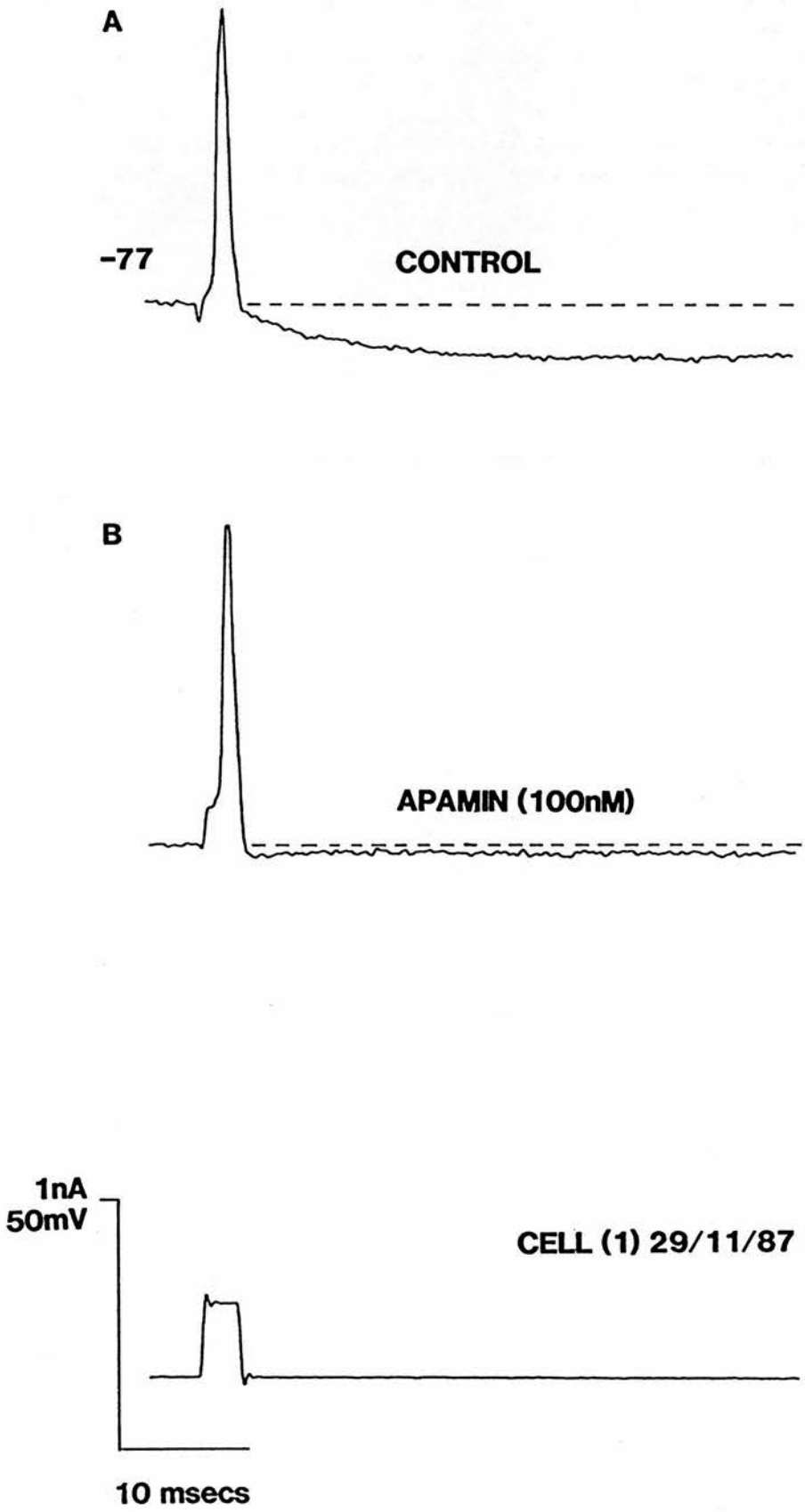

Fig. 3.15

An apparent effect of 5-HT on the amplitude and duration of AHP's evoked following high threshold spike activation in TTX. In control ACSF highthreshold calcium spike actvation evokes a 17mV AHP which slowly decays back to the resting potential (-68mV) after periods of greater than 150ms. Middle trace, bath application of 5-HT (100μM) causes a reduction in the amplitude of the AHP, 10mV peak, and a decrease in the duration when the cell was manually voltage clamped to the resting membrane potential, with depolarising DC current injection. On washout the cell returned to the control resting membrane potential and the AHP recovered to control amplitudes, 17mv peak, and duration.

Fig. 3.15

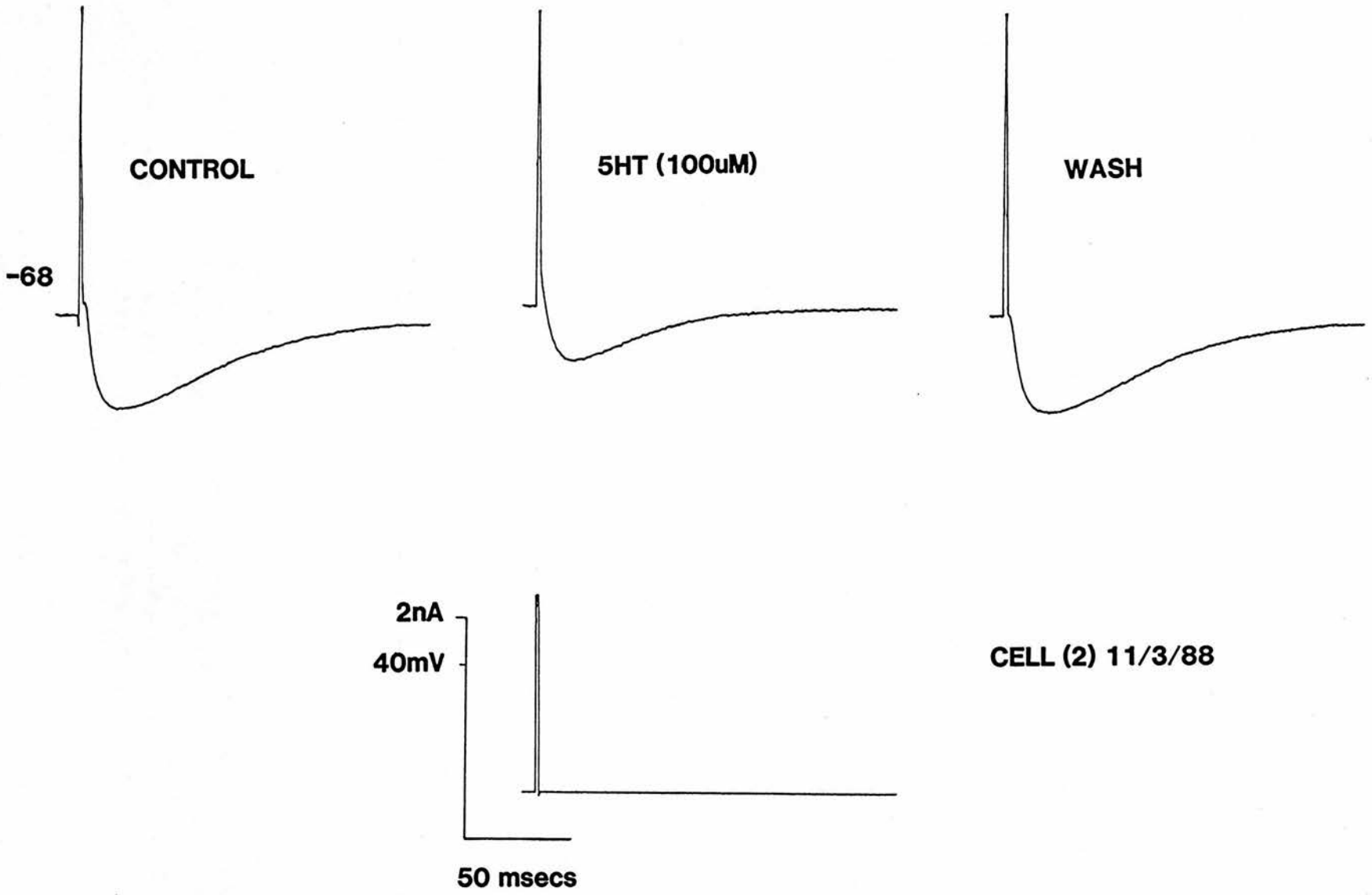

Fig. 3.16

The effect of membrane potential on the decaying phase of hyperpolarising electrotonic potentials. A, hyperpolarising electrotonic potentials from -65mV, in response to a single (200ms) hyperpolarising 0.1na current pulse (bottom trace) have a single exponential charging time course (see Fig. 3.4). The discharging voltage response however has an additional slow component. Manual hyperpolarisation of the membrane potential with hyperpolarising DC current showed that at -75mV the slow component was reduced and at -85mV it was abolished.

Fig. 3.16

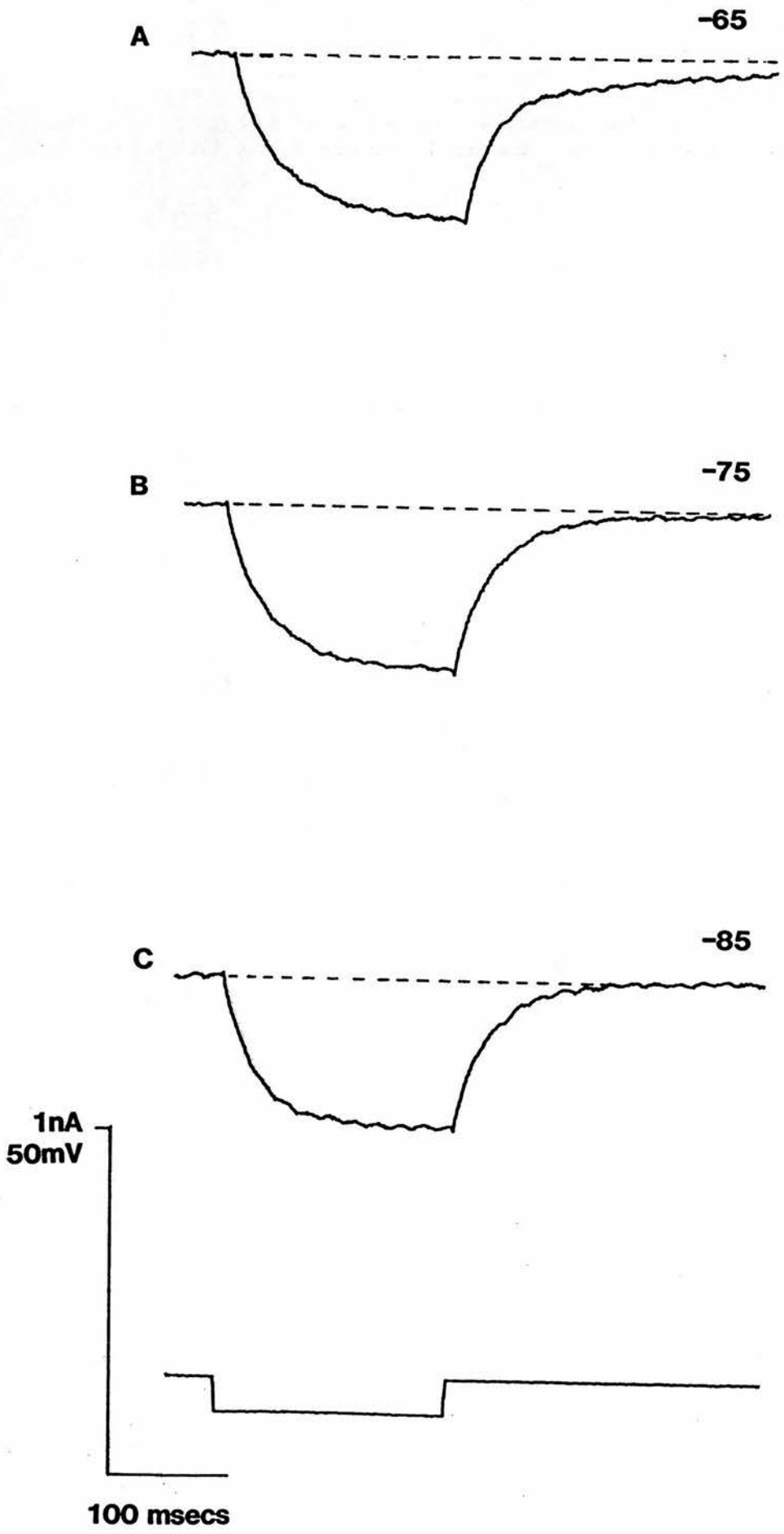

Fig. 3.17

The effect of membrane holding potential on active and passive conductances recorded in voltage clamp conditions. At rest -60mV (A) incremental hyperpolarising step commands (lower trace) evoke graded inward leakage currents. Holding the cell at the more depolarised level of -50mV (B) also caused graded inward leakage currents, however step commands to the more hyperpolarised levels evoke transient outward tail currents on termination of the step command. At a holding potential of -40mV (C) similar hyperpolarising step commands evoke markedly increased leakage currents. The response to the smaller hyperpolarising step commands also show a time dependent inward relaxation and a subsequent inward tail current on termination of the step command. Step commands from -40 to -80mV evoked an ever increasing transient outward tail currents in comparison to step commands to the same potential seen in trace B.

Fig. 3.17

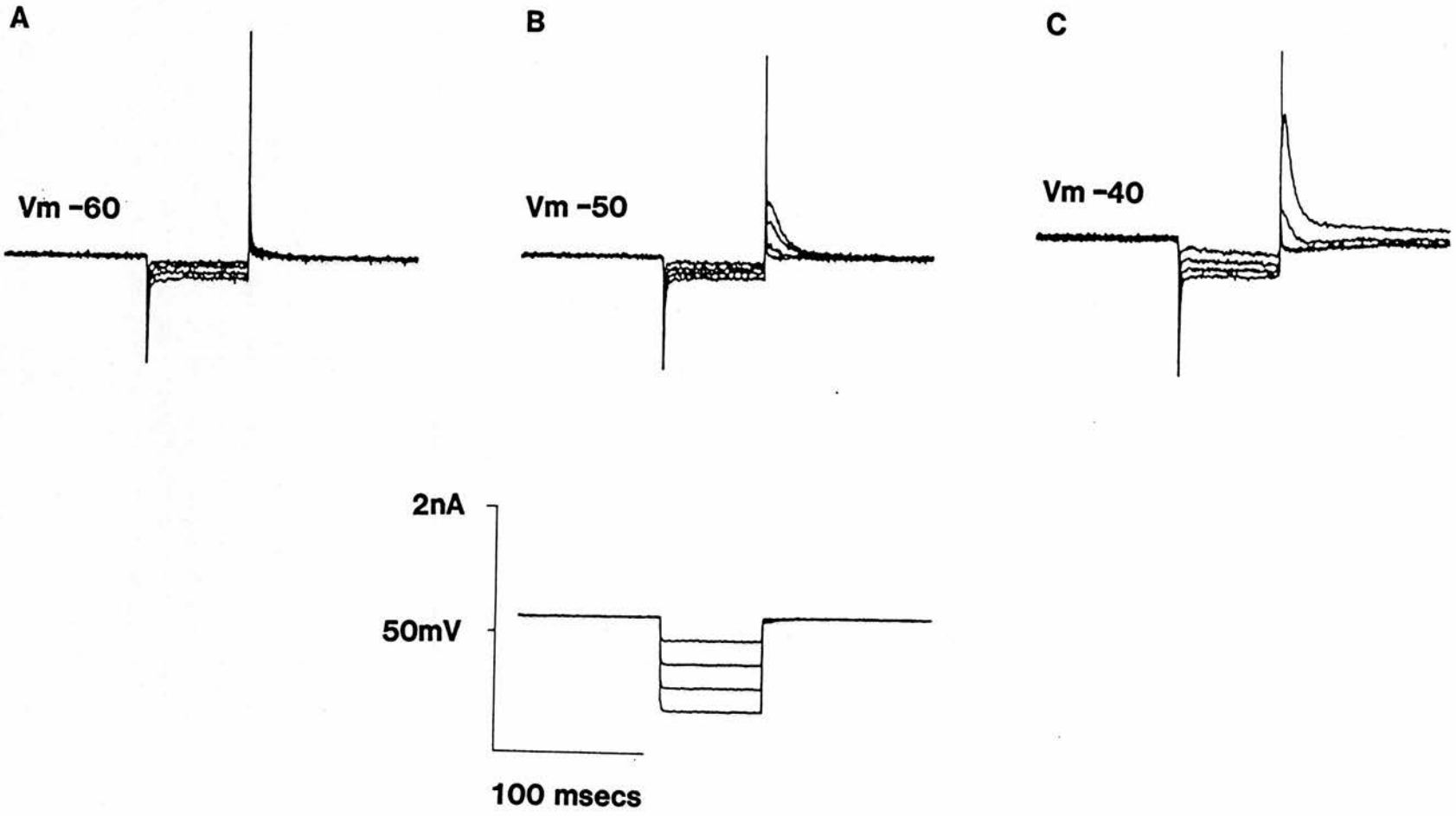

CELL (4) 4/3/88

Fig. 3.18

Steady state voltage - current analysis of membrane currents generated in a single cell held at three different membrane potentials (same cell as Fig. 3.17). At rest (-60mV) hyperpolarising step commands evoked leakage currents which resulted in a linear V/I relationship with a slope that corresponds to a conductance state of 4.3nS. On depolarisation to -55mV the same voltage step commands evoke graded leakage currents that are larger for each incremental step than at -60mV. The V/I plot however remained linear and shows an identical slope conductance of 4.3nS. Further depolarisation to a holding potential of - 40mV caused an inward relaxation to appear in the voltage step commands hence current values were taken when a plateau response had been reached (arrow in Fig. 3.16). Although the V/I plot at -40mV remains linear the slope increased greatly and corresponds to a conductance state of 8.1nS indicating that voltage gated channels had opened.

Fig. 3.18

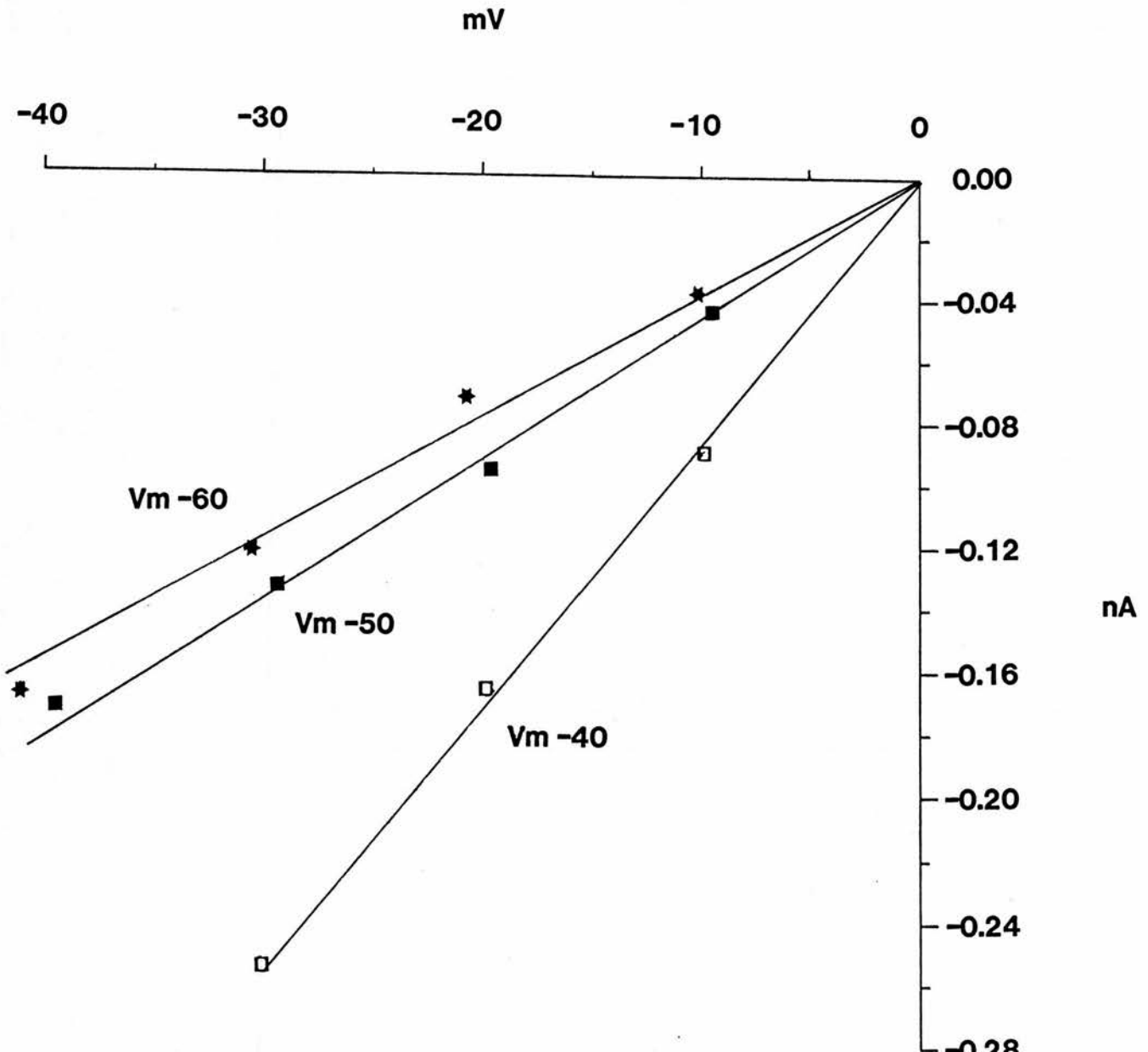

Fig. 3.19

The effect of TEA (10mM) on outward K+ currents. When voltage clamped at rest (-60mV) and stepped to more depolarised levels (C) the currents generated are both voltage and time dependent (A and B). A step from -60 to - 50mV evoked only an outward leakage current. stepping to levels greater than -40mV initially evoked a high amplitude transient outward current (1) followed by a slowly activating outward current (2). Commands to -30mV and above also ellicit an outward tail current on termination of the step command. In the presence of bath applied TEA (10mM) the slowly activating current was greatly reduced and the outward tail current abolished, the amplitude of the fast onset initial transient outward current however remained unchanged.

Fig. 3.19

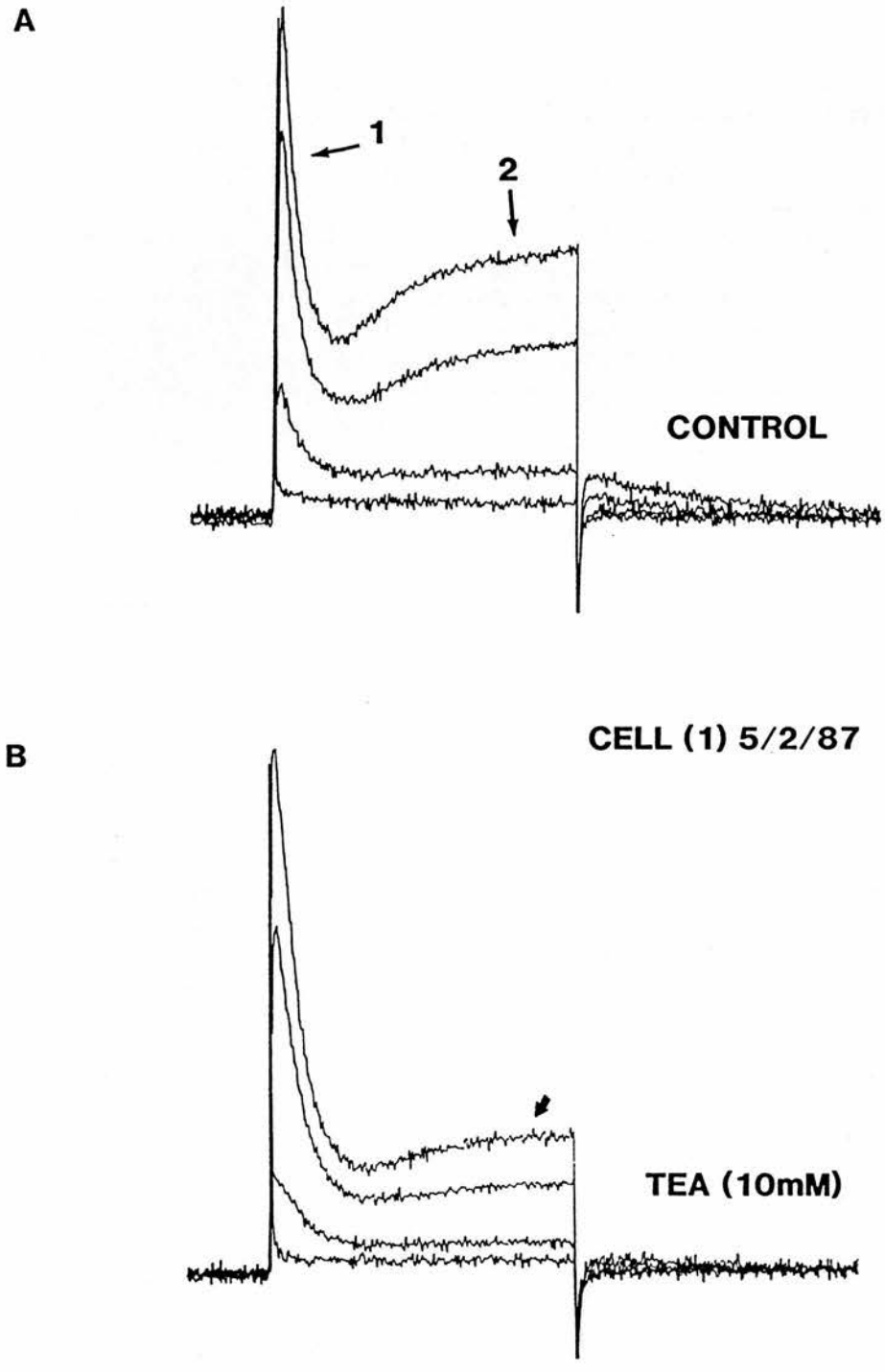

Fig. 3.20

The effect of TEA on IA time constant of inactivation. In control ACSF step depolarisations from -60mV to -25mV evoked a fast TOC which , when ln (1- V/Vmax) was plotted against time (ms), showed a single exponential time constant of inactivation (g) of 6ms during the first 20ms of the decay. Step commands to the same depolarised level in the presence of TEA (10mM) evoked a TOC which showed a time constant of inactivation of 7ms.

Fig. 3.20

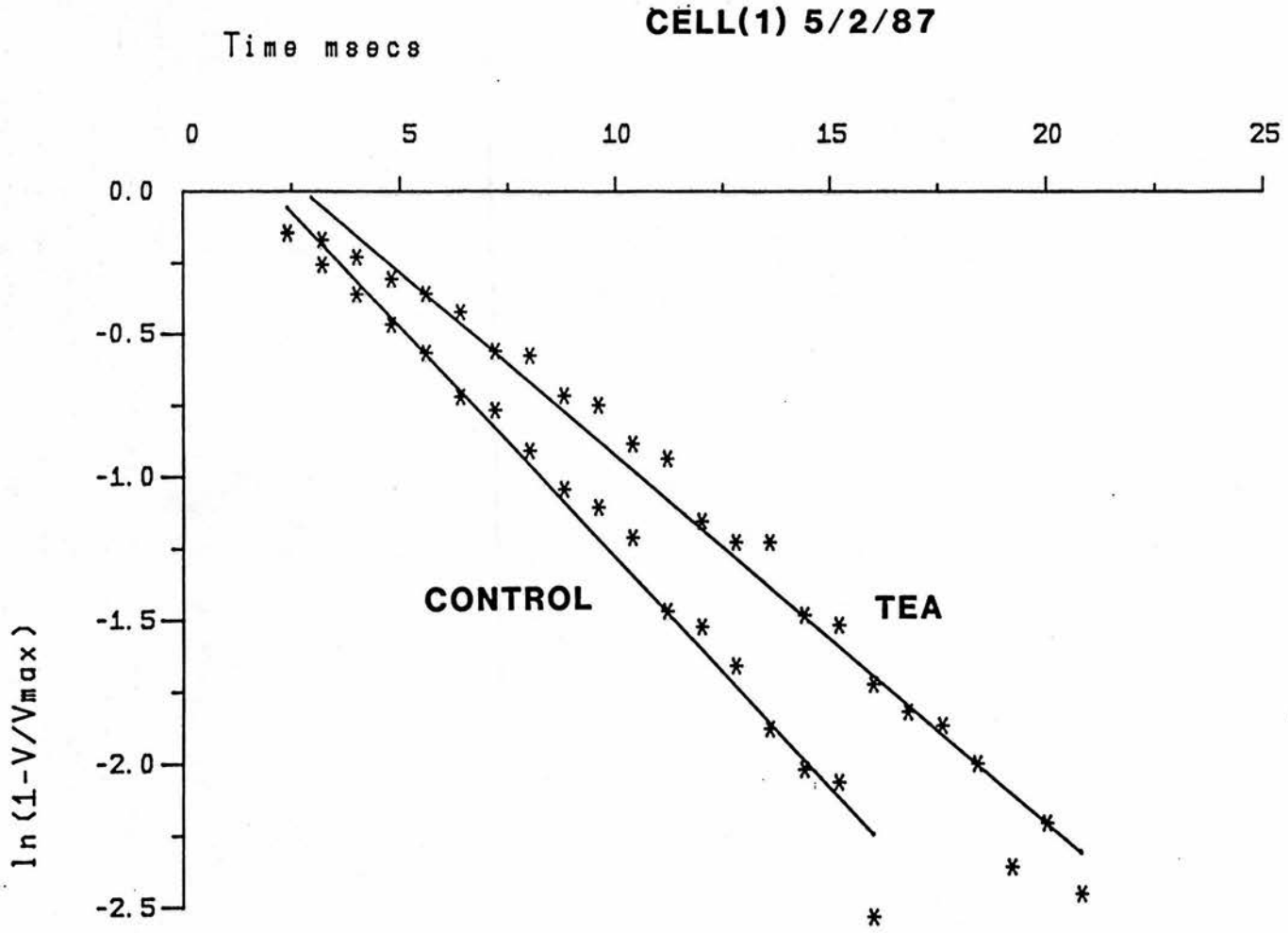
CELL(1) 5/2/87
Time msecs
0
5
10
15
20
25
0.0
-0.5
-1.0
-1.5
-2.0
-2.5
ln(1-V/Vmax)
CONTROL
TEA

Fig. 3.21

The dual pulse voltage clamp protocol used to determine the activation and inactivation characteristics of A like currents. A, activation properties, holding at -67mV and stepping to -52mV in 5mV increments evoked a graded outward transient current (lower trace) following a constant prepulse step command to -87mV (upper trace). To determine inactivation properties, B, prepulse step commands to -97mV in 10mV increments preceded a constant test step command to -52mV (upper trace). Lower trace, currents evoked in reponse to the inactivation protocol. Note in both A and B final trace the current amplitude evoked caused clamping problems in the voltage protocol.

Fig. 3.21

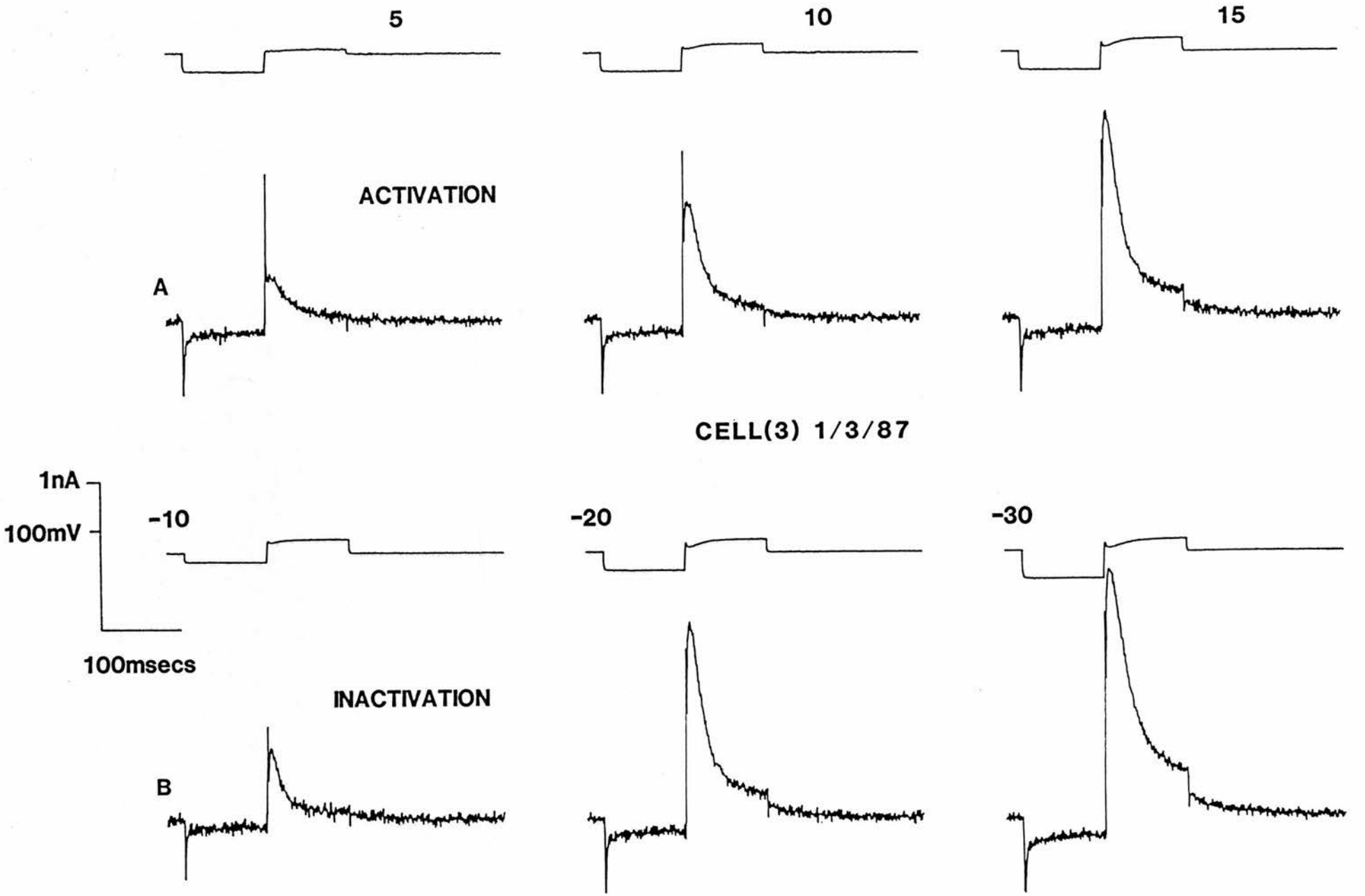
5
10
15
ACTIVATION
A
CELL(3) 1/3/87
1nA
100mV
-10
-20
-30
100msecs
INACTIVATION
B

Fig. 3.22

Plots of ln (1-V/Vmax) against time for currents evoked during activation and inactivation protocols. Both activation and inactivation protocols evoked A like currents that showed single expoential time constants of decay that were dependent on the amplitude of the current evoked. In the same cell as Fig. 3.20 the A current generated (A final trace) (1.39nA) following a fixed prepulse step command to -87mV and a depolarising step command to -52mV showed a time constant of decay of 25ms. During the inactivation protocol a prepulse step command to -97mV followed by a fixed depolarisation to -52mV evoked an A current (1.66nA) that showed a time constant of decay of34ms.

Fig. 3.22

CELL(3) 1/3/88

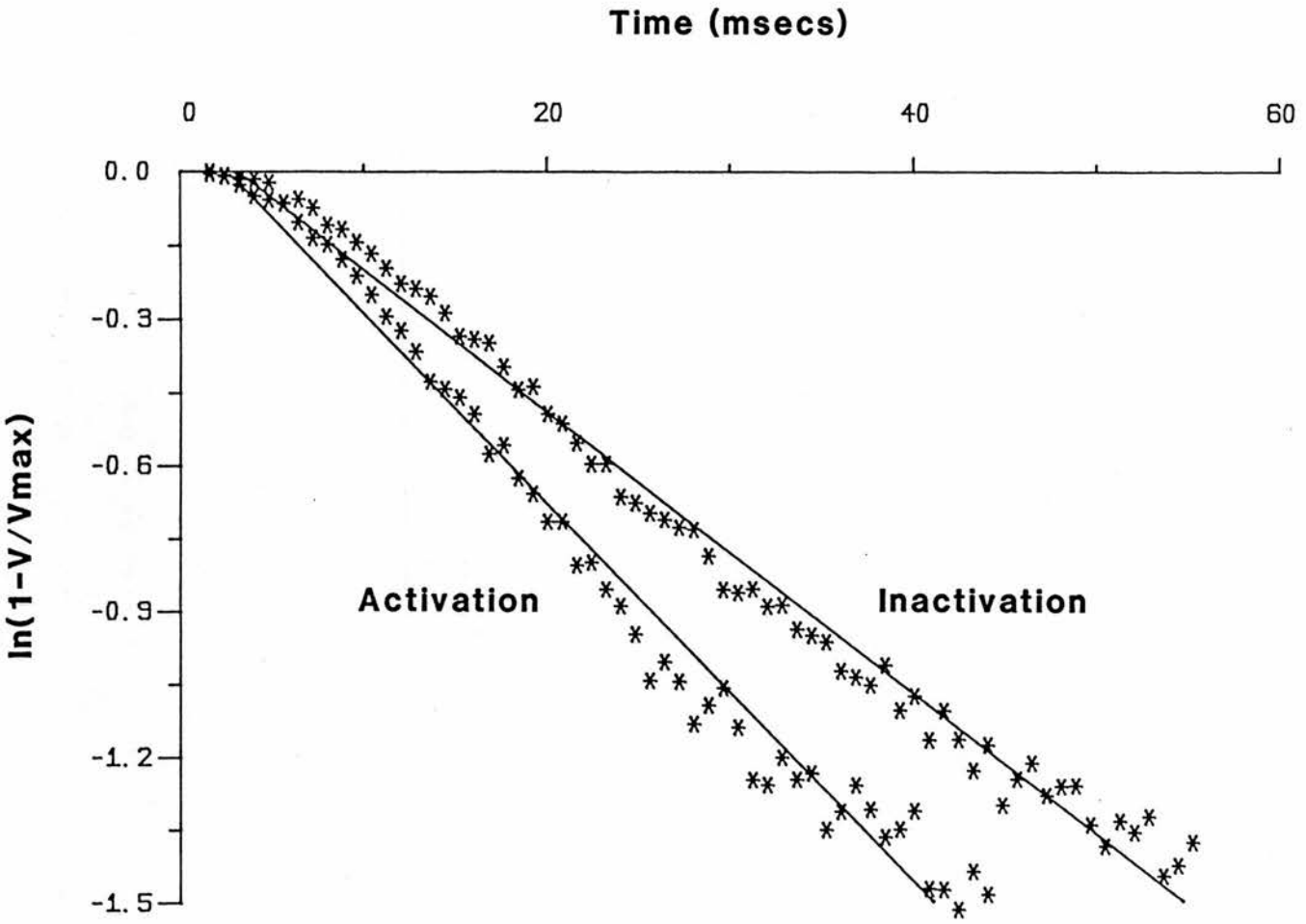

Fig. 3.23

Steady state inactivation curve for normalised A current values (I/Imax) against membrane potential (mV), following the voltage clamp inactivation protocol previously described (Fig. 3.20). Experimental data (open circles) was fitted with an appropriate exponential function (solid line). For details of line fitting see methods section. The inactivation curve produced showed a slope of 3.8mV at the half maximal membrane potential (Vhalf = -89.5mV) and a maximum estimated current (Imax) of 1.9nA.

Fig. 3.23

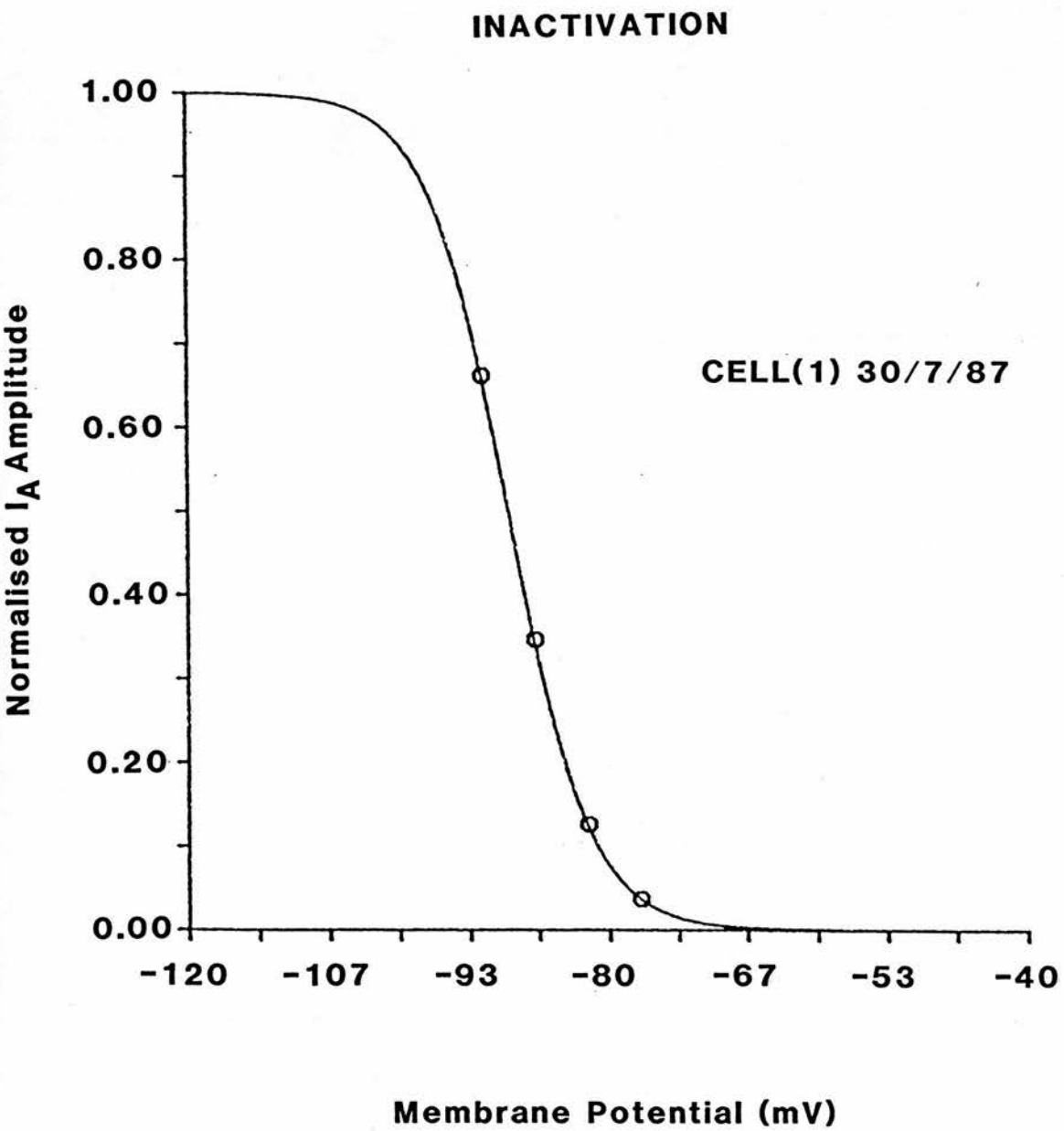
INACTIVATION
1.00
0.80
0.60
0.40
0.20
0.00
Normalised I_A Amplitude
CELL(1) 30/7/87
-120
-107
-93
-80
-67
-53
-40
Membrane Potential (mV)

Fig. 3.24

Steady state activation plot for normalised A current values (I/Imax) against membrane potential (mV). The experimental data (open circles) was fitted with an appropriate exponential function (solid line), for details of curve fitting see methods section. The activation curve produced showed a slope of 4.3mV at a half maximal membrane potential (Vhalf = -49mV) and a maximum estimated current (Imax) of 1.5nA.

Fig. 3.24

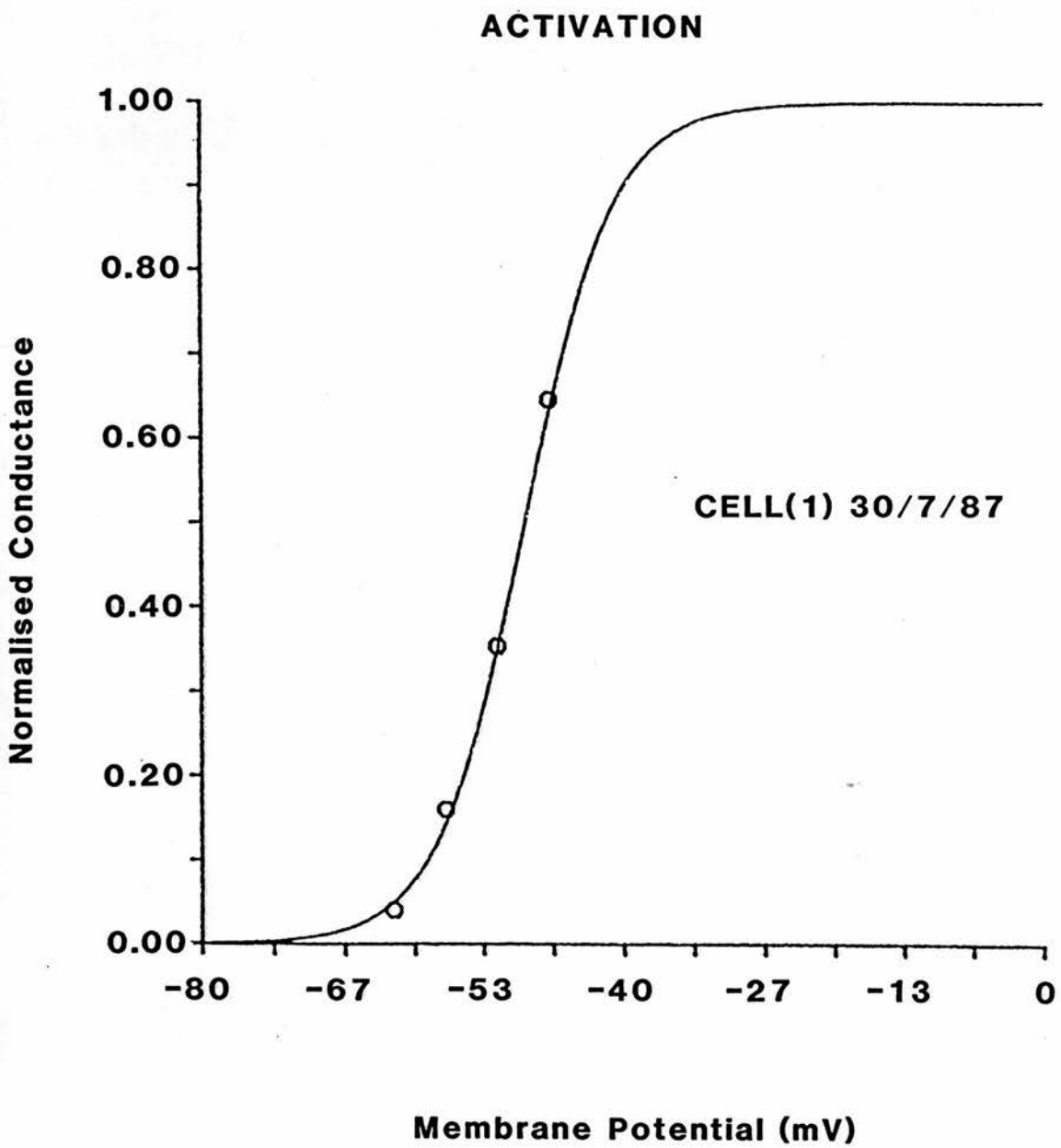
ACTIVATION
1.00
0.80
0.60
0.40
0.20
0.00
Normalised Conductance
CELL(1) 30/7/87
-80
-67
-53
-40
-27
-13
0
Membrane Potential (mV)

Fig. 3.25

The effect of membrane holding potential on steady state inactivation properties. At a holding potential of -50mV, (crosses) the steady state inactivation curve showed a slope of 3.13mV with a half maximal inactivation of -63.27mV and a maximum estimated current (Imax) of 1.24nA. At a holding potential of -60mV the inactivation curve (circles) was parallelly shifted to 7mV more negative potentials. The curve had a slope of 3.48mV with a half maximal inactivation of -70.57mV and a maximum estimated current (Imax) of 0.58nA.

Fig. 3.25

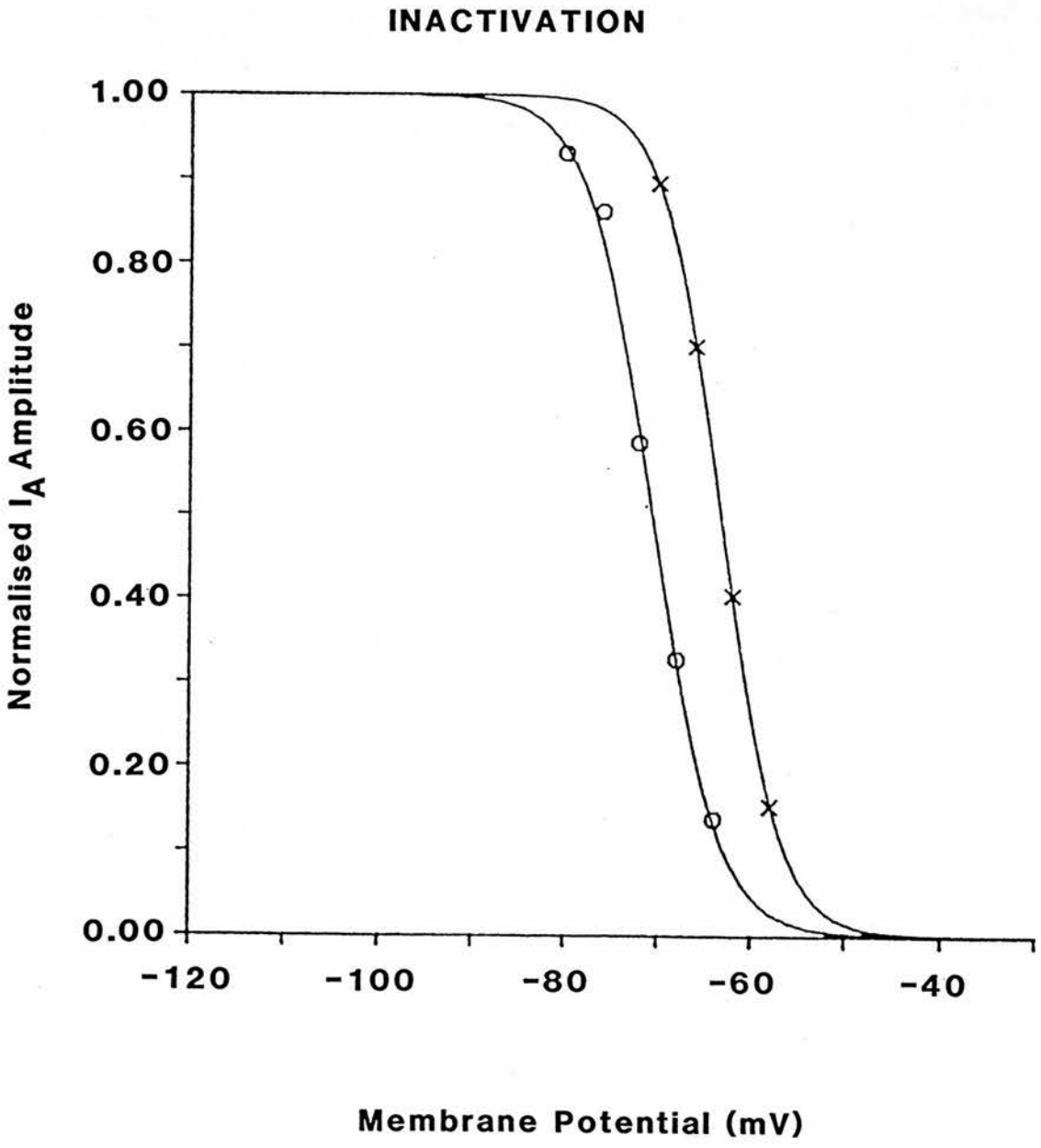

CELL(1) 7/3/88

Fig. 3.26

The effect of 4-AP on A currents evoked during the steady state inactivation protocol. Holding the cell at -67 and stepping to -97mV in 10mV increments (A upper trace) evoked increasing A current peaks (A lower trace) in response to depolarising step commands to -52mV. In the presence of 4-AP (5mM) the A current (B lower trace) was abolished with prepulse steps to -77mV and markedly reduced in both amplitude and duration with prepulse steps to -87 and -97mV (B upper trace). Note with prepulse commands to -77mV in the presence of 4-AP the transient outward current, seen in control ACSF, was replaced by an initial transient inward current (arrow) followed by a delayed outward current which persists even after the termination of the depolarising step command. Increasing the hyperpolarising prepulse to -87mV caused the apppearance of the outward A current and a delay in the onset of the transient inward current (arrow). Note also that with prepulse steps to -97mV the A current decayed with a single exponential of 34ms (Fig. 3.21), in the presence of 4-AP the decay could best be described by double exponential with an initial time constant of 16ms and a slow decay of approximately 198ms.However a problem with inadequate clamping of the A current in control ACSF cannot be over ruled.

Fig. 3.26

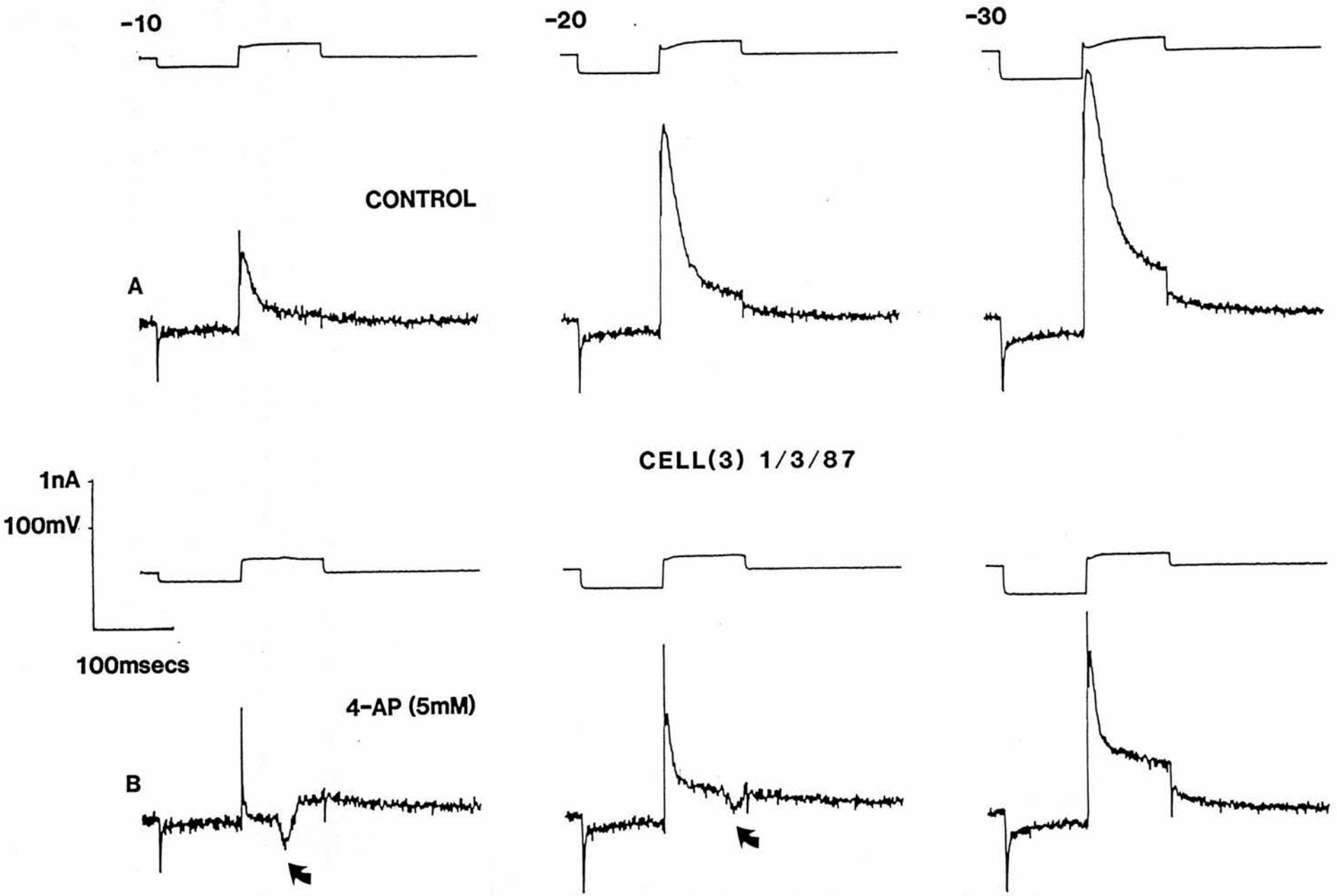

Fig. 3.27

The effect of shortening the duration of the hyperpolarising prepulse on A current amplitude activated by a fixed depolarising step command. A, 20mV depolarising step commands from -63mV when preceded by a 100ms hyperpolarising prepulse to -83mV produces a large 1.8nA transient (τ = 27ms) A current. Shortening the prepulse by 20ms, B, caused no reduction in the peak A current amplitude. Any further reduction in the prepulse duration (C - E) caused a gradual reduction in A current amplitude. In the absence of a hyperpolarising prepulse, F, steps to -43mV from rest elicite little or no A current. Middle trace, the voltage step protocol used to elicit current A - F.

Fig. 3.27

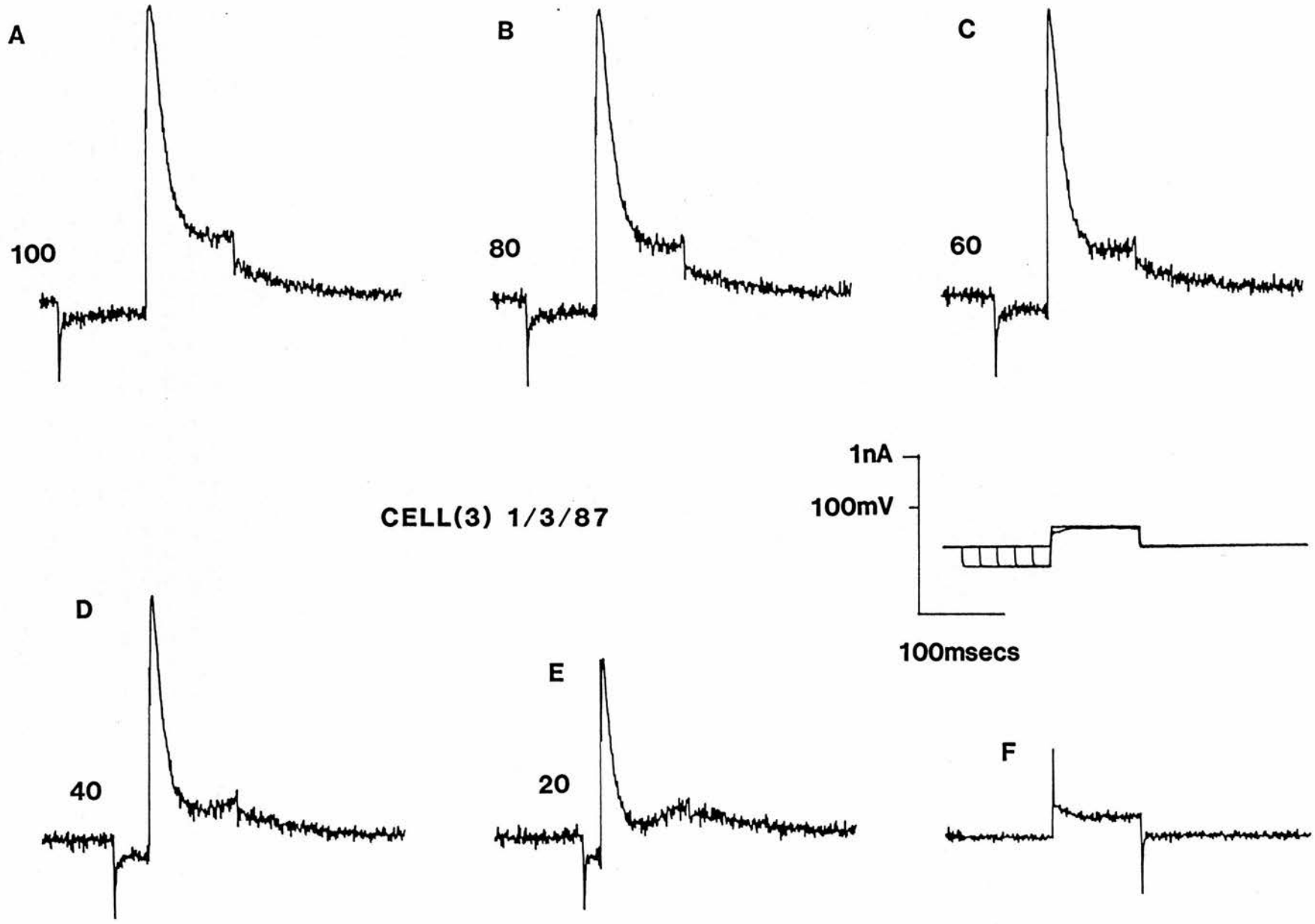

Fig. 3.28

The effect of 4-AP (5mM) on A current activation with time. In control ACSF a dual voltage step protocol (Fig. 3.27) showed an increase in the peak A current evoked (squares) with increasing prepulse duration. The half maximal activation being approximately 14ms and reaching a maximum with hyperpolarising prepulses of 80ms duration. Addition of 4-AP (crosses) caused a marked reduction of the peak A current for all prepulse durations tested, and increased the half maximal activation to 20ms.

Fig. 3.28

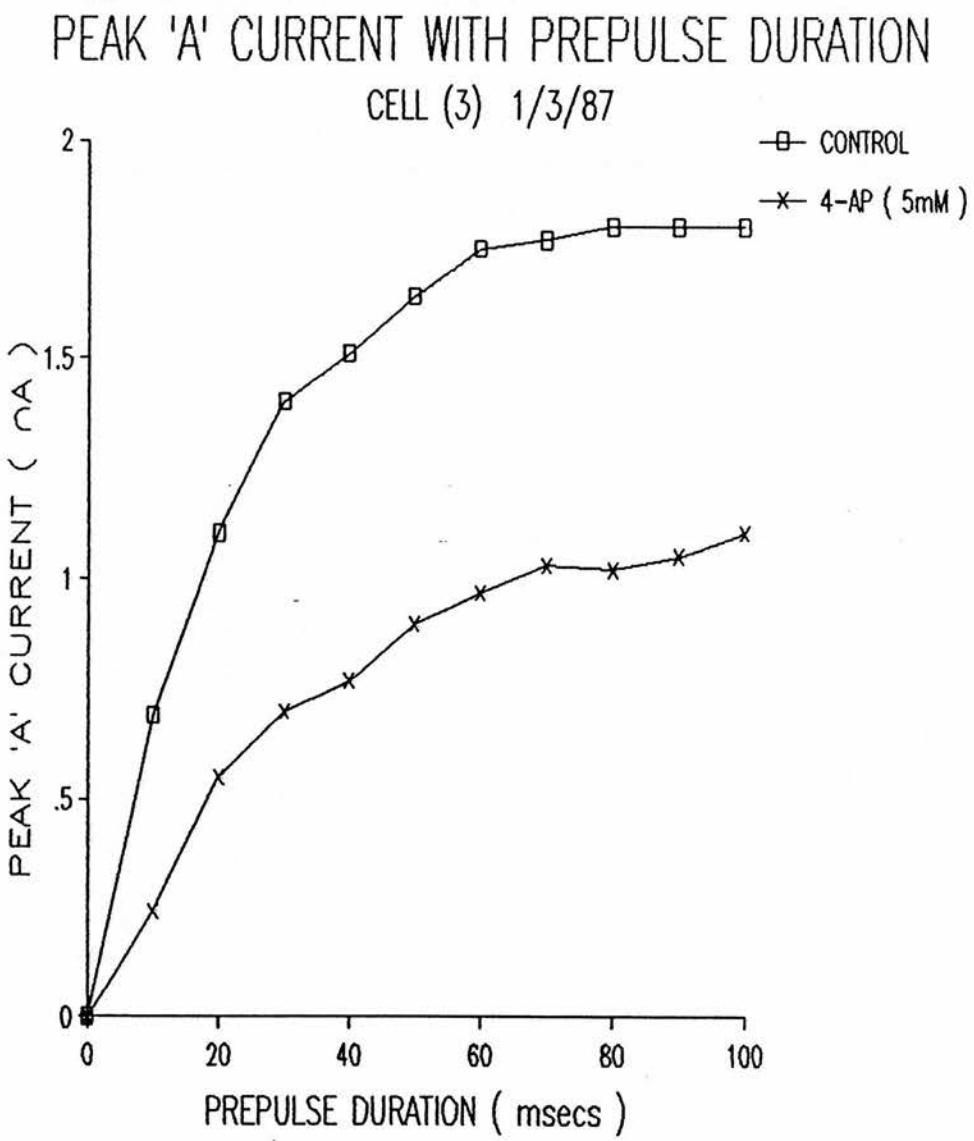
PEAK 'A' CURRENT WITH PREPULSE DURATION
CELL (3) 1/3/87
CONTROL
4-AP (5mM)
PEAK 'A' CURRENT (nA)
2
1.5
1
.5
0
0
20
40
60
80
100
PREPULSE DURATION (msecs)

Fig. 3.29

The effect of 4-AP on the time dependent activation of IA. As shown in the previous Fig. 3.27 IA shows a time dependent activation. Plotting the % activation (Imax - Imax 4-AP) against prepulse duration showed that 4-AP also caused a time dependent blockade of IA. 4-AP caused a 34% inhibition of IA during a 10ms prepulse, this blockade increased with increasing prepulse duration, causing a 61% inhibition of IA with a prepulse of 100ms duration.

Fig. 3.29

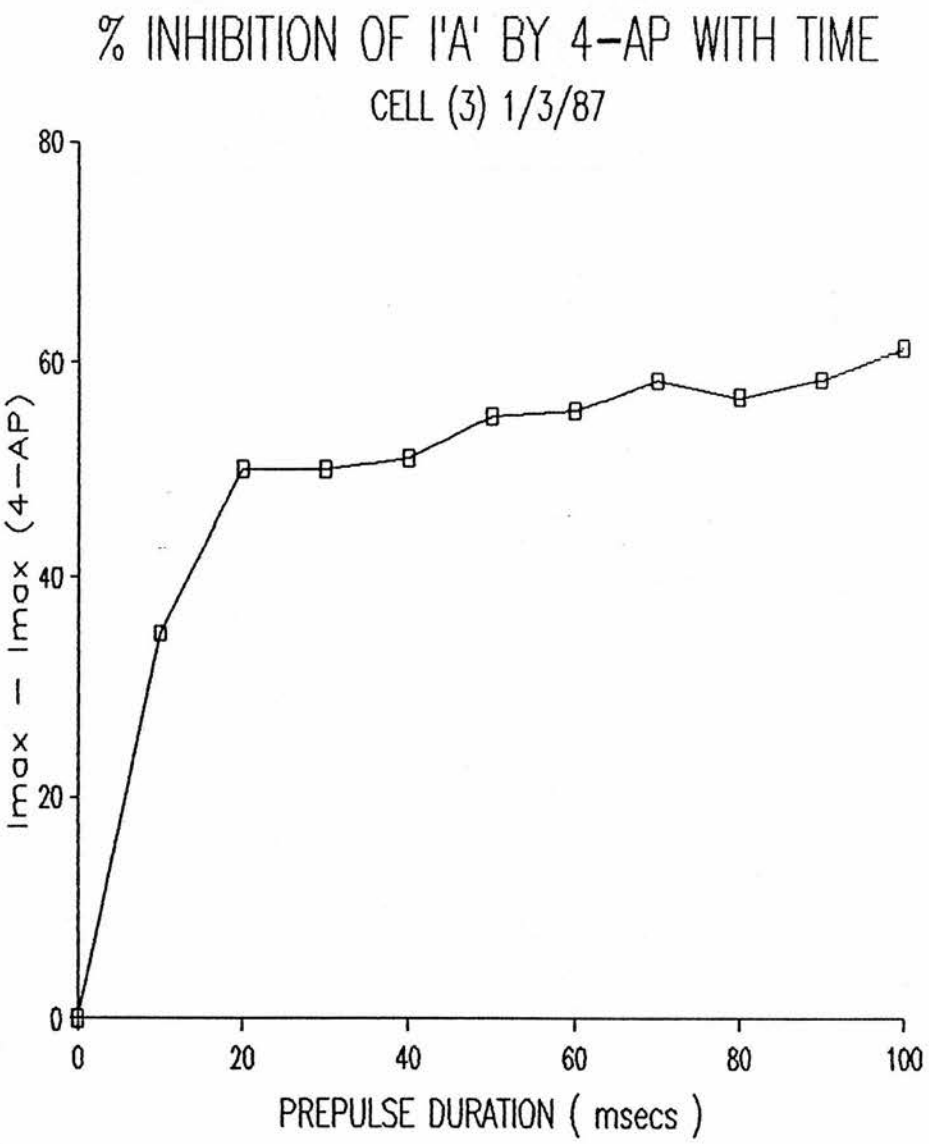
% INHIBITION OF I'A' BY 4-AP WITH TIME
CELL (3) 1/3/87
Imax - Imax (4-AP)
80
60
40
20
0
0
20
40
60
80
100
PREPULSE DURATION (msecs)

Fig. 3.30

The effect of increasing the gap duration between the hyperpolarising prepulse and the voltage step command before, during and after 4-AP (5mM) bath application. Following a step prepulse command to -83mV a gap was introduced before the depolarising step command to -43mV which was increased in 10ms increments. In control ACSF, trace A, increasing the gap duration caused a concomitant decrease in the peak A current evoked by step commands to -43mV. The current decreased to 98% of the maximal reponse with a 10ms gap duration and to 28% with a 90ms gap duration. Bath application of 4-AP, trace B, not only caused a reduction in the peak A current amplitude when no gap was present (1.24nA compared to 1.8nA) but also decreased to 30ms the gap duration after which an A current could still be evoked. On washout, trace C, the A current recovered to 82% of the peak amplitude and the gap duration could be increased to 80ms before the A current was abolished. Lower trace the voltage step protocol used to evoke step currents seen in traces A - C.

Fig. 3.30

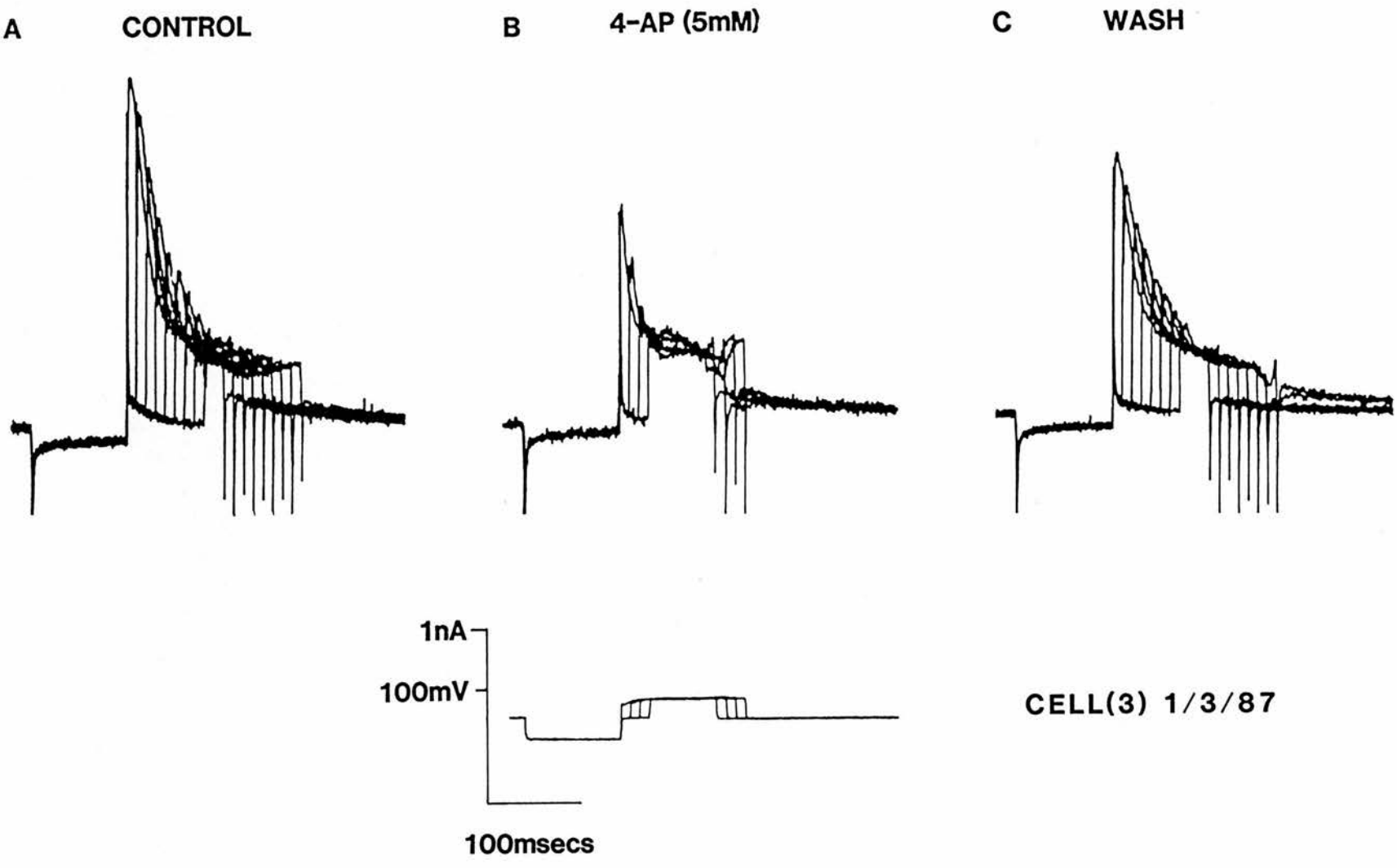

Fig. 3.31

The effect of increasing the gap duration between the hyperpolarising prepulse and the depolarising step command (see Fig. 3.29) before, during and after 4-AP bath applicaton. An increase in the gap duration could be seen to cause a gradual decrease in the A current evoked by fixed voltage commands, reaching near total abolition of the step current with gaps of 90ms duration in control ACSF (squares). During 4-AP application this value was reduced to 30ms together with a concomitant decrease in the peak A current amplitude. On washout the A current recovered to near control values.

Fig. 3.31

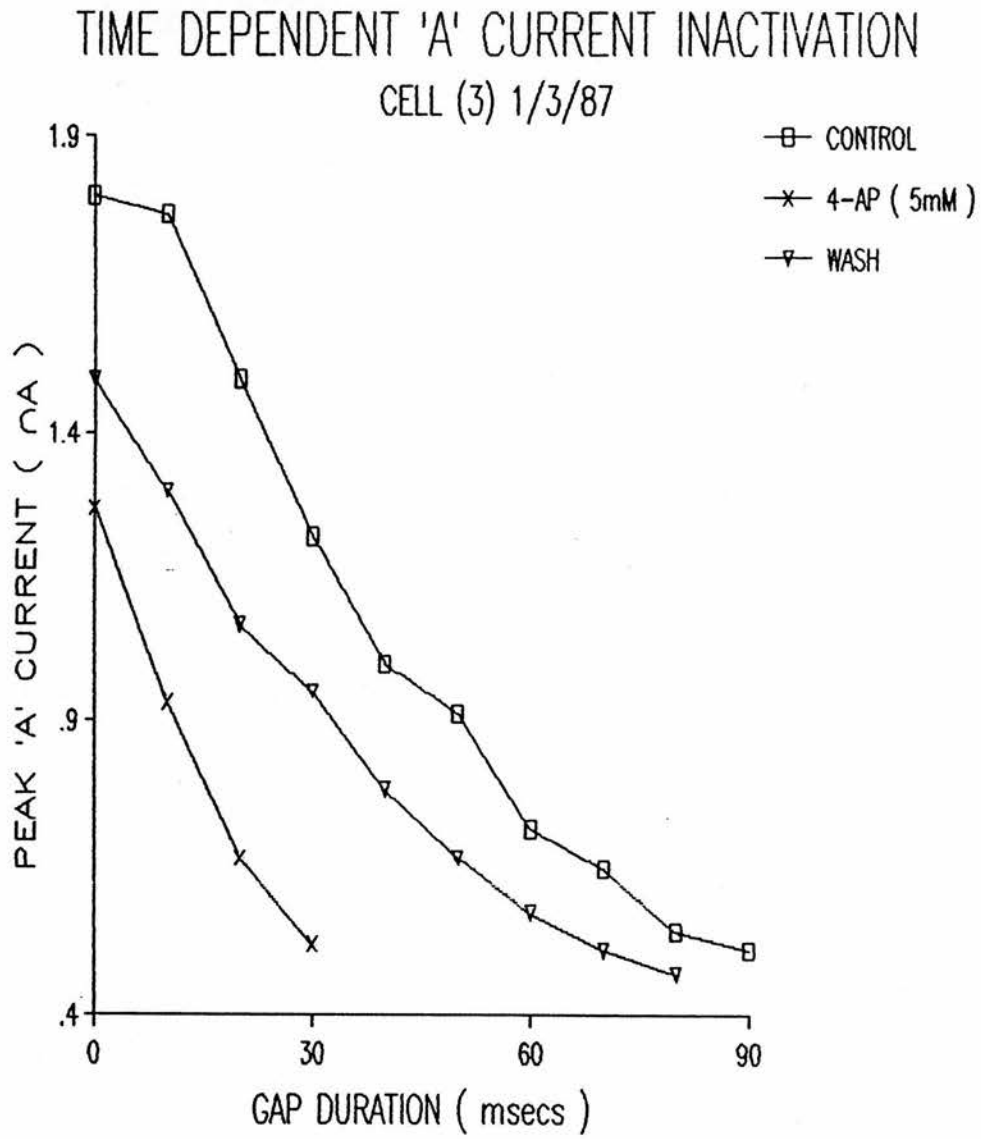
TIME DEPENDENT 'A' CURRENT INACTIVATION
CELL (3) 1/3/87
CONTROL
4-AP (5mM)
WASH
PEAK 'A' CURRENT (nA)
1.9
1.4
.9
.4
0
30
60
90
GAP DURATION (msecs)

Fig. 3.32

The effect of A current activation on the expression of a low threshold transient inward and delayed outward current. Depolarising 100ms step commands to -40mv from a holding potential of -50mV evoked an initial transient inward current (filled triangles) followed by a delayed outward current which persists on termination of the step command. The introduction of graded hyperpolarising pepulse commands caused an increase in the time to peak of the inward transient current. With no prepulse, trace A, the time to peak was 10.4ms, following a prepulse to -70mV, trace B, a small A current delayed the apparent time to peak of the transient inward current by 16.8ms. This appeared to have no effect on the delayed outward tail current. On further hyperpolarisation to potentials greater than-80mV the transient inward current was fully masked by the large transient outward A current. The delayed outward current and the tail currrent could however still be observed. The voltage protocol is shown in trace F.

Fig. 3.32

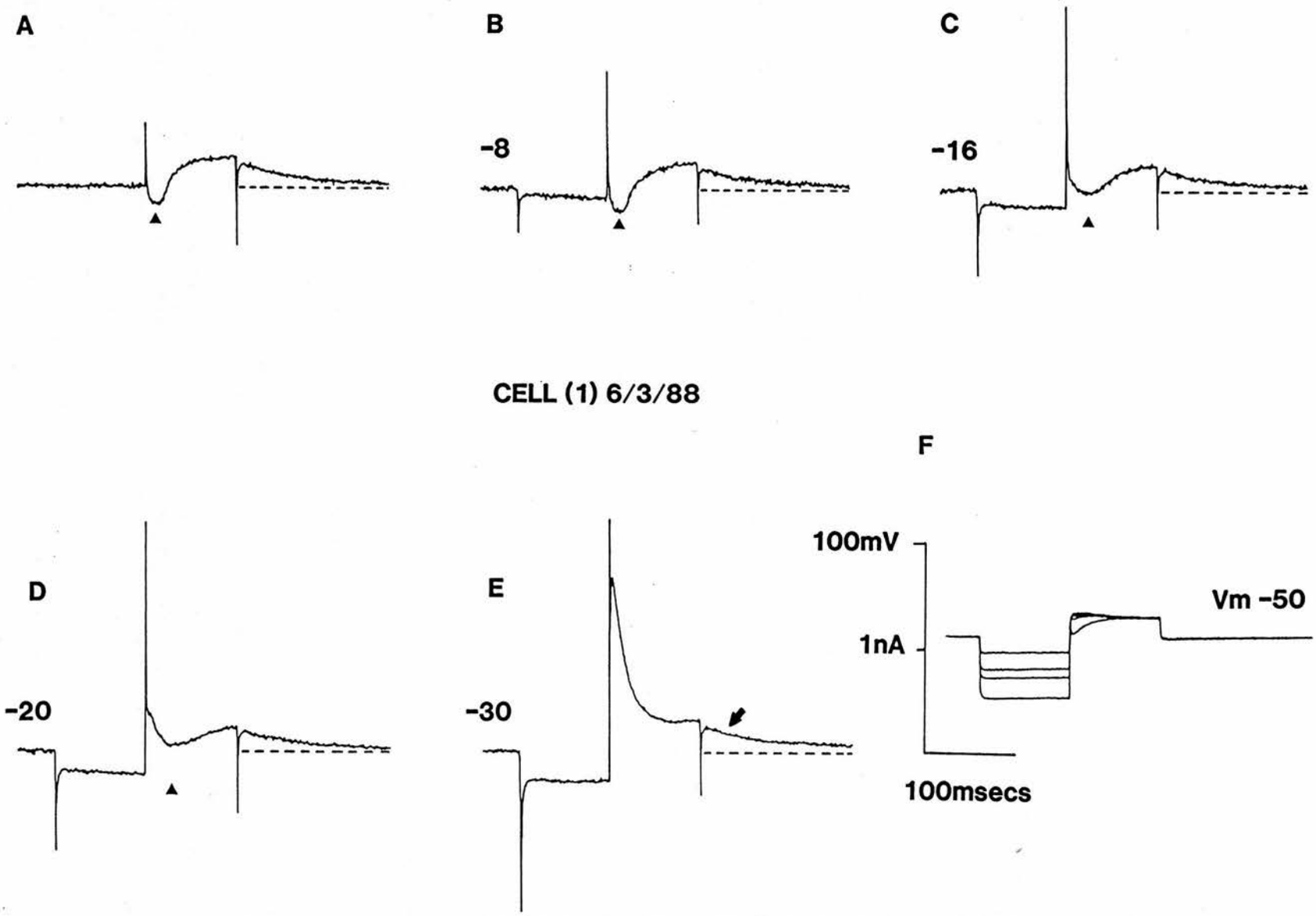

Fig. 3.33

The effect of TEA (10mM) and low calcium, high magnesium (0.2mM, 4mM respectively) on peak A current amplitude. Upper traces the step current generated in response to the voltage step protocol shown in the lower trace. Holding at -57mV and steping to -97mV in 19mV increments caused a graded increase in A current amplitude to be evoked in response to a depolarising step command to -37mV. In control ACSF, trace A, Imax = 1.02nA. When 10mM TEA was substituted for 10mm NaCl in the control ACSF, trace B, a small decrease in the A current amplitude was observed for all prepulse step commands, Imax = 0.8nA (unlike cell (1) 5/2/87 Fig. 3.18) with no apparent change in the duration. In contrast lowering the calcium concentration from 2mM to 0.2mM and replacing the divalent cation concentration by increasing the magnesium concentration to 4mM caused an increase in A current amplitude to be observed for all prepulse step commands, Imax = 1.7nA, together with a reduction in the time course for inactivation. Inactivation g for control Imax was 39.2ms in control ACSF compared to 22.8ms in low Ca2+ ACSF. Note in low Ca2+ ACSF the steady state leakage was larger than in control conditions.

Fig. 3.33

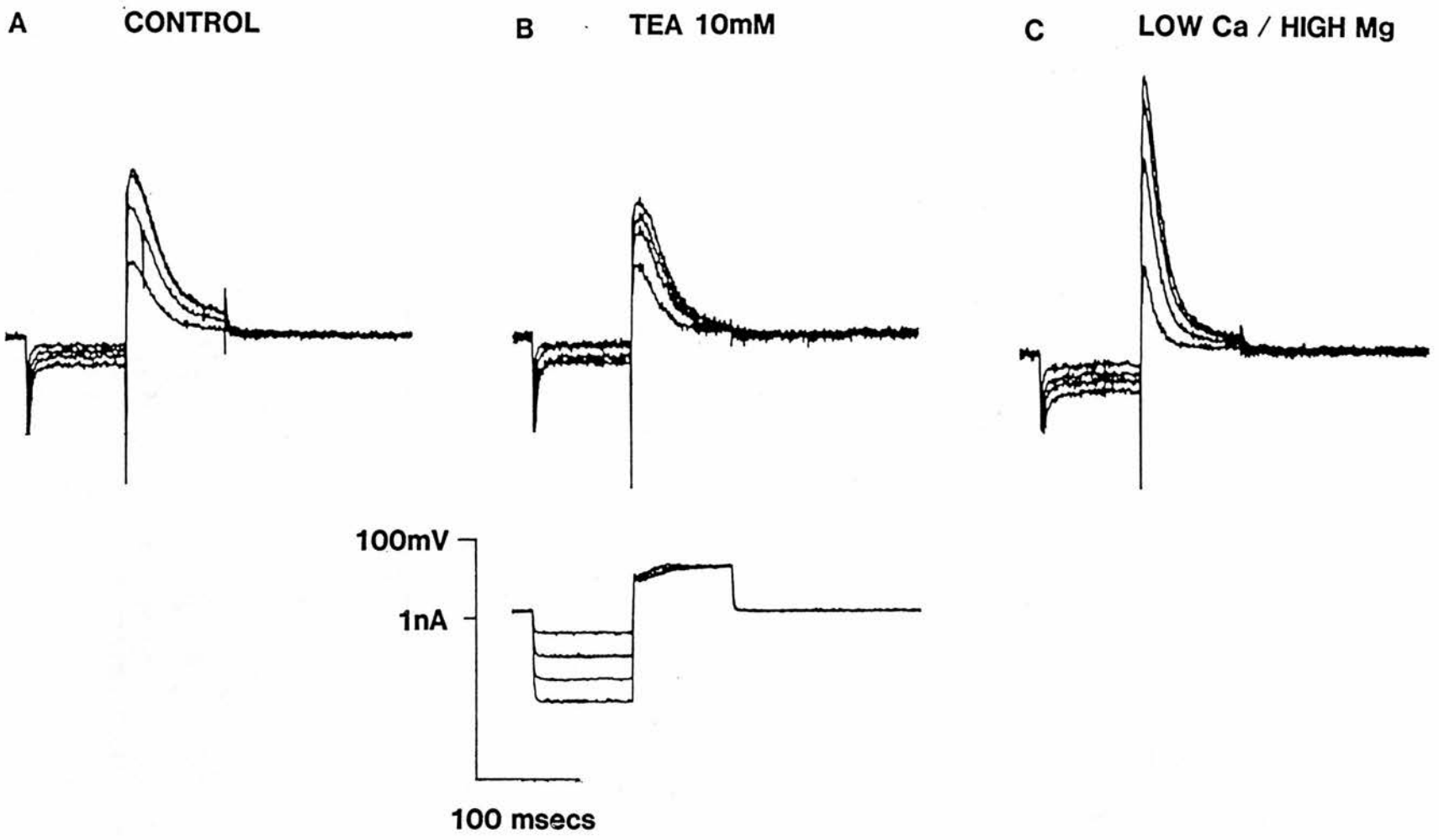

CELL (1) 25/1/87

Fig. 3.34

Steady state inactivation curves before and during bath application of low Ca2+ ACSF. The steady state inactivation curve in control ACSF (circles) calculated from the currents generated in Fig. 3.32 showed a half maximal inactivation (Vhalf) of -68mV, a slope of 7.01mV and a maximum estimated current (Imax) of 1.0nA. Switching to an ACSF containing low calcium, high magnesium caused a hyperpolarising shift in the steady state inactivation curve with Vhalf moving to -71mV, the slope changing to 6.25mV and the Imax increasing to 1.7nA.

Fig. 3.34

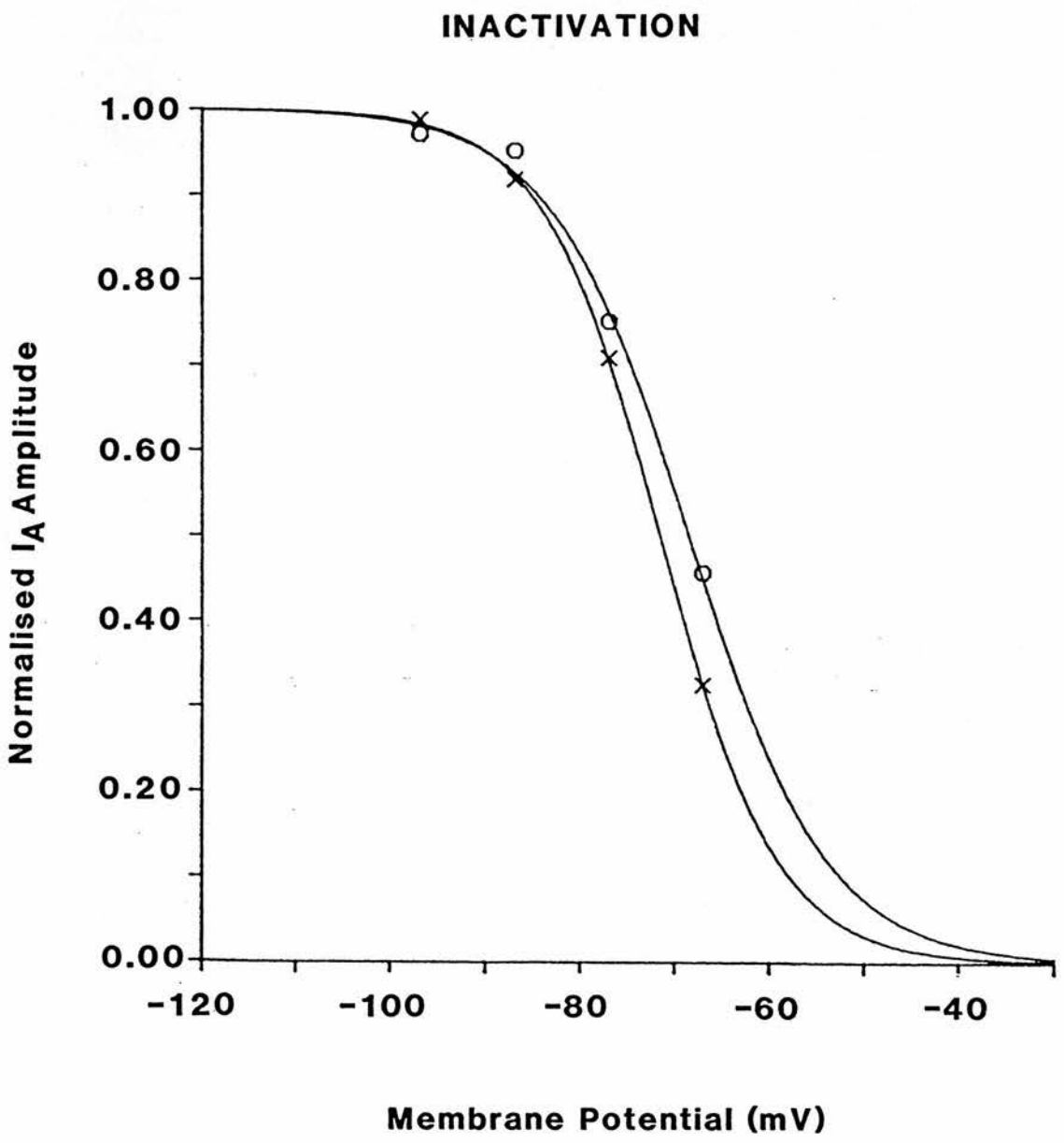
INACTIVATION
1.00
0.80
0.60
0.40
0.20
0.00
Normalised I_A Amplitude
-120
-100
-80
-60
-40
Membrane Potential (mV)
CELL (1) 25/1/87

Fig. 3.35

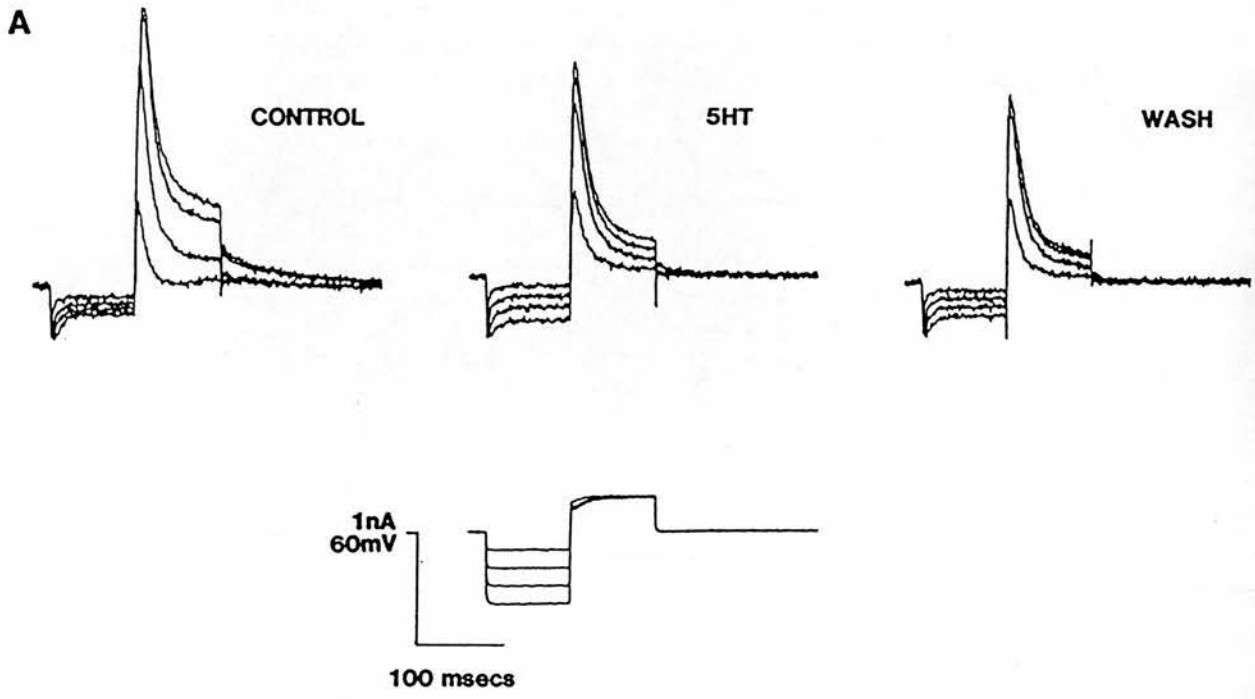

CELL (2) 21/1/87

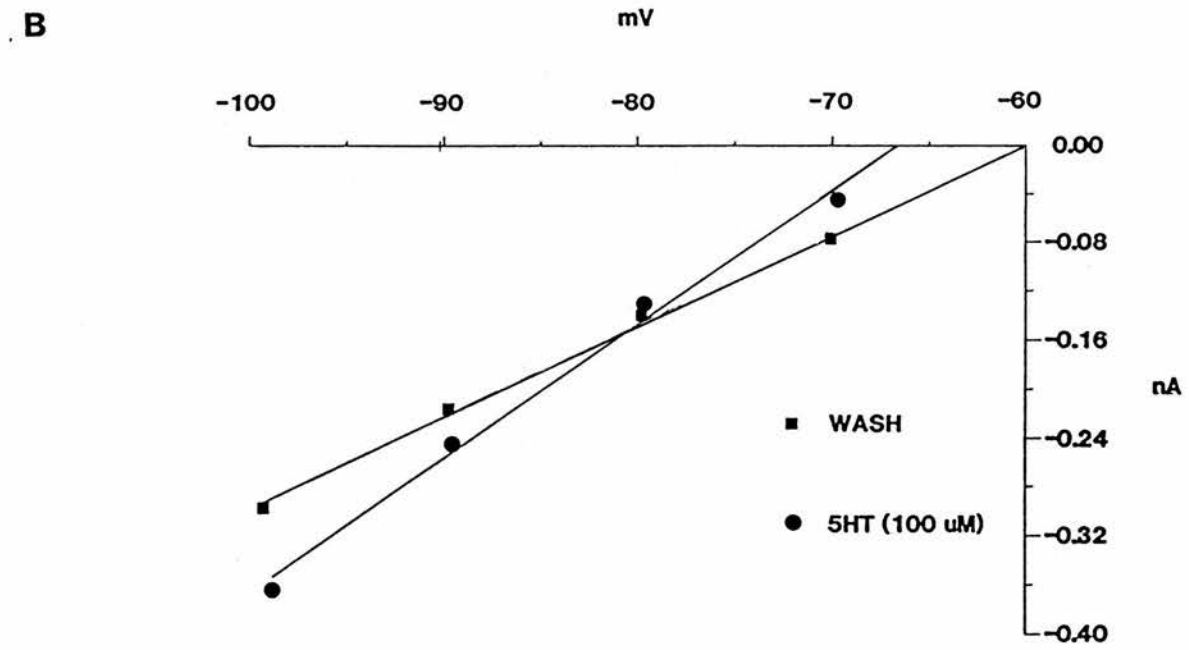

Fig. 3.35

A current responses observed during steady state voltage clamp inactivation protocol before, during and after 5- hydroxytryptamine (5-HT) application. In control ACSF increasing hyperpolarising prepulse commands to - 100mV, in 10mV increments, (A lower trace) evoked a graded increase in A current amplitude (A upper trace) in response to a fixed depolarising step command to -41mV, Imax = 2.53nA. Bath application of 5-HT (100μM) caused a reduction of the A current amplitude for all levels of membrane prepulse hyperpolarisation, Imax = 2.05nA. Note that during 5-HT application a positive DC holding current (0.04nA) was required to maintain the membrane at the control level of -60mv. On washout however the A current amplitude did not recover to control values and did in fact decline further than those values obtained in 5-HT, Imax = 1.78nA. B, the voltage - current relationship derived from the leakage currents evoked during hyperpolarising prepulses during and after 5-HT application. During 5-HT application the voltage - current relationship could be fitted with a linear regression line that showed a slope conductance of 20nS. On washout the slope conductance decreased to 7.1nS. The point of intersection of the two lines indicated a reversal potential of approximately -80mV.

Fig. 3.36

Normalised steady state A current inactivation curves determined before, during and after bath application of 5-HT (100μM). In control ACSF the experimental data (circles) was fitted by a curve that showed a half maximal inactivation potential (Vhalf) of -73mV, an estimated maximal current (Imax) of 2.56nA and a slope of 4.09mV. In the presence of 5-HT (crosses) Vhalf was shifted to -72mV, Imax decreased to 2.03nA and the slope decreased to 5.78mV. On washout the slope returned to near contrl values, 3.65mV, the Vhalf hoever had shifted to -70mV and the Imax had further decreased to 1.75nA.

Fig. 3.36

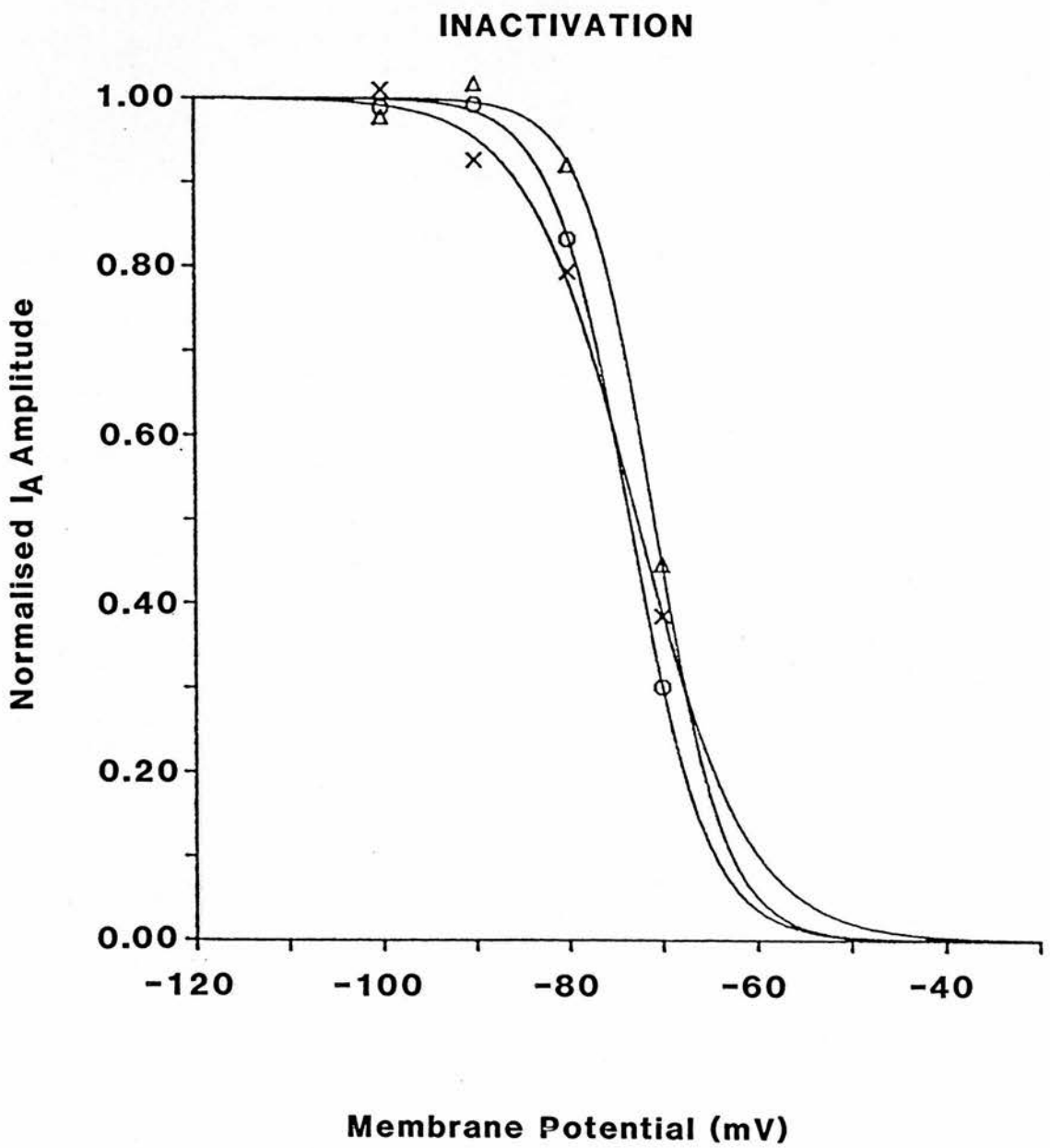

CELL(2) 21/1/88

Fig. 3.37

The effect of noradrenaline (NA) (50μM) on A currents evoked during a dual pulse inactivation protocol. A, upper trace, step currents evoked with graded hyperpolarising prepulse step commands to a maximum of -94mV preceding a fixed depolarisation step to -54mV, lower trace. In the presence of NA the A currents activated by a similar voltage protocol showed a marked reduction in A current amplitude. Imax in control ACSF was 0.63nA compared to an Imax of 0.34nA in NA. B, the voltage - current relationship in control ACSF (squares) showed a slope conductance of 3.7nS which fell to 2.7nS in NA (stars), as estimated from currents produced during hyperpolarising prepulse step commands. The point of intersection of the two regression lines showed the reversal potential for the NA effect to be -80mV.

Fig. 3.37

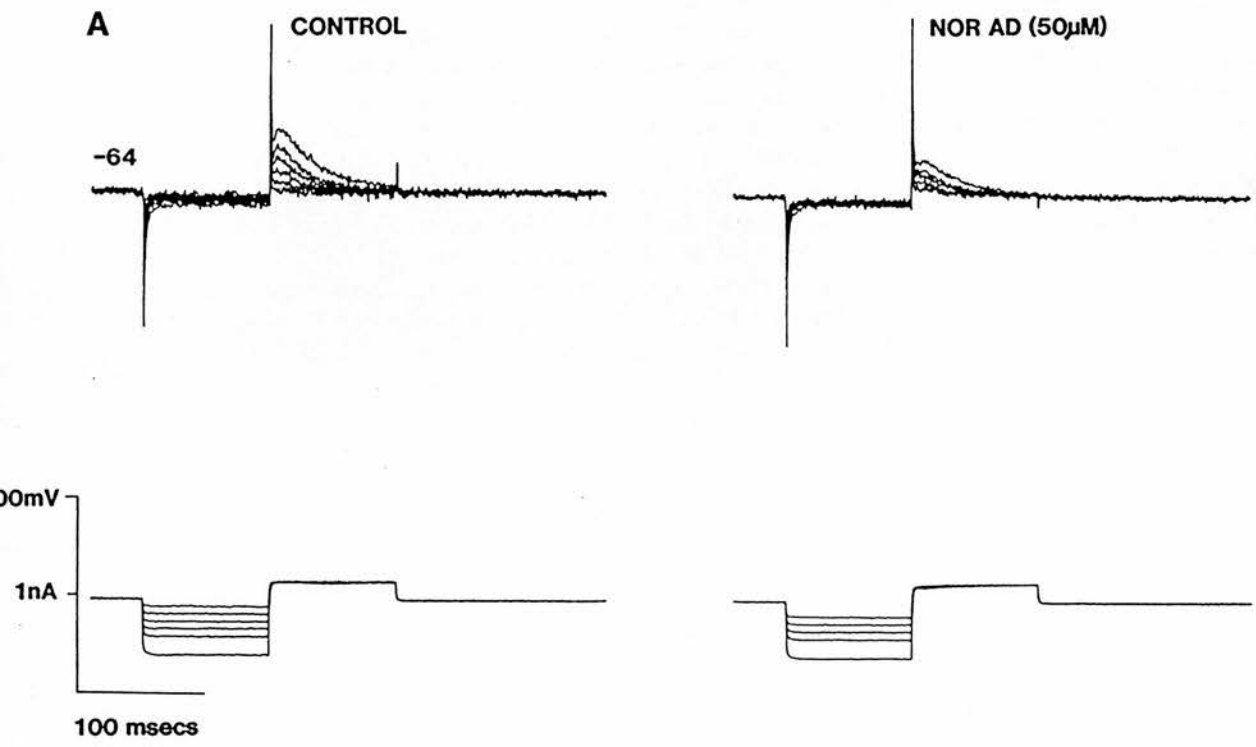

CELL (1) 6/3/88

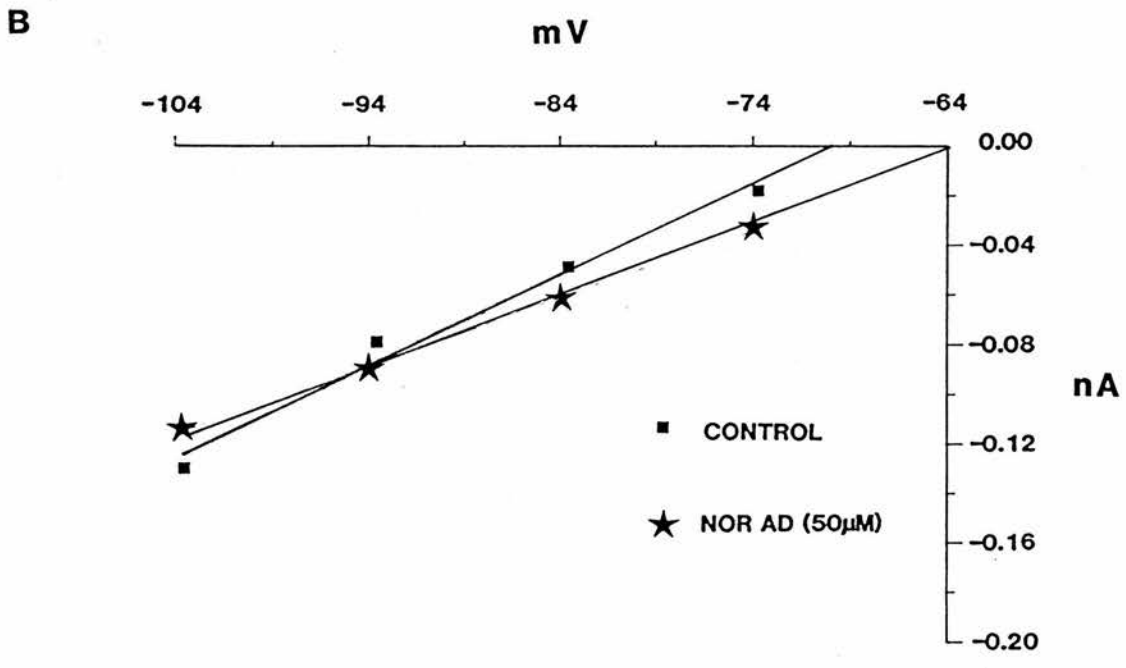

Fig. 3.38

Normalised steady state A current inactivation curve before and during noradrenaline (50μM) bath application. In control ACSF experimental data (circles) was best fitted by a curve that showed a half maximal inactivation (Vhalf) of -82mV with an estimated Imax of 0.69nA and a slope of 5.81mV. Bath application of NA caused a positive shift in the voltage inactivation curve with Vhalf changing to -77mV and Imax reducing to 0.36nA. The slope however remained close to control levels at 5.98mV

Fig. 3.38

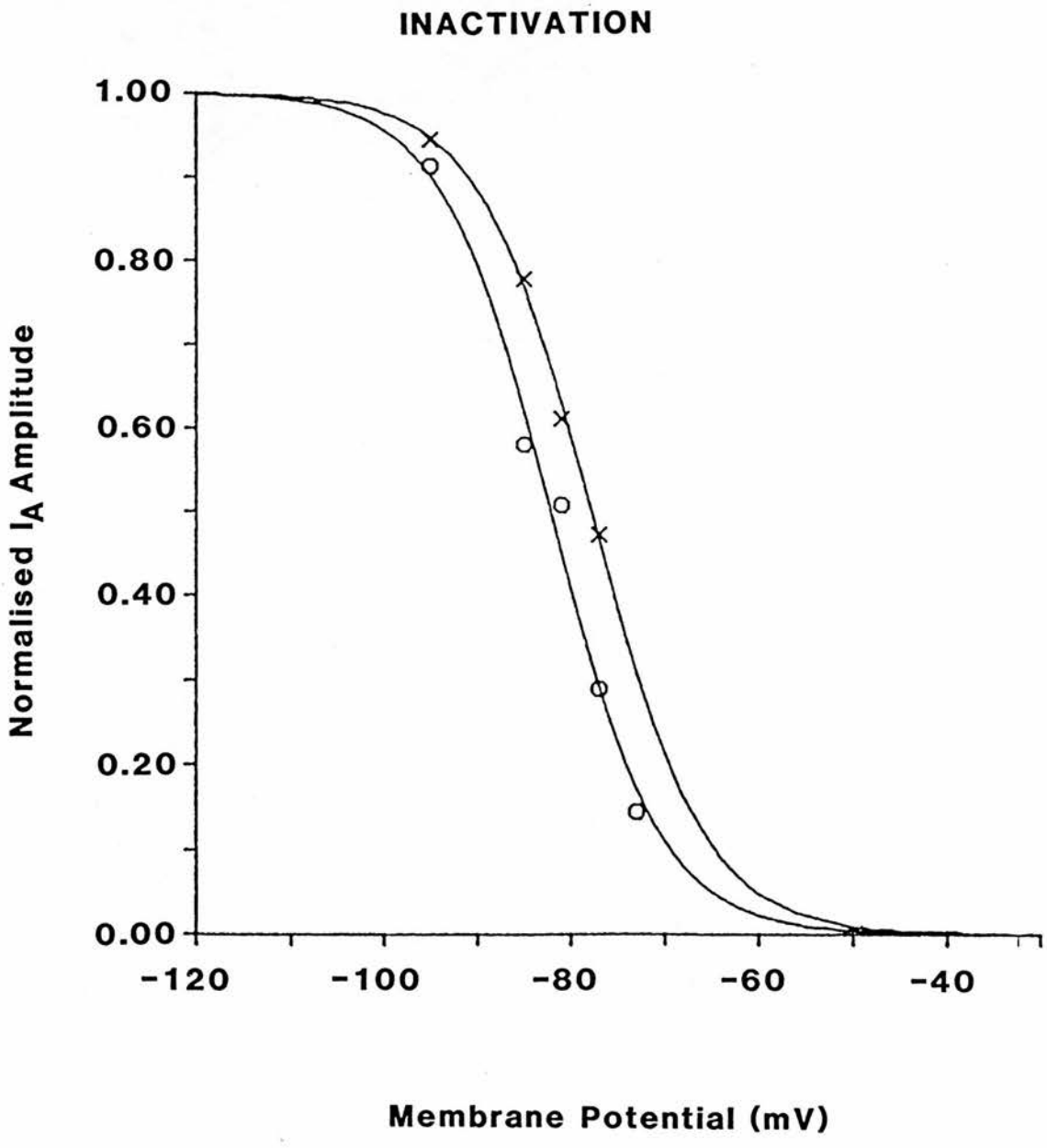

CELL(1) 6/3/88

Fig. 3.39

The effect of repeated bath administration of NA (50μM) on A currents evoked during a dual pulse voltage clamp protocol. On initial application, A, NA caused a reduction in the amplitude of the A currents evoked during a routine dual pulse inactivation protocol. Imax in control ACSF was 3.18nA compared to 1.79 in NA, the Imax recovered to 2.34 after washout. Note that during NA application a hyperpolarising DC current command was required to hold the cell at the resting potential of -60mV. On the third application of NA, B, no change was observed in the holding current, the A current Imax was however reduced from 1.96nA (wash 2) to 1.55nA with a slight recovery on washout to 1.71nA. Lower trace, the voltage clamp protocol used to elicite the step currents seen in A and B.

Fig. 3.39

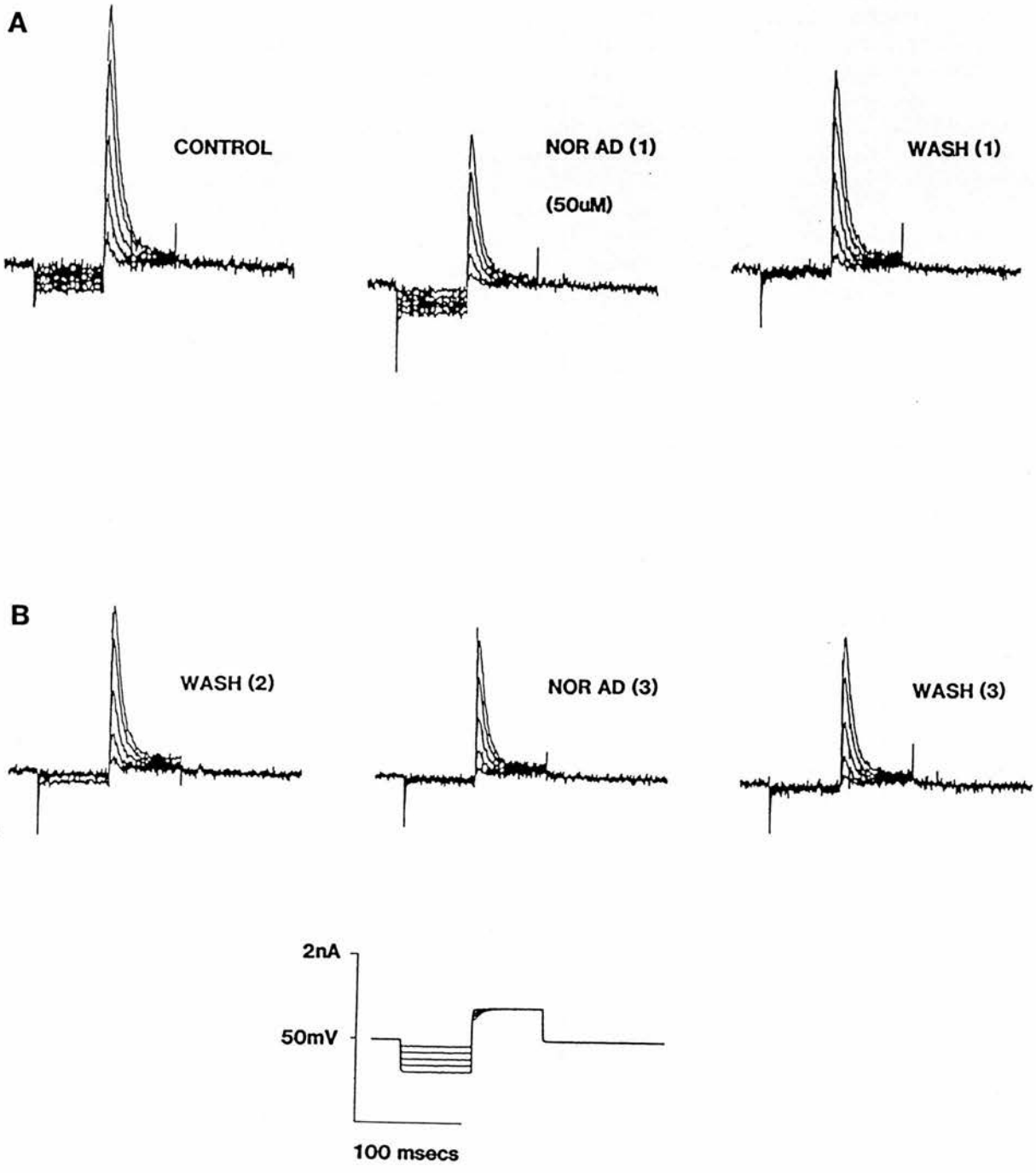
A
CONTROL
NOR AD (1)
(50uM)
WASH (1)
B
WASH (2)
NOR AD (3)
WASH (3)
2nA
50mV
100 msecs

Fig. 3.40

Normalised steady state A current inactivation curves before and during NA bath application for data obtained from Fig. 3.38. In control ACSF the inactivation curve fitted to the experimental data (circles) showed a Vhalf of -74mV and an Imax of 2.86nA. The slope was estimated to be 3.78mV. Addition of NA (crosses) caused a reduction in the Vhalf to -68mV and increased the estimated slope to 2.86mV. The Imax however was markedly reduced to 1.65nA.

Fig. 3.40

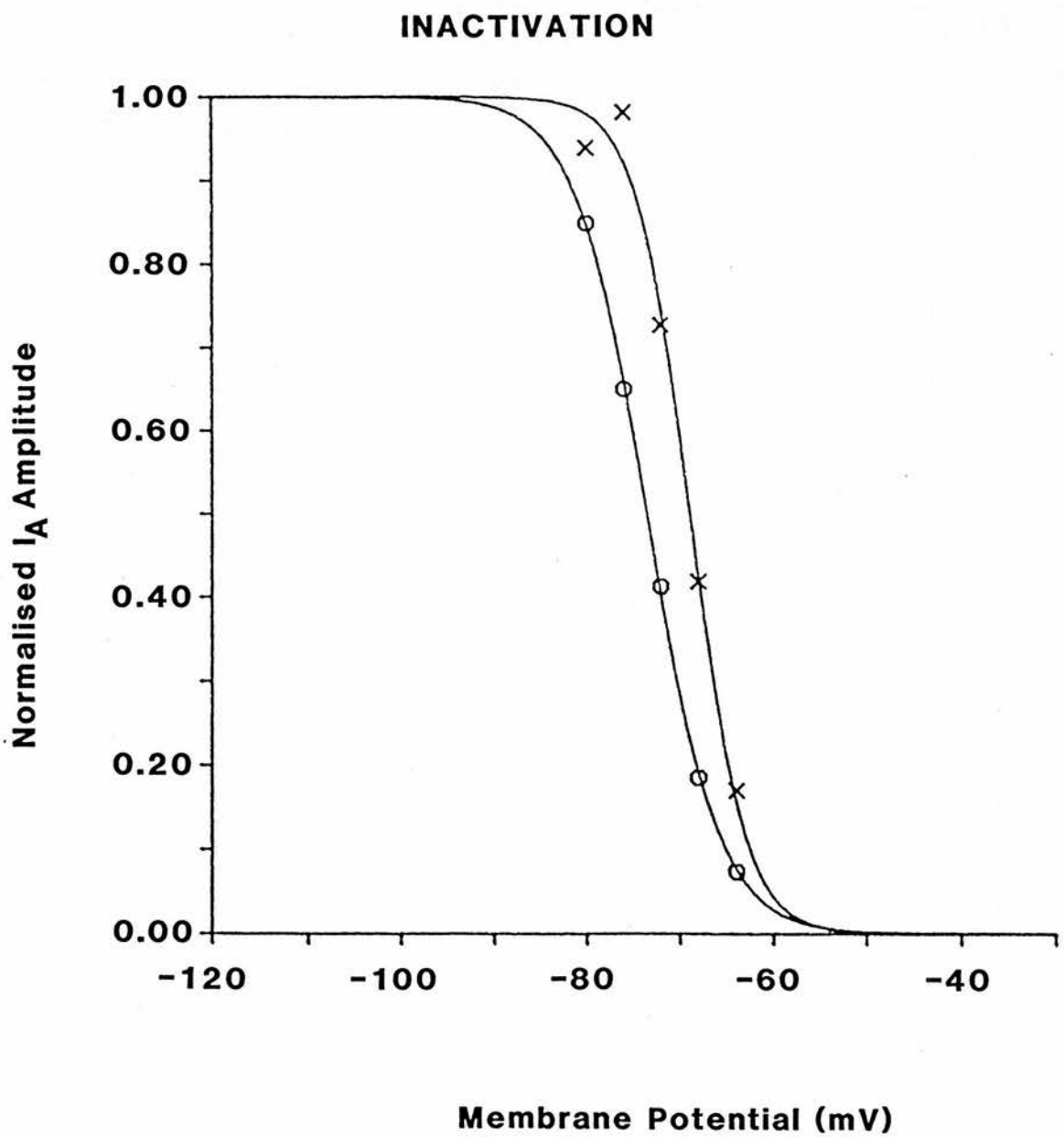

CELL(4) 4/3/88

Fig. 3.41

Normalised steady state A current inactivation curves before and during NA application and subsequent application of 4-AP (5mM). After multiple application of NA the steady state inactivation curves appear inseparable. Both the Vhalf -74mV and the slope 3.9mV being similar in control ACSF (circles) and on NA application (crosses). The maximum estimated current was still seen to decline from 2.14nA in control ACSF to 1.93nA in NA. Subsequent bath application of 4-AP following washout of NA caused a small shift in Vhalf to - 72mV together with a reduction in the estimated Imax to 1.0nA and an increase in the slope to 2.98mV.

Fig. 3.41

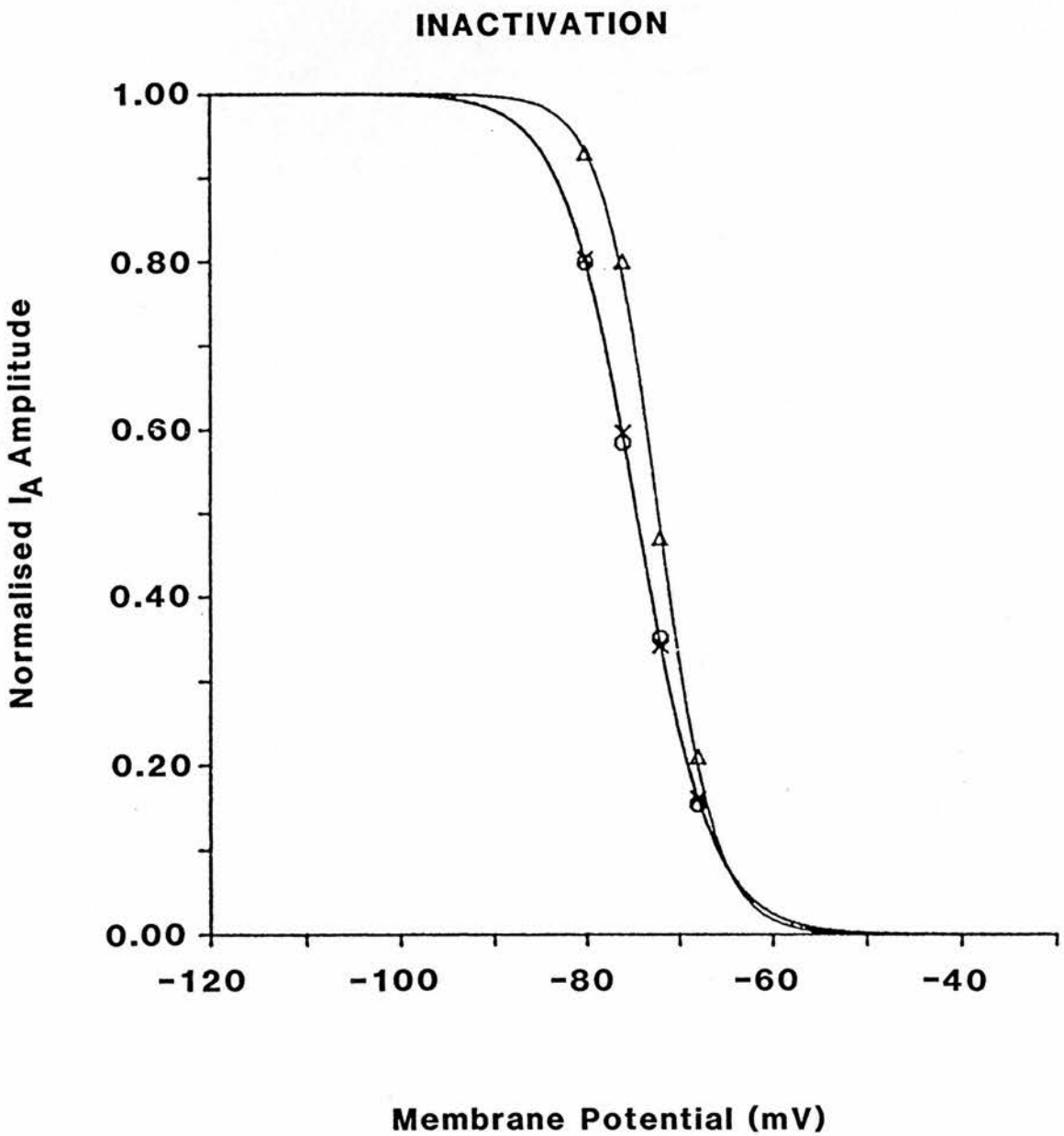
INACTIVATION
1.00
0.80
0.60
0.40
0.20
0.00
Normalised I_A Amplitude
-120
-100
-80
-60
-40
Membrane Potential (mV)
CELL(4) 4/3/88

CHAPTER 4

THE PHARMACOLOGY OF DORSAL RAPHE NEURONES

INTRODUCTION

In the periphery, multiple 5-HT receptor subtypes were demonstrated as early as 1957 by Gaddum & Picarelli. They proposed that in the guinea pig ileum two distinct 5-HT receptors were present, the D and M receptors. It was not until the introduction of radioligand binding and autoradiography that the presence of multiple binding sites were demonstrated in the CNS. In 1979, as in the periphery only two 5-HT binding sites were proposed to exist in the vertebrate CNS. These were the 5-HT_1 and 5-HT_2 binding sites which showed binding preference for ^{3}[H] 5-HT agonists and antagonists respectively (Peroutka & Snyder 1979). The antagonist initially used to discriminate between the two types of binding site, ^{3}[H] spiperone, was shown not to be specific for 5-HT systems and to be a potent antagonist at dopaminergic receptors (Bischoff et al 1980). The introduction of ketanserin a more specific 5-HT_2 ligand (Leysen et al 1981) added further weight to the dual 5-HT binding site theory. In 1982, Laduron et al demonstrated ketanserin binding at high concentrations in the frontal cortex.

Further analysis of the displacement of 5-HT from its binding sites by Pedigo et al (1981) indicated that ^{3}[H] spiperone could label two different binding sites, one with a high nM affinity and a second with a low μM affinity neither of which was believed to be analogous to the 5-HT_2 binding site. These binding sites were subsequently termed the 5-HT_{1A} and 5-HT_{1B} sites respectively. A third type of 5-HT_1 binding site has since been proposed based on a high affinity displacement of ^{3}[H] 5-HT by an ergot derivative mesulergine (Pazos et al 1984) and has been designated the 5-HT_{1C} site.

All of these binding sites have been shown to have their own unique regional distribution. Thus although 5-HT_1 binding sites are present in high concentrations in a multiplicity of brain areas receiving a serotonergic input the individual subtypes have however been demonstrated to show a precise regional distribution. Hence 5-HT_{1A} sites are enriched in the dorsal raphe nucleus, dentate gyrus and septal nucleus, 5-HT_{1B} sites in the substantia nigra, globus pallidus and dorsal subiculum, and 5-HT_{1C} sites are particularly enriched in the choroid plexus (Deshmukh et al 1983, Pazos & Palacios 1985). More recently a fourth 5-HT_1 binding site subtype has been identified in bovine, human and rat brain, labelled the 5-HT_{1D} site and is seen in highest densities in the basal ganglia and caudate nucleus (Heuring &

Peroutka 1987, Herrick-Davis & Titeler 1988, Waeber et al 1988). Finally the 5-HT_3 receptor which was thought for a long time to be expressed only in the periphery has recently been demonstrated to have an equivalent binding site in the rat CNS with high concentrations in cortical and limbic areas (Kilpatrick et al 1987).

It remains uncertain however whether these binding sites can be correlated directly with functionally active 5-HT receptor sub types. The fact that on heating to 60°C these membrane bound sites show a total loss of binding for each of the sub types indicates that they could be membrane bound proteins but not necessarily receptor proteins. Consequently functional correlates are required if the multiple 5-HT binding sites seen using ligand binding and autoradiography are to be established as of physiological significance.

The existence of presynaptic 5-HT autoreceptors that control the release of 5-HT from serotonergic nerve terminals had been demonstrated and shown to be inhibited by methiothepin and quipazine but not by other 5-HT antagonists (cyproheptadine, methysergide, mianserin and spiperone) (Cerrito & Raiteri 1979, Martin & Sanders - Bush 1982a). Due to the significant correlation between the effects of K^+ - evoked ^{3}[H] 5-HT release and ^{3}[H] 5-HT binding but not ^{3}[H] spiperone binding Martin & Sanders - Bush (1982b) concluded that the 5-HT autoreceptor and the 5-HT_1 binding site may be related.

Behavioural studies have also shown that certain 5-HT receptor mediated behaviour such as wet-dog shakes and head twitch appear to be mediated primarily by activation of 5-HT_2 receptors as they can be selectively antagonised by 5-HT_2 ligands such as ketanserin and pirenperone (Yap & Taylor 1983, Colpaert & Janssen 1983a+b). A comparison of the effects of 5-HT ligands on wet-dog shakes and the 5-HT syndrome by Lucki et al (1984) demonstrated that although 5-HT_2 ligands were effective at blocking wet-dog shakes they were ineffective at blocking the 5-HT syndrome. The non-specific 5-$HT_{1/2}$ ligands metergoline and methysergide were however capable of blocking the syndrome suggesting that it may be mediated via 5-HT_1 receptors.

The existance of different types of 5-HT receptors within the CNS has also been proposed in order to explain the electrophysiological differences discovered during single unit recording experiments.

Aghajanian (1981) described three distinct types of 5-HT receptor S_1, S_2 and S_3 based on regional neuronal responses to 5-HT as determined by extracellular unit recording. S_1 receptors were proposed to mediate the excitatory or facilitatory action of 5-HT seen with microiontophoretic application of 5-HT onto facial motoneurones (McCall & Aghajanian 1979). 5-HT did not directly evoke action potential generation but would facilitate the subthreshold or threshold excitatory effects of iontophoretically applied glutamate. This response could be antagonised by methysergide and cyproheptadine. S_2 receptors were proposed to mediate the inhibitory effects of 5-HT and LSD on dorsal raphe firing activity. Hence activation of the S_2 receptors would result in a reduction in the firing activity of serotonergic neurones. Finally S_3 receptors were proposed to mediate the post synaptic inhibitory responses to 5-HT in areas, other than the DR nucleus, and showed only a weak inhibitory response to LSD application (Haigler & Aghajanian 1974, Wang & Aghajanian 1977a) and were insensitive to the 5-HT ligands methysergide and cyproheptadine.

However not all areas of the brain conform to this rather rigid pattern. In an early intracellular study into the action of 5-HT application on hippocampal CA_1 neurones Jahnsen (1980) noted that 50% of cells showed an inhibitory response, 11% showed an excitatory response, 6% a biphasic response and 33% no response at all. Hence it appeared that receptor types may not be homogeneous to a specific brain region or even a single neurone. This may explain the anomalous antagonist responses observed by Segal (1976) in unit recordings from the hippocampus. In this preparation methysergide and cyproheptadine were shown to be potent antagonists of 5-HT induced inhibition of firing.

At the start of this study it was not yet known if the S_2 autoreceptor proposed by Aghajanian to mediate the inhibitory response of dorsal raphe neurones to 5-HT corresponded to any of the proposed 5-HT binding sites or if indeed the autoreceptor was pharmacologically similar to the presynaptic 5-HT_1 autoreceptor mediating 5-HT release from serotonergic neurones. Hence it was thought important to try and elucidate the nature of the somatic autoreceptor on DR neurones and the ionic mechanism that underlies 5-HT induced inhibition of firing. This was greatly helped by the more recent development of more

specific 5-HT ligands which will be discussed when applicable, as will the results from other groups looking at the same problem that have reported findings during the course of this study.

RESULTS

Mechanisms of action of 5-hydroxytryptamine.

During current clamp experiments almost all neurones impaled in the raphe slice preparation (see methods) that showed the characteristic passive membrane properties of serotonergic neurones (see previous chapter) responded to 5-HT superfusion with a membrane hyperpolarisation and a decrease in input resistance. In Fig. 4.1(a) the resting membrane potential of the neurone under study was -66mV in control ACSF, the electrotonic potentials evoked in response to hyperpolarising current steps showed the input resistance (Rm) to be 439MΩ and the time constant (τ) to be 49.2ms. Manual voltage clamping of the resting potential back to the pre 5-HT membrane potential showed 5-HT to induce a reduction in Rm to 195MΩ and τ to 26.4m. On washout the membrane potential returned to control levels and Rm recovered to 405MΩ and τ to 50.3ms. In the same cell current - voltage relationships, Fig. 4.1(B), showed the reversal potential for the 5-HT induced hyperpolarisation to be -80.3mV. This value was close to the value calculated from the Nernst equation for a potassium mediated conductance. In 19 similar experiments 100μM 5-HT caused a -9.1 ± 1.1mV hyperpolarisation and a reduction in Rm from 221 ± 44MΩ to 149 ± 16.4MΩ and τ from 33.2 ± 3.9ms to 22.1 ± 2.0ms. The reversal potential was seen to be -91.6 ± 5.3mV which once again was close to the calculated reversal potential for a potassium mediated conductance (see Figs. 4.18, 4.18 + 4.19). Superfusion with 50μM 5-HT (not shown) evoked a hyperpolarisation of -6.5 ± 0.7mV (n = 6) that was associated with a reduction in Rm from 233 ± 24MΩ (n = 6) to 176 ± 17MΩ (n = 6) and τ from 39.4 ± 8.6ms (n = 6) to 29.1 ± 6.1ms (n = 6).

In a group of experiments designed to show the postsynaptic nature of the 5-HT response the above experiment was repeated in the presence of TTX to block synaptic transmission. In TTX containing ACSF a 0.2nA hyperpolarising current step evoked a steady state voltage deflection of -50mV from the resting membrane potential in the neurone shown in Fig. 4.2, a similar amplitude depolarising current step evoked only a 15mV voltage deflection. Following superfusion with 100μM 5-HT a reduction in the voltage responses to hyperpolarising current steps was observed with τ decreasing from 41.8 to 20.8ms and the current - voltage relationships in the hyperpolarising direction,

Fig. 4.2(B) (lower left quadrant) showing a reduction in the input resistance from 241 to 123MΩ. No apparent effect of 5-HT was observed in voltage deflections in the depolarising direction Fig. 4.2(B) (upper right quadrant). The effect on the hyperpolarising voltage responses was reversed on washout.

In order to determine the increase in outward current flow occurring during superfusion with 5-HT the voltage clamp protocol was employed. In Fig. 4.3(A) the cell was clamped at or near the resting membrane potential of -64mV. In control ACSF, voltage step commands from -64 to -104mV in 10mV increments evoked square step currents which increased linearly with the increase in the voltage step commands. Superfusion with 100μM 5-HT caused a marked increase in the step currents evoked in response to voltage step commands of a similar magnitude as in control ACSF. The linear voltage - current relationship showed an increase in slope conductance from 7.0nS (mean 7.6 ± 1.2nS (n = 6)) in control ACSF to 11.8nS (mean 11.5 ± 1.3nS (n = 6)) during superfusion with 5-HT, Fig. 4.3(B). The reversal potential for the 5-HT effect was -80.3mV (mean -75.5 ± 1.3mV (n = 6)); once again close to the estimated reversal potential for a potassium conductance.

Mechanisms of action of gamma aminobutyric acid (GABA) receptor agonists.

GABA. Since the first direct evidence that GABA acts as an inhibitory transmitter in the mammalian CNS (Krnjevic & Schwartz 1967) subsequent research has demonstrated that GABA - mediated inhibition was due in part to $GABA_A$ receptor activation of a chloride channel, the receptor being selectively blocked by the plant alkaloid bicuculline (Curtis et al 1971). Hence a comparison between 5-HT and GABA mediated events in DR neurones was necessary in order to exclude a possible role of a Cl^- conductance in the 5-HT mediated inhibition.

Using glass microelectrodes filled with 3M KCl DR neurones were loaded with Cl^- during the passage of hyperpolarising current steps. As a consequence the normal chloride driving force could be reversed. Fig. 4.4 shows the effect of superfusion with 10mM GABA on chloride loaded DR neurones. At the resting membrane potential of -52mV in control ACSF the input resistance was 119MΩ and τ was 30.7ms. On superfusion with GABA the membrane potential depolarised by 7mV and Rm

was reduced to 72MΩ and τ to 4.9ms. An extrapolation of the linear current - voltage relationships Fig. 4.4(B) showed the reversal potential for the GABA induced response to be -37mV. Both the Rm and τ returned to the control levels on washout. Under the same chloride load 5-HT was shown on the same cell to evoke a hyperpolarisation asociated with a similar decrease in Rm and τ (see Fig. 4.1).

Baclofen, the $GABA_B$ receptor agonist. This β - p - chlorophenyl derivative of GABA was shown by Hill and Bowery (1981) to bind with high affinity and saturable binding kinetics to a bicuculline insensitive GABA binding site, the $GABA_B$ site. Unlike the $GABA_A$ receptor the $GABA_B$ receptor in hippocampal pyramidal cells is not linked to a chloride channel but to a potassium sensitive increase in conductance (Newberry & Nicoll 1984). In the raphe slice preparation baclofen was seen to cause a membrane hyperpolarisation even on neurones that did not respond to bath application of 5-HT, Fig. 4.5. In this cell electrotonic potentials evoked from rest, -63mV, in response to hyperpolarising current pulses showed a τ of 13ms (mean 21.6 ± 7.6ms (n = 4)) and an Rm of 74MΩ (mean 112 ± 18mV (n = 4)). Superfusion with 100μM 5-HT was ineffective on the membrane potential, the Rm or τ. Bath application of 50μM baclofen however caused a -6mV hyperpolarisation (mean -9.0 ± 2.0mV (n = 4)) and a concomitant reduction in Rm to 58MΩ (mean 76 ± 9MΩ (n = 4)) and τ to 9.5ms (mean 11.5 ± 2.0ms (n = 4)). The reversal potential for the baclofen mediated response, Fig. 4.5(B), was -90mV (mean -90.9 ± 6.4mV (n = 4)). This value was close to the 5-HT reversal potential and also to the reversal potential for the potassium conductance calculated using the Nernst equation.

Mechanisms of action of the putative $5\text{-}HT_{1A}$ agonists.

8-hydroxy-2-(di-n-propylamino)-tetralin (8OH-DPAT). 8OH-DPAT a centrally active 5-HT agonist (Hjorth et al 1982) was shown in binding experiments to selectively displace ^{3}[H] 5-HT from the $5\text{-}HT_{1A}$ binding site in the rat frontal cortex (Middlemiss & Fozard 1983) and has been shown to bind with high affinity in the region of the DR nucleus (Marcinkiewicz 1984). In the same year Hamon et al (1984) demonstrated that 8OH-DPAT was a potent agonist at both pre and post synaptic 5-HT receptors in the rat brain by showing 8OH-DPAT to inhibit ^{3}[H] 5-HT uptake into cortical synaptosomes and to stimulate 5-HT sensitive

adenylate cyclase in homogenates of colliculi from new born rats. Hence it was of interest to determine the effects of 8OH-DPAT on the membrane properties of DR neurones.

8OH-DPAT was found to mimick the action of 5-HT at concentrations an order of magnitude lower than would be required to evoke a similar response with 5-HT. In control ACSF, Fig. 4.6, the resting membrane potential of the neurone under study was -60mV with an input resistance 137MΩ (mean 221 ± 75MΩ (n = 3)) and τ 15.9ms (mean 23.8 ± 7.3ms (n = 3)). Superfusion with 10μM 8OH-DPAT caused a -13mV hyperpolarisation (mean -11 ± 1.0mV (n = 3)) a decrease in Rm to 87MΩ (mean 144 ± 28MΩ (n = 3)) and τ to 8.4ms (mean 16.0 ± 2.8ms (n = 3)). The effect was extremely persistent and only partial recovery occurred after 30 minutes of washing, membrane potential was only restored to -67mV, the Rm to 108MΩ and τ to 14.3ms. The current - voltage relationships generated before and during superfusion with 8OH-DPAT showed a reversal potential for the drug effect of -97mV (mean 89.2 ± 5.1mV (n = 3)). This effect with 10μM proved to be submaximal as 100μM 8OH-DPAT (not shown) could evoke a -15.5 ± 4.5mV (n = 2) hyperpolarisation and decreased Rm from 226 ± 42MΩ (n = 2) to 102 ± 21MΩ (n = 2) and τ from 35.4 ± 2.9ms (n = 2) to 14.6 ± 0.5ms (n = 2). Hence the input resistance was seen to be decreased by 31% during bath application of 10μM 8OH-DPAT and 54% by 100μM 8OH-DPAT. τ was also seen to be altered in a dose dependent fashion with a 44% decrease in 10μM 8OH-DPAT and a 61% decrease in 100μM 8OH-DPAT. In contrast the reversal potential for the 8OH-DPAT effect showed little change with dosage and were -89.2 and -90.4mV respectively. Both potentials are close to that expected for the reversal potential of a potassium mediated event.

Dipropyl-5-carboxamidotryptamine (DP-5-CT). Experiments on the electrically stimulated guinea-pig ileum, that had been proposed as a model for 5-HT_{1A} receptors in the periphery (Fozard & Kibinger 1985), had demonstrated that DP-5-CT was an extremely potent 5-HT_{1A} agonist (Hagenbach et al 1985) it was of interest therefore to see if DP-5-CT was active on the 5-HT receptors in the DR nucleus.

DP-5-CT was indeed found to be a potent agonist, Fig. 4.7(A). At the resting membrane potential of -62mV, in control ACSF , hyperpolarising electrotonic potentials showed the cell to have an input resistance of 118MΩ and a τ of 22.7ms. Superfusion with 10μM DP-5-CT caused a marked, -12mV, hyperpolarisation which was associated

with a decrease in Rm to 67MΩ and τ to 10.9ms. Even after prolonged washing no reversal of the DP-5-CT induced was observed. Consequently DP-5-CT was considered impracticable for further study. Like 5-HT however DP-5-CT showed a reversal potential of action, Fig. 4.7(B), of -90.2mV which was again close to the expected reversal potential for a potassium mediated event.

Buspirone. This pyrimidinylpiperazine derivative has been shown to be a centrally active anxiolytic in man (Goldberg & Finnerty 1979). Structurally unrelated to the better known benzodiazepine anxiolytics, buspirone has been shown not to interact with benzodiazepine or GABA binding sites (Taylor et al 1982). This same group suggested that the anxiolytic effects ascribed to buspirone might involve central dopaminergic mechanisms. However Gozlan et al (1983) showed that buspirone to be a potent displacer of tritiated 8OH-DPAT from its binding site. Hence the anxiolytic effects of buspirone could be mediated by an action at 5-HT_{1A} receptors.

In the dorsal raphe slice buspirone was found to mimick the action of 5-HT on DR neurones and occlude the responses of both 5-HT and baclofen. At the resting membrane potential of -60mV, Fig. 4.8(A), in control ACSF the neurone had an input resistance of 254MΩ (mean 209 ± 21.4 (n = 3)) and a τ of 36.9ms (mean 29.4 ± 5.9ms (n = 3)). Superfusion with 10μM buspirone caused a -17mV hyperpolarisation which was associated with a decrease in Rm to 122MΩ (mean 97 ± 11.0MΩ (n = 3)) and τ to 17.3ms (mean 12.3 ± 4.9ms (n = 3))(Figs. 4.17, 18, 19). In the presence of 10μM buspirone neither baclofen nor 5-HT (not shown) had any marked effect on either the input resistance (139 and 127MΩ respectively), Fig. 4.9, or the τ. The reversal potential for the buspirone evoked response, Fig. 4.8(B) was calculated to be -93.2mV (mean -93.9 ± 4.2mV (n = 3)), Fig. 4.19, which was again close to the that estimated for a potassium mediated event.

Antagonism of 5-HT induced responses.

Methysergide. The classical 5-HT antagonist methysergide (Gyermek 1961, Cottrell 1970) has been shown to be a non - specific ligand at the 5-HT_1 and 5-HT_2 binding sites (Peroutka & Snyder 1979, Leysen 1981) however it has also been shown to be a potent antagonist at the facial motornucleus (McCall & Aghajanian 1979) but not at the dorsal raphe nucleus (Haigler & Aghajanian 1974) as measured by extracellular

unit recording. It was thought important therefore to determine the effect of pretreatment with methysergide on the inhibitory response to 5-HT of serotonergic neurones within the DR nucleus. Superfusion with 100μM methysergide, Fig. 4.10(A), evoked no direct effect on the resting membrane potential of -71mV recorded in control ACSF, neither was there any apparent effect on the input resistance (229MΩ) nor the τ (28.0ms). On subsequent superfusion with 50μM 5-HT in the presence of methysergide a -5mV hyperpolarisation of the membrane potential was observed. This hyperpolarisation when manually voltage clamped to the resting membrane potential was seen to be associated with a decrease in Rm to 163MΩ and a reduction in τ to 18.0ms. This result was similar to that demonstrated earlier for 50μM 5-HT application in the abscence of an antagonist. The reversal potential for the 5-HT induced response, -91mV, was once again close to that estimated for an event mediated by a change in potassium conductance.

Spiperone. Although spiperone had been originally used to distinguish between 5-HT_1 and 5-HT_2 binding sites no investigation into the postsynaptic effects of spiperone on 5-HT mediated events had been demonstrated at the onset of this study.

The data obtained from binding studies indicated that application of low μM concentrations of spiperone could totally inhibit 5-HT_{1A} and 5-HT_2 binding whilst leaving 5-HT_{1B} binding unaffected (Middlemiss & Fozard 1983, Peroutka 1985). It was therefore considered important to study the effects of low μM concentrations on 5-HT induced inhibition of raphe neurones.

In control conditions, Fig. 4.11(A), 100μM 5-HT was seen to evoke a -9mV hyperpolarisation from the resting membrane potential of -60mV. The hyperpolarisation was accompanied by a reduction in Rm from 229 to 187MΩ and τ from 23.0 to 16.7ms. On washout the τ recovered to 34.2ms and Rm to 292MΩ. The membrane potential however remained 7mV more hyperpolarised than the original resting membrane potential. The reversal potential, Fig. 4.11(B), was calculated to be -105mV which once again would indicate a response mediated by a change in the potassium conductance of the membrane.

Bath application of 10μM spiperone was seen to have no direct effect on the resting membrane potential of -67mV, Fig. 4.12, the input resistance however continued to rise from 292 to 322MΩ and τ from 34.2 to 40.0ms as had been shown during washout of 5-HT in control conditions.

After a period of more than 20 minutes superfusion with 10μM spiperone the response to bath application of 100μM 5-HT was seen to be reduced, Fig. 4.13(A), from a -9 to a -6mV hyperpolarisation. This hyperpolarisation was associated with a decrease in Rm from 322 to 286MΩ. In contrast the τ appeared to be only marginally reduced from 40.0 to 39.1ms. On washout the membrane potential returned to the pre - 5-HT membrane potential and Rm recovered to 326MΩ, τ increased to 41.0ms. Current - voltage relationships constructed before and during 5-HT application showed a reversal potential of -112mV which was close to that recorded in control conditions.

The effects of superfusion with 10μM spiperone on 5-HT induced changes in Rm and τ are summarised in Fig. 4.14. In Fig. 4.14(A) the normalised Rm of the membrane can be seen to gradually increase during the course of the experiment. Although an increase in Rm was observed following washout of 5-HT in control conditions an increase in Rm was associated with the application of spiperone on two occasions. Superfusion of spiperone caused at maximum a 60% reduction of the 5-HT induced decrease in Rm even after prolonged incubations in spiperone (149 minutes, results not shown). As would be expected the changes in τ closely followed those observed for Rm. Hence the normalised τ was seen to gradually increase during the course of the experiment. On the initial application of 5-HT τ was seen to be reduced by 42%, following 5-HT application in the presence of spiperone however the τ was only marginally reduced by 4%.

To control for a non - specific blockade of potassium channels by spiperone the membrane response to baclofen was tested following continuous superfusion with spiperone. Fig. 4.15 shows that even after prolonged superfusion with spiperone (> 1hr) baclofen evoked a marked hyperpolarisation of -16mV from the resting membrane potential of -56mV. This hyperpolarisation was associated with a marked reduction of both the Rm from 128 to 89MΩ and τ from 30.0 to 18.0ms. Subsequent washout, for longer than 30 minutes, showed the membrane potential to return to the control level of -56mV and Rm and τ to recover to 112MΩ and 26.0ms respectively.

Current - voltage relationships produced before and during baclofen superfusion, Fig. 4.15(B), showed a reversal potential for the baclofen action of -95mV which was close to that previously observed in control ACSF (see Fig. 4.5(B)).

S_2 (SYNTEX), a putative 5-HT_{1A} antagonist. This putative 5-HT_{1A} antagonist still under development was reported to have a pK_I of 8.1 and a selectivity for the 5-HT_{1A} binding site at concentrations ten fold lower than was required for binding to other 5-HT binding sites (Syntex personal communication).

Addition of 100nM S_2 to the control ACSF had no direct effect on the resting membrane potential, Rm or τ (not shown). In Fig. 4.16(A) in the presence of 100nM S_2 the resting membrane potential was -66mv, the Rm 379MΩ and τ 36.8ms. Superfusion with 100μM 5-HT, in the presence of 100nM S_2, evoked a modest -4mV hyperpolarisation. In addition the Rm was reduced to 284MΩ and τ to 18.0ms. On washout the membrane potential returned to -66mV and the Rm recovered to 379MΩ and τ to 34.2ms. The current - voltage relationships, Fig. 4.16(B), showed the reversal potential for the 5-HT induced effect to be -81mV.

Discussion

In this chapter a post synaptic mechanism has been demonstrated for the inhibitory action of 5-HT on DR neurones. The ionic mechanism underlying this response appears to be the activation of a pure outward potassium conductance. This mechanism is shared by the $GABA_B$ antagonist baclofen and the purported 5-HT_{1A} agonists 8OH-DPAT, buspirone and DP-5-CT but not the $GABA_A$ agonist GABA indicating that the 5-HT response may be mediated at least in part by the activation of a 5-HT_{1A} receptor. Support for this hypothesis came from the observation that the non - specific 5-$HT_{1/2}$ receptor antagonist methysergide was ineffective in blocking the response to 5-HT whereas the 5-$HT_{1A/2}$ antagonist spiperone caused a marked reduction in the 5-HT induced response. The putative 5-HT_{1A} antagonist S_2 however displayed no antagonism of the 5-HT induced response. The results obtained will be discussed in relation to the results reported from other groups during the course of this study.

Bath application of 5-HT was demonstrated to cause a dose dependent hyperpolarisation of DR neurones which was associated with a decrease in the input resistance of the membrane and a concomitant reduction in the membrane time constant. Any one of these three membrane responses would maintain the neurone in a state of decreased excitability during the period of 5-HT mediated synaptic transmission. Primarily the 5-HT induced hyperpolarisation would decrease the neuronal excitability by increasing the size of a depolarising response required to bring the membrane potential to the threshold for action potential generation. The decrease in the input resistance and the membrane time constant act to further reduce the response to excitatory inputs. The decrease in the input resistance dictates that a larger than normal excitatory current flow would be required to evoke a depolarising voltage response of sufficient magnitude to reach the threshold for action potential generation, irrespective of the membrane hyperpolarisation. The decreased membrane time constant although not affecting the amplitude of an excitatory voltage response would reduce the probability of temporal summation of synaptic inputs and hence reduce the integrative properties of the neurone.

In current clamp mode the reversal potential for the 5-HT response (≈ -90mV) was indicative of a response mediated by a change in potassium conductance, as estimated by the Nernst equation. This result is supported by the observations of Aghajanian & Lakoski (1984) who reported that both 5-HT and LSD showed reversal potentials of ≈ -90mV when measured in the presence of 5mM extracellular potassium (6.25mM K^+ was routinely used in this study). This group further demonstrated that raising the extracellular K^+ concentration to 10mM caused an 18mV reduction in the reversal potential for both these compounds (≈ -72mV). This was almost exactly as predicted by the Nernst equation for a pure potassium conductance, despite the fact that the two agonists evoked hyperpolarisations of different magnitudes when applied in similar concentrations.

Although exogenous application of 5-HT evoked a membrane hyperpolarisation which appeared to be mediated by a change in potassium conductance proof was needed that 5-HT was acting on postsynaptic receptors on DR neurones, and not presynaptically thereby altering a tonic input onto serotonergic neurones. The observation that 5-HT could evoke a similar response in TTX to that normally evoked in control ACSF supported the theory that 5-HT was indeed acting at putative postsynaptic 5-HT receptors. It was interesting to note during the course of the TTX experiments that 5-HT had an apparent differential effect on hyperpolarising and depolarising steady state voltage deflections. Hence 5-HT appeared to cause a marked reduction in the amplitude of steady state hyperpolarising voltage deflections without affecting the amplitude of the depolarising responses. This paradox may be explained by refering to Fig. 3.17. In the presence of TTX hyperpolarising voltage step commands from a holding potential of -40mV showed the presence of an non - inactivating outward I_M like current. The I_M current acts as a rectifier and prevents prolonged periods of membrane depolarisation. This I_M channel current is believed to be carried by an outward movement of K^+ ions, consequently the outward K^+ current may occlude the response to 5-HT application during depolarising voltage deflections.

Voltage clamp analysis showed that at a holding potential at or near the resting membrane potential 5-HT application evoked an outward current which was associated with a two fold increase in membrane conductance. These responses would correspond to the hyperpolarisation

and the decrease in the input resistance observed in current clamp conditions. Voltage - current relationships showed a mean reversal potential for the 5-HT mediated conductance change of -75mV (n = 6). This value was again close to the estimated reversal potential of -82mV for a K^+ conductance given an extracellular K^+ concentration of 6.25mM. There does however appear to be a 15mV discrepancy between the 5-HT reversal potential measured in voltage clamp and that measured in current clamp. It was noted that however that the neurones sampled in voltage clamp also displayed more positive than average reversal potentials in current clamp and hence the reversal potential ($\approx$ -91mV) as estimated for the larger number of current clamp records (n = 19) probably reflects the true reversal potential of the 5-HT mediated event.

The proposition that postsynaptic 5-HT receptor activation mediates an outward K^+ current in DR neurones was supported by the observation of Williams (1987) that the 5-HT current reversed from outward to inward at the potassium equilibrium potential and that increasing the extracellular K^+ concentration caused the reversal potential for the 5-HT current to shift towards more positive potentials.

The possibility that a chloride conductance might have been responsible for the 5-HT induced hyperpolarisation was discounted with the observation that following chloride loading of DR neurones GABA, a $GABA_{A/B}$ receptor agonist, evoked a depolarisation in conditions where 5-HT was seen to evoke a hyperpolarisation. Hence under conditions of chloride loading GABA activation of $GABA_A$ receptors and the subsequent increase in chloride conductance (Curtis et al 1971) must predominate over the increase in K^+ conductance associated with the activation of $GABA_B$ receptors (Newberry & Nicoll 1984). The similarity of the reversal potentials evoked by 5-HT in control and chloride loaded neurones implied that the hyperpolarisation seen on 5-HT application was due to a pure K^+ mediated event.

Newberry & Nicoll's observation that in hippocampal neurones baclofen activation of $GABA_B$ receptors evoked a hyperpolarisation that was mediated by an outward K^+ current indicated that baclofen might be used as a control for events mediated by 5-HT activation of putative 5-HT receptors on DR neurones. The response of DR neurones to bath application of baclofen was shown to be similar to that observed in hippocampal neurones, namely a hyperpolarisation and an associated

decrease in the input resistance and membrane time constant. The similarity between the baclofen evoked response and that of 5-HT application was further strengthened with the observation that both agonists showed a reversal potential of ≈ -90mV.

Andrade et al (1986) reported that in hippocampal neurones 5-HT receptors and $GABA_B$ receptors were coupled to the same K^+ channels by a pertussis toxin sensitive GTP binding (G) protein. Although this question was not addressed in this study, Aghajanian's group have demonstrated that in the DR nucleus pertusis toxin pretreatment can block the inhibition of extracellular firing activity evoked by both intravenous and iontophoretic application of baclofen, 5-HT and LSD (Innis & Aghajanian 1987). Further the inhibitory action of baclofen and 5-HT could be mimicked by intracellular injection of the stable GTP analogue GTPγS. The inhibitory actions of GTPγS were not additive with those of either 5-HT or baclofen, suggesting that they share a common effector system (Innis et al 1988). Hence it was concluded that in DR neurones, as in hippocampal neurones, 5-HT and $GABA_B$ receptors are coupled to the same K^+ channels by a pertussis toxin sensitive G protein. This made baclofen an even more suitable candidate to act as a control when studying possible antagonists of the 5-HT induced response than had originally been envisaged.

The results of bath application of the putative $5\text{-}HT_{1A}$ agonists 8OH-DPAT and DP-5-CT and the novel anxiolytic buspirone are compared with baclofen and GABA and summarised for their action on input resistance in Fig. 4.17, their action on τ in Fig. 4.18 and their calculated reversal potential in Fig. 4.19. Apart from GABA all of the above compounds mimicked the hyperpolarising response of DR neurones to 5-HT application. The responses ranged from -6 to -17mV and were seen to be dose dependent in the case of 5-HT and 8OH-DPAT.

Despite the variations observed in the hyperpolarising responses Fig. 4.19 shows that there appears to be no significant difference between the calculated reversal potentials (≈ -90mV) obtained for this group of agonists. Hence this would indicate a common mechanism of action probably by an alteration of an, as yet, uncharacterised potassium conductance. The hypothesis of a shared mechanism of action was supported by the observation that in the presence of buspirone the responses to 5-HT and baclofen were occluded, Fig. 4.9. Unlike the

hyperpolarising response to application of 5-HT and 8OH-DPAT the reversal potential was found to be independent of the concentration of agonist applied.

Although the putative 5-HT_{1A} agonists and baclofen appear to share a common mechanism of action it was noticeable during the course of these experiments that despite the similarity to 5-HT in the rate of onset (2 to 3 minutes) of action the washout period required to show recovery from the baclofen action was dramatically increased. Hence 2 to 5 minutes was usually required for full 5-HT washout whereas 8OH-DPAT required longer than 45 minutes and DP-5-CT did not recover fully even after prolonged periods of washing. This type of prolonged response has previously been reported for the potent but nonselective 5-HT_{1A} agonist LSD (Aghajanian & Lakoski 1984). The observation by Rigdon & Wang (1987) that inhibitors of 5-HT reuptake (imipramine and fluoxetine) caused a decrease in the base line firing rates of DR neurones superfused with phenylephrine indicated that a) in the <u>in vitro</u> DR slice preparation an active persistent reuptake process is present and b) a tonic release of 5-HT must occur within the DR slice. The active reuptake process would be seen to reduce the effective concentration of 5-HT seen at the somatic receptors and also act, in addition to the washout process, to speed the removal of 5-HT from the extracellular fluid. If the putative 5-HT_{1A} agonists and buspirone were not recognised as substrates for the active uptake process this could account for the observation that ten fold higher concentrations of 5-HT were required to evoke hyperpolarising responses of a similar magnitude to those evoked by the above agonists. The absence of an active reuptake process would also result in longer washout periods than would be required for 5-HT. In the rat striatum Schoemaker & Langer demonstrated that 8OH-DPAT showed biphasic binding to striatal membranes. A high affinity binding site (K_d = 0.59nM) was observed that was interpreted to correlate to the 5-HT_{1A} receptor and a low affinity binding site (K_d = 34nM) which, due to inhibition of binding in the presence of the 5-HT uptake inhibitors indalpine and citalopram, was assumed to represent 8OH-DPAT binding to the 5-HT uptake system. If a similar binding was to occur in the DR nucleus and assuming that 8OH-DPAT was not internalised then, on subsequent washout following superfusion with μM 8OH-DPAT concentrations, a slow dissociation from the uptake binding site might allow the continued activation of somatic 5-HT receptors. It is

unlikely however that this is the reason for the prolonged action of these compounds. Firstly because no similar binding has been demonstrated for either DP-5-CT or buspirone, both of which require prolonged periods of washout and secondly it is unlikely that this mechanism would be shared by the $GABA_B$ agonist baclofen. What is more likely is that these compounds show a much higher affinity for their respective receptors and in the absence of an active uptake process simply require longer periods of washout before receptor activation is abolished. It would therefore be of interest to study the action of 5-HT, 8OH-DPAT, DP-5-CT and buspirone in the presence of a 5-HT uptake inhibitor.

A simple rank order of drug potency could however be constructed by measuring the percentage reduction of the Rm and τ in the presence of these compounds. The percentage reduction in Rm summarised in Fig. 4.17 shows that for the lowest concentration of drug treatment the rank order of potency was buspirone > DP-5-CT > 8OH-DPAT > 5-HT, with values ranging from 53% reduction on buspirone application to 24% reduction with 5-HT application. As might be expected GABA acting at both $GABA_A$ and $GABA_B$ showed a greater reduction in Rm than the $GABA_B$ agonist baclofen. Interestingly 5-HT showed a greater reduction of Rm than baclofen at a similar concentration. These two agonists have been demonstrated to activate the same G protein mediated potassium conductance (Innis & Aghajanian 1987) and hence the greater potency of 5-HT may reflect a greater population of 5-HT receptors than $GABA_B$ receptors on DR neurones. Since the time constant for membrane charging is dependent on the input resistance of the neurone it would be expected that the rank order of potency observed for the reduction of Rm would be similarly reflected in the effect on τ. Fig. 4.18 shows this supposition to be true. Hence the order of potency was found to be buspirone > DP-5-CT > 8OH-DPAT > 5-HT. Once again GABA was shown to be more potent than baclofen, the reduction of τ by GABA however did not appear to correlate to the GABA induced reduction in Rm. It is probable that this reflects neuronal damage rather than an intrinsic property of GABA action.

The similarity in the actions of the putative $5\text{-}HT_{1A}$ agonists and those of 5-HT indicated that the somatic 5-HT autoreceptor was most likely of the $5\text{-}HT_{1A}$ subclass. This theory was supported by the observation of Verge et al (1985) who showed that following selective degeneration of serotonergic neurones by intracerebral administration

of 5,7-dihydroxytryptamine a marked reduction in 8OH-DPAT binding in the dorsal raphe nucleus was observed. In contrast, no significant change was detected in the hippocampus or the cerebral cortex. This group concluded that the presynaptic autoreceptor on serotonergic cell bodies and/or dendrites were of the 5-HT_{1A} subtype and distinct from the autoreceptors located on the presynaptic nerve terminals. A similar conclusion was reached by VanderMaelen et al (1986) who examined the effects of intravenous or intraperitoneal buspirone on extracellular single unit recording from the DR nucleus in vivo. Buspirone was shown to cause a dose dependent reduction of DR firing activity which mimicked that of 5-HT and was resistant to picrotoxin which blocked the effects of iontophoretically applied GABA. More conclusive support for the 5-HT_{1A} autoreceptor theory came from the observation that two additional selective 5-HT_{1A} binding ligands ipsapirone (Dompert et al 1985, Glaser et al 1985) and LY 165163 (Ransom et al 1986) evoked inhibitory responses similar to those evoked by 5-HT in serotonergic neurones recorded intracellularly in the DR nucleus (Sprouse & Aghajanian 1987). Two short-chain-substituted piperazines, m-chlorophenylpiperazine (mCPP) and trifluoromethylpiperazine (TFMPP), shown to be specific 5-HT_{1B} ligands (Sills et al 1984) were found to be only weak inhibitors of extracellular single unit activity.

These results together with the results obtained in this study indicate that 5-HT_{1A} receptors probably predominate on the cell body and/or dendrites of DR neurones. However a lesser population of 5-HT_{1B} receptors may also be present. On the other hand it should be noted that Sprouse & Aghajanian (1987) suggested that the weak agonist activity of the 5-HT_{1B} ligands might be due to a residual 5-HT_{1A} agonist action of these compounds at the concentrations used in their study. It was also of interest to note that this group also mentioned that DR neurones showed minimal recovery from bath application of both ipsapirone and LY 165163 even after several hours of washout.

Because of the prolonged duration of action of the selective 5-HT_{1A} agonists the effects of 5-HT antagonists were measured against the response of DR neurones to 5-HT application. Although inconclusive when studied in isolation the results of the antagonist experiments obtained in this study add further weight to the argument that the somatic autoreceptor of DR neurones is of the 5-HT_{1A} subtype.

Methysergide the non-specific 5-$HT_{1/2}$ antagonist had been shown to be ineffective in blocking the inhibitory response of DR neurones to 5-HT application when recorded extracellularly (Haigler & Aghajanian 1974). This was also found to be true in this study when serotonergic neurones were recorded intracellularly. Pretreatment with 100μM methysergide showed no direct effect on the resting membrane potential, Rm or τ of DR neurones. Further 5-HT application in the presence of methysergide evoked a response of similar magnitude to that observed in control ACSF. In contrast spiperone, a non-specific 5-$HT_{1A/2}$ antagonist at concentrations used in this study, was shown to cause a gradual increase in the Rm and τ of DR neurones during the whole duration of application. Spiperone is highly lipophilic and was shown to require a preincubation of at least 1hr before a blockade of the 5-HT evoked hyperpolarisation in CA_1 pyramidal neurones was observed (Andrade & Nicoll 1987(a)). It is probable that an even more prolonged period of preincubation was necessary to overcome spiperone sequestration into lipid stores within the semi-submerged slice used in this study before an effective concentration in the extracellular fluid was achieved. The increase observed in both Rm and τ may be due to a non-specific effect of spiperone on the lipid bilayer of the serotonergic neurones. It is also possible that the increase in Rm and τ was indicative of a blockade of a tonic 5-HT release within the slice. That this could occur was supported by the observation that pretreatment with 10μM spiperone caused a marked (80%) blockade of the 5-HT evoked reduction in both Rm and τ. This antagonism is probably not mediated by an action on 5-HT_2 receptors since methysergide showed a total lack of antagonistic activity and ketanserin, a specific 5-HT_2 antagonist, was demonstrated by Lakoski & Aghajanian (1985) to be ineffective in antagonising 5-HT evoked inhibition of DR firing activity. Using extracellular single unit recording from the DR nucleus Lum & Piercy (1988) have recently demonstrated that low intravenous doses of spiperone antagonised the inhibitory action of 8OH-DPAT on DR neurones but not the dopamine receptor mediated effect of amphetamine on substantia nigra neurones. Further LY 53857, a 5-HT_2 antagonist, was ineffective at blocking the action of 8OH-DPAT in DR neurones. They concluded that the spiperone mediated antagonism of 8OH-DPAT on the DR nucleus represented a blockade of 5-HT_{1A} receptors and not 5-HT_2 or dopamine receptors.

It is interesting to note that although the evidence appears to point to the fact that the somatodendritic autoreceptors of DR neurones are of the 5-HT_{1A} subtype pretreatment with spiperone failed to totally antagonise the response to bath applied 5-HT even after spiperone incubation periods of greater than 1hr. Recently certain β-adrenoceptor antagonsts have been shown to be potent inhibitors of 5-HT_{1A} binding. Sprouse & Aghajanian (1986) demonstrated that the (-) isomer of propranolol rapidly and reversibly blocked the inhibitory effects on dorsal raphe firing of the 5-HT_{1A} selective agonists ipsapirone and 8OH-DPAT. (-) propranolol was however shown to be only a relatively weak antagonist of 5-HT itself. Hence it must be assumed that the endogenous neurotransmitter 5-HT may have actions on dorsal raphe neurones in addition to those mediated by 5-HT_{1A} receptors. It is possible that 5-HT_{1B} receptors are responsible at least in part for the additional action of 5-HT however the development of specific agonists and antagonists to the 5-HT_{1C} and $_{1D}$ will be required before our understanding of the 5-HT response in DR neurones is complete.

The Syntex compound S_2 was reported to show high affinity binding to 5-HT_{1A} binding sites and in a behavioural model for 5-HT action S_2 was seen to be a putative 5-HT_{1A} antagonist. In this study however S_2 was shown to be ineffective in blocking the 5-HT induced response DR neurones and showed no direct effect on passive membrane properties. This anomaly is not uncommon; the buspirone analogue (8-[2-[4-(2-methoxyphenyl)-1-piperazinyl]ethyl]-8-azaspirol[4,5]-decane-7,9-dione (BMY 7378) was shown to potently displace binding of 8OH-DPAT from rat hippocampal membranes and to block the effect of 8OH-DPAT on forskolin stimulated adenylate cyclase activity (Yocca et al 1987) and hence was assumed to be a 5-HT_{1A} antagonist. VanderMaelen et al (1987) however showed that BMY 7378 was a partial agonist on the 5-HT_{1A} receptors in the DR nucleus and inhibited neuronal firing. This would suggest that behavioural antagonism of 8OH-DPAT 5-HT_{1A} receptor activation need not involve a blockade of 5-HT_{1A} somatodendritic autoreceptors on DR neurones activated by 8-OH-DPAT.

In conclusion, the results presented in this chapter are consistent with much of the recent literature on the way in which the activation of 5-HT_{1A} receptors inhibits the activity of dorsal raphe neurones. A more potent, less lipophillic antagonist will be required if the role of this receptor in synaptic transmission is to be demonstrated.

Fig. 4.1

Intracellular current clamp recordings from dorsal raphe neurones in the in vitro slice preparation using 3M KCl glass microelectrodes. In A, (upper trace) electrotonic potentials evoked in response to graded (300ms) hyperpolarising current steps (lower trace) before, during and after superfusion with 100μM 5-HT creatinine sulphate. In control ACSF at the resting membrane potential (-66mV) the membrane input resistance was 439MΩ and the time constant for membrane charging (τ) was 49.2ms. During 5-HT superfusion a membrane hyperpolarisation of -7mV was evoked. Manual voltage clamping at the pre 5-HT membrane potetial showed the input resistance to fall to 195MΩ and τ to 26.4ms. On washout the membrane potential returned to control levels and the input resistance recovered to 405MΩ and τ to 50.3ms. In B, current - voltage relationships, calculated from the records in A, show the reversal potential for the 5-HT induced hyperpolarisation to be -80.3mV. Closed circles, current - voltage before 5-HT administration : open squares data obtained after 5-HT superfusion : closed squares data obtained during 5-HT superfusion.

Fig. 4.1

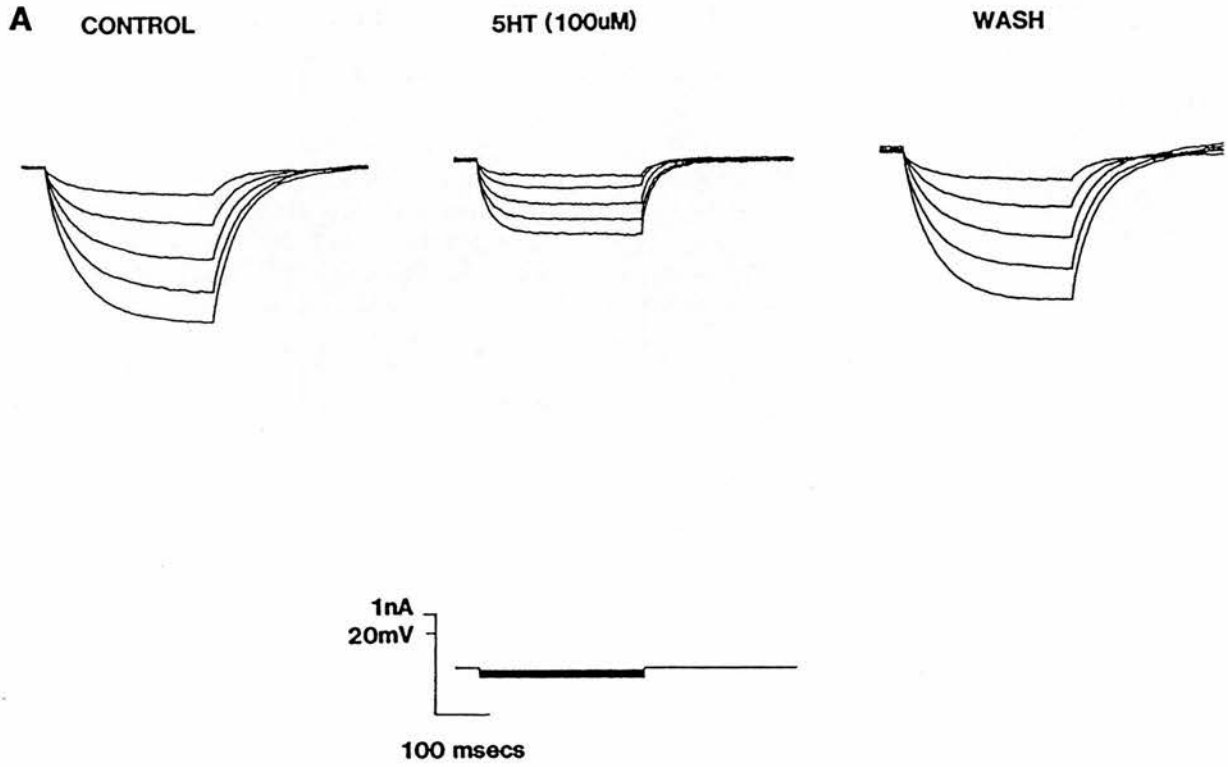
A
CONTROL
5HT (100uM)
WASH
1nA
20mV
100 msecs

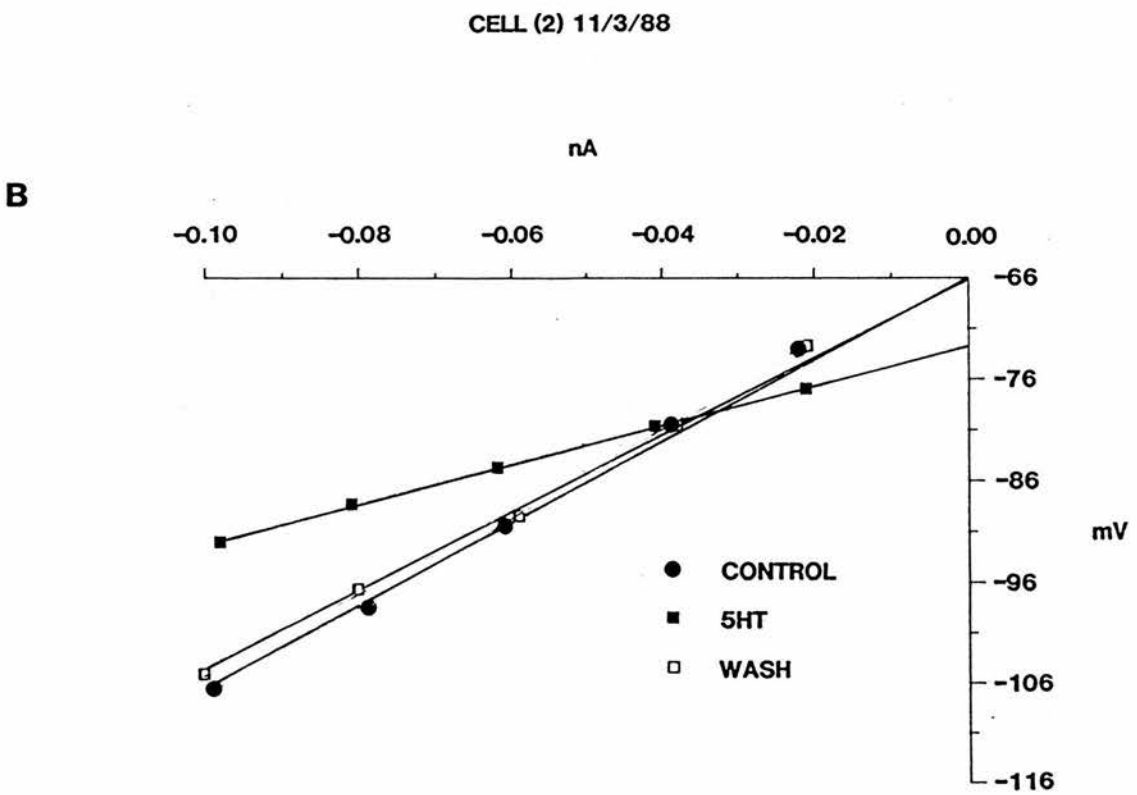
CELL (2) 11/3/88
B
nA
-0.10
-0.08
-0.06
-0.04
-0.02
0.00
-66
-76
-86
-96
-106
-116
mV
CONTROL
5HT
WASH

Fig. 4.2

The effect of 5-HT (100μM) on hyperpolarising and depolarising electrotonic potentials in the presence of TTX (1μM). In A, electrotonic potentials (upper trace) evoked in response to graded hyperpolarising and depolarising current steps (lower trace) before, during and after 5-HT superfusion. At the resting membrane potential of -76mV the electrotonic potentials were clearly asymmetrical and 0.2nA current steps which evoked a steady state 50mV deflection from resting levels in the hyperpolarising direction evoked only a 15mV deflection in the depolarising direction. Superfusion with 5-HT evoked a 10mV hyperpolarisation. Manual voltage clamping to the pre 5-HT membrane potential showed a reduction in the voltage response to hyperpolarising current steps together with a reduction in the time constant for membrane charging (τ) from 41.8 to 20.8ms without appearing to affect the depolarising voltage responses. The effect on the hyperpolarising voltage responses was seen to reverse on washout. In B, current - voltage relationships measured at steady state voltage levels (arrows in A) in the hyperpolarising direction (lower left quadrant) showed a reduction in the input resistance from 241 to 123MΩ during superfusion with 5-HT. No effect of 5-HT was observed on the current - voltage relationships in the depolarising direction (top right quadrant). Closed circles, current - voltage relationship before 5-HT administration : closed triangles current - voltage relationship during 5-HT superfusion.

Fig. 4.2

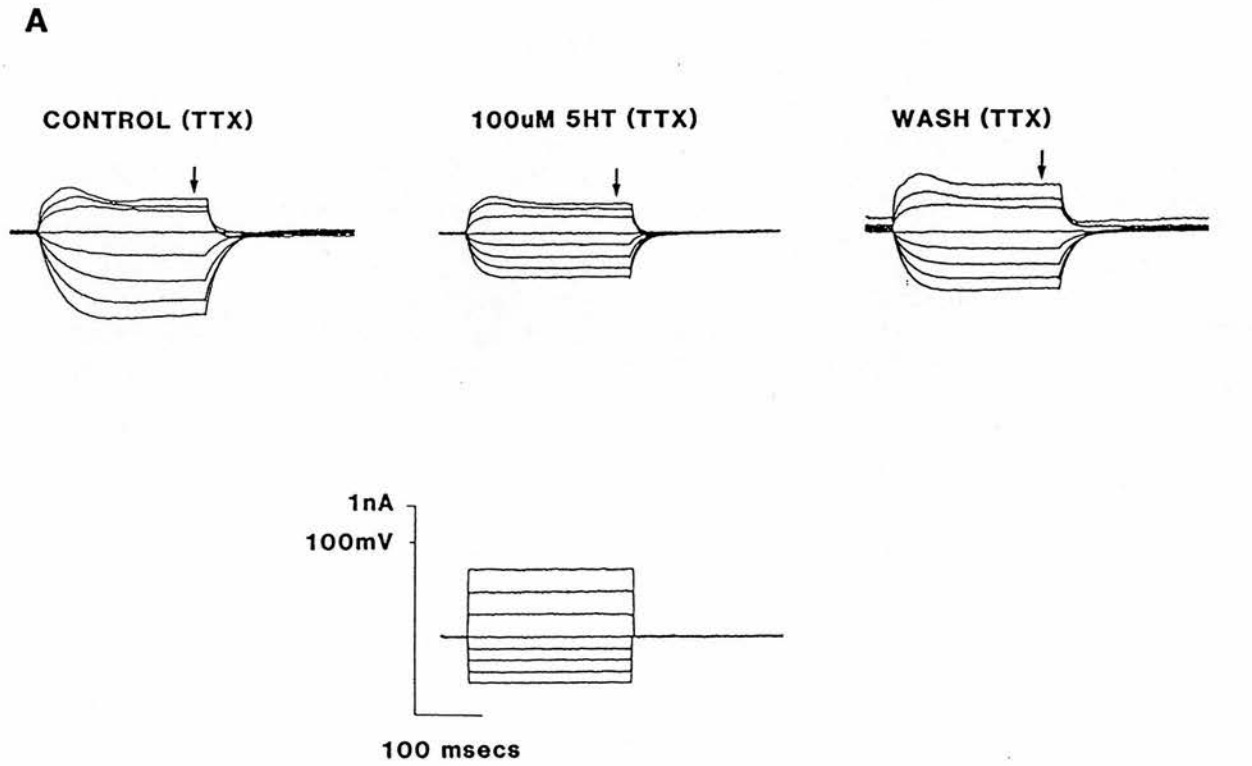
A
CONTROL (TTX)
100uM 5HT (TTX)
WASH (TTX)
1nA
100mV
100 msecs

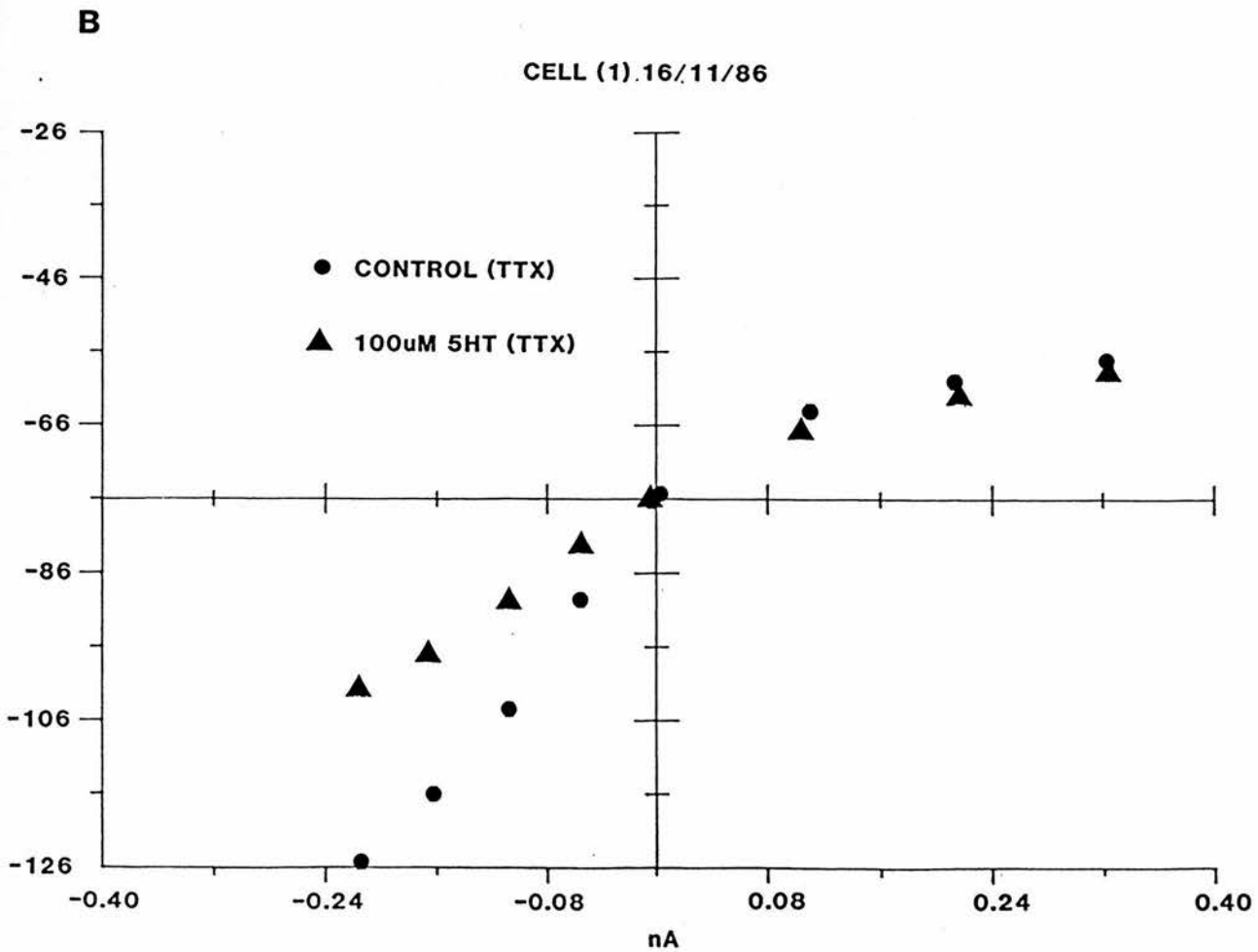
B
CELL (1).16/11/86
-26
-46
-66
-86
-106
-126
CONTROL (TTX)
100uM 5HT (TTX)
-0.40
-0.24
-0.08
0.08
0.24
0.40
nA

Fig. 4.3

Voltage clamp analysis of passive membrane conductance before, during and after bath application of 5-HT (100μM). In A , in the presence of 1μM TTX the cell was voltage clamped at -64mV. Hyperpolarising voltage step commands from -64 to -104mV in 10mV increments evoked graded square step currents which increased linearly with increasing step commands. Superfusion with 5-HT caused a marked increase in the step current evoked by voltage step commands to similar potentials. Note during 5-HT superfusion a 0.07nA DC positive current was required to maintain the cell at the holding potential. The step currents were seen to recover to control levels on washout. In B, voltage - current relationships showed 5-HT to cause an increase in the slope conductance from 7.0 to 11.8nS. The intercept of the two regression lines showed the reversal potential of the 5-HT effect to be -79.3mV.

Fig. 4.3

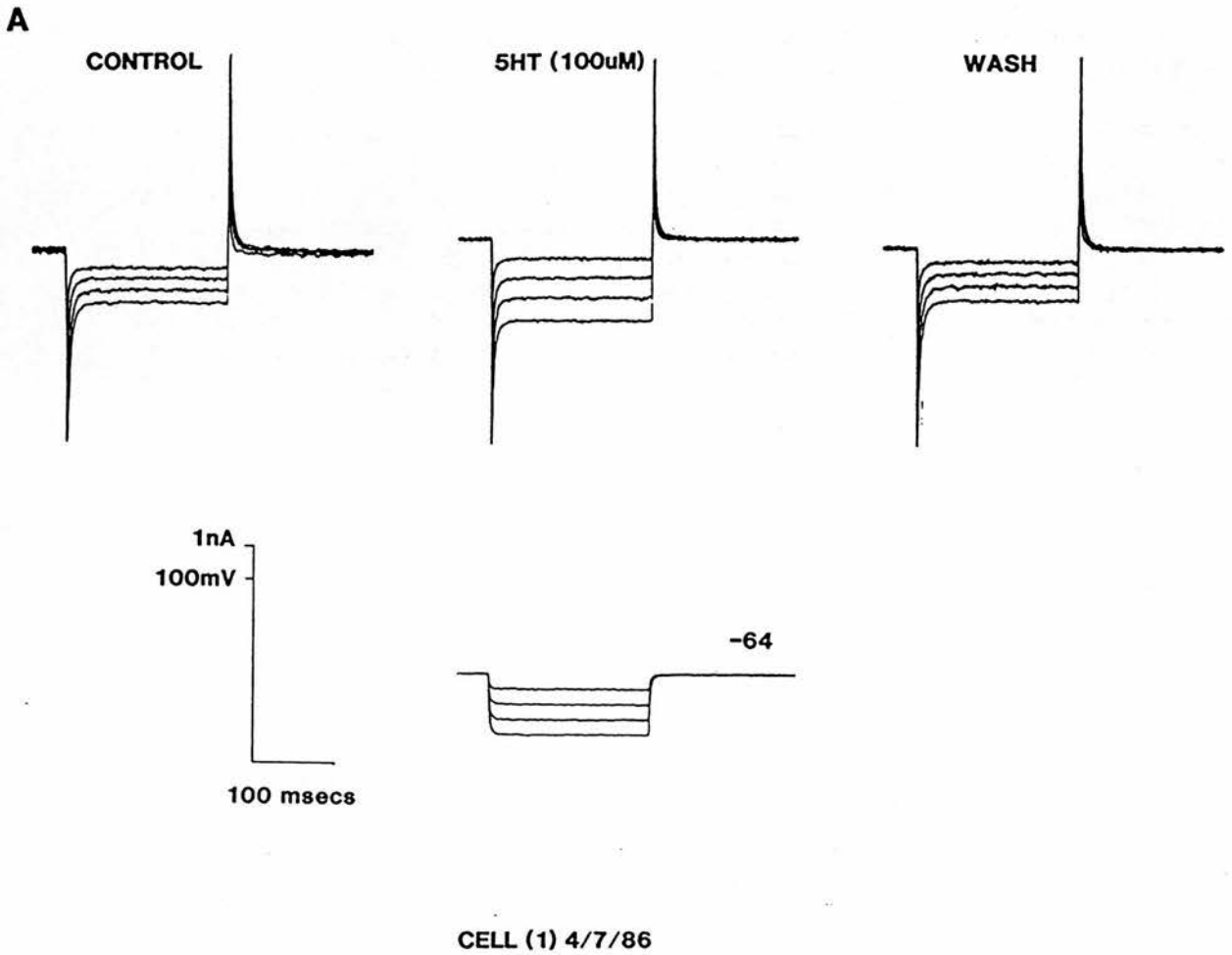
A
CONTROL
5HT (100uM)
WASH
1nA
100mV
-64
100 msecs
CELL (1) 4/7/86
B
mV
-104
-94
-84
-74
-64
0.0
-0.08
-0.16
-0.24
-0.32
-0.40
nA
CONTROL
5HT (100uM)

Fig. 4.4

The effect of gamma aminobutyric acid (GABA) on the resting membrane properties of chloride loaded raphe neurones. In A, chloride loading was achieved by impaling cells with 3M KCl electrodes, hyperpolarising current steps causing the gradual extrusion of Cl ions from the microelectrode into the cell. At rest -52mV Rm was 119MΩ and τ 30.7ms. Bath application of 10mM GABA caused a 7mV depolarisation which when manually offset was seen to be accompanied by a decrease in Rm to72MΩ and τ to 4.9ms. In this cell washout caused the cell to return to a membrane potential more negative than control (-60mV) and both Rm and τ returned to control values. In B, current - voltage relationships before and during superfusion with 10mM GABA. Extrapolation of the regression lines showed a reversal potential for the GABA mediated response of -37mV.

Fig. 4.4

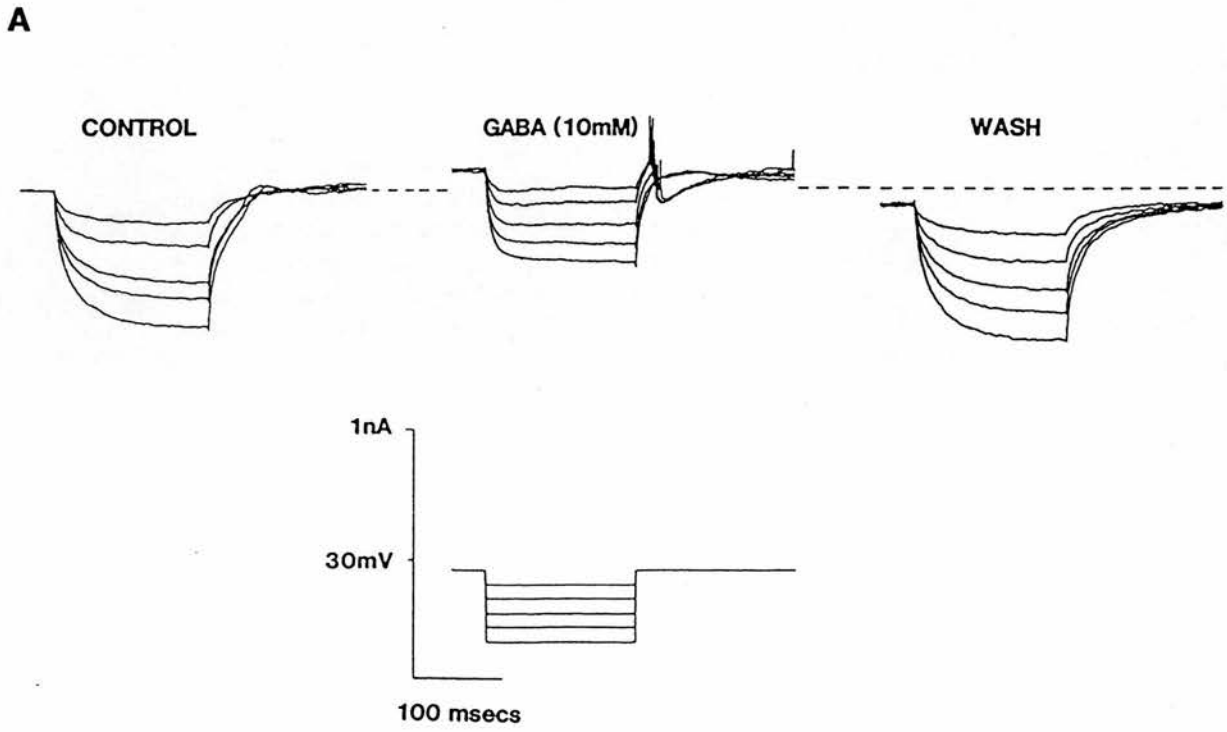
A
CONTROL
GABA (10mM)
WASH
1nA
30mV
100 msecs

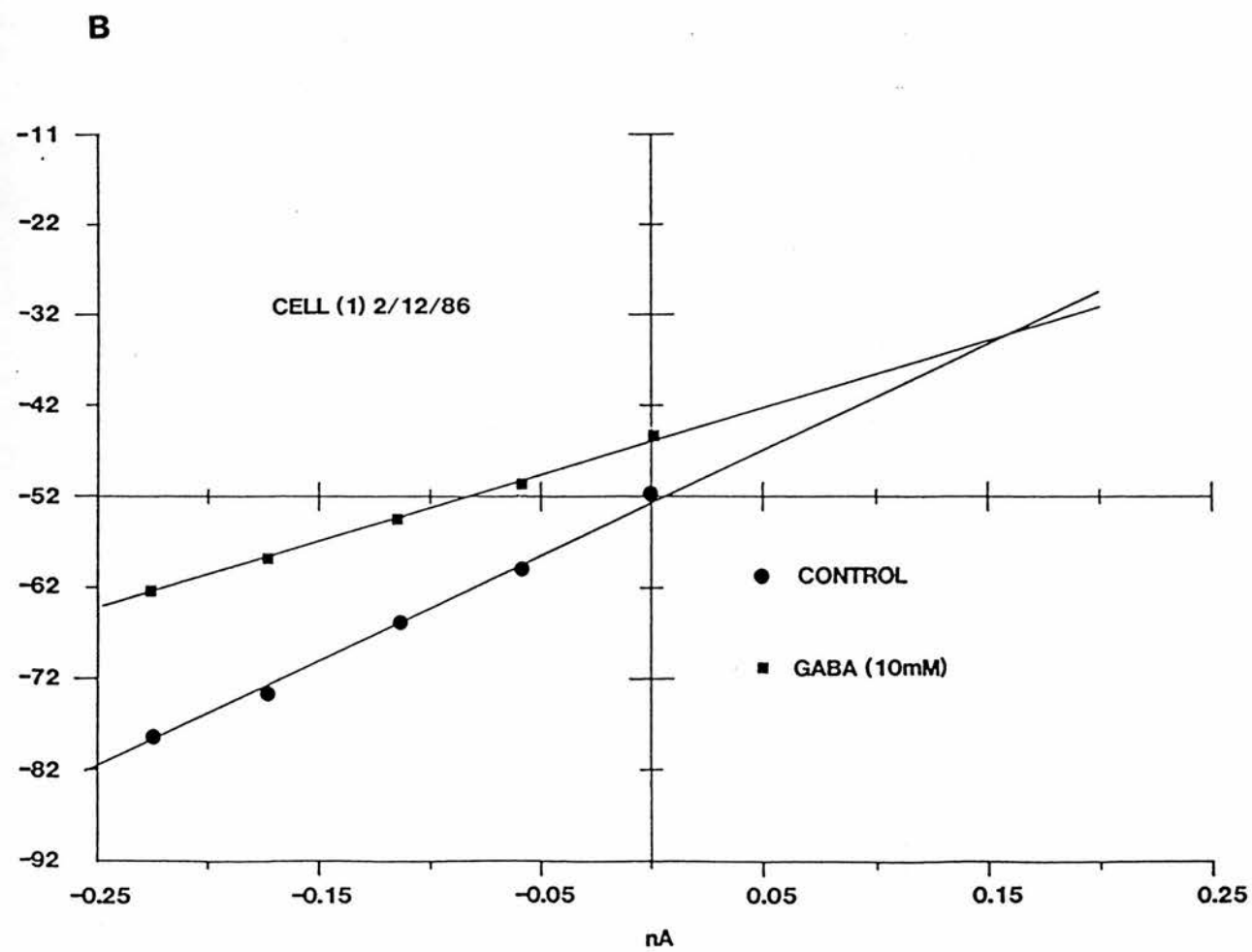
B
-11
-22
-32
-42
-52
-62
-72
-82
-92
CELL (1) 2/12/86
CONTROL
GABA (10mM)
-0.25
-0.15
-0.05
0.05
0.15
0.25
nA

Fig. 4.5

The effect of 50μM baclofen on a raphe neurone that appears unresponsive to superfusion with 100μM 5-HT. In A, electrotonic potentials evoked in respones to hyperpolarising current steps, lower trace. At rest -63mV in control ACSF the Rm was 74MΩ and τ 13ms. Superfusion with 100μM 5-HT was ineffective in changing either Rm or τ. Superfusion with 50μM baclofen however caused a 6mV hyperpolarisation which when manually offset was seen to be accompanied by a decrease in both Rm to 58MΩ and τ to 9.5ms. In B, current - voltage relationships before and during baclofen application. The reversal potential for the baclofen mediated response was shown to be -90mV.

Fig. 4.5

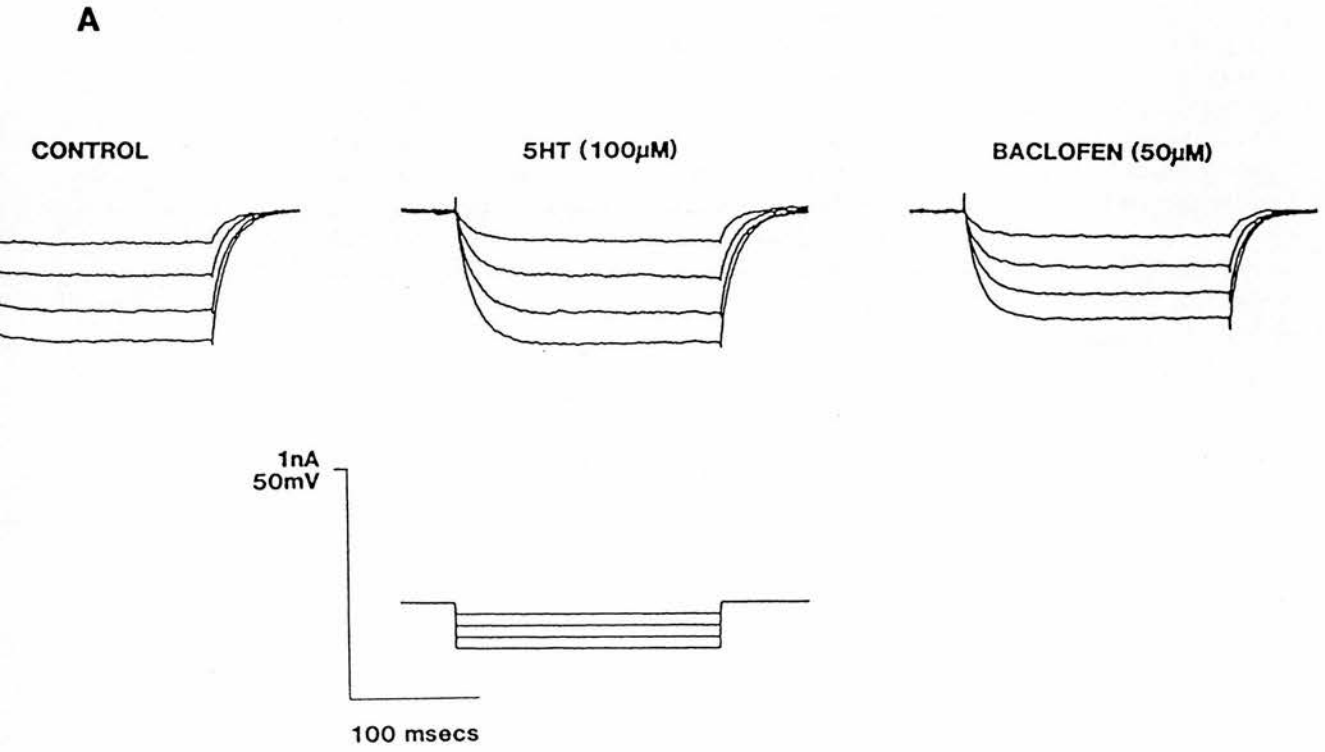
A
CONTROL
5HT (100μM)
BACLOFEN (50μM)
1nA
50mV
100 msecs

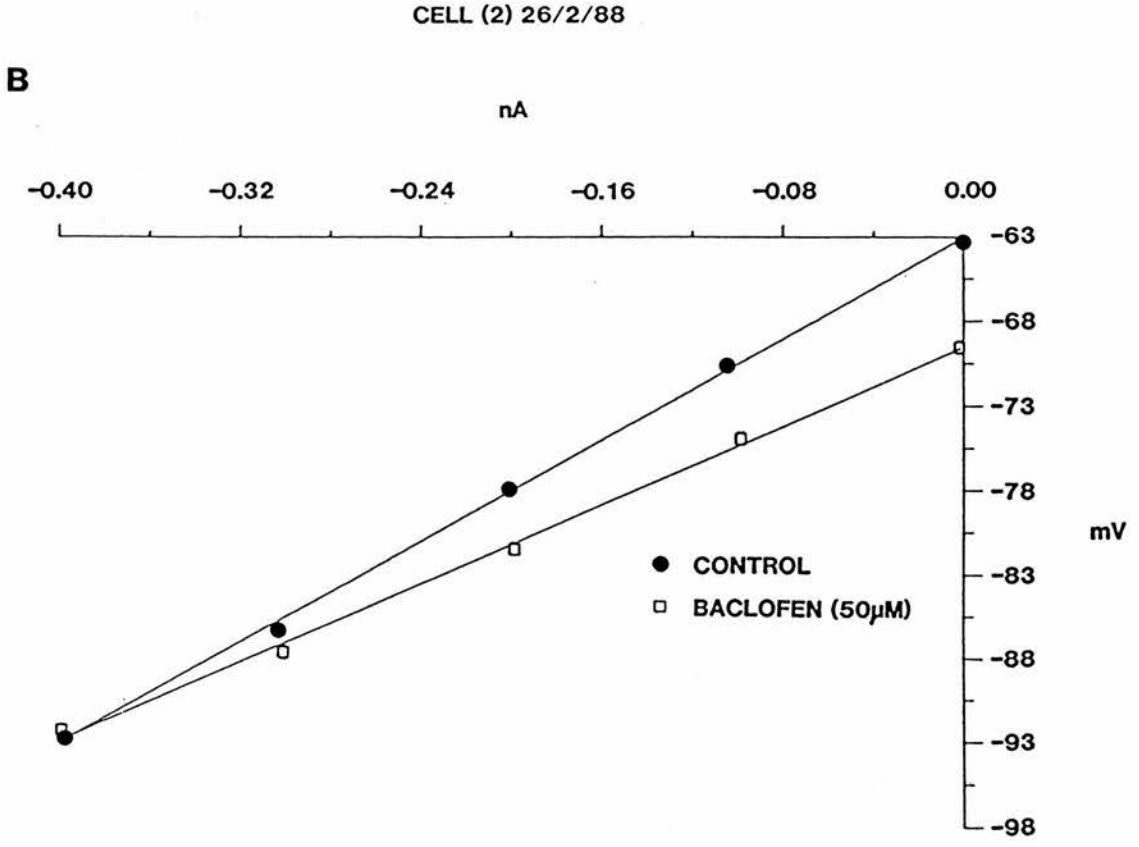
CELL (2) 26/2/88
B
nA
-0.40
-0.32
-0.24
-0.16
-0.08
0.00
-63
-68
-73
-78
-83
-88
-93
-98
mV
CONTROL
BACLOFEN (50μM)

Fig. 4.6

The effect of 8-hydroxy-2-(di-propylammino)-tetralin (8-OH-DPAT) on passive membrane properties of a raphe neurone. In, A electrotonic potentials evoked in response to 150ms hyperpolarising current pulses, lower trace, before, during and after 8-OH-DPAT administration. In control ACSF the resting membrane potential was -60mV with an Rm of 137MΩ and a τ of 15.9ms. Superfusion with 8-OH-DPAT caused a 13mV hyperpolarisation which, when offset, was seen to be accompanied by a reduction of Rm to 87MΩ and τ to 8.45ms. The effect of 8-OH-DPAT was exremely persistant showing only partial recovery after prolonged washing. The membrane potential stabilised at -67mV with Rm recovering to 108MΩ and τ to 14.33ms. In B, current - voltage relationships generated before, during and after 8-OH-DPAT superfusion. The reversal potential, calculated from the point of intersection of the lines of regression, was -89.2mV.

Fig. 4.6

A

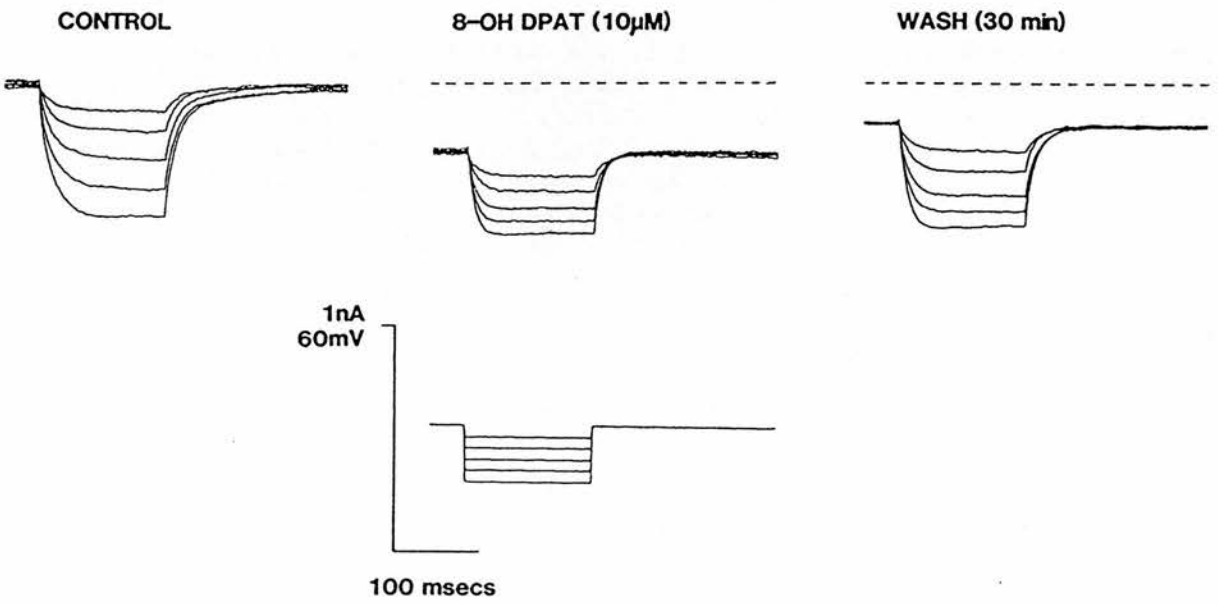
CONTROL
8-OH DPAT (10μM)
WASH (30 min)
1nA
60mV
100 msecs

B

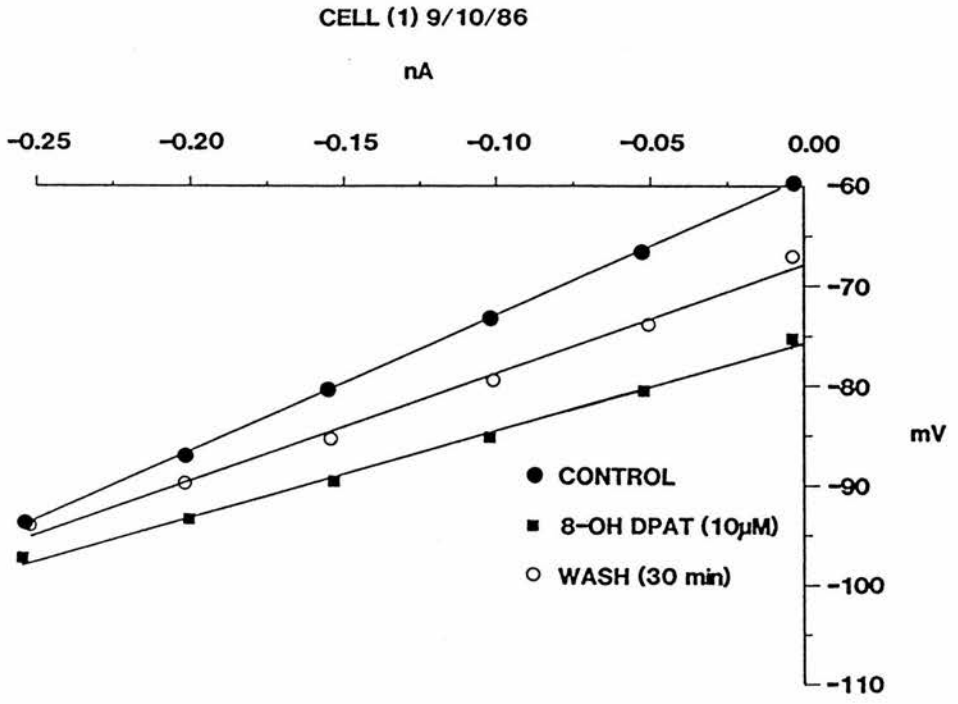
CELL (1) 9/10/86
nA
-0.25
-0.20
-0.15
-0.10
-0.05
0.00
-60
-70
-80
-90
-100
-110
mV
CONTROL
8-OH DPAT (10μM)
WASH (30 min)

Fig. 4.7

The effect of 10μM dipropyl-5-carboxamidotryptamine (DP-5-CT) on passive membrane properties of a raphe neurone. In A, electrotonic potentials evoked in response to graded 200ms hyperpolarising current steps, lower trace. In control ACSF the resting membrane potential was -62mV with an Rm of 118MΩ and τ of 22.7ms. Superfusion with DP-5-CT caused a 12mV hyperpolarisation which, when offset, was seen to be accompanied by a reduction in Rm to 67MΩ and τ to 10.9ms. No recovery of the DP-5-CT induced effect was observed even following prolonged periods of washing. In B, current - voltage relationships before and during DP-5-CT superfusion. The reversal potential, calculated from the extrapolated regression lines, was -90.2mV.

Fig. 4.7

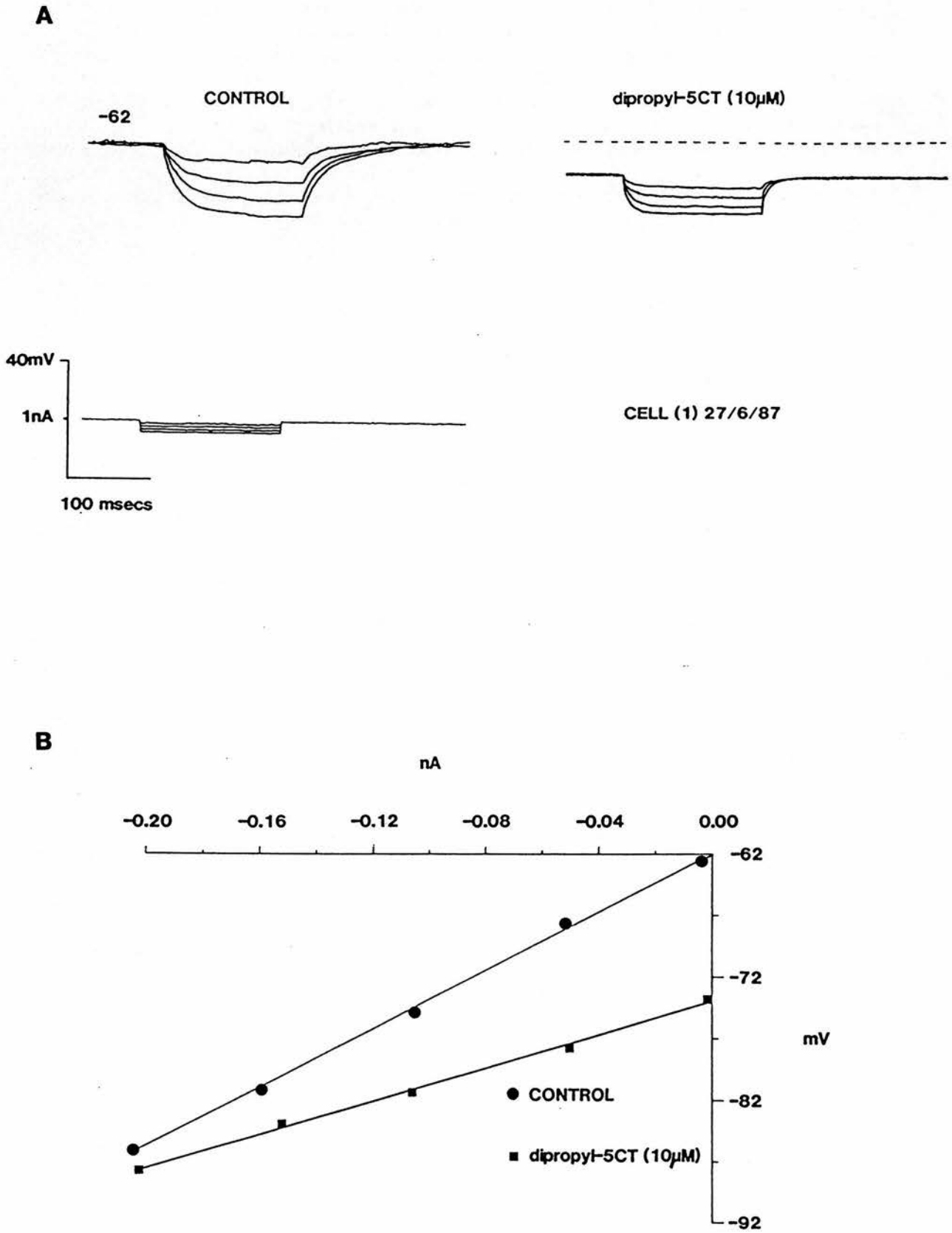
A
CONTROL
-62
dipropyl-5CT (10μM)
40mV
1nA
100 msecs
CELL (1) 27/6/87
B
nA
-0.20
-0.16
-0.12
-0.08
-0.04
0.00
-62
-72
-82
-92
mV
CONTROL
dipropyl-5CT (10μM)

Fig. 4.8

The effect of 10μM buspirone on passive membrane properties of a raphe neurone and the effect of buspirone on subsequent baclofen administration. In A, electrotonic potentials evoked in response to graded 250ms hyperpolarising current step, lower trace. In control ACSF the resting membrane potential was -60mV with an Rm of 254MΩ and a τ of 36.9ms. Superfusion with buspirone caused a 17mV hyperpolarisation which, when offset, was seen to be accompanied by a reduction in Rm to 122MΩ and τ to 17.3ms. In the presence of buspirone 15μM baclofen caused no further change in the membrane potential nor any significant change in either Rm or in τ. In B, current - voltage relationships before and during buspirone superfusion. The reversal potential, calculated from the extrapolated regression lines, was seen to be -93.2mV.

Fig. 4.8

A

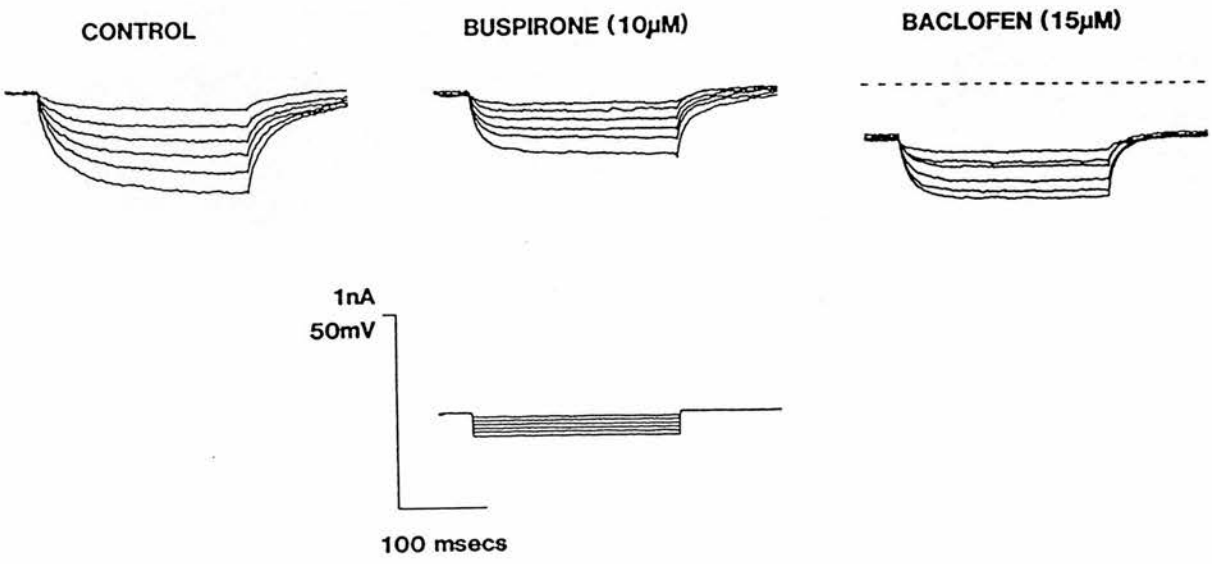

CELL (1) 27/3/88

B

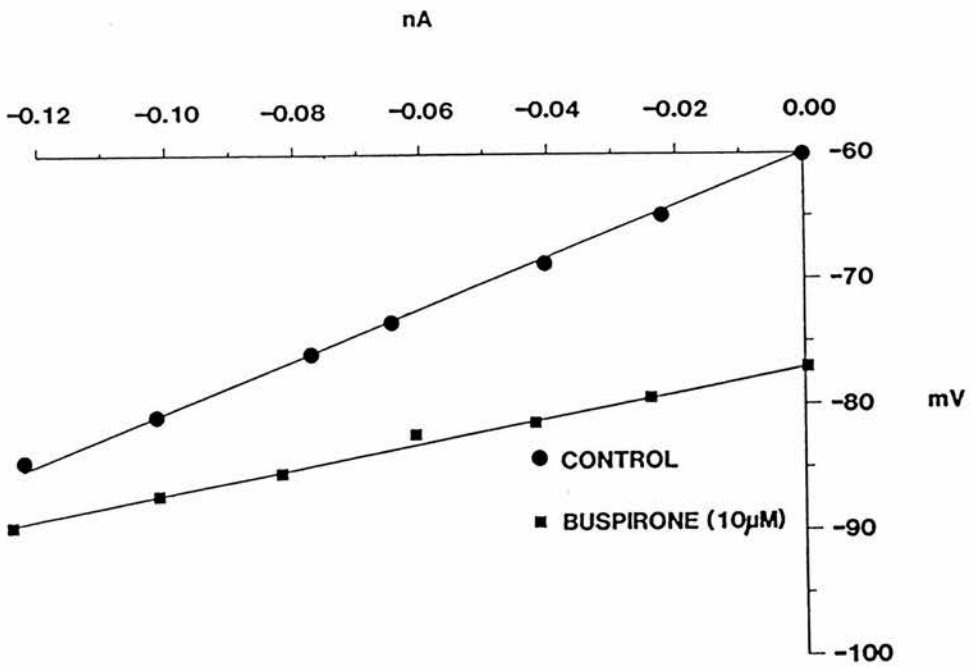

Fig. 4.9

The effect of buspirone pretreatment on current - voltage relationships obtained in the presence of 100μM 5-HT and 15μM baclofen. In the same cell as Fig. 4.8 buspirone caused a reduction in Rm from 254MΩ in control ACSF to 122MΩ (closed circles). Washing (open squares) failed to remove the effects of buspirone. Subsequent application of both 100μM 5-HT (closed squares) or 15μM baclofen (stars) caused no significant change in Rm, 127 and 139MΩ respectively.

Fig. 4.9

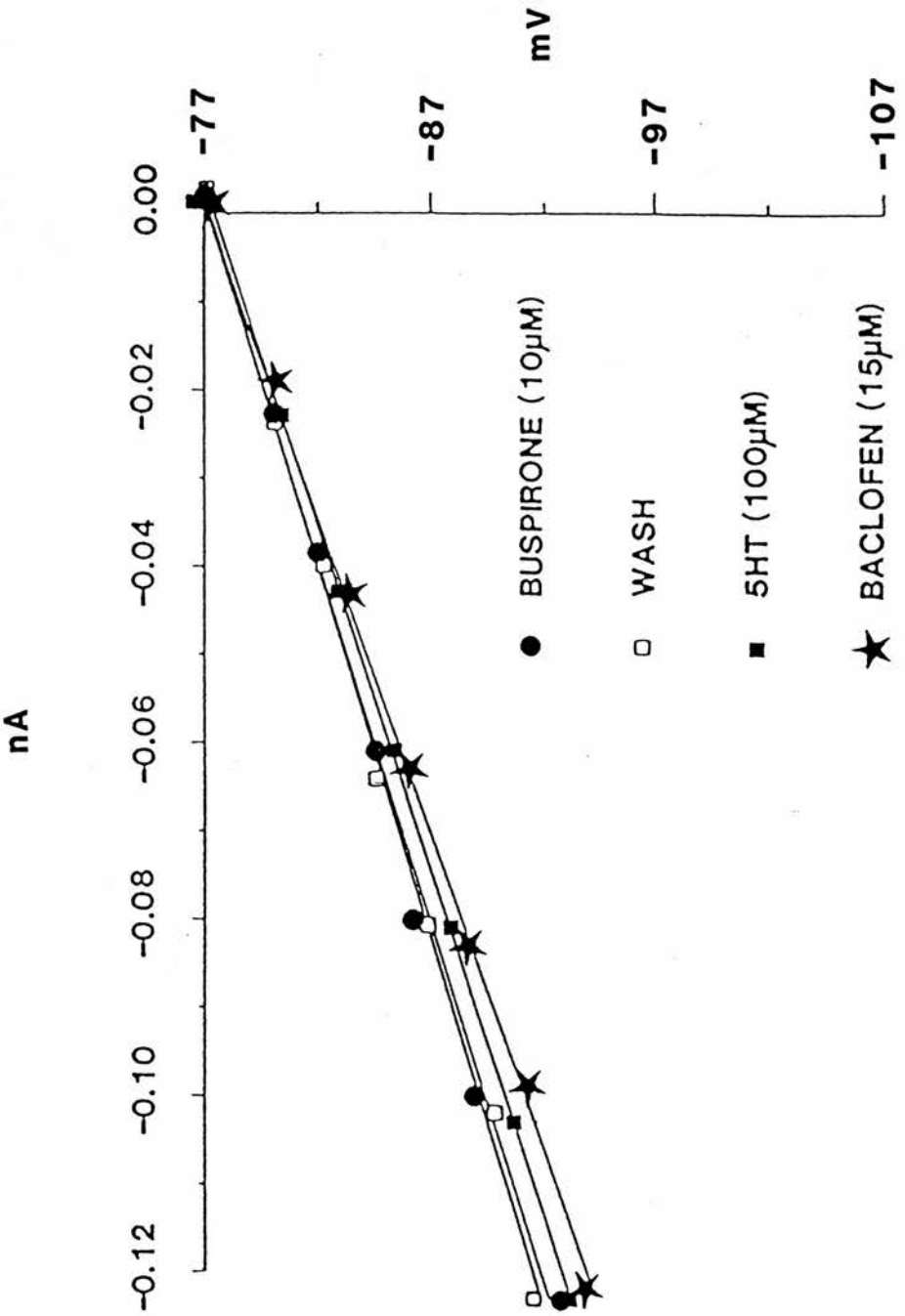
CELL (1) 27/3/88
nA
0.00
-0.02
-0.04
-0.06
-0.08
-0.10
-0.12
-77
-87
-97
-107
mV
BUSPIRONE (10μM)
WASH
5HT (100μM)
BACLOFEN (15μM)

Fig. 4.10

The effect of 100μM methysergide pretreatment on 5-HT evoked changes in passive membrane properties of a raphe neurone. In A, electrotonic potentials evoked in response to graded 100ms hyperpolarising current steps, lower trace. Pretreatment with 100μM methysergide had no direct effect on the resting membrane potential of -71mV nor Rm 229MΩ or τ 28ms. Superfusion with 50μM 5-HT evoked a 5mV hyperpolarisation which, when offset, was seen to be accompanied by a reduction of both Rm to 163MΩ and τ to 18ms. In B, current - voltage relationships before and during superfusion with 5-HT in the presence of methysergide. The reversal potential, calculated from the intercept of the regression lines, was -91mV.

Fig. 4.10

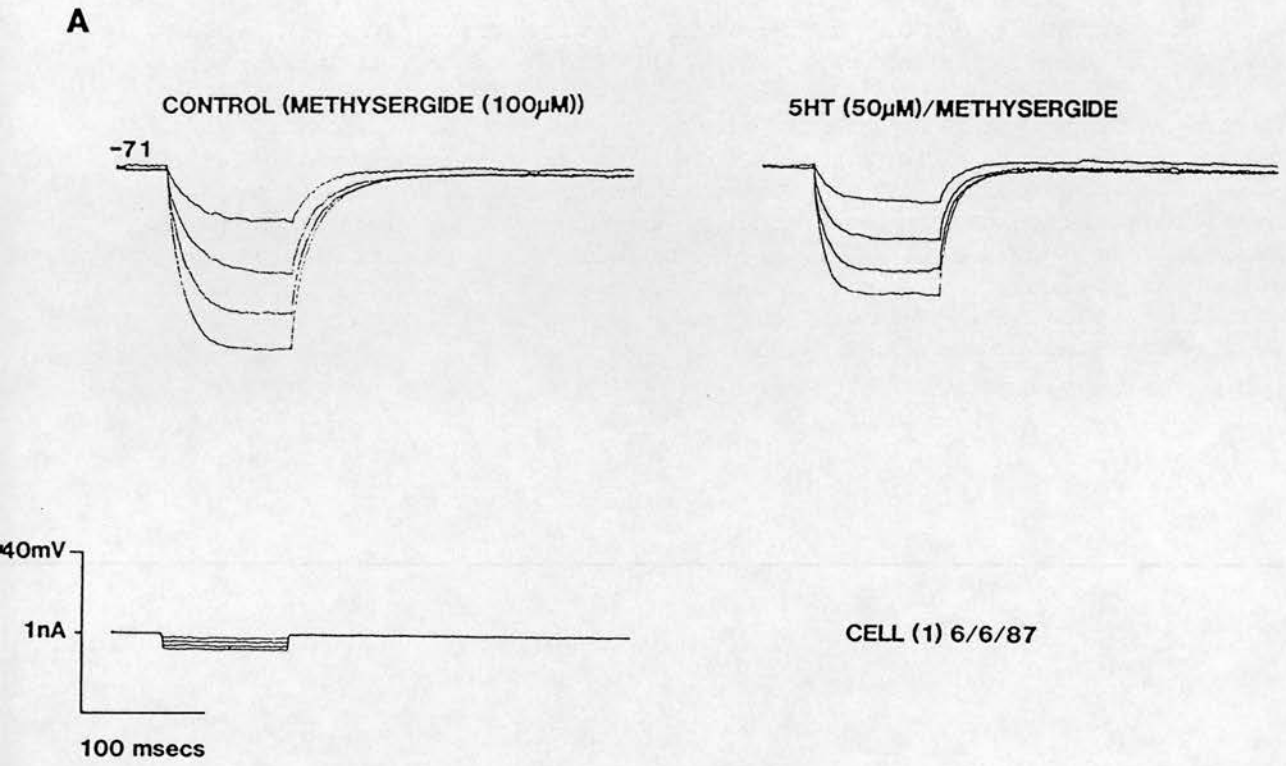
A
CONTROL (METHYSERGIDE (100μM))
5HT (50μM)/METHYSERGIDE
-71
40mV
1nA
100 msecs
CELL (1) 6/6/87

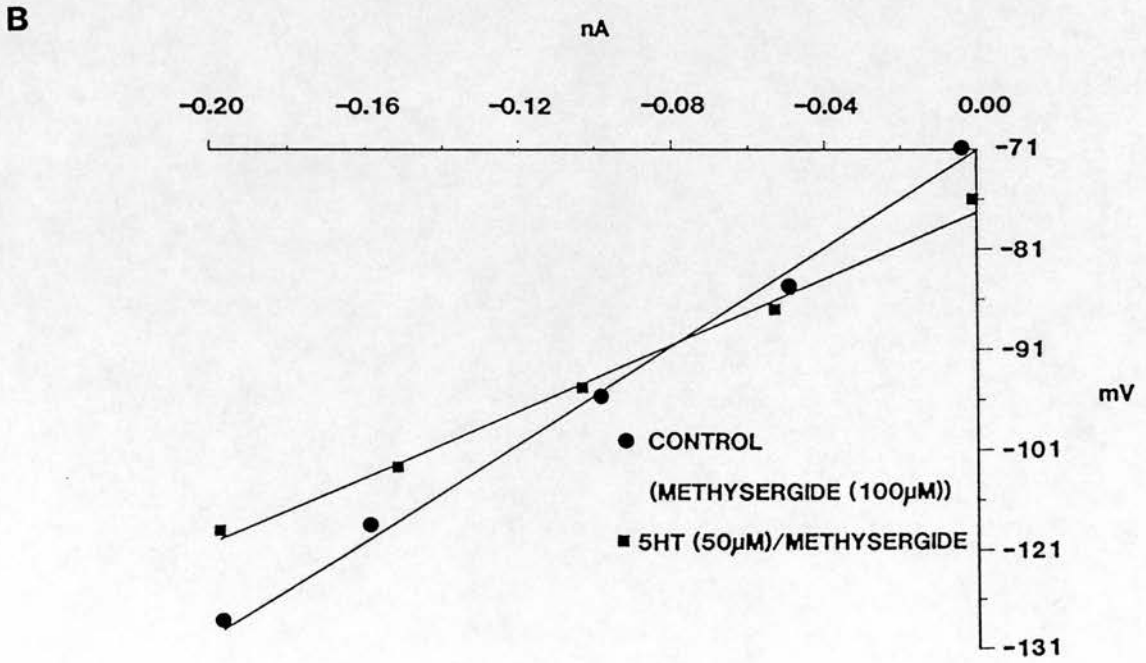
B
nA
-0.20
-0.16
-0.12
-0.08
-0.04
0.00
-71
-81
-91
-101
-121
-131
mV
CONTROL
(METHYSERGIDE (100μM))
5HT (50μM)/METHYSERGIDE

Fig. 4.11

The control effect of 100μM 5-HT on the passive membrane properties of the neurone that appeared to be unaffected by spiperone in Fig. 4.12. In A, electrotonic potentials evoked in response to graded 250ms hyperpolarising current steps, lower trace, before, during and after superfusion with 5-HT. In control ACSF the resting membrane potential was -60mV with an Rm of 229MΩ and a τ of 23ms. Superfusion with 100μM 5-HT caused a 9mV hyperpolarisation which, when offset, was seen to be accompanied by a reduction in Rm to 187MΩ and τ to 16.7ms. On washout the cell remained 7mV more hyperpolarised than the original resting membrane potential, Rm however increased to 292MΩ and τ to 34.2ms. In B, current - voltage relationships before and during 5-HT superfusion. The reversal potential, calculated from the extrapolated point of intersection of the lines of regression, was -105mV.

Fig. 4.11

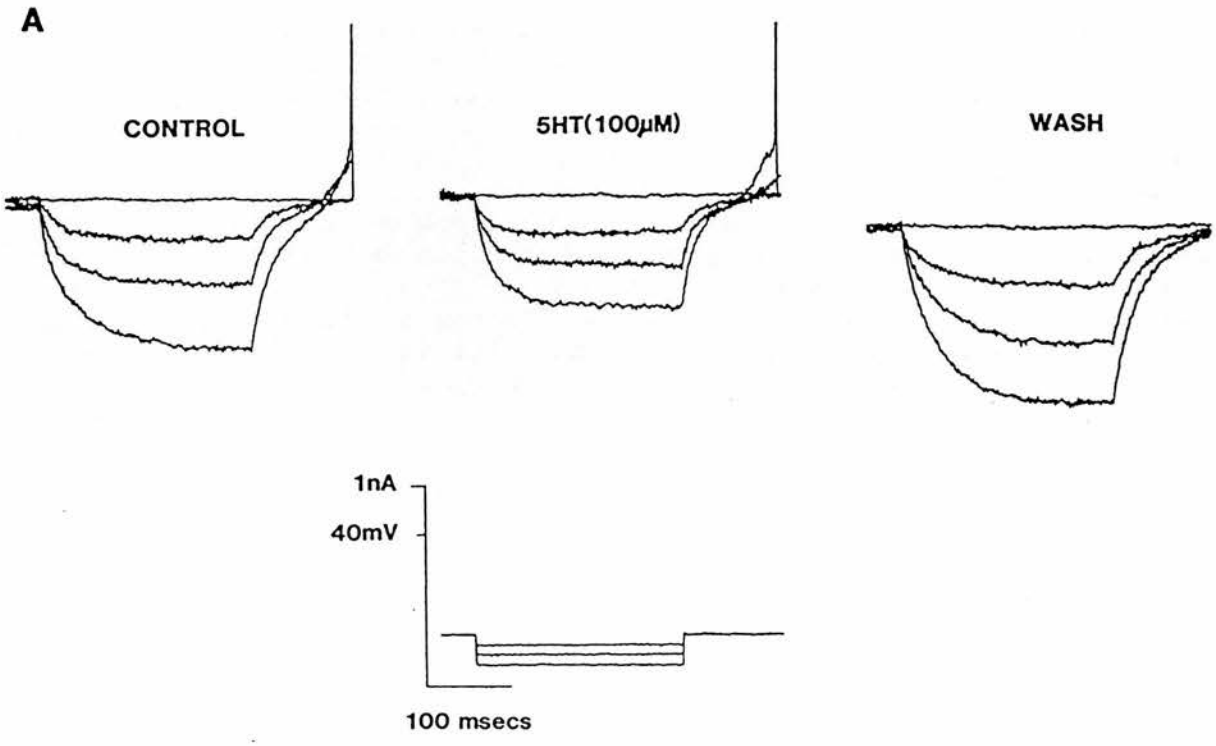

CELL (4) 16/2/88

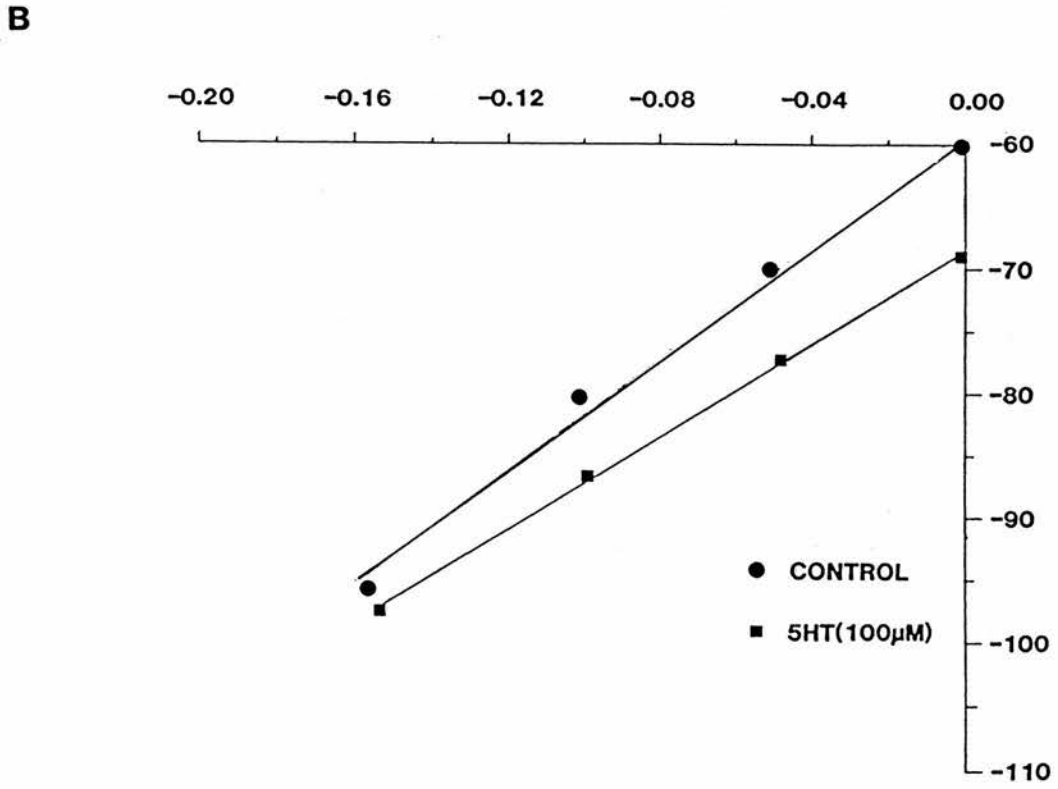

Fig. 4.12

The effect of spiperone on the passive membrane properties of the same raphe neurone as shown in Fig. 4.11. In A, electrotonic potentials evoked in response to hyperpolarising current steps, lower trace, before and during spiperone superfusion. In control ACSF the resting membrane potential was -67mV with an Rm of 292MΩ and a τ of 34.2ms. Superfusion with 10μM spiperone had no effect on the resting membrane potential however Rm increased to 322MΩ and τ to 40ms as it had done during the washout of 5-HT (see Fig. 4.11) . In B, current-voltage relationships before and during spiperone superfusion. No intersection of the two regression lines was observed indicating that spiperone appeared to have no direct effect on any one particular ionic conductance.

Fig. 4.12

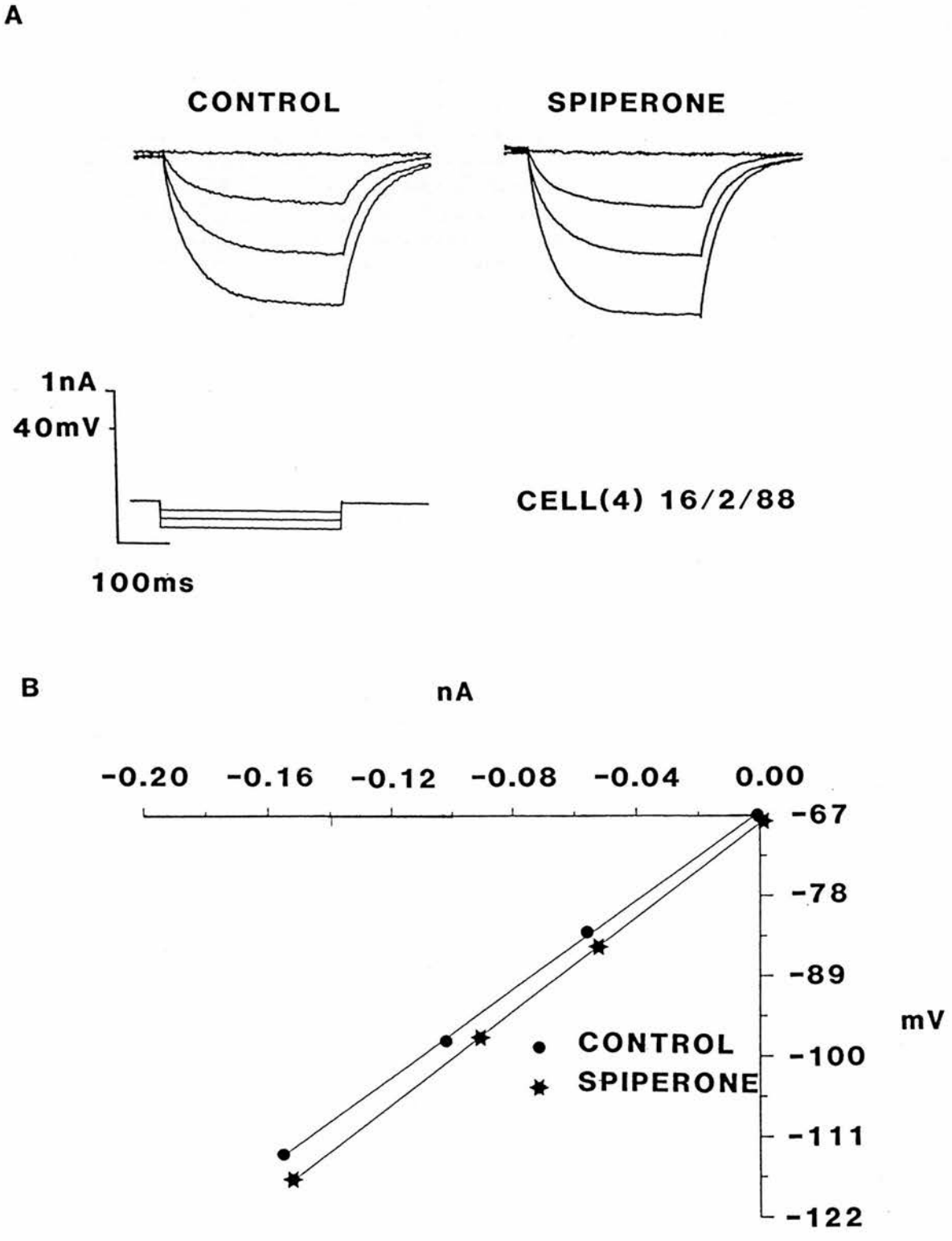
A
CONTROL
SPIPERONE
1nA
40mV
100ms
CELL(4) 16/2/88
B
nA
-0.20
-0.16
-0.12
-0.08
-0.04
0.00
-67
-78
-89
-100
-111
-122
mV
CONTROL
SPIPERONE

Fig. 4.13

The effects of 100μM 5-HT on passive membrane properties of a raphe neurone during continuous (20min) 10μM spiperone superfusion in the same neurone as that shown in Figs. 4.11 and 4.12. In A, electrotonic potentials evoked in response to graded 250ms hyperpolarising current steps, lower trace, before, during and after superfusion with 5-HT. In the presence of spiperone containing ACSF 5-HT evoked a 6mV hyperpolarisation which, when offset, was seen to be associated with a decrease in Rm from 322 to 286MΩ and τ was marginally reduced from 40 to 39.1ms. On washout the resting membrane potential returned to -67mV and Rm increased to 326MΩ and τ to 41ms. In B, current-voltage relationships before and during 5-HT superfusion in the presence of continuously perfused spiperone.The reversal potential, calculated from the point of intersection of the two lines of regression, was -112mV.

Fig. 4.13

A

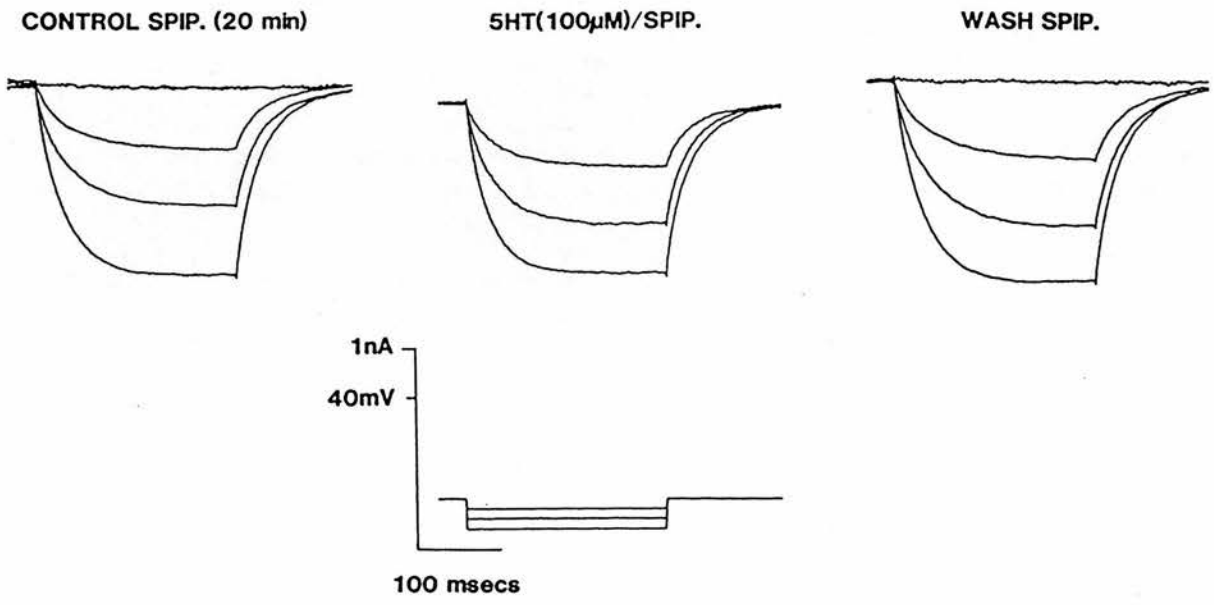

CELL (4) 16/2/88

B

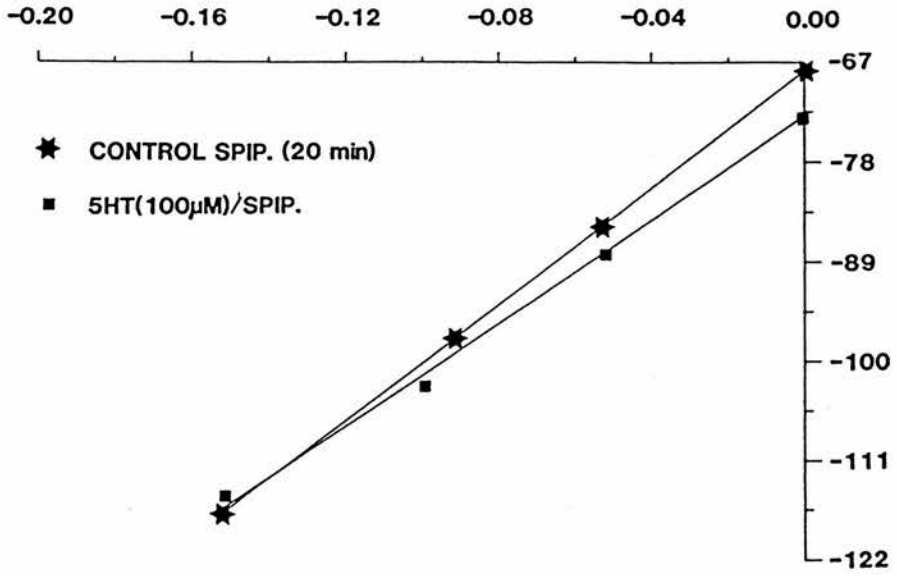

Fig. 4.14

The effects of 100μM 5-HT superfusion on Rm and τ before and during superfusion with 10μM spiperone. In A, in control ACSF 5-HT caused a 30% reduction in Rm. In the presence of spiperone the same concentration of 5-HT caused only a 10% reduction in Rm. Note that during the course of spiperone superfusion the Rm was seen to gradually increase. In B, 5-HT was seen to cause a 42% reduction of τ in control ACSF. Following spiperone superfusion this was reduced to a 5% reduction in τ. As with Rm τ was seen to gradually increase during the course of spiperone treatment.

Fig. 4.14

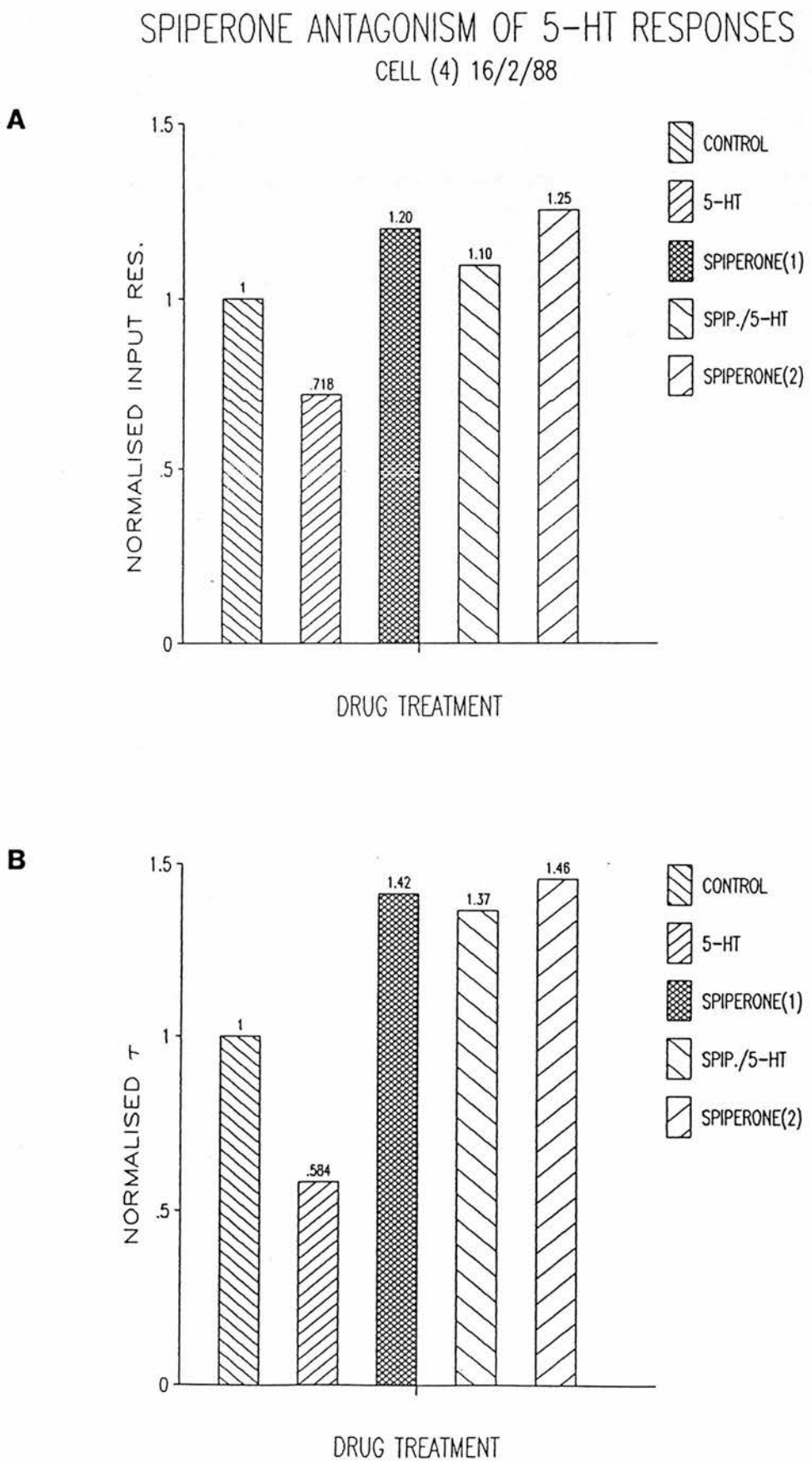
SPIPERONE ANTAGONISM OF 5-HT RESPONSES
CELL (4) 16/2/88
A
NORMALISED INPUT RES.
1.5
1
.5
0
1
.718
1.20
1.10
1.25
CONTROL
5-HT
SPIPERONE(1)
SPIP./5-HT
SPIPERONE(2)
DRUG TREATMENT
B
NORMALISED τ
1.5
1
.5
0
1
.584
1.42
1.37
1.46
CONTROL
5-HT
SPIPERONE(1)
SPIP./5-HT
SPIPERONE(2)
DRUG TREATMENT

Fig. 4.15

The effect of continuous 10μM spiperone superfusion on changes in passive membrane properties evoked by 60μM baclofen. In A, electrotonic potentials evoked in response to 100ms hyperpolarising current steps, lower trace, before, during and after baclofen superfusion in the presence of spiperone. In spiperone containing ACSF the resting membrane potential was -56mV with an Rm of 128MΩ and τ 30ms. After prolonged superfusion with spiperone 60μM baclofen causes a 16mV hyperpolarisation which, when offset, was seen to be associated with a decrease in Rm to 89MΩ and τ to 18ms. On washing for greater than 30 minutes the membrane potential returned to -56mV and Rm recovered to 112MΩ and τ to 26ms. In B, current-voltage relationships before and during baclofen superfusion. The reversal potential, calculated from the extrapolated point of intersection of the lines of regression, was -95mV.

Fig. 4.15

A

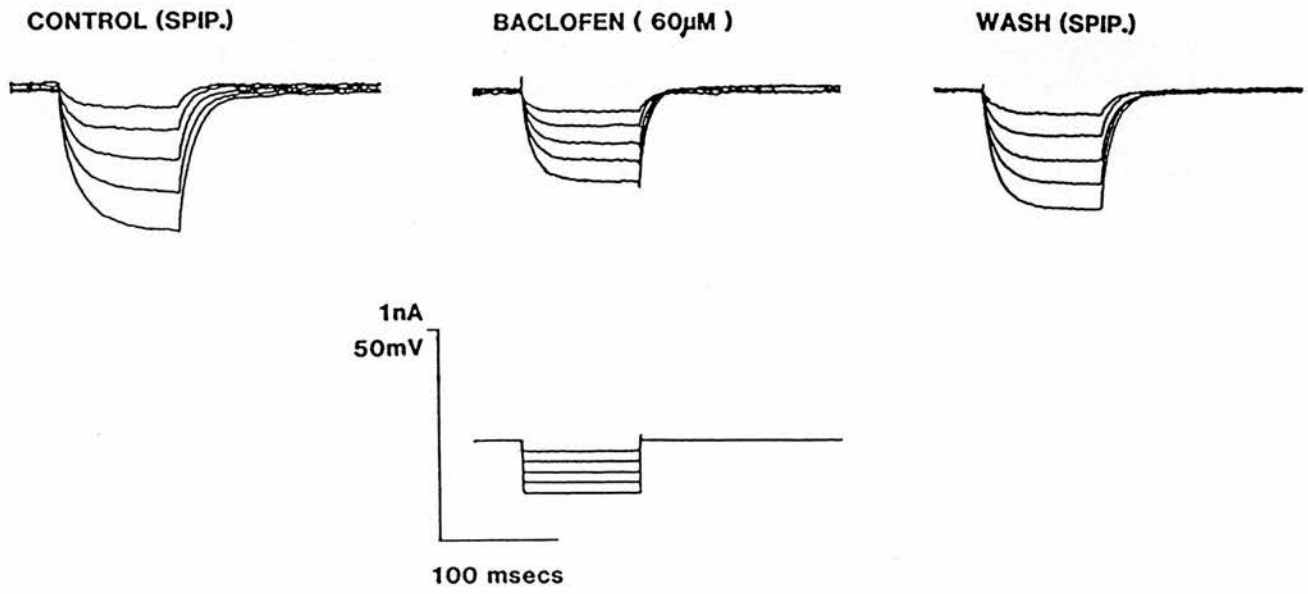

CELL (4) 19/2/88

B

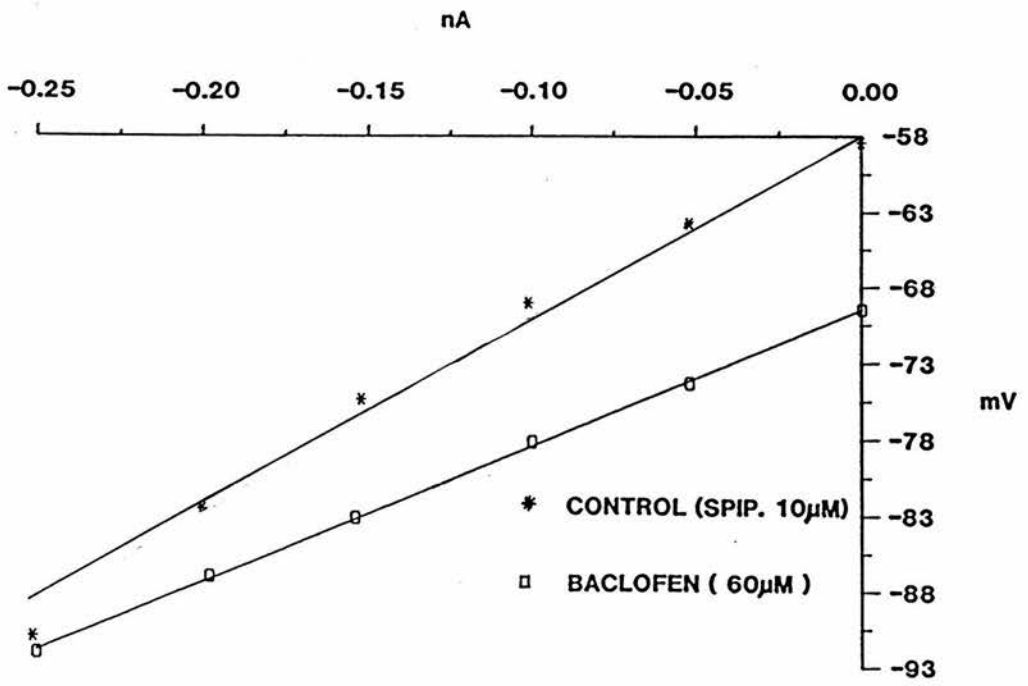

Fig. 4.16

The effect of a putative 5-HT_{1A} antagonist S_2 (SYNTEX) on passive membrane properties before during and after superfusion with 100μM 5-HT. In A, elelectrotonic potentials evoked in resonse to 200ms graded hyperpolarising current steps, lower trace, in the presence of continuously superfused S_2. In S_2 containing ACSF the resting membrane potential was -66mV with an Rm of 388MΩ and τ 36.8ms. Superfusion of 5-HT in the presence of S_2 caused a modest 4mV hyperpolarisation which, when offset was seen to be associated with a reducton of Rm to 284MΩ and τ to 18ms. On washout the resting membrane potential returned to -66mV and Rm recovered to 379MΩ and τ to 34.2ms. In B, current-voltage relationships during and after superfusion with 5-HT in the presence of S_2. The reversal potential, shown from the point of intersection of the two regression lines, was -81mV.

Fig. 4.16

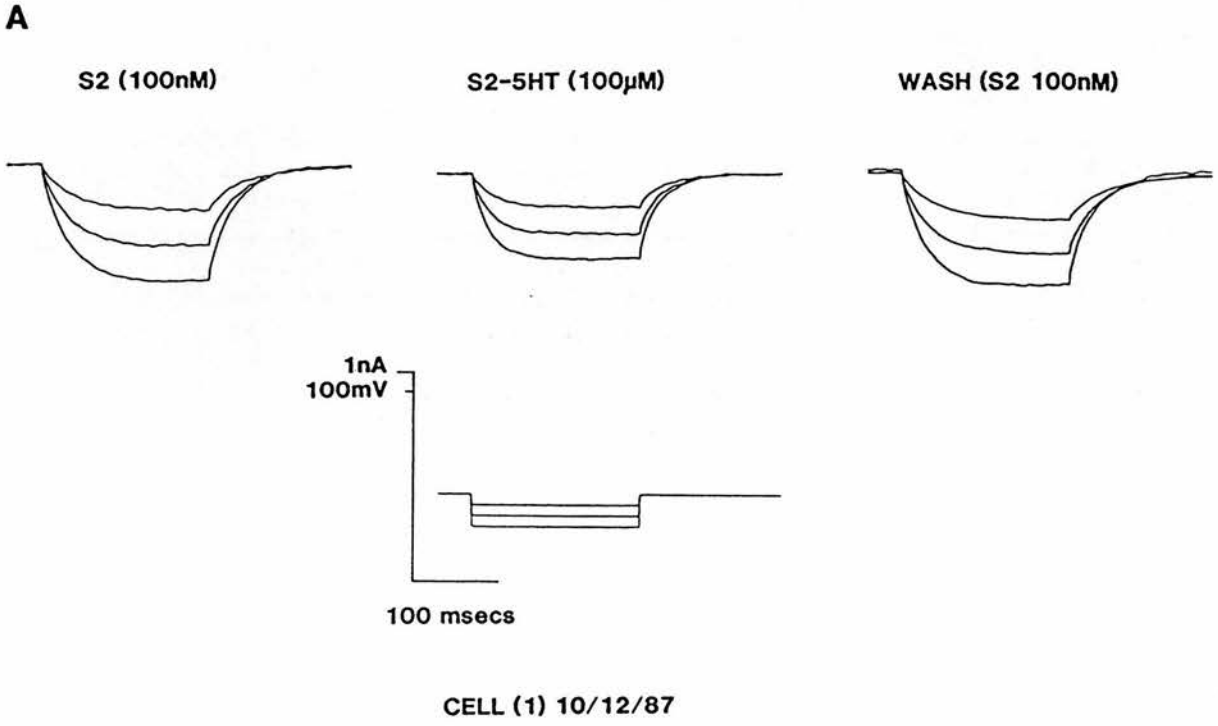
A
S2 (100nM)
S2-5HT (100μM)
WASH (S2 100nM)
1nA
100mV
100 msecs
CELL (1) 10/12/87

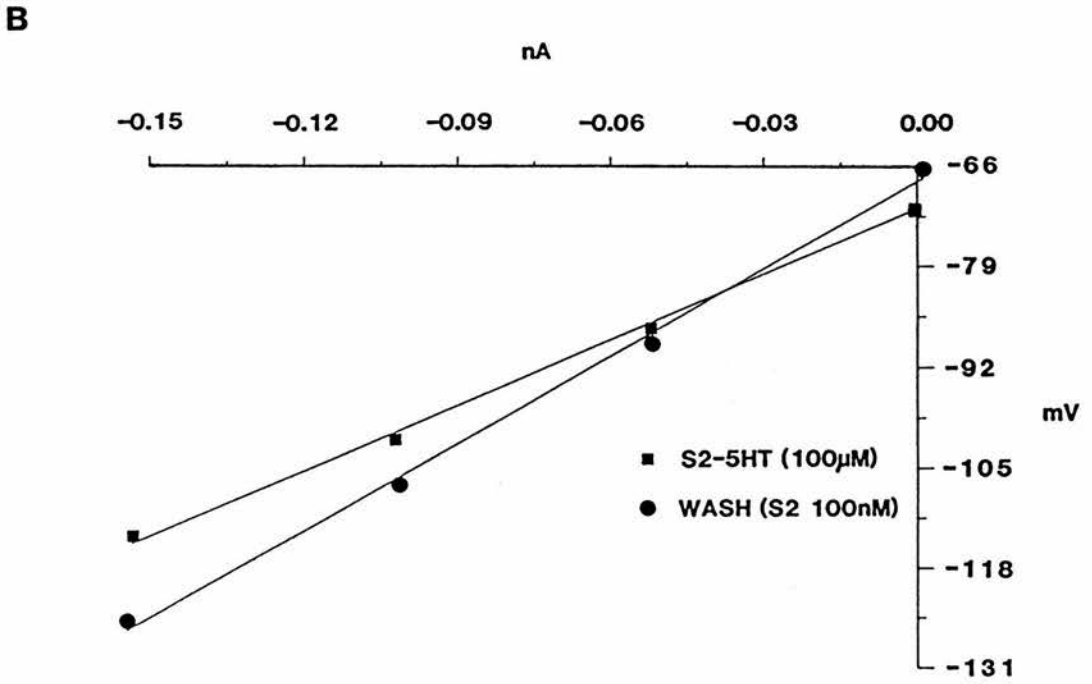
B
nA
-0.15
-0.12
-0.09
-0.06
-0.03
0.00
-66
-79
-92
-105
-118
-131
mV
S2-5HT (100μM)
WASH (S2 100nM)

Fig. 4.17

The effects of drug treatment on the input resistance of raphe neurones. A decrease in Rm was observed with all drug treatments. When the % change in Rm was plotted against drug treatment a rank order of potency was seen that showed for the 5-HT_{1A} agonists buspirone > DP-5-CT > 8-OH-DPAT > 5-HT at the concentrations shown in the annotation to the right of the histogram. The reduction in Rm was seen to range from 53% during buspirone superfusion to 24% with 5-HT superfusion. Baclofen was seen to cause a similar reduction in Rm, 21%, than 5-HT. GABA however caused a 39% reduction in Rm.

Fig. 4.17

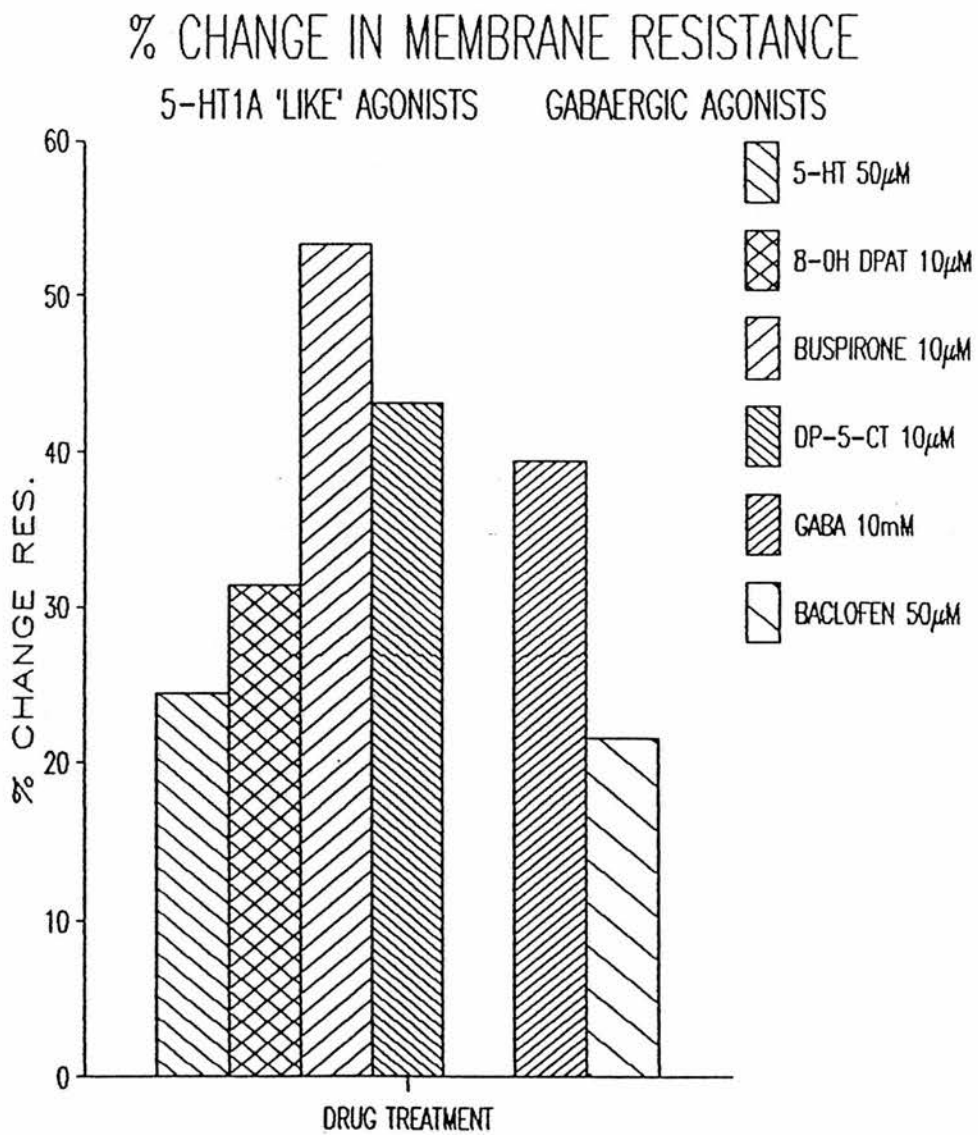
% CHANGE IN MEMBRANE RESISTANCE
5-HT1A 'LIKE' AGONISTS
GABAERGIC AGONISTS
% CHANGE RES.
60
50
40
30
20
10
0
DRUG TREATMENT
5-HT 50μM
8-OH DPAT 10μM
BUSPIRONE 10μM
DP-5-CT 10μM
GABA 10mM
BACLOFEN 50μM

Fig. 4.18

The effects of drug treatment on the time constant for membrane charging of raphe neurones. A decrease in τ was observed with all drug treatments. When the % change in τ was plotted against drug treatment a rank order of potency similar to that shown in Fig. 4.17 for the 5-HT_{1A} agonists was observed, hence buspirone > DP-5-CT > 8-OH-DPAT > 5-HT. The reduction in τ mirrored the reduction in Rm, hence buspirone was seen to reduce τ by 59% and 5-HT by 27%. Once again baclofen caused a similar reduction in τ, 23%, than 5-HT. GABA was seen to cause a marked reduction in τ, 84%, this was thought to be due to cell damage.

Fig. 4.18

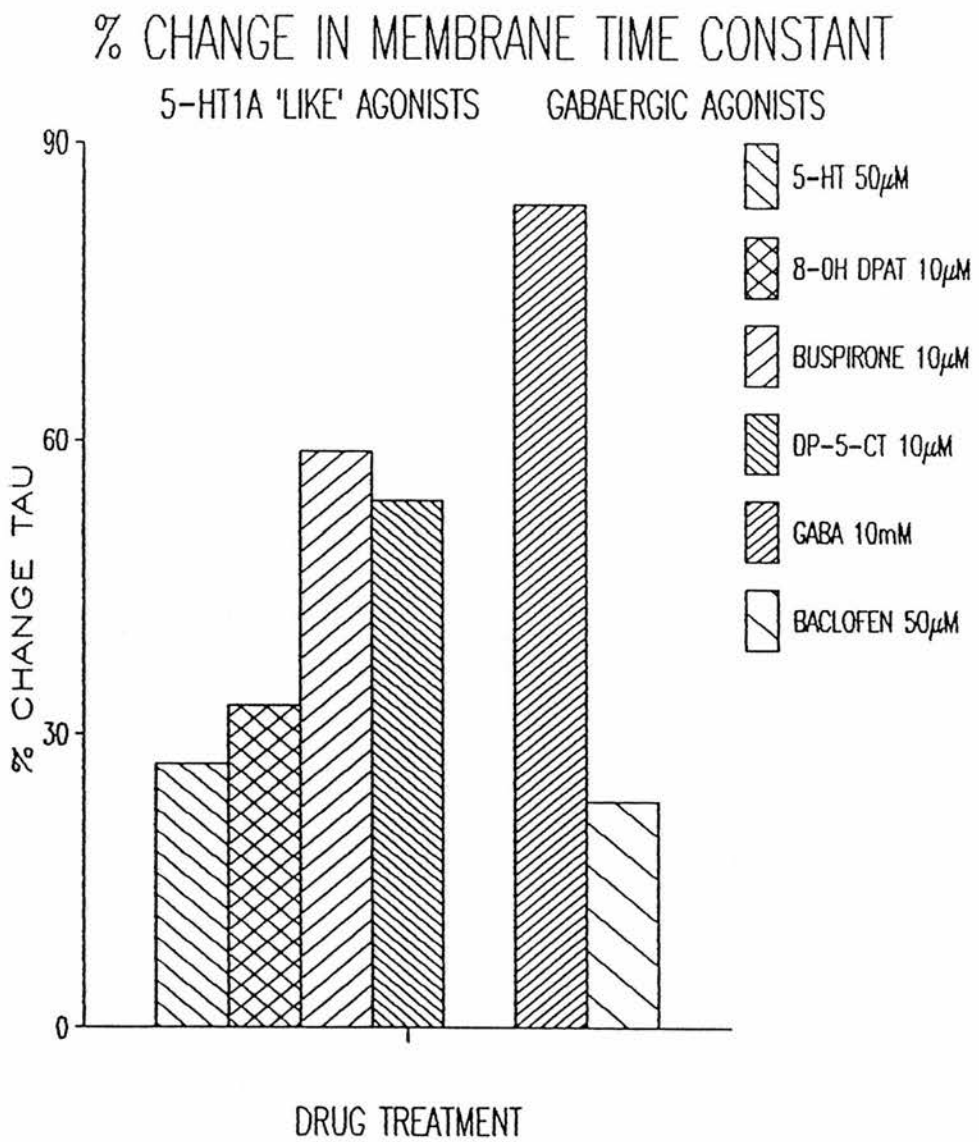
% CHANGE IN MEMBRANE TIME CONSTANT
5-HT1A 'LIKE' AGONISTS
GABAERGIC AGONISTS
90
60
30
0
% CHANGE TAU
5-HT 50μM
8-OH DPAT 10μM
BUSPIRONE 10μM
DP-5-CT 10μM
GABA 10mM
BACLOFEN 50μM
DRUG TREATMENT

Fig. 4.19

The reversal potentials of differing drug treatments on raphe neurones. Irrespective of the concentration of 5-HT or the 5-HT_{1A} agonists applied the reversal potential was seen to be approximately -90mV. This was also found to be true of baclofen suggesting that these compounds share a common potassium mediated mechanism of action. The GABA evoked response however was seen to show a reversal potential of -37mV.

Fig. 4.19

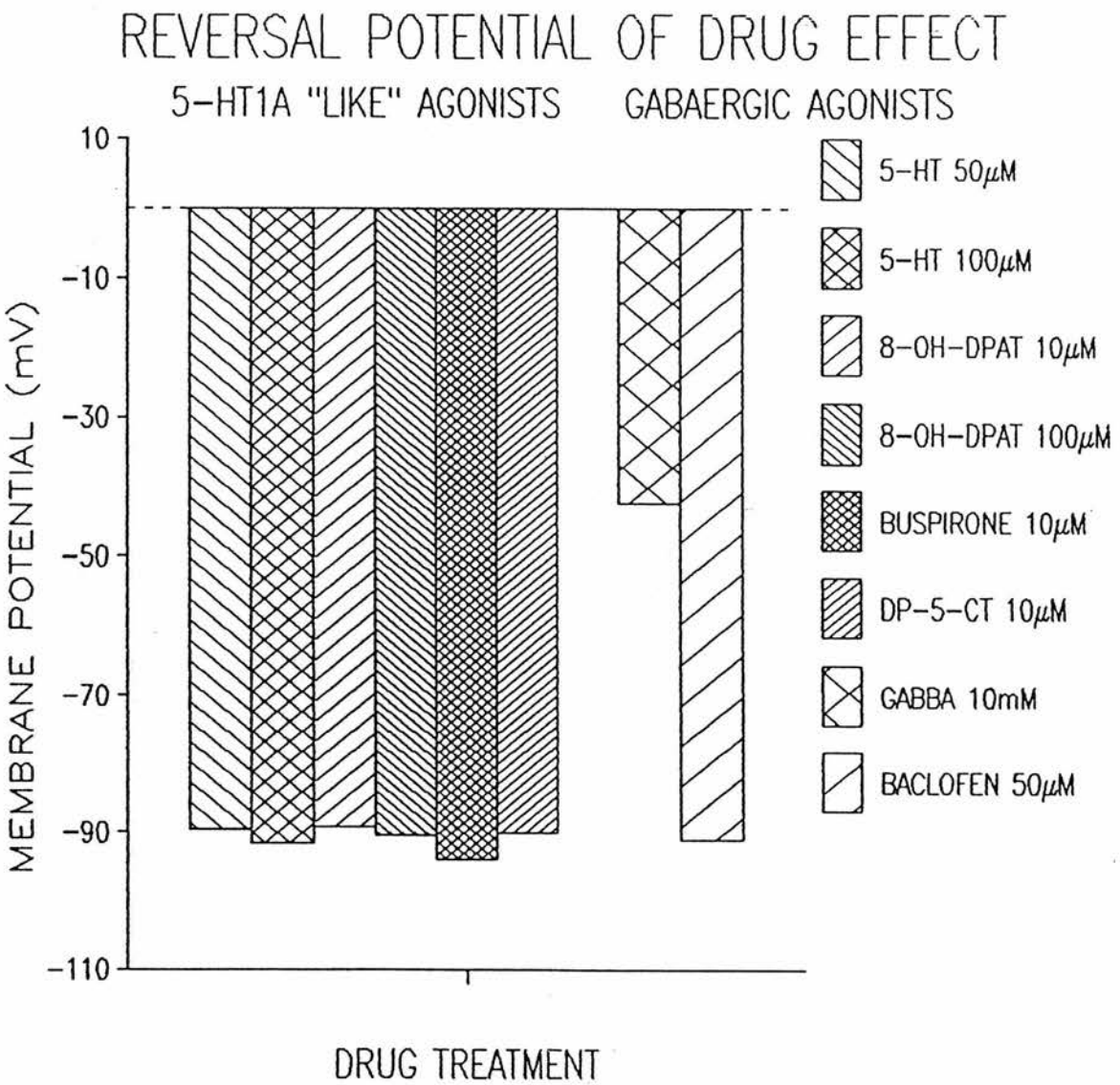
REVERSAL POTENTIAL OF DRUG EFFECT
5-HT1A "LIKE" AGONISTS
GABAERGIC AGONISTS
MEMBRANE POTENTIAL (mV)
10
-10
-30
-50
-70
-90
-110
5-HT 50μM
5-HT 100μM
8-OH-DPAT 10μM
8-OH-DPAT 100μM
BUSPIRONE 10μM
DP-5-CT 10μM
GABBA 10mM
BACLOFEN 50μM
DRUG TREATMENT

CHAPTER 5

DISCUSSION

The results of this study indicate that not only do DR neurones posses the necessary passive and active membrane properties required to maintain a slow rhythmic firing pattern but there also appears to be an autoinhibition of cell firing due to the hyperpolarising action of 5-HT acting on proposed 5-HT_{1A} autoreceptors.

This action of 5-HT on somatic autoreceptors within the DR nucleus could be considered a postsynaptic action of 5-HT consequently it was of interest to compare the biophysical and pharmacological data obtained in this study with that reported for the biophysical properties and action of 5-HT at two other post synaptic 5-HT receptor sites, namely the hippocampal pyramidal CA_1 neurones and at the facial motonucleus (FMN). Both of these areas have been shown to receive a dense 5-HT innervation with the hippocampus being primarily innervated from the dorsal and median raphe nuclei (Saavedra et al 1974, Crunelli & Segal 1985). The source of the serotonergic innervation to the FMN is at present uncertain. In the cat efferent projections from the medullary and dorsal raphe have been identified. It is possible that these may be projections from serotonergic neurones (Holstege et al 1984).

Passive membrane properties.

The passive membrane properties of the three areas showed distinct and characteristic values. Hence of the three neuronal types DR neurones can be seen to be most responsive to small excitatory inputs with an Rm of 203MΩ and a τ of 29ms. FMN neurones on the other hand would be particularly unresponsive to small excitatory synaptic inputs with an Rm of 8.9MΩ and τ 2.9ms (Larkman & Kelly 1987). Hippocampal CA_1 neurones would show an intermediate response to any synaptic input since the Rm is 48MΩ and τ 18.5ms (personal observation, Brown et al 1981). This may in part reflect the physiological roles that have been ascribed to these areas. Hence for DR neurones, which have been associated with temperature control, sleep and waking, reproductive behaviour and aggression (Messing 1978), the ability to respond rapidly to a continually changing environment would be essential. The CA_1 neurones of the hippocampus which have been associated with learning and memory (Collingridge et al 1983, Gustafsson & Wigstrom 1986) would not require the rapid response pattern of DR neurones but would presumably require a

response to graded informational inputs. At the opposite extreme to DR neurones FMN neurones which control movement of the facial musculature would require a large synaptic input before signal transmission occurred. Hence acting to reduce the possibility of muscular spasm.

The values of Rm and τ calculated for the individual neuronal types can be used to give an indication of the neuronal size (see methods). Hence the estimated radii for hippocampal CA_1 and FM neurones appear to be similar at approximately 50μm. By comparison DR neurones are seen to be more compact with an estimated radius of 33μm. These are generally larger than would be observed with stained neurones and probably reflects the fact that these neurones are not simple spheres and that the calculation does not account for the contribution of the dendritic arborizations to the membrane capacitance.

Interestingly the hippocampal CA_1 and FM neurones display more negative resting potentials ($\approx$ -70mV) than those displayed by DR neurones (-59mV), which taken together with their lower input resistances indicate that CA_1 and FM neurones show a greater resting potassium conductance than DR neurones.

Active membrane properties.

Unlike DR neurones neither CA_1 nor FM neurones show spontaneous rhythmic action potential generation in the in vitro preparation, this must in part be due to the more hyperpolarised resting membrane potentials shown by these neurones. All three neuronal types show a threshold for action potential generation of approximately -55mV hence the CA_1 and FM neurones would require a depolarisation 10mV greater than that required for DR neurones to initiate any intrinsic pacemaker activity.

That hippocampal neurones have the capability to demonstrate pacemaker activity is witnessed by the fact that CA_1 neurones show the whole collage of active conductances reported for DR in this study, and more. Unfortunately due to the fragility of the preparation and the extremely low input resistance FM neurones have not yet been successfully voltage clamped. Hence inferences will be made from other motoneurone types where voltage clamping has been successfully

achieved, namely spinal motoneurones (SM). Although not ideal, voltage responses in current clamp mode indicate the presence of particular conductances in the FM preparation.

The self reinforcing four stage pacemaker potential shown in DR neurones was observed to be initiated by the onset of an all or none action potential.

In the presence of TTX depolarising current step commands evoke low threshold depolarising prepotentials which are sensitive to external Co^{2+} and Cd^{2+} in both DR neurones (this study) and hippocampal CA_1 neurones (Brown & Griffith 1983). In both neuronal types this depolarising prepotential has been shown to result from a voltage dependent inward Ca^{2+} current. A prepotential preceding spike generation has been observed in FM neurones (Larkman et al, in press) which may be generated by the inward I_i current observed in SM neurones (Schwindt & Crill 1980). Activated at potentials 10mV more positive than rest, it is thought to correspond to a low threshold calcium current.

Perhaps more importantly for the self reinforcing pacemaker activity of DR neurones a de-inactivation of a low threshold Ca^{2+} current occurs during membrane hyperpolarisation. This de-inactivation resulted in a rebound low threshold Ca^{2+} prepotential on termination of transient hyperpolarising current steps. This I_{Ca} which activates at potentials negative to rest and inactivates near to rest appears to be absent in both FM/SM and CA_1 neurones.

Unlike motoneurones a further Ca^{2+} conductance has been demonstrated in both CA_1 neurones (Brown & Griffith 1983) and DR neurones (this study). In both preparations this current activates at levels more depolarised than the low threshold Ca^{2+} current and is thought to be representative of a calcium spike of dendritic origin. In a recent study Pitler & Landfield (1987) demonstrated that in CA_1 neurones the high threshold inward Ca^{2+} current amplitude was decreased with repetitive activation in caesium loaded cells. Hence it would appear that Ca^{2+} mediated inactivation of I_{Ca} may be an important mechanism to regulate the influx of Ca^{2+} into CNS neurones.

It is probable that in all three neuronal types the low threshold Ca^{2+} prepotential triggers the activation of the all or none TTX sensitive sodium spike. In DR and CA_1 neurones this sodium spike acts as the trigger of a high threshold Ca^{2+} spike which in turn would add to the observed duration of the recorded action potential.

When recorded under current clamp conditions all three neuronal types show the presence of an AHP following action potential generation, the magnitude and duration of which varies from preparation to preparation. The AHP in DR neurones was shown to be sensitive to Ca^{2+} channel blockers, inhibited by application of apamin and reversed at the K^+ equilibrium potential. Hence a calcium dependent K^+ conductance, I_{AHP}, was seen to underlie the AHP. In hippocampal neurones two conductances have been demonstrated to contribute to the AHP. I_c (Brown & Griffith 1983) which shows TEA sensitivity and is responsible for the early fast hyperpolarisation, and I_{AHP} (Lancaster & Adams 1986) an apamin sensitive current responsible for the slow decay of the AHP. Both I_c and I_{AHP} are calcium dependent outward K^+ currents (Storm 1987).

In FM neurones the fast and slow AHP's are separated by a transient delayed depolarisation (DD) (Larkman et al, in press). The DD in SM neurones has been proposed to be of dendritic origin and mediated by either an Na^+ (Traub & Llinas 1977) or Ca^{2+} conductance (Walton & Fulton 1986). It is probable that the fast and slow AHP seen in FM neurones correspond to the apparent Ca^{2+} dependent fast (I_{KF}) and slow (I_{KS}) outward K^+ currents reported by Schwindt & Crill (1981). The sensitivity of I_{KF} to TEA and the insensitivity of I_{KS} was reminiscent of I_c and I_{AHP} reported in hippocampal neurones. This was further supported by the observation that the slow AHP in cat SM neurones was blocked by apamin administration without affecting the fast AHP (Zhang & Krnjevic 1987).

The rate of depolarisation following the activation of an AHP in DR neurones was further slowed by the activation of a voltage and time dependent outward K^+ current I_A which could be inhibited by 4-AP and not TEA. This current was de-inactivated with hyperpolarisation from the resting membrane potential and activated on subsequent depolarisation. The half maximal inactivation occurred at -71mV and the half maximal activation at -46mV with both inactivation and activation curves showing an e fold increase in current amplitude following a 5mV change in the membrane potential. Hence the inactivation and activation characteristics fall within the potential range traversed by the membrane potential during pacemaker activity. The rate of decay of I_A was seen to range from 17 to 46ms. However the inactivation and activation are sufficiently slow to ensure that the decay of the membrane hyperpolarisation following an AHP lasts for

greater than 150ms. Similar characteristics have been demonstrated for I_A currents seen in hippocampal CA_1 neurones. However the half maximal activation and inactivation potentials are seen to be shifted 10mV in the hyperpolarising direction (Numann et al 1987). This would be expected since the resting membrane potential of CA_1 neurones is also 10mV more hyperpolarised than that of DR neurones. A second deviation from the characteristics shown by DR I_A is that CA_1 I_A shows a biphasic exponential decay (Gustafsson et al 1982, Storm 1986) in control ACSF unlike DR neurones which only appear to show a biphasic decay in the presence of 4-AP.

The overlap observed in the activation and inactivation curves indicated that at rest DR neurones show a degree of I_A activation which would act to increase the threshold for action potential generation. Storm (1987) noted that in CA_1 neurones not only did 4-AP cause a reduction in the amplitude of I_A but also caused an increase in the action potential spike duration, suggesting that in these neurones I_A might play a part in spike repolarisation. However it was noted that the effect of I_A on repolarisation was secondary to that of I_C. It is interesting to note that Zhang & Krnjevic (1986) demonstrated that in cat SM neurones 4-AP caused a marked increase in the duration of antidromically evoked action potentials together with a contradictory decrease in AHP amplitude and increase in AHP duration. If 4-AP was acting specifically to block I_A then an increase in the spike duration may be expected if I_A was activated at rest, as with CA_1 neurones. A concomitant reduction in the duration of the AHP would also be expected and not an increase as observed. It was concluded that 4-AP partially blocked Ca^{2+} activated K^+ channels. It has to be noted that this group used leakage of particularly high concentrations of 4-AP (0.5 - 1.0M), at these concentration it is probable that 4-AP would affect K^+ conductances other than just I_A. The increased spike duration and reduced AHP amplitude would indicate an action on I_C, I_{AHP} may be insensitive to 4-AP and hence increase in duration due to the increased Ca^{2+} entry during the spike. Consequently there is no direct evidence for the existence of I_A in motoneurones.

In DR neurones I_A was demonstrated to be opposed by an inward Ca^{2+} conductance (de-inactivated by the AHP) which drives the membrane potential towards the threshold for action potential generation following the decay of I_A. Hence a reduction in the extracellular

concentration of Ca^{2+} was observed to cause an increase in the amplitude of I_A. No such opposing current has been demonstrated in either CA_1 or FM neurones. Conversely a reduction in the amplitude of I_A has been observed in CA_1 neurones following Ca^{2+} channel blockade (Thompson 1977, Gustafsson et al 1982, Zbicz & Weight 1985, Numann et al 1987). A positive shift in the activation / inactivation properties was probably responsible for these observations.

The remaining outward regulatory current to be discussed is the non - inactivating K^+ current, I_M. Dingledine et al (1977) had observed that ACh application onto CA_1 neurones caused an increase in cell firing which was associated with an increase in the membrane input resistance. The excitatory action of ACh was demonstrated to be due to an ACh receptor mediated inhibition of an outward K^+ current, I_M, in vertebrate neurones (Brown & Adams 1980). I_M has since been shown to mediate the muscarinic excitation of CA_1 neurones (Halliwell & Adams 1982) and play a role in accommodation of CA_1 firing (Madison & Nicoll 1984). Unlike CA_1 neurones where I_M appears to be active at the resting membrane potential (Malenka et al 1986) I_M in DR neurones requires membrane depolarisation before activation occurs hence acting to prevent prolonged neuronal depolarisation and also contributing to accommodation of DR firing. No evidence, as yet, has been reported for the existence of an I_M like current in FM neurones.

Unlike CA_1 or FM neurones DR neurones show a linear current - voltage relationship in the hyperpolarising direction with voltage deflections to approximately -100mV. Deflections to more negative potentials than this demonstrate the occurrence of anomalous rectification. It is unlikely that DR neurones would ever be hyperpolarised to such an extent <u>in vivo</u> and hence the physiological relevance of this current is obscure. FM and CA_1 neurones however both show anomalous rectification with hyperpolarising steps to -80mV and beyond. The current underlying the anomalous rectification in hippocampal CA_1 neurones has been designated I_Q (Halliwell & Adams 1982) and been shown to be a time dependent activation of an inward K^+ conductance. A similar current to I_Q was reported by Barrett et al (1980) in SM neurones and was also proposed to account for hyperpolarising aspects of anomalous rectification. The physiological significance of this current is hard to quantify. However this group

proposed that the current may be activated during the AHP and act to regulate the discharge frequencies of SM neurones, a similar function for I_Q in CA_1 neurones would seem probable.

It can be seen from the above discussion that the three neuronal types have in common a number of active membrane currents. What appears to differentiate DR neurones from CA_1 and FM neurones in their ability to generate self reinforcing pacemaker activity is a) a resting membrane potential close to the threshold for action potential generation, b) a particularly high membrane input resistance and c) the presence of an inward Ca^{2+} conductance activated by membrane hyperpolarisation.

Although these three neuronal types share a number of active membrane currents it can be seen that a given neurotransmitter acting to reduce an active current in one nucleus may be ineffective or increase the same conductance in either of the other two nuclei. Such is the case with 5-HT.

This study has demonstrated that the 5-HT evoked hyperpolarisation of DR neurones and the associated decrease in input resistance and time constant for membrane charging was mediated by an increase in K^+ conductance that did not appear to be due to a direct action on any of the active conductances mentioned previously. The pharmacological profile, ie the full agonist properties of the 5-HT_{1A} ligands 8OH-DPAT, DP-5-CT, and buspirone, and the antagonistic action of spiperone and (-) propranolol (Sprouse & Aghajanian 1986) but not methysergide or ketanserin (Lakoski & Aghajanian 1984), indicated that the effect was mediated primarily by the activation of 5-HT_{1A} autoreceptors. The inability of spiperone to fully block the action of 5-HT and the weak agonist activity of TFMPP and mCPP (Sprouse & Aghajanian 1988) demonstrated the heterogeneity of 5-HT receptor subtypes on DR neurones. The somatodendritic 5-HT_{1A} receptors of DR neurones have subsequently been shown to be coupled to a pertussis toxin sensitive G protein that mediates K^+ channel activity (Innis & Aghajanian 1987, 1988). This pertussis toxin sensitive G protein has also been shown to mediate the hyperpolarising action of baclofen acting on $GABA_B$ receptors.

In contrast to the effect of 5-HT on DR neurones, a depolarising response to 5-HT was observed in FM neurones (VanderMaelen & Aghajanian 1980, Larkman & Kelly 1987). In vivo extracellular unit recording had demonstrated that 5-HT and DOM (2,5-dimethoxy-4-

methylamphetamine), a putative 5-HT receptor agonist, facilitated the excitatory action of glutamate on DR neurones an action that could be inhibited by both methysergide and ketanserin (McCall & Aghajanian 1979, Penington & Reiffenstein 1986). Hence a 5-HT_2 receptor subtype was proposed to mediate the excitatory response to 5-HT of FM neurones. Subsequent intracellular recording studies could not definitely confirm this hypothesis. Methysergide was shown to fully antagonise the the depolarisation and associated increase in input resistance and time constant evoked by 5-HT application. Conversely ketanserin and ritanserin did not fully block the 5-HT response (Larkman & Kelly 1988). Further methiothepin, a non specific 5-HT_1 receptor antagonist, was ineffective in blocking the 5-HT induced response and 8OH-DPAT failed to mimic the depolarising response to 5-HT. This work was complemented by the observations of Connell & Wallis (1988) who demonstrated that, in SM neurones, the depolarising response to 5-HT could be potently inhibited by methysergide and modestly antagonised by ketanserin but not methiothepin or the 5-HT_3 antagonist MDL 72222. Of the 5-HT agonists available neither 8OH-DPAT nor RU 24969 mimicked the depolarising response to 5-HT whereas a rank order of potency of 5-HT > αMe5-HT > 5-CT > 5-MeOT was obtained for these 5-HT analogues. This group concluded that although the receptor profile was not 5-HT_3 like, it did not clearly coincide with that for either 5-HT_1 like or 5-HT_2 receptors. Hence two conclusions may be drawn from the above data 1) that 5-HT acts to depolarise FM (and SM) neurones by an action on a novel subclass of 5-HT receptor or 2) that 5-HT acts on multiple 5-HT receptors to produce the overall depolarising response, as appears to be the case for DR neurones. This second option may explain why α-methyl-5-HT, a purported 5-HT_2 agonist, evokes a depolarising response as does 5-carboxamidotryptamine (5-CT) but not 8OH-DPAT or RU 24969. 5-CT is a non specific agonist at 5-$HT_{1A/B/D}$ subtypes (Peroutka 1988) and hence may evoke a response by an action at the 5-HT_{1D} receptor subtype.

Despite complications with the pharmacological profiles of both FM and DR neurones it appears that the opposite effects of 5-HT application on neuronal excitability at these distinct nuclei can be attributed to the activation of different receptor subtypes, the 5-HT_2 and 5-HT_{1A} respectively.

In the hippocampus autoradiographic studies have demonstrated that the CA_1 region contains an extremely large concentration of 5-HT_{1A} binding sites (Deshmukh et al 1983, Marcinkiewicz 1984, Glaser & Traber 1985, Pazos & Palacios 1985). Extracellular single unit recording had mainly demonstrated an inhibitory effect of 5-HT on CA_1 neurones (Segal 1980, Rowan & Anwyl 1985, Beck & Goldfarb 1985, Penington & Reiffenstein 1986, Ropert 1988). Excitatory responses to 5-HT application had however also been reported (Rowan & Anwyl 1985). Some confusion arose in these extracellular studies over the action of 5-HT antagonists on the reported hyperpolarising action of 5-HT. Segal (1980) had originally shown methysergide and cyproheptadine to inhibit the 5-HT induced decrease in firing rates. In a later study Penington & Reiffenstein (1986) reported that methysergide, cyproheptadine, metergoline and ketanserin were all ineffective in antagonising the 5-HT induced response.

Two comprehensive intracellular studies have demonstrated 5-HT to evoke a biphasic response in CA_1 neurones, a hyperpolarisation followed by a depolarisation (Andrade & Nicoll 1987, Colino & Halliwell 1987). Unfortunately although these papers showed a similarity in the response to 5-HT they reached different conclusions as to some of the underlying mechanisms. It is important to note that the biphasic response to 5-HT appears to show a regional distribution. Hence Colino & Halliwell demonstrated that septal CA_1 neurones responded mainly with a hyperpolarisation whereas temporal CA_1 neurones mainly showed a biphasic response. This may in part explain the differing responses observed in extracellular studies.

Both the hyperpolarisation and the depolarisation are mediated by changes in K^+ conductance of the membrane. The hyperpolarisation and associated reduction in input resistance was mediated by a 5-HT stimulated K^+ conductance. The depolarisation and associated increase in input resistance was mediated by a 5-HT reduction in K^+ conductance. Like the autoreceptor of DR neurones the 5-HT receptor mediating the hyperpolarisation was assumed to be of the 5-HT_{1A} subtype. Hence the 5-HT response could be antagonised by spiperone, methiothepin, cyproheptadine and mianserin. 8OH-DPAT showed only weak agonist activity even at micromolar concentrations and could partially block the response to 5-HT (Andrade & Nicoll 1987(a), Wu et al 1988). This partial agonist activity was mimicked by both buspirone and ipsapirone (Andrade & Nicoll 1987(b)). These results were further

supported by the inhibitory action of 8OH-DPAT, buspirone and ipsapirone on population spike activity (Beck et al 1985, Rowan & Anwyl 1987). Colino and Halliwell (1986) had however reported that nM concentrations of 8OH-DPAT completely abolished the hyperpolarisation and resistance decrease induced by 5-HT. This same group later reported an antagonistic action of nM concentrations of ipsapirone. Although these results are contradictory for the mechanism of action of these purported 5-HT_{1A} agonists the conclusion that the receptor mediating the hyperpolarising response was of a 5-HT_{1A} subtype remains valid. A similar hyperpolarisation was demonstrated for baclofen on CA_1 neurones (Newberry & Nicoll 1984 & 1985, Inoue et al 1985). This hyperpolarisation was mediated by an increase in K^+ conductance similar to that evoked by 5-HT. It was subsequently shown that both 5-HT and baclofen act on seperate receptors (Dutar & Nicoll 1988) which are directly coupled to the same potassium channel by a pertussis sensitive G protein (Andrade et al 1986, Clarke et al 1987) as appears to be the case for DR neurones.

Unlike the 5-HT effect on DR neurones and the baclofen effect on CA_1 neurones, 5-HT evokes a rebound depolarisation of CA_1 neurones. This rebound depolarisation was independent of the initial hyperpolarisation since it could still be evoked following blockade of the hyperpolarising response by spiperone. The greatest dichotomy exists over the mechanisms underlying the depolarising response. Colino and Halliwell reported the depolarisation to be mediated via a suppression of both an intrinsic membrane conductance and I_m with both RU 24969 and ICS 205-930, a 5-HT_3 ligand, antagonising the response to 5-HT. In contrast Andrade and Nicoll reported that the depolarisation was unaffected by ketanserin, mianserin, methysergide and ICS 205-930. The 5-HT induced depolarisation was not mimicked by 8OH-DPAT or TFMPP and was proposed to result from a decrease in a resting potassium current and not blockade of I_m or I_{AHP}.

That I_{AHP} may have been implicated in the depolarising response came from the observation that a decrease in AHP amplitude occurs with the same time course of action as the depolarising response. Further more the reduction in AHP amplitude was still observed following the blockade of the depolarising response. Madison and Nicoll (1986) had demonstrated that NA acting to activate adenylate cyclase caused a small depolarisation and a reduction in AHP size. This effect on AHP amplitude could be mimicked by applying 8-bromo-cyclic AMP. The

effects of 5-HT on hippocampal adenylate cyclase activity is unclear with some groups claiming that 5-HT_{1A} ligands inhibit activity (De Vivo & Maayani 1986, Bockaert et al 1987) whilst others claim that 5-HT_{1A} receptors mediate stimulation of adenylate cyclase activity (Markstein et al 1986). However following inhibition of the 5-HT mediated hyperpolarisation and blockade of the AHP with 8-bromo-cyclic AMP 5-HT still produced a depolarising response. Hence 5-HT appears to exhibit a third direct effect on CA_1 neurones by reducing I_{AHP} thereby causing a reduction in accomodation. This effect was reminiscent of the action of NA, DA and histamine on AHP production in CA_1 neurones (Madison & Nicoll 1982, Haas & Konnerth 1983, Malenka & Nicoll 1986). The action of 5-HT on AHP amplitude may be due to a receptor mediated activation of protein kinase C which has been shown to abolish AHP production in hippocampal neurones (Malenka et al 1986). The possible receptor subtype/s mediating this and the depolarising response remains unclear however the resistance to antagonism by ketanserin, spiperone, methysergide and mianserin would indicate that these responses are not mediated by 5-$HT_{1A/C}$ or 5-HT_2 receptors. An effect on 5-HT_3 receptors may be indicated due to the antagonism of the depolarising response by ICS 205-930 (Colino & Halliwell) however two factors argue against this 1) the lack of activity of the same compound in the hands of Andrade and Nicoll and 2) reported responses to peripheral 5-HT_3 receptor activation indicated a rapid depolarisation (Akasu et al 1987) which is not compatible with the long duration rebound depolarisation observed in hippocampal neurones.

The inhibition of the 5-HT induced response reported by RU 24969 would at first glance appear to indicate a possible 5-HT_{1B} receptor mediated event. RU 24969 however has been demonstrated to be a potent 5-HT_{1B} agonist (Peroutka 1986) and hence would be expected to produce a depolarisation and / or a decrease in AHP amplitude if this receptor was involved. TFMPP another putative 5-HT_{1B} agonist has no direct effect on CA_1 neurones hence RU 24969 may be acting as an antagonist at another as yet unidentified 5-HT receptor.

Interestingly methysergide which was shown to be ineffective in antagonising the 5-HT induced hyperpolarisation of DR neurones was shown to be a partial agonist at the proposed CA_1 5-HT_{1A} receptor (Andrade & Nicoll 1987, Yakel et al 1988). When viewed together with the partial agonist / antagonist response to the 5-HT_{1A} ligands 8OH-DPAT, ipsapirone, buspirone and gepirone of CA_1 neurones a question

must arise as to the real similarity of these two purported 5-HT_{1A} receptors. More recently a genomic clone G-21 has been shown to encode the 5-HT_{1A} receptor (Fargin et al 1988). Originally cloned as a possible β adrenergic receptor, the clone showed a greater affinity for 5-HT than adrenergic ligands. The rank order of potency of ligand binding was 8OH-DPAT > ipsapirone $\approx$ 5-HT > buspirone >> dopamine > adrenaline = histamine. Competition studies demonstrated the receptor to have two affinity states for ligand binding K_H and K_L. For 5-HT binding K_H was 0.27 $\pm$ 0.07nM and K_L was 63 $\pm$ 5.5nM. This dual affinity state may explain the full agonist properties of 5-HT_{1A} ligands on DR neurones compared to the partial agonist / antagonist properties on CA_1 neurones. It may be speculated that the preponderance of the 5-HT_{1A} receptors on DR neurones are in the high affinity state whereas those on CA_1 neurones are in the low affinity state. The remarkable sequence similarity between the 5-HT_{1A} receptor and adrenergic receptors would explain the ability of the β adrenergic antagonists pindolol and (-) propranolol to antagonise 5-HT activation of 5-HT_{1A} receptors. If this cloned 5-HT_{1A} receptor can be isolated and expressed in the plasma membrane of an oocyte it would be of interest to see to which of the above pharmacological profiles it more closely resembles.

The similarity in the protein structure of the 5-HT_{1A} receptor for other nonserotonergic receptors and the use of non specific antagonists has complicated our understanding of 5-HT receptor characterisation in specific brain regions. With the introduction of new more specific 5-HT_{1A} antagonists such as NAN-190 (1-(2-methoxyphenyl)-4-[4-(2-phthalimmido)butyl]piperazine) (Glennon et al 1988(a + b)) the ability to show the true receptor profile of DR and CA_1 neurones will be greatly enhanced. Hence the possibility that the weak agonist activity of the 5-HT_{1B} ligands TFMPP and mCPP on DR neurones might result from a residual 5-HT_{1A} receptor activity could be tested.

The ability to accurately predict the physiological mechanisms underlying specific receptor activation is of major importance. Recent ligand binding studies have demonstrated the absence of 5-HT_{1B} binding sites in the human brain (Hoyer et al 1986, Pazos et al 1987). Consequently responses designated as being mediated by 5-HT_{1B} receptors in the rat must be assumed either non existent in the human brain or to be mediated by another 5-HT receptor subtype. The latter

theory would seem more probable as it would be inconceivable that the human brain functioned without presynaptic 5-HT autoreceptors which have been reported to be of the 5-HT_{1B} subtype in rats (Engel et al 1986, Maura et al 1986).

The monophasic response shown to 5-HT by both the FM and DR may not be typical of the rest of the CNS. Indeed multiple responses have now been demonstrated in lateral septal neurones, deep cerebellar nuclei neurones and cortical neurones (Joels et al 1986, Gardette et al 1987, Davies et al 1987). Hence it is becoming more and more important to determine specific receptor activity. The ability to record intracellularly from two areas of the CNS that show the relatively simple but opposite monophasic response to 5-HT will in the future lead to a greater understanding of the responses that mediate 5-HT induced multiple responses. At present we can only generalise, hence it appears that the hyperpolarisation observed in CA_1 neurones is mediated by a mechanism that is similar to the 5-HT_{1A} receptor mediated hyperpolarisation in DR neurones. The depolarisation however shows a different and as yet uncharacterised pharmacological profile to that of the probable 5-HT_2 receptor mediated depolarisation in FM neurones.

Conclusion.

This study has demonstrated that the passive membrane properties of DR neurones ensure that even very small postsynaptic current flow would be capable of causing a marked membrane potential perturbation. If an EPSP reaches threshold for action potential generation this will initiate the start of a four stage pacemaker potential. A range of both time and voltage dependent active membrane properties have been shown to be present that activate during the four stage cycle to maintain a steady rhythmical self reinforcing firing pattern. Of primary importance in maintaining the low frequency firing rate is the de-inactivation of an A current by membrane hyperpolarisation during the post spike AHP. This current acts to delay the return to the resting membrane potential and has been shown to be cut short by the excitatory neurotransmitter NA. The active current that appears to differentiate DR neurones from neurones that do not show a pacemaker activity is an inward Ca^{2+} current that de-inactivates with membrane

hyperpolarisation. This current drives the membrane potential towards the threshold for action potential generation following the decay of the AHP and hence ensures the initiation of the next four stage cycle.

The firing rate is further regulated by an apparent tonic release of 5-HT from either dendritic stores or recurrent axon collaterals. This tonic release of 5-HT acting via a 5-HT_{1A} receptor G protein complex activates an uncharacterised outward K^+ conductance, hyperpolarising the neurone and decreasing its input resistance and reducing its excitability. It is proposed that the mechanism of action of the novel anxiolytics such as buspirone, ipsapirone and gepirone may in part be due to their 5-HT_{1A} agonist activity on DR autoreceptors hence decreasing the downstream activity of 5-HT on postsynaptic receptors in areas such as the hippocampus, amygdala, septum, and substantia nigra.

Only the development of more selective agonists and antagonists for 5-HT receptor subtypes will allow a fuller characterisation of the 5-HT receptor subtypes located on the cell bodies of serotonergic DR neurones.

ABBREVIATIONS

ACSF	Artificial cerebrospinal fluid
AHP	Afterhyperpolarisation
4-AP	4-Aminopyridine
CNS	Central nervous system
5,7DHT	5,7 Dihydroxytryptamine
DP-5-CT	Dipropyl-5-carboxamidotryptamine
DPSP	Depolarising postsynaptic potential
DR	Dorsal raphe
DRG	Dorsal root ganglion
DRN	Dorsal raphe nucleus
DTX	Dendrotoxin
FMN	Facial motonucleus
GABA	Gamma aminobutyric acid
GTP	Guanosine triphosphate
HEPES	N-2-Hydroxyethylpiperazine-N'-2-ethanesulfonic acid
HPLC	Highperformance liquid chromatography
5-HT	5-Hydroxytryptamine, serotonin
5-HTP	5-Hydroxytryptophan
IO	Inferior olivary
IPSP	Inhibitory postsynaptic potential
LSD	Lysergic acid diethylaminde
MAO	Monoamine oxidase
mCPP	m-Chlorophenylpiperazine
NA	Noradrenaline
8-OH-DPAT	8-Hydroxy-2-(di-n-propylamino)-tetralin
PBS	Phosphate buffered saline
p-CPA	p-Chlorophenylalanine
TFMPP	Trifluoromethylpiperazine
TOC	Transient outward current
TTX	Tetrodotoxin

Adams, P.R., Brown, D.A., & Constanti, A. (1982). M-currents and other potassium currents in bullfrog sympathetic neurones. J. Physiol. 330, 537-572.

Adrien, J., & Lanfumey, L. (1986). Ontogenesis of unit activity in the raphe dorsalis of the behaving kitten: its relationship with the state of vigilance. Brain Res. 366, 10-21.

Aghajanian, G.K. (1976). LSD and 2-bromo-LSD: comparison of effects on serotonergic neurones and on neurones in two serotonergic projection areas, the ventral lateral geniculate and amygdala. Neuropharmacol. 15, 521-528.

Aghajanian, G.K. 1981. The modulatory role of serotonin at multiple receptors in brain. In Serotonin Neurotransmission and Behaviour. Jacobs.B.L, and Gelperin., editors. MIT Press, Cambridge Massachusetts. 156-185.

Aghajanian, G.K. (1985). Modulation of a transient outward current in serotonergic neurones by $'_1$-adrenoceptors. Nature 315, 501-503.

Aghajanian, G.K., & Asher, I.M. (1971). Histochemical fluorescence of raphe neurones: selective enhancement by tryptophan. Science 172, 1159-1161.

Aghajanian, G.K., Foote, W.E., & Sheard, M.H. (1968). Lysergic acid diethylamide: sensitive neuronal units in the midbrain raphe. Science 161, 706-708.

Aghajanian, G.K., Graham, A.W., & Sheard, M.H. (1970). Serotonin-containing neurones in brain: depression of firing by monoamine oxidase inhibitors. Science 169, 1100-1102.

Aghajanian, G.K., & Haigler, H.J. (1974). L-Tryptophan as a selective histochemical marker for serotonergic neurones in single-cell recording studies. Brain Res. 81, 364-372.

Aghajanian, G.K., Kuhar, M.J., & Roth, R.H. (1973). Serotonin-containing neuronal perykarya and terminals: differential effects of p-chlorophenylalanine. Brain Res. 54, 85-101.

Aghajanian, G.K., & Lakoski, J.M. (1984). Hyperpolarisation of serotonergic neurones by serotonin and LSD: studies in brain slice showing increased K^+ conductance. Brain Res. 305, 181-185.

Aghajanian, G.K., & VanderMaelen, C.P. (1982). Intracellular recordings from serotonergic dorsal raphe neurones: pacemaker potentials and the effect of LSD. Brain Res. 238, 463-469.

Aghajanian, G.K., & VanderMaelen, C.P. (1982). Intracellular identification of central noradrenergic and serotonergic neurones by a new double labeling procedure. J. Neurosci. 2 No.12, 1786-1792.

Aghajanian, G.K., & Wang, R.Y. (1977). Habenular and other midbrain raphe afferents demonstrated by a modified retrograde tracing technique. Brain Res. 122, 229-242.

Akasu, T., Hasuo, H., & Tokimasa, T. (1987). Activation of 5-HT_3 receptor subtypes causes a rapid excitation of rabbit parasympathetic neurones. B. J. Pharmac. 91, 453-455.

Alger, B.E., & Nicoll, R.A. (1980). Spontaneous inhibitory post-synaptic potentials in hippocampus: mechanisms for tonic inhibition. Brain Res. 200, 195-200.

Andersen, P., Bliss, T.V.P., & Skrede, K.K. (1971). Unit analysis of hippocampal population spikes. Exp. Brain Res. 13, 208-221.

Andrade, R., Malenka, R.C., & Nicoll, R.A. (1986). A G protein couples serotonin and $GABA_B$ receptors to the same channels in hippocampus. Science 234, 1261-1264.

Andrade, R., & Nicoll, R.A. (1987). Pharmacologically distinct actions of serotonin on single pyramidal neurones of the rat hippocampus recorded in vitro. J. Physiol. 394, 99-124.

Andrade, R., & Nicoll, R.A. (1987). Novel anxiolytics descriminate between postsynaptic serotonin receptors mediating different physiological responses on single neurones of the rat hippocampus. Naunyn-Schmeideberg's Arch. Pharmac. 336, 5-10.

Banks, B.E.C., Brown, C., Burgess, G.M., Burnstock, G., Claret, M., Cocks, T.M., & Jenkinson, D.H. (1979). Apamin blocks certain neurotransmitter-induced increases in potassium permeability. Nature 282, 415-417.

Baraban, J.M., & Aghajanian, G.K. (1980). Suppression of firing activity of 5-HT neurones in the dorsal raphe by alpha-adrenoceptor antagonists. Neuropharmacol. 19, 355-363.

Baraban, J.M., & Aghajanian, G.K. (1981). Noradrenergic innervation of serotonergic neurones in the dorsal raphe: demonstration by electron microscopic autoradiography. Brain Res. 204, 1-11.

Baraban, J.M., Wang, R.Y., & Aghajanian, G.K. (1978). Reserpine suppression of dorsal raphe neuronal firing: mediation by adrenergic system. Eur. J. Pharm. 52, 27-36.

Barrett.E.F,, & Barrett.J.N, (1976). Separation of two voltage-sensitive potassium currents, and demonstration of a tetrodotoxin-resistant calcium current in frog motoneurones. J. Physiol. 255, 737-744.

Barrett.E.F,, Barrett.J.N,, & Crill.W.E, (1980). Voltage-sensitive outward currents in cat motoneurones. J. Physiol. 304, 301-324.

Beck, S.G., Clarke, W.P., & Goldfarb, J. (1985). Spiperone differentiates multiple 5-hydroxytryptamine responses in rat hippocampal slices in vitro. Eur. J. Pharm. 116, 195-197.

Beck, S.G., & Goldfarb, J. (1985). Serotonin produces a reversible concentration dependent decrease of population spikes in rat hippocampal slices. Life Sci. 36, 557-563.

Belin.M.F,, Nanopoulos.M.D,, Aguera.M,, Steinbusch.H,, Verhofstad.A,, Maitre.M,, & Pujol.J.F, (1983). Immunohistochemical evidence for the presence of gamma aminobutyric acid and serotonin in one nerve cell. A study of the rat using antibodies to glutamate decarboxylase and serotonin. Brain Res. 275, 329-339.

Bernado.L.S,, & Prince.D.A, (1982). Dopamine modulates a Ca^{2+} - activated potassium conductance in mammalian hippocampal pyramidal cells. Nature 297, 76-79.

Bischoff, S., Bittiger, H., & Krauss, J. (1980). In vivo [^{3}H]spiperone binding to the rat hippocampal formation: involvement of dopamine receptors. Eur. J. Pharm. 68, 305-315.

Bjorklund, A., Nobin, A., & Stenevi, U. (1973). The use of neurotoxic dihydroxytryptamines as tools for morphological studies and localized lesioning of central indolamine neurones. Z. Zellforsch. 145, 479-501.

Bkaily, G., Sperelakis, N., Renaud, J-F., & Payet, M.D. (1985). Apamin, a highly specific Ca^{2+} blocking agent in heart muscle. Am. J. Physiol. 248, H745-H749.

Blankenship, J.E. (1976). Tetrodotoxin: from poison to powerful tool. Persp. Biol. Med. 19, 509-523.

Bobillier, P., Seguin, S., Petitjean, F., Salvert, D., Touret, M., & Jouvet, M. (1976). The raphe nuclei of the cat brain stem: a topographical atlas of their efferent projections as revealed by autoradiography. Brain Res. 113, 449-486.

Bockaert, J., Dumuis, A., Bouhelal, R., Sebben, M., & Cory, R.N. (1987). Piperazine derivatives including the putative anxiolytic drugs buspirone and ipsapirone, are agonists at 5-HT_{1A} receptors negatively coupled with adenylate cyclase in hippocampal neurones. Naunyn-Schmeideberg's Arch. Pharmac. 335, 588-592.

Bourque, C.W., & Brown, D.A. (1987). Apamin and d-tubocurarine block the after-hyperpolarisation of rat supraoptic neurosecretory neurones. Neurosci. Letts. 82, 185-190.

Bowker, R.M., Reddy, V.K., Fung, S.J., Chan, J.Y.H., & Barnes, C.D. (1987). Serotonergic and non-serotonergic raphe neurones projecting to the feline lumbar and cervical spinal cord: a quantitative horseradish peroxidase-immunocytochemical study. Neurosci. Letts. 75, 31-37.

Bowker, R.M., Westlund, K.N., Sullivan, M.C., Wilber, J.F., & Coulter, J.D. (1983). Descending serotonergic, peptidergic and cholinergic pathways from the raphe nuclei: a multiple transmitter complex. Brain Res. 288, 33-48.

Bramwell, G.J., & Goyne, T. (1973). Responses of midbrain neurones to iontophoretically applied 5-hydroxytryptamine. Br. J. Pharmac. 357P.

Brown, D.A. (1988). M-currents: an update. TINS 11 No.7, 294-299.

Brown, D.A., & Adams, P.R. (1980). Muscarinic suppression of a novel voltage-sensitive K^+ current in a vertebrate neurone. Nature 283, 673-676.

Brown, D.A., & Griffith, W.H. (1983). Calcium-activated outward current in voltage-clamped hippocampal neurones of the guinea-pig. J. Physiol. 337, 287-301.

Brown, T.H., Fricke, R.A., & Perkel, D.H. (1981). Passive electrical constants in three classes of hippocampal neurones. J. Neurophysiol. 46 No.4, 812-827.

Burlhis, T.M., & Aghajanian, G.K. (1987). Pacemaker potentials of serotonergic dorsal raphe neurones: contribution of a low-threshold Ca^{2+} conductance. Synapse 1, 582-588.

Carbone, E., & Lux, H.D. (1984). A low voltage-activated, fully inactivating Ca channel in vertebrate sensory neurones. Nature 310, 501-502.

Carlsson, A., & Lindqvist, M. (1970). Accumulation of 5-hydroxytryptophan in mouse brain after decarboxylase inhibition. J. Pharm. Pharmac. 22, 726-727.

Cerrito, F., & Raiteri, M. (1979). Serotonin release is modulated by presynaptic autoreceptors. Eur. J. Pharm. 57, 427-430.

Chazal, G., & Ralston, H.J., III (1987). Serotonin-containing structures in the nucleus raphe dorsalis of the cat: an ultrastructural analysis of dendrites, presynaptic dendrites, and axon terminals. The Journal of Comparative Neurology 259, 317-329.

Cherubini, E., & Lanfumey, L. (1987). An inward calcium current underlying regenerative calcium potentials in rat striatal neurones in vitro enhanced by BAY K 8644. Neurosci. 21 No.3, 997-1005.

Cherubini, E., & Williams, J.T. (1988). Nifedipine-sensitive calcium currents in rat locus coeruleus neurones in vitro. J. Physiol. 401, 66P.

Clarke, W.P., De Vivo, M., Beck, S.G., Maayani, S., & Goldfarb, J. (1987). Serotonin decreases population spike amplitude in hippocampal cells through a pertusis toxin substrate. Brain Res. 410, 357-361.

Colino, A., & Halliwell, J.V. (1986). 8-OH-DPAT is a strong antagonist of 5-HT action in rat hippocampus. Eur. J. Pharm. 130, 151-152.

Colino, A., & Halliwell, J.V. (1987). Differential modulation of three separate K-conductances in hippocampal CA1 neurones by serotonin. Nature 328, 73-77.

Collingridge, G.L., Kehl, J.S., & McLennan, H. (1983). Excitatory amino acids in synaptic transmission in the schaffer collateral-commissural pathway of the rat hippocampus. J. Physiol. 334, 33-46.

Colpaert, F.C., & Janssen, P.A.J. (1983). The head-twitch response to intraperitoneal injection of 5-hydroxytryptamine in the rat: antagonist effects of purported 5-hydroxytryptamine antagonists and of pirenperone, an LSD antagonist. Neuropharmacol. 22 No.8, 993-1000.

Colpaert, F.C., & Janssen, P.A.J. (1983). A characterisation of LSD-antagonist effects of pirenperone in the rat. Neuropharmacol. 22 No.8, 1001-1005.

Connell, L.A., & Wallis, D.I. (1988). Responses to 5-hydroxytryptamine evoked in the hemisected spinal cord of the neonate rat. Br. J. Pharmac. 94, 1101-1114.

Connor, J.A. (1978). Slow repetitive activity from fast conductance changes in neurones. Fed. Proc. 37, 2139-2145.

Connor, J.A., & Stevens, C.F. (1971). Voltage clamp studies of a transient outward membrane current in gastropod neural somata. J. Physiol. 213, 21-30.

Conrad, L.C.A., Leonard, C.M., & Pfaff, D.W. (1973). Connections of the median and dorsal raphe nuclei in the rat: an autoradiographic and degeneration study. J. Comp. Neur. 156, 179-206.

Constanti, A., & Sim, J.A. (1987). Calcium-dependent potassium conductance in guinea-pig olfactory cortex neurones in vitro. J. Physiol. 387, 173-194.

Cottrell, G.A. (1970). Direct postsynaptic resposes to stimulation of serotonin-containing neurones. Nature 225, 1060-1062.

Crunelli, V., Forda, S., Brooks, P.A., Wilson, K.C.P., Wise, J.C.M., & Kelly, J.S. (1983). Passive membrane properties of neurones in the dorsal raphe and periaqueductal grey recorded in vitro. Neurosci. Letts. 40, 263-268.

Crunelli, V., & Segal, M. (1985). An electrophysiological study of neurones in the rat median raphe and their projections to septum and hippocampus. Neurosci. 15 No.1, 47-60.

Curtis, D.R., Duggan, A.W., Felix, D., & Johnston, G.A.R. (1971). Antagonism between bicuculline and GABA in the cat brainstem. Brain Res. 33, 69-96.

Dahlstrom, A., & Fuxe, K. (1965). Evidence for the existence of monoamine containing neurones in the central nervous system. I. Demonstration of monoamines in the cell bodies of brain stem neurones. Acta. Physiol. Scand. 232, 1-55.

Davies, M.F., Deisz, R.., Prince, .A., & Peroutka, S.J. (1987). Two distinct effects of 5-hydroxytryptamine on single cortical neurones. Brain Res. 423, 347-352.

De Vivo, M., & Maayani, S. (1986). Characterization of the 5-hydroxytryptamine$_{1A}$ receptor-mediated inhibition of forskolin-stimulated adenylate cyclase activity in guinea pig and rat hippocampal membranes. J. Pharm. Exp. Ther. 238 No.1, 248-253.

Dekin, M.S., & Getting, P.A. (1984). Firing pattern of neurones in the nucleus tractus solitarius: modulation by membrane hyperpolarisation. Brain Res. 324, 180-184.

Deshmukh, P.P., Yamamura, H.I., Woods, L., & Nelson, D.L. (1983). Computer-assisted autoradiographic localization of subtypes of serotoninl receptors in rat brain. Brain Res. 288, 338-343.

Dingledine, R., Dodd, J., & Kelly, J.S. (1977). Ach-evoked excitation of cortical neurones. J. Physiol. 273, 79P.

Docherty, R.J., Dolly, J.O., Halliwell, J.V., & Othman, I. (1983). Excitatory effects of dendrotoxin on the hippocampus in vitro. J. Physiol. 336, 58P-59P.

Dompert, W.U., Glaser, T., & Traber, J. (1985). ^{3}H TVX Q 7821: identification of 5-HT_1 binding sites as target for a novel putative anxiolytic. Naunyn-Schmeideberg's Arch. Pharmac. 328, 467-470.

Dudar, J.D. (1974). In vitro excitation of hippocampal pyramidal cell dendrites by glutamic acid. Neuropharmacol. 13, 1083-1089.

Dunlap, K., & Fischbach, G.D. (1978). Neurotransmitters decrease the calcium component of sensory neurone action potentials. Nature 276, 837-839.

Dutar, P., & Nicoll, R.A. (1988). A physiological role for $GABA_B$ receptors in the central nervous system. Nature 332, 156-158.

Engel, G., Gothert, M., Hoyer, D., Schlicker, E., & Hillenbrand, K. (1986). Identity of inhibitory presynaptic 5-hydroxytryptamine (5-HT) autoreceptors in the rat brain cortex with 5-HT_{1B} binding sites. Naunyn-Schmeideberg's Arch. Pharmac. 332, 1-7.

Fargin, A., Raymond, J.R., Lohse, M.J., Kobilka, B.K., Caron, M.G., & Lefkowitz, R.J. (1988). The genomic clone G-21 which resembles a a-adrenergic receptor sequence encodes the 5-HT_{1A} receptor. Nature 335, 358-360.

Fedulova, S.A., Kostyuk, P.G., & Veselovsky, N.S. (1985). Two types of calcium channel in the somatic membrane of new-born rat dorsal root ganglion neurones. J. Physiol. 359, 431-446.

Finkel, A.S., & Redman, S. (1984). Theory and operation of a single microelectrode voltage clamp. J. Neurosci. Meth. 11, 101-127.

Fowler, J.C., Greene, R., & Weinreich, D. (1985). Two calcium-sensitive after-hyperpolarisations in visceral sensory neurones of the rabbit. J. Physiol. 365, 59-75.

Fox, A.P., Nowycky, M.C., & Tsien, R.W. (1987). Single-channel recordings of three types of calcium channels in chick sensory neurones. J. Physiol. 394, 173-200.

Fozard, J.R., & Kilbinger, H. (1985). 8-OH-DPAT inhibits transmitter release from guinea-pig enteric cholinergic neurones by activating 5-HT_{1A} receptors. Br. J. Pharmac. 86, 601P.

Frankenhauser, B., & Hodgkin, A.L. (1957). The action of calcium on the electrical properties of squid axons. J. Physiol. 137, 218-244.

Freedman, J.E., & Aghajanian, G.K. (1987). Role of phosphoinositide metabolites in the prolongation of afterhyperpolarisations by $'_1$-adrenoreceptors in dorsal raphe neurones. J. Neurosci. 7 No.12, 3897-3906.

Gaddum, J.H. (1953). Antagonism between lysergic acid diethylamide and 5-hydroxytryptamine. J. Physiol. 121, 15P.

Gaddum, J.H. (1961). Push-pull cannulae. J. Physiol. 155, 1P-2P.

Gallager, D.W., & Aghajanian, G.K. (1976). Effect of antipsychotic drugs on the firing of dorsal raphe cells. II. Reversal by picrotoxin. Eur. J. Pharm. 39, 357-364.

Gallager, D.W., & Aghajanian, G.K. (1976). Inhibition of firing of dorsal raphe by tryptophan and 5-hydroxtryptophan: blockade by inhibiting serotonin synthesis with Ro-4-4602. Neuropharmacol. 15, 149-156.

Gardette, R., Krupa, M., & Crepel, F. (1987). Differential effects of serotonin on the spontaneous discharge and on the excitatory amino acid-induced responses of the deep cerebellar nuclei neurones in rat cerebellar slices. Neurosci. 23 No.2, 491-500.

Ginsborg, B.L. (1973). Eletrical changes in the membrane in junctional transmission. Biochimica et Biophysica Acta 300, 289-317.

Glaser, T., & Traber, J. (1983). Buspirone: action on serotonin receptors in calf hippocampus. Eur. J. Pharm. 88, 137-138.

Glaser.T,, Rath.M,, Traber.J,, Zilles.K,, & Schleicher.A, (1985). Autoradiographic identification and topographical analyses of high affinity serotonin receptor subtypes as a target for the novel putative anxiolytic TVX Q 7821. Brain Res. 358, 129-136.

Glennon, R.A., Naiman, N.A., Lyon, R.A., & Titeler, M. (1988). Arylpiperazine derivatives as high-affinity 5-HT_{1A} serotonin ligands. J. Med. Chem. 31, 1968-1971.

Glennon, R.A., Naiman, N.A., Pierson, M.E., Titeler, M., Lyon, R.A., & Weisberg, E. (1988). NAN-190: an arylpiperazine analog that antagonizes the stimulus effects of the 5-HT_{1A} agonist 8-hydroxy-2-(di-n-propylamino)tetralin (8-OH-DPAT). Eur. J. Pharm. 154, 339-341.

Goldberg, H.L., & Finnerty, R.J. (1979). The comparative efficacy of buspirone and diazepam in the treatment of anxiety. Am. J. Psychiat. 136, 1184-1187.

Gozlan, H., El Mestikawy, S., Pichat, L., Glowinski, J., & Hamon, M. (1983). Identification of presynaptic serotonin autoreceptors using a new ligand: ^{3}H-PAT. Nature 305, 140-142.

Gustafsson, B., Galvan, M., Grafe, P., & Wigstrom, H. (1982). A transient outward current in a mammalian central neurone blocked by 4-aminopyridine. Nature 299, 252-254.

Gustafsson, B., & Wigstrom, H. (1986). Hippocampal long-lasting potentiation produced by pairing single volleys and brief conditioning tetani evoked in seperate afferents. J. Neurosci. 6 No.6, 1575-1582.

Gyermek, L. (1961). 5-Hydroxytryptamine antagonists. Pharmac. Rev. 13, 399-439.

Haas, H.L., & Konnerth, A. (1983). Histamine and noradrenaline decrease calcium-activated potassium conductance in hippocampal pyramidal cells. Nature 302, 432-434.

Haas, H.L., Schaerer, B., & Vosmansky, M. (1979). A simple perfusion chamber for the study of nervous tissue slices in vitro. J. Neurosci. Meth. 1, 323-325.

Hagenbach, A., Hoyer, D., Kalkman, H.O., & Seier, M.P. (1986). N,N Dipropyl-5-carboxamidotryptamine (DP-5-CT), an extremely potent and selective 5-HT_{1A} agonist. Br. J. Pharmac. 87, 139P.(Abstract)

Haigler, H.J., & Aghajanian, G.K. (1974). Peripheral serotonin antagonists: failure to antagonize serotonin in brain areas receiving a prominent serotonergic input. J. Neural Trans. 35, 257-273.

Haigler, H.J., & Aghajanian, G.K. (1974). Lysergic acid diethylamide and serotonin: a comparison of effects on serotonergic neurones and neurones receiving a serotonergic input. J. Pharm. Exp. Ther. 188 No.3, 688-699.

Halliwell, J.V., & Adams, P.R. (1982). Voltage-clamp analysis of muscarinic excitation in hippocampal neurones. Brain Res. 250, 71-92.

Halliwell, J.V., Othman, I.B., Pelchen-Matthews, A., & Dolly, J.O. (1986). Central action of dendrotoxin: selective reduction of a transient K conductance in hippocampus and binding to localised acceptors. Proc. Nat. Acad. Sci. USA 83, 493-497.

Hamon, M., Bourgoin, S., Gozlan, H., Hall, M.D., & Goetz, C. (1984). Biochemical evidence for the 5-HT agonist properties of PAT (8-hydroxy-2-(di-n-propylamino)teralin) in the rat brain. Eur. J. Pharm. 100, 263-276.

Harandi, M., Aguera, M., Gamrani, H., Didier, M., Maitre, M., Calas, A., & Belin, M.F. (1987). y-Aminobutyric acid and 5-hydroxytryptamine interrelationship in the rat nucleus raphe dorsalis: combination of radioautographic and immunocytochemical techniques at light and electron microscopy levels. Neurosci. 21 No.1, 237-251.

Henry, F., Faudon, M., & Ternaux, J-P. (1982). In vivo release of serotonin in two raphe nuclei (raphe dorsalis and magnus) of the cat. Brain Res. Bull. 8, 123-129.

Herrick-Davis, K., & Titeler, M. (1988). Detection and characterisation of the serotonin 5-HT_{1D} receptor in rat and human brain. J. Neurochem. 50 No.5, 1624-1631.

Heuring, R.E., & Peroutka, S.J. (1987). Characterisation of a novel ^{3}H-5-hydroxtryptamine binding site subtype in bovine brain membranes. J. Neurosci. 7 No.3, 894-903.

Hill, D.R., & Bowery, N.G. (1981). ^{3}H-baclofen and ^{3}H-GABA bind to bicuculline-insensitive $GABA_B$ sites in rat brain. Nature 290, 149-152.

Hjorth, S., Carlsson, A., Lindberg, P., Sanchez, D., Wikstrom, H., Arvidsson, L.B., Hacksell, U., & Nilsson, J.L.G. (1982). 8-Hydroxy-2-(di-n-propylamino)tetralin, 8-OH-DPAT, a potent and selective simplified ergot cogener with central 5-HT-receptor stimulating activity. J. Neural Trans. 55, 169-188.

Hodgkin, A.L., & Huxley.A.F, (1952). A quantitative description of membrane current and its application to conduction and excitation in nerve. J. Physiol. 117, 500-544.

Hodgkin, A.L., & Katz, B. (1949). Effect of temperature on electrical activity of giant axon of squid. J. Physiol. 109, 240-249.

Hokfelt, T., Ljungdahl, A., Steinbusch, H., Verhofstad, A., Nilsson, G., Brodin, E., Pernow, B., & Goldstein, M. (1978). Immunocytochemical evidence of substance P-like immunoreactivity in some 5-hydroxytryptamine-containing neurones in the rat central nervous system. Neurosci. 3, 517-538.

Holstege.G.H,, Tan.J,, Vanl Ham.J,, & Bos.A, (1984). Mesencephalic projections to the facial nucleus in the cat. An autoradiographical tracing study. Brain Res. 311, 7-22.

Hotson, J.R., & Prince, D.A. (1980). A calcium-activated hyperpolarisation follows repetative firing in hippocampal neurones. J. Neurophysiol. 43 No.2, 409-419.

Hoyer, D., Pazos, A., Probst, A., & Palacios, J.M. (1986). Serotonin receptors in the human brain. I. Characterization and autoradiographic localization of $5\text{-}HT_{1A}$ recognition sites. Apparent absence of $5\text{-}HT_{1B}$ recognition sites. Brain Res. 376, 85-96.

Innis, R.B., & Aghajanian, G.K. (1987). Pertusis toxin blocks $5\text{-}HT_{1A}$ and $GABA_B$ receptor-mediated inhibition of serotonergic neurones. Eur. J. Pharm. 143, 195-204.

Innis, R.B., Nestler, E.J., & Aghajanian, G.K. (1988). Evidence for G protein mediation of serotonin- and $GABA_B$- induced hyperpolarisation of dorsal raphe neurones. Brain Res. 459, 27-36.

Inoue, M., Matsuo, T., & Ogata, N. (1985). Baclofen activates voltage-dependent and 4-aminopyridine sensitive K^+ conductance in guinea pig hippocampal pyramidal cells maintained in vitro. Br. J. Pharmac. 84, 833-841.

Jahnsen, H. (1980). The action of 5-hydroxytryptamine on neuronal membranes and synaptic tramsmission in area CA1 of the hippocampus in vitro. Brain Res. 197, 83-94.

Jahnsen, H., & LLinas, R. (1984). Ionic basis for the electroresponsiveness and oscillatory properties of guinea-pig thalamic neurones in vitro. J. Physiol. 349, 227-247.

Joels, M., Twery, M.J., Shinnick-Gallagher, P., & Gallagher, J.P. (1986). Multiple actions of serotonin on lateral septal neurones in rat brain. Eur. J. Pharm. 129, 203-204.

Johnston, D., Hablitz, J.J., & Wilson, W.A. (1980). Voltage clamp discloses slow inward current in hippocampal burst-firing neurones. Nature 286, 391-393.

Kasai, H., Kameyama, K., Yamaguchi, K., & Fukuda, J. (1986). Single transient K channels in mammalian sensory neurones. Biophys. J. 49, 1243-1247.

Kawai, T., & Watanabe, M. (1986). Blockade of Ca-activated K conductance by apamin in rat sympathetic neurones. Br. J. Pharmac. 87, 225-232.

Kilpatrick, G.J., Jones, B.J., & Tyers, M.B. (1987). Identification and distribution of 5-HT_3 receptors in rat brain using radioligand binding. Nature 330, 746-748.

Kita, T., Kita, H., & Kitai, S.T. (1986). Electrical membrane properties of rat substantia nigra compacta neurones in an in vitro slice preparation. Brain Res. 372, 21-30.

Koe, K., & Wiessman, A. (1966). p-Chlorophenylalanine: a specific depletor of brain serotonin. J. Pharm. Exp. Ther. 154 No.3, 499-516.

Krnjevic, K., Lamour, Y., MacDonald, J.F., & Nistri, A. (1978). Depression by manganese and cobalt of monosynaptic Ia excitatory post-synaptic potential in cat spinal cord. J. Physiol. 289, 82P-83P.

Krnjevic, K., & Schwartz, S. (1967). The action of gamma aminobutyric acid on cortical neurones. Exp. Brain Res. 3, 320-336.

Kuno, M., & Weakly, J.N. (1972). Quantal components of the inibitory synaptic potential in spinal motoneurones of the cat. J. Physiol. 224, 287-303.

Laduron, P.M., Janssen, P.F.M., & Leysen, J.E. (1982). In vivo binding of [^{3}H]ketanserin on serotonin S_2-receptors in rat brain. Eur. J. Pharm. 81, 43-48.

Lakoski, J.M., & Aghajanian, G.K. (1985). Effects of ketanserin on neuronal responses to serotonin in the prefrontal cortex, lateral geniculate and dorsal raphe nucleus. Neuropharmacol. 24 No.4, 265-273.

Lancaster, B., & Adams, P.R. (1986). Calcium-dependent current generating the afterhyperpolarisation of hippocampal neurones. J. Neurophysiol. 55 No.6, 1268-1282.

Larkman, P.M., & Kelly, J.S. (1988). The effects of serotonin (5-HT) and antagonists on rat facial motoneurones in the in vitro brainstem slice. J. Neurosci. Meth. 24 No.2, 199.

Larkman, P.M., Penington, N.J., & Kelly, J.S. (in press). Electrophysiology of adult rat facial motoneurones : The effects of serotonin (5-HT) in a novel in vitro brainstem slice. J. Neurosci. Meth.

Leger, L., Charnay, Y., Dubois, P.M., & Jouvet, M. (1986). Distribution of enkephalin-immunoreactive cell bodies in relation to serotonin-containing neurones in the raphe nuclei of the cat: immunohistochemical evidence for the coexistence of enkephalins and serotonin in certain cells. Brain Res. 362, 63-73.

Leysen, J.E., Awouters, F., Kennis, L., Laduron, P.M., Vandenberk, J., & Janssen, P.A.J. (1981). Receptor binding profile of R 41 468, a novel antagonist at 5-HT_2 receptors. Life Sci. 28, 1015-1022.

Li, C-l., & McIlwain, H. (1957). Maintainance of resting membrane potentials in slices of mammalian cerebral cortex and other tissues in vitro. J. Physiol. 139, 178-190.

LLinas, R., & Sugimori, M. (1980). Electrophysiological properties of the in vitro purkinje cell somata in mammalian cerebellar slices. J. Physiol. 305, 171-195.

LLinas, R., & Sugimori, M. (1980). Electrophysiological properties of in vitro pukinje cell dendrites in mammalian cerebellar slices. J. Physiol. 305, 197-213.

LLinas, R., & Yarom, Y. (1981). Properties and distribution of ionic conductances generating electroreponsiveness of mammalian inferior olivary neurones in vitro. J. Physiol. 315, 569-584.

LLinas, R., & Yarom, Y. (1981). Electrophysiology of mammalian inferior olivary neurones in vitro. Different types of voltage-dependent ionic conductances. J. Physiol. 315, 549-567.

Loizou, L.A. (1969). Projections of the nucleus locus coeruleus in the albino rat. Brain Res. 15, 563-566.

Lucki, I., Nobler, M.S., & Frazer, A. (1984). Differential actions of serotonin antagonists on two behavioural models of serotonin receptor activation in the rat. J. Pharm. Exp. Ther. 228 No.1, 133-139.

Lum, J.T., & Piercey, M.F. (1988). Electrophysiological evidence that spiperone is an antagonist of 5-HT_{1A} receptors in the dorsal raphe nucleus. Eur. J. Pharm. 149, 9-15.

Madison, D.V., & Nicoll, R.A. (1982). Noradrenaline blocks accommodation of pyramidal cell discharge in the hippocampus. Nature 299, 636-638.

Madison, D.V., & Nicoll, R.A. (1984). Control of the repetitive discharge of rat CA1 pyramidal neurones in vitro. J. Physiol. 354, 319-331.

Malenka, R.C., Madison, D.V., Andrade, R., & Nicoll, R.A. (1986). Phorbol esters mimic some cholinergic actions in hippocampal pyramidal neurones. J. Neurosci. 6 No.2, 475-480.

Malenka, R.C., & Nicoll, R.A. (1986). Dopamine decreases the calcium-activated afterhyperpolarisation in hippocampal CA1 pyramidal cells. Brain Res. 379, 210-215.

Marcinkiewicz, M., Verge, D., Gozlan, H., Pichat, L., & Hamon, M. (1984). Autoradiographic evidence for the heterogeneity of 5-HT_1 sites in the rat brain. Brain Res. 291, 159-163.

Markstein, R., Hoyer, D., & Engel, G. (1986). 5-HT_{1A}-receptors mediate stimulation of adenylate cyclase in rat hippocampus. Naunyn-Schmeideberg's Arch. Pharmac. 333, 335-341.

Martin, L.L., & Sanders-Bush, E. (1982). The serotonin autoreceptor: antagonism by quipazine. Neuropharmacol. 21, 445-450.

Martin, L.L., & Sanders-Bush, E. (1982). Comparison of the pharmacological characteristics of 5-HT_1 and 5-HT_2 binding sites with those of serotonin autoreceptors which modulate serotonin release. Naunyn-Schmeideberg's Arch. Pharmac. 321, 165-170.

Marwaha, J., & Aghajanian, G.K. (1982). Relative potencies of '$_1$ and '$_2$ antagonists in the locus coeruleus, dorsal raphe and dorsal lateral geniculate nuclei: an electrophysiological study. J. Pharm. Exp. Ther. 222 No.2, 287-293.

Maura, G., Roccatagliata, E., & Raiteri, M. (1986). Serotonin autoreceptor in rat hippocampus: pharmacological characterisation as a subtype of the 5-HT_1 receptor. Naunyn-Schmeideberg's Arch. Pharmac. 334, 323-326.

Mayer, M.L., & Sugiyama, K. (1988). A modulatory action of divalent cations on transient outward current in cultured rat sensory neurones. J. Physiol. 396, 417-433.

McMcall, R.B., & Aghajanian, G.K. (1979). Serotonergic facilitation of facial motoneurone excitation. Brain Res. 169, 11-27.

Messing, R.B. (1978). Behavioural effects of serotonin neurotoxins: an overview. Annal. N. Y. Acad. Sci. 305, 480-491.

Middlemiss, D.N., & Fozard, J.R (1983). 8-Hydroxy-2-(di-n-propylamino)tetralin discriminates between subtypes of the 5-HT_1 recognition site. Eur. J. Pharm. 90, 151-153.

Mosko, S.S., Haubrich, D., & Jacobs, B.L. (1977). Serotonergic afferents to the dorsal raphe nucleus: evidence from HRP and synaptosomal uptake studies. Brain Res. 119, 269-290.

Mosko, S.S., & Jacobs, B.L. (1977). Electrophysiological evidence against negative neuronal feedback from the forebrain controlling midbrain raphe unit activity. Brain Res. 119, 291-303.

Mosko.S.S,, & Jacobs.B.L, (1976). Recording of dorsal raphe unit activity in vitro. Neurosci. Letts. 2, 195-200.

Mourre, C., Hugues, M., & Lazdunski, M. (1986). Quantitative autoradiographic mapping in rat brain of the receptor of apamin a polypeptide toxin specific for one class of Ca^{2+}-dependent K^+ channels. Brain Res. 382, 239-249.

Murase, K., & Randic, M. (1983). Electrophysiological properties of rat spinal dorsal horn neurones *in vitro*: calcium-dependent action potentials. J. Physiol. 334, 141-153.

Neher, E. (1971). Two fast transient components during voltage clamp on snail neurones. J. Gen. Physiol. 58, 36-53.

Newberry, N.R., & Nicoll, R.A. (1984). Direct hyperpolarising action of baclofen on hippocampal pyramidal cells. Nature 308, 450-452.

Newberry, N.R., & Nicoll, R.A. (1985). Comparison of the action of baclofen with y-aminobutyric acid on rat hippocampal pyramidal cells in vitro. J. Physiol. 360, 161-185.

Nicoll, R.A., Alger, B.E., & Jahr, C.E. (1980). Enkephalin blocks inhibitory pathways in the vertebrate CNS. Nature 287, 22-25.

Noble, D. (1985). Ionic mechanisms in rhythmic firing of heart and nerve. TINS, Vol.8, 499-504.

Nowycky, M.C., Fox, A.P., & Tsien, R.W. (1985). Three types of neuronal calcium channel with different calcium agonist sensitivity. Nature 316, 440-443.

Numann, R.E., Wadman, W.J., & Wong, R.K.S. (1987). Outward currents of single hippocampal cells obtained from the adult guinea-pig. J. Physiol. 393, 331-353.

Ogren, S.O., Berge, O-G., & Johansson, C. (1985). Involvement of spinal serotonergic pathways in nociception but not in avoidance learning. Psychopharmac. 87, 260-265.

Orrego, F. (1979). Criteria for the identification of central neurotransmitters and their application to studies with some nerve tissue preparations *in vitro*. Neurosci. 4, 1037-1057.

Paxinos, G., and C. Watson. 1982. The rat brain in stereotaxic coordinates, Academic Press, Sydney.

Pazos, A., Hoyer, D., & Palacios, J.M. (1984). The binding of serotonergic ligand to the porcine choroid plexus: characterisation of a new type of serotonin recognition site. Eur. J. Pharm. 106, 539-546.

Pazos, A., & Palacios, J.M. (1985). Quantitative autoradiographic mapping of serotonin receptors in the rat brain. I. Serotonin-1 receptors. Brain Res. 346, 205-230.

Pazos, A., Probst, A., & Palacios, J.M. (1987). Serotonin receptors in the human brain --III. Autoradiographic mapping of serotonin-1 receptors. Neurosci. 21 No.1, 97-122.

Pedigo, N.W., Yamamura, H.I., & Nelson, D.L. (1981). Discrimination of multiple [^{3}H]5-hydroxytryptamine binding sites by the neuroleptic spiperone in rat brain. J. Neurochem. 36 No.1, 220-226.

Penington, N.J., & Reiffenstein, R.J. (1986). Possible involvement of serotonin in the facilitatory effect of a hallucinogenic phenethylamine on single facial motoneurones. Can. J. Physiol. Pharmacol. 64, 1302-1309.

Penington, N.J., & Reiffenstein, R.J. (1986). Lack of effect of antagonists on serotonin-induced inhibition in rat hippocampus. Can. J. Physiol. Pharmacol. 64, 1413-1418.

Pennefather, P., Lancaster, B., Adams, P.R., & Nicoll, R.A. (1985). Two distinct Ca-dependent K currents in bullfrog sympathetic ganglion cells. Proc. Nat. Acad. Sci. USA 82, 3040-3044.

Peroutka, S.J. (1985). Selective labeling of 5-HT_{1A} and 5-HT_{1B} binding sites in bovine brain. Brain Res. 344, 167-171.

Peroutka, S.J. (1986). Pharmacological differentiation and characterisation of 5-HT_{1A}, 5-HT_{1B}, and 5-HT_{1C} binding sites in rat frontal cortex. J. Neurochem. 47, 529-540.

Peroutka, S.J., & Snyder, S.H. (1979). Multiple serotonin receptors: differential binding of [^{3}H]5-hydroxytryptamine, [^{3}H]lisergic acid diethylamide and [^{3}H]spiroperidol. Mol. Pharmac. 16, 687-699.

Pitler, T.A., & Landfield, P.W. (1987). Probable Ca^{2+}-mediated inactivation of Ca^2 currents in mammalian brain neurones. Brain Res. 410, 147-153.

Ransom, R.W., Asarch, K.B., & Shih, J.C. (1986). [3H]1-[2-(4-aminophenyl)ethyl]-4- (3-trifluoromethylphenyl)piperazine: a selective radioligand for 5-HT_{1A} receptors in rat brain. J. Neurochem. 46 No.1, 68-75.

Reisine, T.D., Soubrie, P., Artaud, F., & Glowinski, J. (1982). Involvement of leteral habenula-dorsal raphe neurones in the differential regulation of striatal and nigral serotonergic transmission in cats. J. Neurosci. 2 No.8, 1062-1071.

Rigdon, G.C., & Wang, C.M. (1987). Serotonin reuptake blockers inhibit the firing rate of serotonergic neurones of the dorsal raphe in vitro. Soc. Neurosci. Abstr. 13, 1648.

Roizen, M.F., & Jacobowitz, D.M. (1976). Studies on the origin of innervation of the noradrenergic area bordering on the nucleus raphe dorsalis. Brain Res. 101, 561-568.

Ropert, N. (1988). Inhibitory action of serotonin in CA1 hippocampal neurones in vitro. Neurosci. 26 No.1, 69-81.

Rowan, M.J., & Anwyl, R. (1985). The effects of prolonged treatment with tricyclic antidepressants on the actions of 5-hydroxytryptamine in the hippocampal slice of the rat. Neuropharmacol. 24 No.2, 131-137.

Rowan, M.J., & Anwyl, R. (1987). Neurophysiological effects of buspirone and ipsapirone in the hippocampus: comparison with 5-hydroxtryptamine. Eur. J. Pharm. 132, 93-96.

Saavedra, J.M., Brownstein, ., & Palkovits, M. (1974). Serotonin distribution in the limbic system of the rat. Brain Res. 79, 437-441.

Sada, H., Sada, S., & Sperelakis, N. (1986). Recovery of the slow acion potential is hastened by the calcium slow channel agonist, BAY-K-8644. Eur. J. Pharm. 120, 17-24.

Schoemaker, H., & Langer, S.Z. (1986). [^{3}H]8-OH-DPAT labels the serotonin transporter in the rat striatum. Eur. J. Pharm. 124, 371-373.

Schwartzkroin, P.A. (1975). Characteristics of CA1 neurones recorded intracellularly in the hippocampal in vitro slice preparation. Brain Res. 85, 423-436.

Schwindt, P.C., & Crill, W.E. (1981). Differential effects of TEA and cations on outward currents of cat motoneurones. J. Neurophysiol. 46 No.1, 1-16.

Schwindt.P,, & Crill.W, (1980). Role of a persistent inward current in motoneurone bursting during spinal seizures. J. Neurophysiol. 43 No.5, 1296-1318.

Scuvee-Moreau, J.J., & Dresse, A.E. (1979). Effects of various antidepressant drugs on the spontaneous firing rate of locus coeruleus and dorsal raphe neurones of the rat. Eur. J. Pharm. 57, 219-225.

Segal, M. (1976). 5-HT antagonists in rat hippocampus. Brain Res. 103, 161-166.

Segal, M. (1985). A potent transient outward current regulates excitability of dorsal raphe neurones. Brain Res. 359, 347-350.

Sills, M.A., Wolfe, B.B., & Frazer, A. (1984). Determination of selective and nonselective compounds for the 5-HT$_{1A}$ and 5-HT$_{1B}$ receptor subtypes in rat frontal cortex. J. Pharm. Exp. Ther. 231, 480-487.

Sprouse, J.S., & Aghajanian, G.K. (1986). (-)-Propranolol blocks the inhibition of serotonergic dorsal raphe cell firing by 5-HT$_{1A}$ selective agonists. Eur. J. Pharm. 128, 295-298.

Sprouse, J.S., & Aghajanian, G.K. (1987). Electrophysiological responses of serotonergic dorsal raphe neurones to 5-HT$_{1A}$ and 5-HT$_{1B}$ agonists. Synapse 1, 3-9.

Sprouse, J.S., & Aghajanian, G.K. (1988). Responses of hippocampal pyramidal cells to putative serotonin 5-HT$_{1A}$ and 5-HT$_{1B}$ agonists: a comparative study with dorsal raphe neurones. Neuropharmacol. 27, 707-715.

Steinbusch, H.W.M. (1981). Distribution of serotonin-immunoreactivity in the central nervous system of the rat - cell bodies and terminals. Neurosci. 6 No.4, 557-618.

Steindler, D.A., Isaacson, L.G., & Trosko, B.K. (1983). Combined immunocytochemistry and autoradiographic retrograde axonal tracing for identification of projection neurones. J. Neurosci. Meth. 9, 217-228.

Stern, W.C., Johnson, A., Bronzino, J.D., & Morgane, P.J. (1979). Influence of electrical stimulation of the substantia nigra on spontaneous activity of raphe neurones in the anesthetized rat. Brain Res. Bull. 4, 561-565.

Stern, W.C., Johnson, A., Bronzino, J.D., & Morgane, P.J. (1979). Effects of electrical stimulation of the lateral habenula on single-unit activity of raphe neurones. Exp. Neurol. 65, 326-342.

Storm, J.F. (1987). Action potential repolarisation and a fast after-hyperpolarisation in rat hippocampal pyramidal cells. J. Physiol. 385, 733-759.

Storm.J, (1986). A-current and Ca-dependent transient outward current control the iniatial repetitive firing in hippocampal neurones. Biophys. J. 49, 396a.

Taber-Pierce, E., Foote, W.E., & Hobson, J.A. (1976). The efferent connection of the nucleus raphe dorsalis. Brain Res. 107, 137-144.

Taber-Pierce, E., Lichentenstein, E., & Feldman, S.C. (1985). The somatostatin systems of the guinea-pig brainstem. Neurosci. 15 No.1, 215-235.

Takeuchi, Y., Kojima, M., Matsuura, T., & Sano, Y. (1983). Serotonergic innervation on the motoneurones in the mammalian brainstem. Light and electron microscopic immunohistochemistry. Anat. Embryol. 167 No.3, 321-333.

Tanaka, K., Minota, S., Kuba, K., Koyano, K., & Abe, T. (1986). Differential effects of apamin on Ca^{2+}-dependent K^{+} currents in bullfrog sympathetic ganglion cells. Neurosci. Letts. 69, 233-238.

Taylor, D.P., Allen, L.E., Becker, J.E., Crane, M., Hyslop, D.K., & Riblet, L.A. (1984). Changing concepts for the biochemical action of the anxioselective drug, buspirone. Drug Dev. Res. 4, 95-108.

Thompson, S.H. (1977). Three pharmacologically distinct potassium channels in molluscan neurones. J. Physiol. 265, 465-488.

Thompson, S.H. (1982). Aminopyridine block of transient potassium current. J. Gen. Physiol. 80, 1-18.

Traub.R.D,, & Llinas.R, (1977). The spatial distribution of ionic conductances in normal and axotomised motorneurones. Neurosci. 2, 829-849.

Trulson, M.E. (1985). Simultaneous recording of dorsal raphe unit activity and serotonin release in the striatum using voltammetry in awake, behaving cats. Life Sci. 37, 2199-2204.

Trulson, M.E., Howell, G.A., Brandstetter, J.W., Fredrickson, M.H., & Fredrickson, C.J. (1982). In vitro recording of raphe unit activity: evidence for endogenous rhythms in presumed serotonergic neurones. Life Sci. 31, 785-790.

Tsien.R.W,, Lipscombe.D,, Madison.D.V,, Bley.K.R,, & Fox.A.P, (1988). Multiple types of neuronal calcium channels and their selective modulation. TINS 11 No.10, 431-437.

Ungerstedt, U. 1984. Measurement of neurotransmitter release by intracranial dialysis. In Measurement of Neurotransmitter Release In Vivo. C.A. Marsden, editor. J.Wiley & Sons Ltd, . 81-105.

Van der Kooy, D., & Hattori, T. (1980). Bilaterally situated dorsal raphe cell bodies have only unilateral forebrain projections in rat. Brain Res. 192, 550-554.

Van der Kooy, D., & Hattori, T. (1980). Dorsal raphe cells with collateral projections to the caudate-putamen and substantia nigra: a fluorescent retrograde double labeling studt in the rat. Brain Res. 186, 1-7.

VanderMaelen, C.P., & Aghajanian, G.K. (1980). Intracellular studies showing modulation of facial motoneurone excitability by serotonin. Nature 287, 346-347.

VanderMaelen, C.P., & Aghajanian, G.K. (1983). Evidence for a calcium-activated potassium conductance in serotonergic dorsal raphe neurones. Soc. Neurosci. Abs. 9, 500.

VanderMaelen, C.P., Matheson, G.K., Wilderman, R.C., & Patterson, L.A. (1986). Inhibition of serotonergic dorsal raphe neurones by systemic and iontophoretic administration of buspirone, a non-benzodiazepine anxiolytic drug. Eur. J. Pharm. 129, 123-130.

Verge, D., Daval, G., Patey, A., Gozlan, H., El Mestikawy, S., & Hamon, M. (1985). Presynaptic 5-HT autoreceptors on serotonergic cell bodies and/or dendrites but not terminals are of the 5-HT_{1A} subtype. Eur. J. Pharm. 113, 463-464.

Waeber, C., Schoeffter, P., Palacios, J.M., & Hoyer, D. (1988). Molecular pharmacology of 5-HT_{1D} recognition sites: radioligand binding studies in human, pig and calf brain membranes. Naunyn-Schmeideberg's Arch. Pharmac. 337, 595-601.

Walton, K., & Fulton, B.P. (1986). Ionic mechanism underlying the firing properties of rat neonatal motoneurones studied in vitro. Neurosci. 19 No.3, 669-683.

Wang, R.Y., & Aghajanian, G.K. (1977). Inhibition of neurones in the amygdala by dorsal raphe stimulation: mediation through a direct serotonergic pathway. Brain Res. 120, 85-102.

Wang, R.Y., & Aghajanian, G.K. (1977). Antidromically identified serotonergic neurones in the rat midbrain raphe: evidence for collateral inhibition. Brain Res. 132, 186-193.

Wang, R.Y., & Aghajanian, G.K. (1982). Correlative firing patterns of serotonergic neurones in rat dorsal raphe nucleus. J. Neurosci. 2 No.1, 11-16.

Werman, R. (1966). A review: Criteria for identificationof a CNS transmitter. J. Comp. Biochem. Physiol. 18, 745-766.

Williams, J.T. (1987). Inwardly rectifying potassium currents induced by 5-HT in dorsal raphe neurones. Soc. Neurosci. Abstr. 13, 1650.

Williams, J.T., North, R.A., Shefner, S.A., Nishi, S., & Egan, T.M. (1984). Membrane properties of rat locus coeruleus neurones. Neurosci. 13 No.1, 137-156.

Wilson, W.A., & Goldner, M.M. (1975). Voltage clamping with a single microelectrode. J. Neurobiol. 6 No.4, 411-422.

Wong, R.K.S., & Prince, D.A. (1981). Afterpotential generation in hippocampal pyramidal cells. J. Neurophysiol. 45 No.1, 86-97.

Wu, P.H., Gurevich, N., & Carlen, P.L. (1988). Serotonin-1A receptor activation in hippocampal CA1 neurones by 8-hydroxy-2-(di-n-propylamino)tetralin, 5-methoxytryptamine and 5-hydroxytryptamine. Neurosci. Letts. 86, 72-76.

Yakel, J.L., Trussell, L.O., & Jackson, M.B. (1988). Three serotonin responses in cultured mouse hippocampal and striatal neurones. J. Neurosci. 8 No.4, 1273-1285.

Yamamoto, C. (1972). Intracellular study of seizure-like after discharges elicited in thin hippocampal sections in vitro. Exp. Neurol. 35, 154-164.

Yap, C.Y., & Taylor, D.A. (1983). Involvement of 5-HT_2 receptors in the wet-dog shake behaviour induced by 5-hydroxytryptophan in the rat. Neuropharmacol. 22 No.7, 801-804.

Yocca.F.D,, Hyslop.D.K,, Smith.D.W,, & Maayani.S, (1987). BMY 7378, a buspirone analog with high affinity, selectivity and low intrinsic activity at the 5-HT_{1A} receptor in rat and guinea pig hippocampal membranes. Eur. J. Pharm. 137, 293-294.

Yoshimura, M., & Higashi, H. (1985). 5-Hydroxytryptamine mediates inhibitory postsynaptic potentials in rat dorsal raphe neurones. Neurosci. Letts. 53, 69-74.

Yoshimura, M., Higashi, H., & Nishi, S. (1985). Noradrenaline mediates slow excitatory synaptic potentials in rat dorsal raphe neurones in vitro. Neurosci. Letts. 61, 305-309.

Zbicz, K.L., & Weight, F.F. (1985). Transient voltage and calcium-dependent outward currents in hippocampal CA3 pyramidal neurones. J. Neurophysiol. 53 No.4, 1038-1058.

Zhang, L., & Krnjevic, K. (1986). Effects of 4-aminopyridine on the action potential and the after-hyperpolarisation of cat spinal motoneurones. Can. J. Physiol. Pharmacol. 64, 1402-1406.

Zhang, L., & Krnjevic, K. (1987). Apamin depresses selectively the after-hyperpolarisation of cat spinal motoneurones. Neurosci. Letts. 74, 58-62.